The involvement of kynurenine pathway in neuroinflammation and neurodegeneration: New insight for therapeutic

Gloria Castellano González

A thesis of The Australian School of Advanced Medicine, Faculty of Human Sciences, Macquarie University, submitted in fulfilment of the requirements for the degree of Doctor of Philosophy.

Supervisor:

Prof. Gilles J. Guillemin

Co-supervisors:

Prof. Bruce J. Brew

Prof. Francesca Fallarino

December 2014

Declaration of originality

I hereby declare that the work presented in this thesis has not been submitted for a higher degree to any other university or institution. To the best of my knowledge this submission contains no material previously published or written by another person, except where due reference is stated otherwise. Any contribution made to the research by others is explicitly acknowledged.

Gloria Castellano González

Australian School of Advanced Medicine
Faculty of Human Science
Macquarie University

22nd of December 2014

Acknowledgements

This work would not have been possible without the support, inside and outside the lab, of many people who made this journey so much more enriching.

First, I would like to thank my supervisor Prof. Gilles J. Guillemin for giving me the opportunity of undertake a PhD project in his group, for his confidence, understanding and friendship. Also for always supporting me and my ideas or projects and make them possible. To my co-supervisor, Prof. Bruce J. Brew for his critical advice, adding a clinical point of view to my research. Also to my co-supervisor Prof. Francesca Fallarino, for her infinite knowledge and passion for research, which was contagious. Thanks for your mentorship and friendship.

A special thank you for Dr. Alban Bessede, whose pass through our lab marked a before and after in my PhD. Thanks for your advice and support as a friend and as a researcher. Also to Karina Ghisoni and Roberta Martins, whose exchange in our lab brought as many laughs as share of knowledge.

During my candidature I have experienced several changes in laboratory locations, which has allowed me to grow as a researcher, to build friendships and to work with many wonderful colleagues. To past and present members at our Neuroinflammation group: Dr Anna Zinger, Dr Gayathri Sundaram, Dr Nady Brady, Dr Jong-min Lee, Dr David Lovejoy, Dr Edwin Lim, Josien de Brie, Ariel Seaton, thank you all for your knowledge and assistance. To Vanessa Tan and Dr Benjamin Heng for their unconditional help and availability. To Kelly Jacobs for our work as a team in KMO and especially to Dr Seray Adams, my best friend, I don't know what would have I done without you! To all the members at our new MND group for sharing their expertise in new techniques and support, especially to Dr Emily Don for her expertise in cloning. To ASAM, at Macquarie University, and its members, for welcoming us, especially to Phil Bokiniec for the last minute checks and Dr Kayla Viegas, for all her help and being a great friend. To SoMS, at UNSW, for supporting my PhD candidature and to its members, especially to Sonia Bustamante, Dr Helder Marcal, Dr Nicolas Pichaud and Prof Nicodemus Telda for their expertise, knowledge and advice in specific techniques. To Dr Claire Goldsbury, who first supervised me in Sydney and introduced me to research. I would also like to thank Dr David Brown and Dr Lucette Cysique in AMR, St Vincents Hospital for their knowledge and advice in

neuroinflammation and statistics and especially to Dr Simon Jones, for his assistance with the flow cytometer, support and valuable advice.

A special thank to all the members of the Experimental Medicine Department in the University of Perugia: Prof Ursula Grohmann, Prof Paolo Puccetti, Prof Maria L Belladonna, Prof Ciriana Orabona, Prof Roberta Bianchi, Dr Carmine Vacca, Dr Maria T Pallotta, Dr Davide Matino, Elisa Albini, Alberta Iacono, Selina Polani, Giuseppe Paolicelli, etc. Thank you all for making my exchange in the lab an unforgettable experience, for your unsurpassed knowledge and kindness. Especially to Dr Claudia Volpi, for your unconditional support, laughter and friendship, and to Marco Gargaro and Giada Mondanelli, for all the good times inside and outside the lab, for your support always and for the many Italian vocabulary you taught me.

Finally, I would like to thank my family who have closely and unequivocally supported me despite the distance and to Craig for his unconditional support, encouragement and understanding at all times.

Publications

Book chapters

- Jun Sasaki and Masaki Kichida (2011) *"Curcumin: Biosynthesis, Medicinal Uses and Health Benefits"*. Nova Publishers. Chapter: Curcumin: Medicinal properties, Molecular targets and biological mechanisms.

Journal publications

- NADY BRAIDY, PABLO MUÑOZ, ADRIAN G PALACIOS, GLORIA CASTELLANO-GONZÁLEZ AND GILLES J. GUILLEMIN (2012*)* "Recent rodent models for Alzheimer's disease: clinical implications and basic research". *Journal of Neural transmission* 119 (2): 173-195.

- MUSTHAFA M. ESSA, RESHMI K. VIJAYAN, GLORIA CASTELLANO- GONZÁLEZ, MUSTAQ A. MEMON, NADY BRAIDY AND GILLES J. GUILLEMIN (2012) "Neuroprotective Effect of Natural Products Against Alzheimer's Disease" *Neurochemical research*

- GLORIA CASTELLANO-GONZÁLEZ, NICOLAS PICHAUD, J. WILLIAM O. BALLARD, ALBAN BESSEDE, HELDER MARCAL AND GILLES J. GUILLEMIN (2014) "Epigallocatechin-3-gallate induces oxidative phosphorylation by activating Cytochrome c oxidase in human primary neurons and astrocytes" *J. Neurochem* (*submitted*). **Chapter 6**.

- GLORIA CASTELLANO- GONZÁLEZ, KELLY JACOBS, EMILY DON, SERAY ADAMS, DAVID B. LOVEJOY, BRUCE J. BREW AND GILLES J. GUILLEMIN (2014) "Activation of Kynurenine 3-monooxygenase interferes with cellular bioenergetics" (*in progress*). **Chapter 5.**

- GLORIA CASTELLANO- GONZÁLEZ, KELLY JAKOBS, DAVID LOVEJOY BRUCE J. BREW AND GILLES J. GUILLEMIN (2014) "Physiological regulation of the Kynurenine pathway. Understanding the role of KP in health and pathology" (*in progress*). **Literature review**.

Conference proceedings

Poster presentations

- International congress of neuroimmunology, Mainz, Germany, 2014.

Title: "*Immunoregulatory function of adult primary astrocytes: The role of Kynurenines"* Gloria Castellano González, Simon Jones, Marco Gargaro, Giada Mondanelli, Gayathri Sundaram, Alban Bessede, Gilles J. Guillemin and Francesca Fallarino.

- International Congress of immunology, Milano, Italy, 2013.

Title: "*High doses of CpG oligodeoxynucleotides stimulate a tolerogenic TLR9-TRIF pathway*" Claudia Volpi, Gloria Castellano González, Francesca Fallarino, Ursula Grohmann and Paolo Puccetti.

- VI neurotoxicity society meeting, Valdivia, Chile, 2013.

Title: "*Bioenergetics modulation by a natural molecule as a target for neuroprotection*". Gloria Castellano González, Alban Bessede, Helder Marcal and Gilles J. Guillemin

- International Society for Tryptophan Research, Sydney, Australia, 2012.

Title: "*Natural modulators of the kynurenine pathway: A Novel application to combat neurodegeneration*". Gloria Castellano González, Helder Marcal, Alban Bessede and Gilles J. Guillemin

- Drug discovery symposium (UNSW) Sydney, Australia, 2011.

Title: *"Screening for natural inhibitor of the kynurenine pathway enzymes".* Gloria Castellano González, Helder Marcal, Alban Bessede and Gilles J. Guillemin

Oral presentations

- Lifesyle Approaches for the Prevention of Alzheimer's Disease, Perth, Australia, 2012.

Title: "*Natural inhibitors of the Kynurenine pathway: Novel applications in Alzheimer's Disease treatment.*" Gloria Castellano González, Helder Marcal, Alban Bessede and Gilles J. Guillemin

Abstract

Mitochondrial dysfunction, glutamate excitotoxicity and neuroinflammation are involved in the pathogenesis of numerous neurological disorders. It has been shown that these deleterious aspects are interconnected and induced through an imbalance in the Kynurenine pathway (KP) metabolism. The KP is the main catabolic route of tryptophan (TRP) that ultimately leads to nicotinamide adenine dinucleotide (NAD^+). The KP is activated under inflammatory conditions, which leads to an increase in the KP metabolite, L-kynurenine (KYN), in the periphery and central nervous system (CNS). KYN is essential in regulating acute inflammatory responses, by mediating tolerance. However, in the brain, increased levels of KYN can potentially lead to neurotoxic KYN metabolites, predominantly through Kynurenine-3-monooxigenase (KMO) driven degradation. Therefore, the initial acute anti-inflammatory response of KP activation may thereafter contribute to neurodegeneration. Evidence is lacking on how KYN could regulate neuroinflammation in the CNS and why the KP shifts from being a protective response from the organism to exacerbate the CNS pathology.

The work presented in this thesis demonstrates that increased levels of KYN regulate astrocytic responses to inflammation. Furthermore, abnormalities in KP metabolite levels can promote neuroinflammatory responses. We also showed that one of the causes of KMO driven KP dysregulation is mitochondrial dysfunction and that by increasing mitochondrial complex IV activity we could potentially drive KYN degradation through the Kynurenine amino transferase (KAT) branch, which promotes the synthesis of neuroprotective metabolites.

In conclusion, neurological disorders involving neuroinflammation and mitochondrial impairment, will favour the KMO branch of the KP. This may subsequently lead to the long-term effect of KP imbalance, driving the KP towards the neurotoxic metabolites, exacerbating oxidative stress glutamate excitotoxicity and neuroinflammation. Therefore, limiting KMO activity, either with pharmacological inhibitors or by restoring the metabolic balance, could moderate the KP-mediated neurotoxicity, being a potential treatment for neurodegenerative diseases.

Table of Contents

List of Figures

List of Tables

List of Abbreviations

2-DG	2-Deoxy-D-Glucose
3-HAA	3-hydroxyanthranilic acid
3-HAAO	3-hydroxyanthranilic acid oxygenase
3-HK	3-hydroxykynurenine
3-NPA	3-nitropropionic acid
AADAT	Aminoadipate aminotransferase
ACMS	Aminocarboxymuconate semialdehyde
ACMSD	Aminocarboxymuconate semialdehyde decarboxylase
AD	Alzheimer's Disease
AhR	Aryl hydrocarbon receptor
AHRE	Aryl hydrocarbon response element
ALS	Amyotrophic Lateral Sclerosis
AM	Antimycin A
AMP	Adenosine monophosphate
AMPAR	AMPA receptors
AMPK	AMP-Activated protein kinase
AP	Activator protein family
APC	Allophycocyanin
APCs	Antigen-presenting cells
ARNT	AhR Nuclear translocator

ASAT	Aspartate aminotransferase
Aβ	β-Amyloid peptides
BBB	Blood-brain barrier
BCA	Bicinchoninic acid
BDNF	Brain derived neurotrophic factor
BSA	Bovine serum albumin
CaMKKβ	Calmodium-dependent protein kinase kinase β
CCBL	Cysteine conjugate beta-lyase
CCL	CC-chemokine ligand
CcO	Cytochrome c Oxidase (mitochondrial complex IV)
CCR	C-C chemokine receptor
cDNA	Complementary DNA
CNS	Central nervous system
COX	Cyclo oxygenase
CSF	Cerebrospinal fluid
CTLA4	Cytotoxic T-lymphocyte antigen 4
CXCR	C-X-C chemokine receptor
CYP1A1	Cytochrome P4501A1
DAPI	4',6-diamidino-2-phenylindole

DC	Dendritic cells
DNA	Deoxyribonucleic acid
DNase I	Deoxyribonuclease I
dNTPs	Deoxynucleotide triphosphates
DRE	Dioxin response element
EAE	Experimental Autoimmune Encephalomyelitis
ECM	Extracellular matrix
EDTA	Ethylenediaminetetraacetic acid
EGCG	Epigallocatechin-3-gallate
ER	Endoplasmic reticulum
ETS	Electron transport system
FAD	Flavin adenine dinucleotide
FBS	Fetal bovine serum
FCCP	Carbonyl cyanide-4-(trifluoromethoxy)phenylhydrazone
FITC	Fluorescein isothiocyanate
GABA	γ-aminobutyric acid
GAPDH	Glyceraldehyde phosphate dehydrogenase
GARP	Glycoprotein-A repetitions predominant protein
GFAP	Glial fibrillary acidic protein

GITR-L	Glucocorticoid inducer tumor necrosis factor receptor ligand
GluR	Glutamate receptor
GOT	Glutamic oxaloacetic transaminase
GPR	G-protein coupled receptor
GTK	Glutamine transaminase K
H_2O_2	Hydrogen peroxide
HAAO	3-hydroxyanthranilate 3,4-dioxygenase
HBSS	Hank's Balanced Salt Solution
HD	Huntington Disease
HEK	Human Embrionic Kidney
HIV	Human Immunodeficiency virus
HO-1	HemeOxigenase -1
HPLC	High performance liquid chromatography
HPRT	Hypoxanthine-guanine phosphoribosyltransferase
HRP	Horseradish peroxidase
IDO	Indoleamine, 2-3 dioxygenase
IFN	Interferon
IGF	Insulin Growth Factor
IL	Interleukin
IRF	IFN-regulatory factor

KAT	Kynurenine aminotransferase
KMO	Kynurenine 3-monooxygenase
KO	Knock Out
KP	Kynurenine pathway
KYN	Kynurenine
KYNA	Kynurenic acid
KYNU	L-kynurenine hydrolase
LAP	Latency-associated peptide
LB	Lysogeny broth
LC	Latent TGF-β complex
LDH	Lactate dehydrogenase
LLC	Large soluble latent TGF-β complex
LPS	Lipopolysaccharide
LTBP-1	Latent TGF-β-binding protein
MAP2	Microtubule-associated protein 2
MAPK	Mitogen-activated protein kinase
MCP-1	Monocytic chemoattractant-1
MHC	Major histocompatibility complex
MIP	Macrophage inflammatory proteins

MMP	Matrix metalloproteinases
MPP^+	1-methyl-4-phenylpyridinium
MPTP	1-methyl-4-phenyl-1,2,3,6-tetra-pyridine
mRNA	Messenger RNA
MS	Multiple sclerosis
MSC	Mesenchymal stromal cells
nAChRs	α-7-nicotinic acethylcholine receptors
NAD	Nicotinamide adenine dinucleotide
NADP	Nicotinamide adenine dinucleotide phosphate
NF-κB	Nuclear factor-κB
NMDA	N-methyl-D-aspartate
NMDAR	N-methyl-D-aspartate receptor
NMDAR	NMDA receptor
NO	Nitric oxide
NOS	Nitric oxide synthase
O^{2-}	Superoxide anion radical
OCR	Oxygen consumption rate
ODN	Oligodeoxynucleotides
OXPHOS	Oxidative phosphorylation

PAI	Plasminogen activator inhibitor
PARP	poly (ADP-ribose) polymerase
PBS	Phosphate Buffer Saline
PD	Parkinson's Disease
PE	Phycoerythrin
PFA	Paraformaldehyde
PGC-1α	Proliferator-activated receptor ϒ coactivator 1α
PI	Propidium iodide
PI3K	Phosphatidylinositol 3-kinase
PIC	Picolinic acid
PKA	Protein kinase A
PLP	Pyridoxal-5 phosphate
QPRT	Quinolinate phosphoribosyltransferase
QUIN	Quinolinic acid
RNA	Ribonucleic acid
ROS	Reactive oxygen species
ROX	Residual oxygen consumption
RT-PCR	Reverse transcriptase-polymerase chain reaction
SDS	Sodium dodecyl sulphate

SLC	Small latent TGF-β complex
SN	Substantia nigra
SNpc	Substantia nigra pars compacta
SOCS	Suppressor of cytokine signalling 3
SOD	Superoxide dismutase
SRC	Spare Respiratory Capacity
STAT	Signal transducer and activator of transcription
Treg	Regulatory T cell
TBP	TATA-binding protein
TBS	Tris-Buffered Saline
TCA	tricarboxylic acid
TCCD	2,3,7,8-Tetrachlorodibenzo-p-dioxin
TDO	Tryptophan, 2-3 dioxygenase
Tfam	Mitochondrial transcription factor A
TGF	Transforming Growth Factor
TLR	Toll-like receptors
TMPD	*N*,*N*,*N*′,*N*′-Tetramethyl-*p*-phenylenediamine
TNF	Tumour Necrosis Factor
Tr1	Type 1 regulatory T cells
TRP	L-Tryptophan

UHPLC	Ultra High performance liquid chromatography
uPA	urokinase Plasminogen Activator
uPAR	uPA receptor
WT	Wild Type
β2M	β-2 microglobulin
Δp	Electrochemical proton motive force
ΔpH_m	Mitochondrial pH gradient
$\Delta\Psi_m$	Mitochondrial membrane potential

Chapter 1

Literature Review

The ***kynurenine pathway*** (KP) represents the main route for the catabolism of tryptophan (TRP) that ultimately leads to nicotinamide adenine dinucleotide (NAD^+). TRP is an amino acid required for protein synthesis and other important metabolic functions, but animals do not possess the enzymatic machinery to synthesize it and it must be obtained from external sources. Tryptophan can be found in blood bound to albumin, but only the free form can cross the blood-brain barrier (BBB) by the competitive and nonspecific L-type amino acid transporter (1). In the nervous system and gut, tryptophan is a required substrate for the synthesis of serotonin, whereas in the pineal gland, it is required for the synthesis of melatonin. Also, when niacin content in the diet is insufficient for metabolic requirements, tryptophan is necessary for the synthesis of the essential cellular cofactor NAD^+ (2).

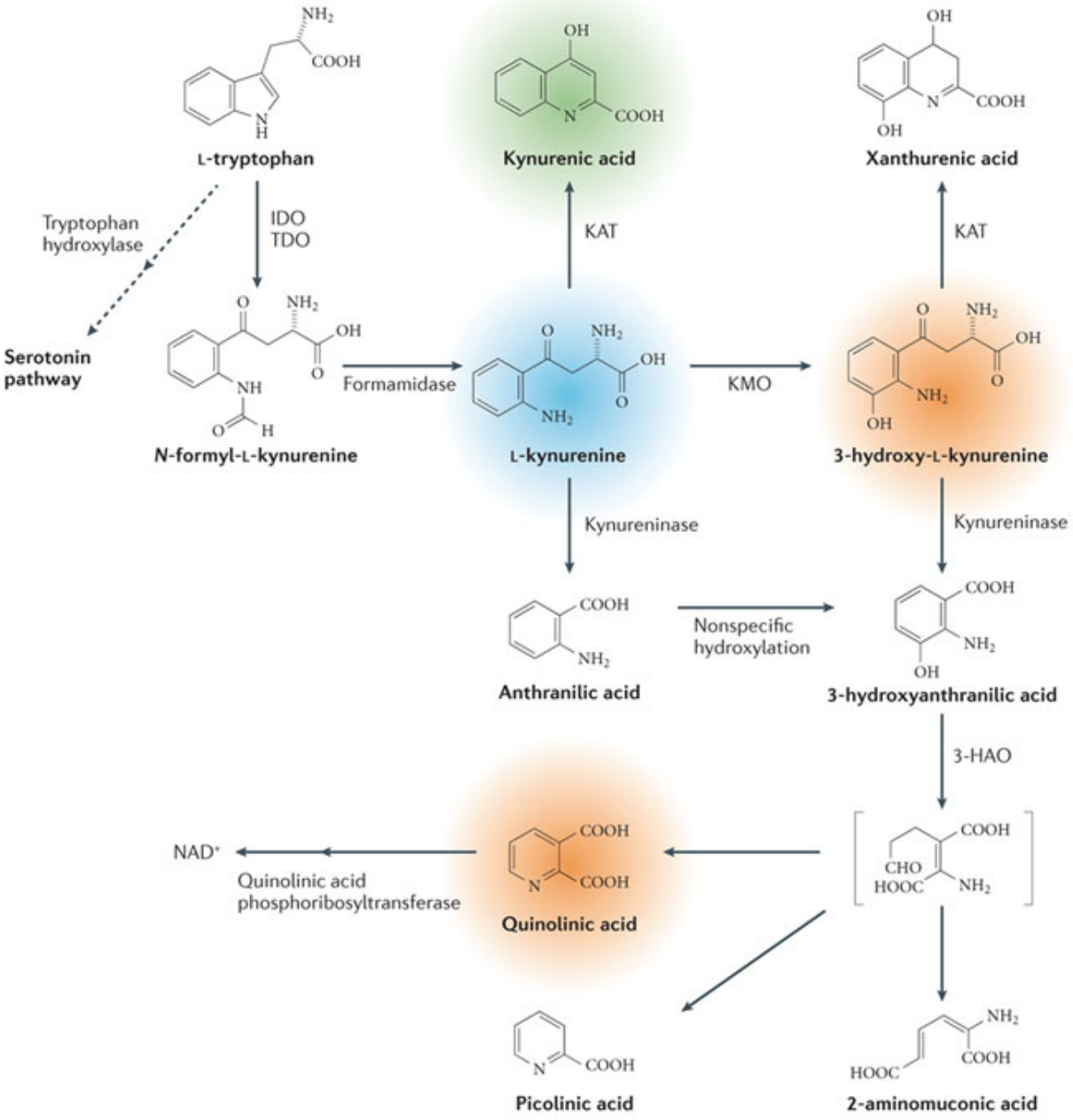

Figure 1.1: The Kynurenine Pathway

KP scheme showing the most relevant metabolites. Figure from Vecsei et al. (3)

1.1 Modulators of the kynurenine pathway

The KP is regulated by several endogenous molecules that are related to inflammation, energy metabolism, Redox balance and glutaminergic transmission. Its complex regulatory mechanisms, together with its abnormalities being implicated in many neurodegenerative diseases (section 1.4), highlight the importance of adequate KP balance to maintain physiological homeostasis.

1.1.1 The KP switch: IDO-1, IDO-2 and TDO

The enzyme that catalyses the first and rate limiting step of TRP catabolism is either tryptophan 2,3-dioxygenase (TDO) or indoleamine 2,3-dioxygenase (IDO-1 and IDO-2) (4, 5). Although TDO and IDO have identical biochemical activity, they share no significant sequence homology (10% amino acid homology) (6). Moreover, TDO and IDO have different substrate specificities. While IDO-1 (and IDO-2, generally less efficiently) can cleave several indole-containing compounds, including D- and L-TRP, serotonin, tryptamine and 5-hydroxytryptophan (7), TDO is enantiomer specific and can only cleave L-TRP (8)

TDO is active as a homotetramer; the heme and L-TRP are necessary for its oligomerization and activity. The complete formation of the active site requires tetrameric organization, as the domains that form the active site are far apart in the monomer (9). TDO is constitutively active in liver and can also be found in the brain (9). Furthermore, it has been shown that TDO is expressed in glioma cells and other cancer cells. In these cells, an increase in its expression is not only correlated with malignancy and proliferation of the tumour cell, but also with a promotion of tolerogenic immune response (10). Accordingly, studies have demonstrated that TDO is important in controlling overreaction to LPS challenge, by regulating the pro-inflammatory response to endotoxin (11). TDO is inducible by TRP and glucocorticoids (12). It is responsible for modulating circulating TRP levels (13), as well as the acute increase of systemic KYN/TRP ratio after an inflammatory insult (11).

IDO-1 is expressed in many cells including endothelial cells, smooth muscle cells, fibroblasts, astrocytes, macrophages, microglia and dendritic cells (DCs). Its most potent stimulant is interferon gamma (IFN-γ) (14), which induces both the gene expression and enzymatic activity of IDO-1 (15). IDO-1 has been extensively studied in immunology and its regulation is discussed in more detail below.

IDO-2 can be found adjacent to the IDO-1 gene on chromosome 8 in both mice and humans. This suggests the gene arose via gene duplication (16). They share significant identity at the amino acid level (43% in both human and mouse proteins) (16), but phylogenetic analysis has revealed that, unlike IDO-1, an IDO-2 like protein can also be found in lower vertebrates including chickens, fish and frogs (17). IDO-2

differs with IDO-1 in its expression pattern and signalling pathway. It is detected in human liver, epididymis and kidney (18). IDO-2 has also been detected in gastric, colon and renal tumours and its expression may be up regulated in response to IFN-γ (19). Although IDO-2 has been shown to enzymatically cleave TRP, it has very low activity. In addition, it has been estimated that there are a high proportion of individuals that possess single nucleotide polymorphisms that eliminate enzymatic activity of IDO-2, without an evident pathology (5). Therefore, the physiological roles of IDO-2, as well as its optimal activation conditions, are yet to be discovered.

Heme-mediated modulation of IDO and TDO

Both, IDO and TDO belong to the family of heme-containing oxidoreductases. The ferrous form of the enzyme present at the centre of the heme ring inserts molecular oxygen on the second and third carbons of the indole motif of TRP, which produces L -N -formylkynurenine that subsequently degrades to KYN (Figure 1.1). Regulatory mechanisms by co-factors are likely to be shared by IDO and TDO. However, this thesis will focus on IDO-1, due to the lack of knowledge regarding IDO-2 and the structural differences in TDO.

<u>Positive regulators</u>

IDO is a monomeric protein that contains protoporphyrin IX as its prosthetic group. Activation of IDO requires reduction of its ferric (Fe^{3+}) heme to ferrous (Fe^{2+}) heme. Several electron donors have been proposed as biological reductants of IDO. Superoxide anion radical (O^{2-}) is the most studied, and it has been shown that O^{2-} not only acts as a co-factor, but also as a substrate for IDO by incorporating the oxygen into TRP (20). Superoxide dismutase (SOD), which catalyze the degradation of O^{2-}, can inhibit IDO activity (21), supporting O^{2-} activity as a positive activator of IDO. Conversely, O^{2-} is not able to maintain the maximal steady state activity of IDO and reduced flavine mononucleotide, biopterin (22) and cytochrome b5 (23) have been suggested as more likely electron donors for IDO. Additionally, *NADH*, under aerobic conditions, can act as a reducing cofactor to form the dioxygen adduct of IDO. Interestingly, considering that KP leads to the formation of NAD, a relationship between NAD and TRP metabolism is observed. NADH activates the first and rate limiting reaction in the KP that leads to its own formation (24).

Negative regulators

On the other hand, hydrogen peroxide (H2O2) inactivates IDO by oxidizing the heme iron to ferric. There is evidence that NOS-derived nitric oxide (NO) may regulate IDO expression. NO reduces the IDO protein content by accelerated proteasomal degradation and NO adducts of IDO are believed to be involved in decreasing IDO catalytic activity by binding to its heme group (25). NO could also inhibit TDO activity in a similar mechanism to that of IDO by out-competing O_2 for the vacant coordination site (26). IFN-γ not only induces IDO but also L-arginine metabolism through nitric oxide synthase (NOS), producing NO, which in turn down regulates IDO. It is important to note that by activating the Arginase I-dependent L-Arginine metabolism, immune regulatory functions are enhanced. Activation of Arginase I would decrease L-Arginine available for NO synthesis and the reduction of NO could increase IDO activity, favouring tolerance. However, much NO-mediated pathogenicity depends of peroxynitrite. Peroxynitrite is formed by the combination of NO and superoxide produced by inflammatory cells to defend against pathological insults. Peroxynitrite more strongly inhibits IDO activity by nitration of different tyrosines, oxidation of cysteine residues, or sulfhydryl oxidation (27).

Immune regulators of IDO-1

Many soluble and membrane-bound factors mediate IDO-1 induction, but IFN-γ (Type II) is the main inducer of IDO-1 in the majority of cell types. Type I interferons (IFN-α and IFN-β) have also been reported to induce IDO-1 (14, 28). Interferon-dependent IDO induction is mediated by IFN-regulatory factor (IRF)-1 and signal transducer and activator of transcription (STAT)-1 (29).

Additional cytokines can regulate IDO-1 expression, mainly acting as positive regulators of IFN-dependent mechanisms. These include tumor necrosis factor (TNF)-α (30), interleukin (IL)-2 and IL-12 (31).

IDO IFN-independent induction is mediated by the p38 and JNK mitogen-activated protein kinase (MAPK), phosphatidylinositol 3-kinase (PI3K), and the nuclear factor-κB (NF-κB) pathways. This has been shown in lipopolysaccharide (LPS), TNF-α, IL-6 or IL-1β –mediated IDO induction (32, 33).

Toll-like receptors (TLRs) play an essential role in the generation of innate and adaptive antimicrobial immune responses through recognition of conserved pathogen-associated molecular patterns. After elimination of the pathogen, anti-inflammatory signals are necessary to restore homeostatic balance. IDO-1 seems to be the down-stream effector of the secondary regulatory mechanism of TLRs activation. TLR-3 activation, with dsRNA (34, 35), TLR-4 activation by LPS (36), TLR-7 with unmethylated oligodeoxynucleotides (ODN) sequences containing unmethylated GpC motifs (37), TLR-9 with ODN-CpG (37, 38) or Thymosin α1 (39) induce IRF-3, stimulating the production of type I INF and consequently IDO expression. Targeting TLR-2 and-5 also leads to the expression of IDO (40).

Other IDO inducers involved in immunity include CD28 and cytotoxic T-lymphocyte antigen 4 (CTLA4) molecules from T cells through binding CD80/ CD86 in DC (41-44), CD40 (45), soluble CD200 (a cell surface glycoprotein highly expressed on myeloid cells) (46), anti- FcεRI (receptor for IgE) (47), dexamethasone inducer of glucocorticoid inducer tumor necrosis factor receptor ligand (GITR-L) and glucocorticoids (48), prostaglandin E2 (49), cyclooxygenases (COXs) (50) and hemeoxigenase -1 (HO-1) (51).

Additionally inflammatory mediators released from necrotic cells, a mechanism to alert the immune system of abnormal cell death, also enhance IDO expression. These include adenosine triphosphate (ATP) (52) and hemoglobin (53).

Interestingly, IDO-1 has been shown to have not only TRP catalytic function, but also to act as an intracellular signal transducer that mediates long-term tolerance. This activity involves transforming growth factor (TGF)-β signalling, which induces phosphorylation of IDO. Phosphorylated IDO then, acting as a signal transducer, activates the non-canonical NF-kB pathway and the nuclear translocation of p52-RelB to its target genes (IDO, TGF-β and type I interferons), thus promoting a stable regulatory phenotype in DCs (54).

On the other hand, IDO can be post transcriptionally down regulated through the suppressor of cytokine signalling (SOCS)-3. Autocrine or paracrine IL-6 activates SOCS-3, which binds to IDO, targeting it for ubiquitination and subsequent

proteasome degradation, and thereby promoting immunity (55). Additional negative regulators include IL-4, which has been previously described an inhibitor of IFN-γ-mediated IDO induction (56)

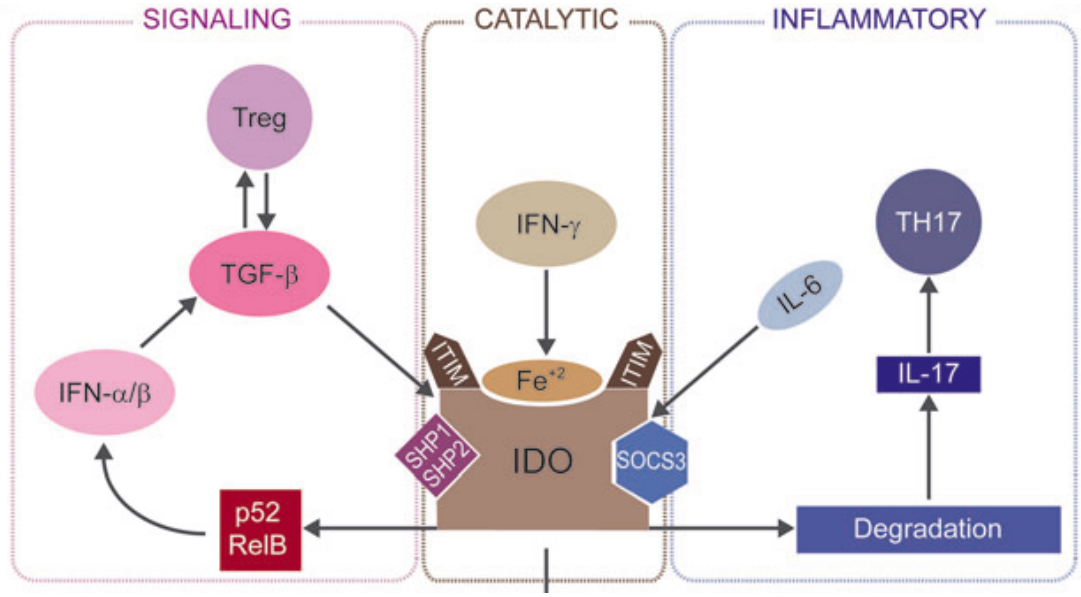

Figure 1.2: The complexity of IDO-1 control by immune regulators

IFN-γ drives intense enzymatic (catalytic) IDO activity, resulting in high-level production of KYN. TGF-β can maintain an IDO-dependent regulatory environment with IDO mainly functioning as a signalling molecule. Both mechanisms are abruptly interrupted by IL-6, which drives IDO degradation. Figure from Fallarino et al. (57).

Overall, the majority of the stimuli known to activate IDO-1 are closely related to inflammatory processes, being involved in innate and adaptive immunity (57). Acute IDO-1 activation prevents exaggerated inflammatory responses in the host against pathogens or an inflammatory trigger (11, 58), and long-term activation prevents different forms of autoimmunity and/or immunopathology (59, 60). Therefore, its acute and chronic activation in neurological diseases where immunity plays an important pathological role, such as MS, could be a defence response from the organism (61, 62).

Activation of the KP and IDO activity in the periphery is a common feature of many non-autoimmune neurological disorders. This supports the idea that there is also an inflammatory component to these pathologies (63-66). Nevertheless, what remains to be elucidated is whether IDO activation in the periphery is a reflection of the neuroinflammatory processes happening in the CNS or the neurodegenerative

disease has its origins outside the CNS.

Either way, what seems to direct the course of the neurological pathology is whether the branch of the KP through KYN is further metabolised (67) (Figure 1.1). Endogenous mediators are involved in directing the KYN through its different options.

1.1.2 First option: Kynurenine 3-Monooxygenase branch

Kynurenine 3-Monooxygenase (KMO) is the first enzyme of the "neurotoxic" branch of the KP. KMO is an oligomeric protein that contains non-covalently bound flavin adenine dinucleotide (FAD). It belongs to the monooxygenase family and it is located in the outer mitochondrial membrane where it converts KYN to 3-hydroxykynurenine (3-HK).

KMO catalyses the incorporation of one atom of molecular oxygen into KYN in the presence of nicotinamide adenine dinucleotide phosphate (NADP)H as an electron donor. The reaction is comprised of two half-reactions: (1) During the reductive reaction, the prosthetic group FAD is reduced to $FADH_2$ by NADPH, and (2) during the oxidative reaction, $FADH_2$ acts as an electron donor and is oxidised by oxygen to FAD, with the subsequent hydroxylation of KYN (68). Therefore, NADPH, O_2 and KYN are the substrates for KMO.

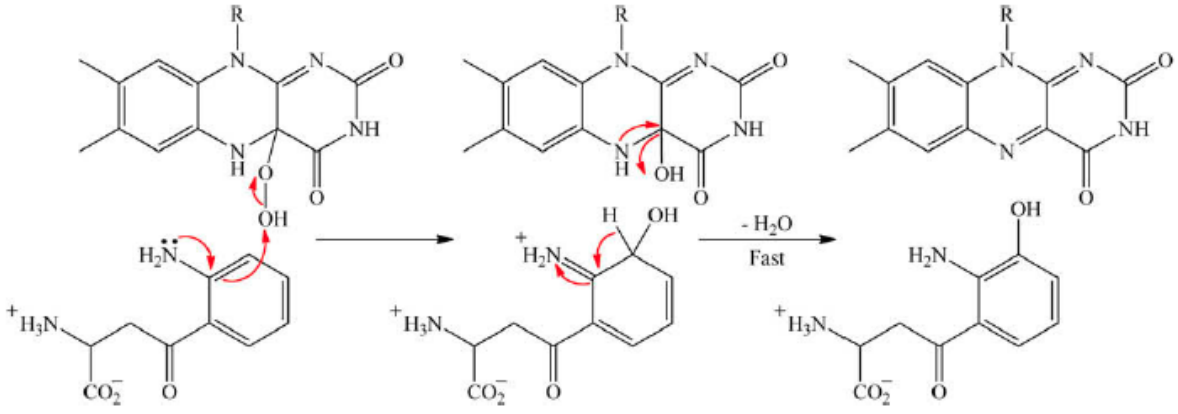

Figure 1.3: The hydroxylation of KYN

Oxygen transfer from the flavin hydroperoxide of KMO first forms the hydroxiflavin-non-aromatic intermediate, which decays rapidly to the oxidised flavin-product complex. Figure from Palfey et al. (69).

Studies on the recombinant enzyme showed that the optimum pH for KMO activity is 7.5. In addition, KMO is highly specific for L-Kynurenine, and is not able to hydroxylase other hydroxyl acceptors, such as kynurenic acid, anthranilic acid, tryptophan, p-hydroxybenzoate and the d-isomer of kynurenine (70)

The aromatic substrate, KYN, acts as an effector for NADPH by modulating the rate at which NADPH reduces the flavin. This (1) couples aromatic substrate acquisition to hydride transfer, and ultimately hydroxylation, and (2) prevents the reduction of the flavin in the absence of the aromatic substrate that, in FAD enzymes, results in the loss of reducing equivalents and in the formation of hydrogen peroxide during re-oxidation of the FAD cofactor (68). However, the product of the reaction (3-HK) can also act as an effector for NADPH, which will reduce FAD to $FADH_2$, but as 3-HK is not the substrate of the reaction, the following $FADH_2$ oxidation will lead to the formation of hydrogen peroxide and subsequent neurotoxic effects of 3-HK overproduction (70). In addition, the NADPH-dependent reduction of FAD is not specific for the native substrate (KYN), but it can recognize substrate-like molecules. This should be taken into account when designing KMO inhibitors because, aside from inhibiting 3-HK production, they could also increase hydrogen peroxide formation, depending on the mechanism of action (68).

KMO: from gene, to cellular protein localization, to tissue

The KMO (KMO; EC 1.14.13.9) gene contains at least 15 exons, spanning approximately 68 kilobase (Kb). By genomic sequence it has been determined that the KMO gene overlaps with the OPN3 gene on chromosome 1q43 and that the two genes are transcribed from opposite strands (71). At least three isoforms produced by alternative splicing have been described for KMO. However, two of them are only based on cDNA data and just one isoform (canonical sequence) has been characterised at the protein level (486 aa). The two alternative isoforms (473 and 452 aa respectively) differ from the canonical sequence by missing the amino acids between positions 367 and 400. This region has been demonstrated to be important for the subcellular localization of the enzyme, but not for the enzymatic activity. A single amino acid polymorphism (SAP) has been described for KMO, involving a change from arginine to cysteine at position 452 (70, 72). Arginine confers positive charge at the C-terminus, which is essential for mitochondrial targeting. Furthermore, it has been shown that a mutation of the C-terminus Arginine in pig KMO decreases

KMO activity by 40 % (73). Changes in the c-terminus region will affect cellular localization of KMO but they do not necessarily result in loss of activity (73). Therefore, KMO derived from the canonical sequence will be localised on the outer mitochondrial membrane. However, alternative splicing or SAP have been described in the literature leading to cytosolic KMO, which may or may not be as active as the canonical KMO.

Brain contains low activity of KMO equally distributed in all regions. The highest specific KMO activity is detected in liver and kidney (74)

Negative regulators of KMO

KMO is sensitive to inhibition by anions in both half-reactions. It appears to bind one or more ions in the proximity of the active site. This has direct influence on the flavin conformational changes (68). Cl- ions compete with NADPH for the enzyme sites that interact with the pyrophosphate moiety of NADPH, thereby decreasing its affinity. By interacting with a second phosphate-binding site, different from NADPH, pyridoxal-5 phosphate (PLP), the active form of vitamin B6, can also decrease NADPH affinity for the enzyme (70).

Positive regulators of KMO

The first positive regulator to consider is its substrate. Binding of KYN stimulates the first half reaction rate by ≈ 2500-fold (69).

KMO expression can also be activated under inflammatory stimuli, IFN-γ being the most common stimulus because of its ability to induce IDO (75). Moreover, LPS (76) and IL1-β (77) can also induce KMO expression independently of IFN-γ. These inflammatory molecules are well-described IDO-1 activators, and activation of KMO occurs after IDO activation. This indicates that the IDO-mediated increase of KYN could be responsible for KMO activation, instead of direct activation by cytokines. Further characterization of specific physiological activators of KMO is required in order to better understand its role on different pathologies.

1.1.3 Second option: Kynurenine aminotransferase branch

Kynurenine amino transferases (KATs) are the enzymes responsible for the first step in the “neuroprotective” branch of the KP. KATs catalyse the irreversible transamination of KYN to produce Kynurenic acid (KYNA). KYNA synthesis involves

two steps: (1) KYN transamination to a side chain α-ketoacid intermediate that is unstable and (2) rapid intramolecular cyclization of the intermediate to KYNA, being only the first step dependent on KATs (Figure 1.4). Consequently, the equilibrium always proceeds to KYNA formation. Four KATs are considered to be involved in KYNA synthesis in the central nervous system: KAT-1, -2, -3 and -4. In addition to their role in KYNA production, KATs exhibit transaminase activity with many amino acids, and they can use several α-keto acids as amine acceptors. The specificity for the amino acid and α-keto acid is different depending on the KAT.

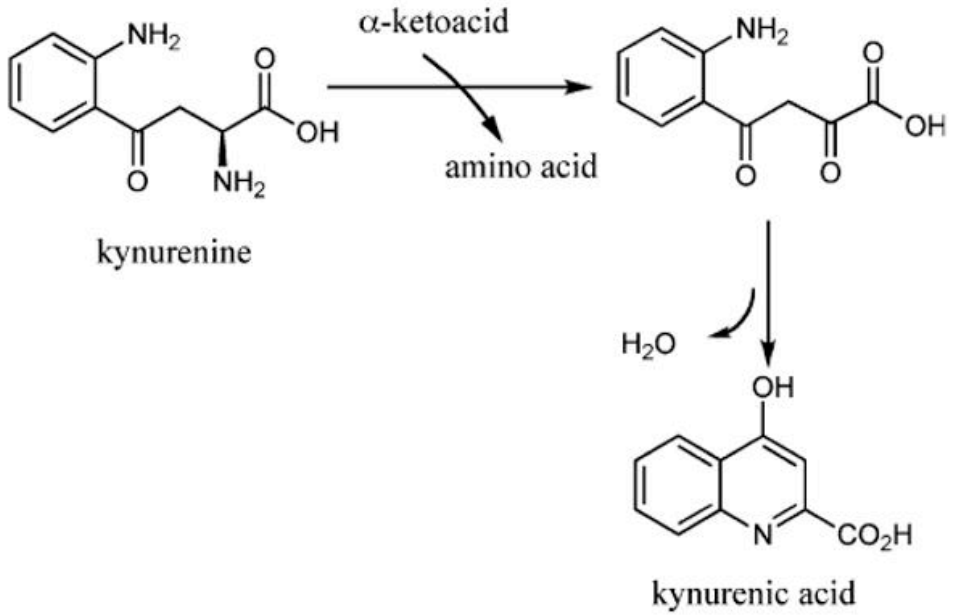

Figure 1.4: Reaction for KYNA synthesis

Figure from Han et al. (78).

KAT-1 is also known as glutamine transaminase K (GTK) or cysteine conjugate beta-lyase (CCBL)-1, as it has transaminase activity for several substrates. However, it is more specific for large, neutral/aromatic/sulphur-containing amino acids, such as glutamine, phenylalanine, leucine, KYN, methionine, tyrosine, histidine, cysteine, and aminobutyrate (79). Even though mice and human KAT-1 behave similarly, they show differences in substrate preference. For example, while mice KAT is more efficient towards phenylalanine, human KAT prefers glutamine (80). Among different α-ketoacids, α-Ketoleucine, glyoxylate, phenylpyruvate, mercaptopyruvate, α-ketobutyrate, mecaptopyruvate, oxaloacetate and pyruvate are the more efficient amino-acceptors for KAT-1.

Additional major biological roles of KAT-1 include closing the methionine salvage pathway (81) and maintaining the levels of phenylpyruvate. KAT-1 has high affinity for phenylpyruvate as a co-substrate and can catabolize its degradation in the presence of KYN (80, 82). Phenylpyruvate is associated with phenylketonuria pathology and its accumulation can produce brain damage (83). KAT-1 can also catalyse the non-physiological beta-elimination reactions with cysteine S-conjugates containing a good leaving group attached at the sulphur (84). These elimination reactions may lead to the bioactivation of certain sulphur-containing fragments, resulting in toxicity to brain. Indeed it has been proposed as a contributing factor to cell death in the substantia nigra observed in Parkinson's Disease (PD) (85). Increased levels of KYN would, therefore, be a mechanism of neuroprotection. This would not only avoid accumulation of phenylpyruvate, but also competitively inhibit the CCBL-1-mediated production of neurotoxic fragments.

KAT-2 is also a multifunctional aminotransferase, localised in the mitochondria. It was first named aminoadipate aminotransferase (AADAT), and it catalyses the transamination of both KYN and aminoadipate (aminoadipate being the best amino acid substrate for KAT-2), but also methionine and glutamate. Aminoadipate is the degradation product of the amino acid lysine, and can occur naturally in the brain. It can act as a selective toxin for glial cells (86) and at high concentrations it enhances glutamate excitotoxicity (80). Therefore, KAT-2 neuroprotective activity could be due to a combination of KYNA synthesis and aminoadipate neutralization. KAT-2, like other KATs, can use many α-keto acids as its amino group acceptors, but the more efficient ones are α-oxoglutarate, α-oxocaproic acid, phenylpyruvate and α-oxo- γ-methiol-butyric acid (80, 87).

KAT-2 is considered to be the principal isoform responsible for KYNA synthesis in the brain because, among all the KATs, this is the one that shows the highest selectivity for KYN (88, 89). Cerebral KAT-2 is located mainly in astrocytes, which are the major source of KYNA in the brain (90)

KAT-3 or cysteine conjugate beta-lyase (CCBL)-2, has high sequence identity and a similar transaminase profile to KAT-1. However, it differs in some biochemical and structural properties. KAT-3 is efficient in catalysing the transamination of glutamine, histidine, methionine, phenylalanine, asparagine, cysteine, and KYN. Differently to

KAT-1, KAT-3 prefers hydrophilic substrates (such as asparagine) (91). KAT-3 can use 13 α-keto acids as co-substrates (92), with glyoxylate, α-ketocaproic acid, phenylpyruvate, α-ketobutyrate, α-keto-methylthiobutyric acid, α-ketovalerate, indo-3-pyruvate, p-hydroxy-phenylpyruvate, mercaptopyruvate, and oxaloacetate being the best amino group acceptors for mKAT-3 (91). Similar to KAT-1, KAT-3 was also reported to have cysteine conjugate beta-lyase activity (91).

KAT-4 is also called mitochondrial aspartate aminotransferase (ASAT) or glutamic oxaloacetic transaminase (GOT)-2. KAT-4 is localised in the mitochondria and catalyses the reversible transamination of oxaloacetate to aspartate (93). This reaction is an essential component of the malate-aspartate shuttle, which is a key mechanism for transferring reducing equivalents from the cytosol into mitochondria in brain. Mitochondrial aspartate can be transported to the cytosol to eventually form malate. Malate can carry electrons into the mitochondria and produce NADH, when oxidised to oxaloacetate. KAT-4 –mediated transamination of oxaloacetate to aspartate allows the shuttle to restart (83). In conjunction, KAT-4 catalyses the conversion of glutamate to α-ketoglutarate (94). This reaction allows the glutamate to enter into the tricarboxylic acid cycle, as well as the re-synthesis of glutamate from tricarboxylic acid cycle intermediates. KAT-4 shows high transamination activity towards glutamate, aspartate, phenylalanine, tyrosine, and cysteine. However, it only has detectable activity towards KYN; therefore, its role in de-novo synthesis of KYNA in the brain is controversial (89, 95).

KAT positive regulators

Even though KYN is not a positive activator of KAT, the high Km values of all KATs will assure that rising levels of endogenous KYN result in a proportional increase of KYNA (78).

KAT-catalysed transamination requires the co-substrate PLP. Administration of vitamin B6 has been shown to increase plasma levels of KYNA (96). Several α-keto acids are also necessary as a co-substrate for KAT activity, and increased levels of those in cortical slices have been found to increase KYNA turnover (82). However, it should be taken into account that some α-ketoacids can also be the product of KAT-mediated amino acid transamination, and may act as inhibitors when they accumulate.

KAT negative regulators

KATs catalyse transamination of several amino acids; therefore, concentrations of these substrates should be considered when studying KAT activity, as they may competitively inhibit KYNA synthesis. Studies has shown that tryptophan, glutamine, phenylalanine, or cysteine inhibit human KAT-1 activity at the low milimolar range (79). Similarly, methionine, histidine, glutamine, leucine, cysteine, phenylalanine and 3-HK can significantly decrease mouse KAT-3 activity (91). Aminoadipate, asparagine, glutamate, histidine, cysteine, lysine, 3-HK, and phenylalanine decrease human KAT-2 activity. However, none of them are effective competitive inhibitors in the presence of KYN, as KAT-2 has strong affinity for KYN (80). On the other hand, mouse KAT-4 catalysed KYNA production can be competitively inhibited by aspartate and glutamate due to the high selectivity of KAT-4 for these amino acids (95). Since aspartate and glutamate are the most abundant proteinogenic amino acids in mouse brains, the contribution of KAT-4 to KYNA formation in mouse brains would be limited (95).

Some α-keto acids can also inhibit KAT. Han et al found that indo-3-pyruvate significantly inhibits KAT-2 (80), but not KAT-3 (91).

Mitochondrial inhibition may also affect KAT activity. 1-methyl-4-phenylpyridinium (MPP+) and 3-nitropropionic acid (3-NPA), inhibitors of mitochondrial complex I and II respectively, decrease KYNA synthesis in rat brain. Whereas MPP+ seemed to affect only KAT-2 (97), 3-NPA impaired the activity of both KAT-1 and KAT-2 (98). The dramatic decrease of KYNA in rat brain after glucose depravation (99), gives further evidence that impaired cellular energy metabolism can down regulate KAT activity. Glucose availability is required for the synthesis of α-keto acids, which are necessary co-substrates in the enzymatic KYN transamination process of KAT (100). Furthermore, astrocytic KYNA formation is reduced by neuronal signals such as glutamate and other depolarizing stimuli. This could be related to the higher energy demand associated with restoring the resting membrane potentials and the consequent decrease of co-substrate availability for KATs (99).

1.1.4 The forgotten option: Kynureninase

The enzyme, Kynureninase (KYNU), is a member of the aminotransferase superfamily (known as KATs) with homodimeric structure and containing PLP as a co-factor

(101). KYNU can catalyse the hydrolysis of KYN to give anthranilic acid (AA), but its main activity is catalysing the hydrolysis of 3-HK to produce 3-hydroxyanthranilic acid (3-HAA). Both reactions produce L-alanine as a second product.

Human KYNU has approximately a 100-fold preference for 3-HK compared to KYN (102) and, therefore, KYN will preferably undergo the KMO or KAT branch depending on the cell type. Nevertheless, KYN degradation through KYNU should be considered in cells that do not express active KMO (such astrocytes) (103), as there is no competition with 3-HK for the enzyme.

1.2 Neuroactive metabolites of the KP

Alterations to the branch that predominantly metabolises KYN will affect the levels of the different neuroactive KP metabolites (Figure 1.1). Each KP metabolite has a specific activity in the CNS and understanding these functions is necessary in order to relate KP abnormalities with a particular pathology. Table 1.1 summarise KP metabolites involvement in glutamate excitotoxicity, inflammation and oxidatite stress.

1.2.1 L-Kynurenine

L-Kynurenine (KYN) is the first stable metabolite of the KP. Studies have shown that is taken up into brain at a significant rate by the large neutral amino acid carrier (L-system) of the BBB (104). This should be taken into account when looking at the KYN concentration in cerebrospinal fluid (CSF), as its up regulation in the periphery is quickly reflected in CNS. In fact, only 40% of the KYN is locally generated in the CNS, whereas 60% is taken up from the blood (105).

Transfer of KYN across the BBB is saturable, suggesting that molecules competing for the same transporter (such 3-HK) may each contribute significantly to the cerebral pool of KYN (104).

In addition to its function as a precursor of other kynurenines, KYN has immunomodulatory activity. Tryptophan catabolism activation in several antigen-presenting cells (APCs) has been shown to suppress allogeneic T-cell proliferation and differentiate naïve T cells into regulatory T cells (Tregs). This effect is mediated by both TRP starvation and increase of kynurenines (106-109). Moreover, KYN has

been found to selectively induce apoptosis in effector T cells (110), thus, favouring an immunosuppressive response. The mechanisms underlying KYN immunosuppressive action were largely unknown, until recent studies demonstrated that KYN is an endogenous Aryl hydrocarbon receptor (AhR) agonist (10, 11). AhR is a ligand-activated transcription factor that regulates several immune processes (described in detail in section 1.3). Activation of AhR by KYN has different effects depending on the cell type. While it can promote cell survival and motility in glioblastoma, it reduces leukocyte proliferation, suppressing cellular and humoral immune responses (10). Additional immunoregulatory activities of KYN-mediated AhR activation include: differentiation of naïve T cells to $Foxp3^+$ Tregs (111), and increase of IL-10 cytokine production and IDO-1 expression in response to TLR ligands in bone marrow DCs and splenic DCs (58). Vogel at al showed that IDO-1 may also be induced by AhR activation *in vivo* (112). IDO-1 catalyses KYN synthesis, which in turn activates AhR. Overall, this results in a positive feedback loop that prolongs AhR immunosuppressive activity. Findings from a recent study also support the role of KYN-mediated AhR activation in down regulating inflammatory responses. It was found that both KYN and AhR are essential in primary endotoxemia resistance (11).

In addition to its role in immune regulation, KYN has also been observed to participate in cellular redox balance; thus, by acting as an antioxidant, it may prevent neurotoxicity (113).

1.2.2 Kynureninic acid

KYNA is a downstream product of KYN, produced by the action of KATs. The most relevant targets for KYNA are in the CNS; however, it cannot cross the BBB and its presence in the brain relies on its production by astrocytes (104). KYNA was first described as a competitive antagonist of glutamate receptors (GluR), equally inhibiting the three ionotropic excitatory receptors: NMDA receptor (NMDAR), AMPA receptors (AMPAR) and kainite receptors (114). However, this activity requires high micromolar concentrations of KYNA (115). Its activity as an endogenous NMDAR inhibitor requires lower concentrations when targeting the glycine-binding site (116),its main target. Additional targets have been described for KYNA. Alongside its activity on NMDAR in the CNS, it has an important role as a negative allosteric modulator of the α-7-nicotinic acethylcholine receptors (nAChRs) (117). nAChRs are expressed in the pre-synaptic axonal terminals of the striatum and mediate glutamate

release. KYNA, at low micromolar range, suppresses presynaptic glutamate release (118). Although synaptic communication requires glutamate, excessive glutamate release and signalling through ionotropic GluR leads to excitotoxicity. KYNA-mediated suppression of glutamate release, synergistically with its activity on NMDAR, potentiates its neuroprotective role on glutamate excitotoxicity. On the other hand, it should be taken into consideration that, under non-excitotoxic conditions, inhibition of NMDAR by KYNA in brain specific regions could affect cognitive, learning and memory functions (119).

Neuroinflammation mediated by resident or infiltrating immune cells is another factor to consider in synaptic alterations. It has been shown that activation of metabotropic GluR 4 in immune cells induces a tolerogenic immune response in an experimental autoimmune encephalomyelitis (EAE) mouse model (120). Therefore, in some neurodegenerative disease where neuroinflammation plays a crucial role, increase of KYNA (with subsequent decrease of glutamate on the inflammatory site) could exacerbate inflammation and synaptic pathology.

KYNA is also the endogenous ligand of the G-protein coupled receptor 35 (GPR35). By activating GPR35 in astrocytes, KYNA has been found to modulate Ca^{2+} fluxes affecting the release of synaptic transmitters, with an overall effect of decreasing excitatory synaptic currents in neuronal circuits (121). This finding further potentiates its neuroprotective role, especially under excitotoxic conditions. GPR35 is also expressed in immune cells and the gastrointestinal tract. Moreover, Wang et al demonstrated that its activation with KYNA modulates the immune response of these cells (122). However, further characterization of GPR35 function and localization is needed to attribute new physiological activities of KYNA. Another described target of KYNA in the periphery is AhR. Activation of AhR by KYNA in inflammatory conditions can increase IL-6 production with the same pattern as dioxin (123). Activation of GPR35 and AhR, as well as expression of glutamate receptors in immune cells, points towards a possible role of KYNA in immune regulation.

Finally KYNA also has antioxidant properties, as it can scavenge hydroxyl, superoxide anion and other free radicals (124).

Table 1.1: Physiological activity of KP metabolites

	GLUTAMINERGIC TRANSMISSION	INFLAMMATION	OXIDATIVE STRESS
KYN		Ligand of **AhR**	Antioxidant
KYNA	Antagonist of **NMDAR**, **AMPAR** Antagonist of **nAChRs**	Ligand of **GPR35** Ligand of **AhR**	Antioxidant
QUIN	Activates **glutamate release** Inhibition of **glutamate up take** **NMDAR** agonist	Induces CNS **inflammation**	Induce **NO** and **SO^{2-}** Form complexes with **Zn**, **Fe** and **Cu**
3-HK			Induces **ROS** production Redox homeostasis at low concentrations
3-HAA		**T reg** differentiation Induces **HO-1** Apoptosis effector T cells	Antioxidant
AA		Inhibit Th1 and Th17 **Tolerance**	
PIC			**Metal chelator**
XA	**mGlu2R** and **mGlu3R** agonist **VGLUT** inhibitor		
CA		Agonist **mGlu4R**	

1.2.3 Quinolinic acid

Quinolinic acid (QUIN) is one of the downstream products of the KMO branch and is the reason why this branch is named "neurotoxic". QUIN is an excitotoxin due to its selective stimulation of NMDAR, which is primarily expressed in neuronal cells (125). However, QUIN has more affinity for some NMDAR subunits, making its excitotoxic properties selective for the subgroup containing NR2A and NR2B subunits. As these subunits are more concentrated in some regions of the brain (for example NR2B in the forebrain), QUIN mainly affects these same areas (126). QUIN can potentiate its own toxicity and that from other excitatory amino acids under energy deprived conditions (127). In addition, QUIN contributes to excessive microenvironment glutamate concentrations by stimulation of synaptosomal glutamate release by

neurons (128) and inhibition of astrocytic glutamate up take from the synapsis and glutamate to glutamine recycling by inhibiting glutamine synthase (129). QUIN has also been shown to increase the reactive oxygen species (ROS) nitric oxide and superoxide by NMDAR-dependent Ca^{2+} entry (130). This induces NOS and reduces SOD activity (131). QUIN has also been show to interact with some metals, increasing oxidative damage. It reduces copper and zinc-dependent SOD activity and forms complexes with Fe2+, which induce hydroxyl radical formation. It is also responsible for lipid peroxidation (132, 133), DNA damage, activation of poly (ADP-ribose) polymerase (PARP) and NAD+ depletion (134). Activated astrocytes and microglia become associated with damaged neurons and QUIN can induce an inflammatory cascade in those cells. It has been demonstrated that QUIN induces astrogliosis by NMDA activation (135) and local inflammation by inducing cytokine and chemokine production, particularly monocytic chemoattractant-1 (MCP-1), IL-8, C-X-C chemokine receptor (CXCR)-4, C-C chemokine receptor (CCR)-5 and IL-1β by astrocytes and monocytic lineage (136, 137). MCP-1 production by astrocytes is highly activated by QUIN, which leads to further recruitment of monocytic lineage cells and activation of the inflammatory cascade (138).

Additional neurotoxic activity by QUIN includes induction of astrocytic and neuronal apoptosis by a caspase-3-dependent mechanism and a decrease of neuronal and astrocytic autophagy (Reviewed in (139)).

Conversely, QUIN activity can be protective in the periphery, where it has a role in maintaining peripheral tolerance by inducing selective thymocyte and Th1 cell death, but not Th2 (140). Additionally, it can confer tolerogenic properties to DCs (141). QUIN cannot cross the BBB, so changes in the periphery are unlikely to increase its neurotoxic activity (104).

1.2.4 3-Hydroxykynurenine, 3-Hydroxyanthranilic acid and Anthranilic acid

Electrophysiological studies of 3-HK, 3-HAA and AA have shown no direct effects of these metabolites on neuronal activity (142). They primarily behave as pro- and anti-oxidants in the brain.

3-HK is the first downstream product of the KMO branch. It has been described as a powerful generator of ROS and a potentially endogenous neurotoxin. Studies in neuronal cultures *in vitro* showed that 3-HK induces ROS-dependent apoptosis of neurons through H_2O_2 production, as oxidative stress can be suppressed by addition of Catalase but not SOD (143). 3-HK-mediated H_2O_2 generation can be a consequence of autoxidation (144) or activation of neuronal xanthine oxidase, which catalyses xanthine or hypoxanthine oxidation, thereby generating H2O2 (145). On the other hand, Wang et al observed that the source of ROS induced by 3-HK in endothelial cells is superoxide, as this was reduced by SOD. In this study, 3-HK increased the activity of nicotinamide adenine dinucleotide phosphate [NAD(P)H] oxidase, which is involved in the innate immune response by generating superoxide products against pathogens (146). In both cases, the final result is high ROS production, which involves the uptake of 3-HK by sodium-dependent neutral amino acid transporters (147).

Other studies show that 3-HK may induce toxicity via downstream mechanisms of ROS, and that cellular uptake is not needed (144). However, larger amounts of 3-HK are required to generate pathological extracellular levels of ROS. It has been proposed that 3-HK mediated toxicity involves pathological calcium release from the endoplasmic reticulum (ER), likely through ROS-mediated inhibition of Ca^{2+} -ATPase in the ER. This would lead to increased cytosolic Ca^{2+} levels, which are then taken up by mitochondria, causing a collapse of the mitochondrial membrane potential (144).

Nevertheless, it is important to note that 3-HK pro-oxidant activity has only been shown at non-physiological concentrations. At physiological or pathological concentrations 3-HK seems to be responsible for maintaining cellular redox homeostasis. It can prevent oxidative damage from O_2^-, OH and NO through its scavenging activity. Furthermore, both 3-HK and 3-HAAO can inhibit spontaneous lipid peroxidation in supernatants from cerebral cortex rats (148). More evidence regarding the 3-HK concentration-dependent activity has been provided using human primary astrocytes and neurons, where lower concentrations of 3-HK increase NAD^+, but high concentrations have opposite effect (149). However, when evaluating 3-HK neurotoxic activity *in vivo*, it should be considered that 3-HK and QUIN can synergistically induce NMDAR activation and ROS production, thus reducing the pathological concentrations of QUIN and 3-HK (150).

An additional activity of 3-HK is the amelioration of clinical symptoms in allergic airway inflammation (151) and in chronic Chagas disease (152), thus suggesting a possible role in immunoregulation.

3-HK can cross the BBB through the large neutral amino acid carrier (the same way as KYN); therefore, an increase of this metabolite in the periphery will be reflected in the CNS (104). Some studies propose that, once in the brain, 3-HK is sequestered and degraded into the neurotoxic QUIN (153). A recent review describes in detail the properties and biological activities of 3-HK (154).

3-HAA can be produced from AA by a non-specific hydroxylation, but also from 3-HK through KYNU. 3-HAA has a similar structure to 3-HK and shares its ROS-inducing and antioxidant properties (148, 155). As an antioxidant, it can inhibit low-density lipoprotein (LDL) oxidation (156). However, the most relevant role of 3-HAA is in inflammation, where it regulates the inflammatory response to tolerance. It has pro-apoptotic activity in activated T cells (157) with specificity for Th1 (140). It inhibits antigen specific proliferation in an early phase of lymphocytes (158) and it converts naïve T cells into $Foxp3^+$ Treg (108). Moreover, it induces TGF-β expression in DCs, which in turn promotes Treg formation (61). Of more relevance in the CNS, 3-HAA has been shown to suppress glial inflammatory cytokine and chemokine production by inducing the expression of HO-1 (159).

3-HAA does not readily cross the BBB, therefore it must be locally produced to be active in the brain (104).

AA is synthetised from KYN by KYNU through an alternative arm of the KP. AA also has immunomodulatory activity by interacting with copper and forming anti-inflammatory complexes that remove the hydroxyl radicals from the inflammatory site (160). However, its regulatory properties have been further studied using its synthetic derivate N-(3,4-dimethoxycinnamonyl) anthranilic acid (Tranilast). This drug has been found to inhibit the activation of myelin-specific Th1 and Th17 cells in EAE mice model (161), attenuate inflammation in collagen-induced arthritis (162) and it is approved in the U.S. for treatment of allergic rhinitis, atopic dermatitis and some forms of asthma (163).

AA can cross the BBB through passive diffusion at a significant rate; however, its transfer appears to be limited by plasma protein binding (104).

1.2.5 Picolinic acid

Picolinic acid (PIC) is a downstream product of 3-HAA. The enzyme implicated in its production is amino-ß-carboxymuconate-semialdehyde decarboxylase (ACMSD). At high concentrations PIC can have antiviral and anti-microbial activity (164, 165). Studies show that PIC also exhibits neuroprotective activity through its metal chelator properties, reducing the neurotoxic effect of QUIN-Fe^{2+} complexes (Reviewed at (166)). Additionally, *in vitro* studies suggest that PIC can influence the immune response by enhancing IFN-γ mediated NOS expression and induction of the macrophage inflammatory proteins (MIP)-1α and 1β in macrophages (167).

1.2.6 Nicotinamide Adenine Dinucleotide

Nicotinamide adenine dinucleotide (NAD^+) is the final product of the KP. Quinolinic acid phosphoribosyl transferase (QPRT) converts QUIN to nicotinic acid adenine ribonucleotide, which is further metabolised to NAD^+. NAD^+ has been identified as an essential cofactor for several enzyme-catalysed oxidative reactions. It also serves as an electron transporter in the mitochondrial electron transport system to produce ATP, and plays a key role in glutathione metabolism and the NADPH-dependant thioredoxin system. These activities are all involved in antioxidant defence and detoxification. Further implications include DNA repair, gene silencing and cellular energy sensing (Reviewed in (168)). Promotion of NAD^+ synthesis may be of interest in oxidative stress conditions, where NAD^+ is depleted, in order to maintain mitochondrial function and neuronal energy supply.

1.2.7 New players of the KP: Cinnabarinic acid, Xanturenic acid and Quinaldic acid

Xanturenic acid (XA) is a metabolite of the 3-HK via the intermediate 4-(2-amino-3-hydroxyphenyl) 2,4– dioxobutanoate through the action of KAT-1 and -2. It has been identified, *in vitro* and *in vivo,* as an allosteric agonist of endogenous Group II (mGlu2 and mGlu3) metabotropic GluR, which is predominantly distributed in the presynaptic region, consistent with its role as inhibitory receptor (169). Group II mGluRs play a role in the pathogenesis of schizophrenia and some of its agonists are a

potential new class of antipsychotics (170). In addition, XA has also been reported to be a vesicular glutamate transporter (VGLUT) inhibitor, which is important in the uptake of glutamate into vesicles in the presynaptic terminal (171). Either by activating mGluR2/3 or by blocking VGLUT, the final effect of XA is sensory inhibition of the glutamatergic transmission with reduction of excitatory postsynaptic potentials. Therefore, XA dysregulation should be taken into consideration in the pathophysiology of neurological and psychiatric disorders (172).

Cinnabarinic acid (CA) is a metabolite of the 3-HAA. In neurons, it can partially activate type 4 metabotropic GluR-4 and non-identified off-target pathways, providing neuroprotection against excitotoxic stimuli (173). Moreover, mGlu4 receptors are also expressed in peripheral cells and their activation in dendritic cells drive naïve T cells to Treg (120). In accordance, a recent study found that activation of mGlu4 receptor by CA confers full protection against EAE by boosting a tolerogenic immune response (174). However, CA protection against EAE does not fully account for mGlu4 receptor activation; therefore, new targets for CA with implications in immune response are yet to be elucidated.

Quinaldic acid (QA) is formed by the de-hydroxylation of KYNA (Figure 1.5); nevertheless, the enzyme catalysing the reaction is unknown. Few studies have investigated QA and its physiological function remains highly unknown. Our group has observed alterations of QA in CSF and serum in different pathologies. Moreover, it can be produced by human primary neurons and affect their susceptibility towards a neurotoxic challenge (Lee J.M., et al., unpublished data). These findings indicate that QA may have an effect on neuronal activity.

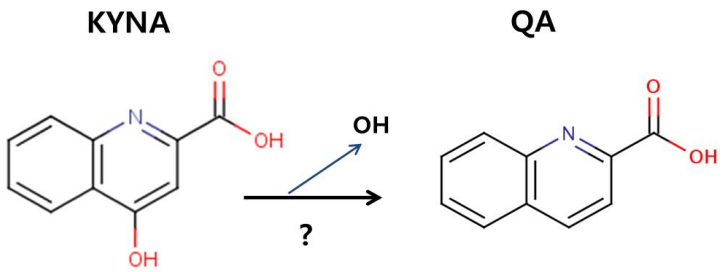

Figure 1.5: Proposed reaction for QA production

QA is formed by the de-hydroxylation of KYNA. However, the enzyme mediating this process remains to be elucidated.

1.3 Aryl hydrocarbon receptor. Target for KP metabolites

AhR (Aryl hydrocarbon receptor) is a ligand-operated transcription factor, which belongs to the basic helix-loop-helix (bHLH) Per-ARNT-Sim (PAS) superfamily that can be activated by a broad array of synthetic and natural ligands. It was initially described as the receptor mediating the toxicological effects of dioxins and other pollutants. However, the immune and liver defects observed in AhR deficient mice suggested that AhR has a physiological role and also reveals that endogenous AhR ligands may be involved on its activity (175, 176). Several dietary compounds, endogenous metabolites and products of the commensal microbiota have been shown to activate AhR signalling (177) and the type of signalling is ligand-specific (178). In Table 1.2, we summarize some of those ligands and their AhR-mediated activity. Ligands of our interest are the group of tryptophan metabolites, especially products of the KP (KYN, KYNA and XA) (10, 11, 123, 179). But additional indoles derivates of TRP have also shown to activate AhR (111, 180, 181). Additionally, potential new AhR ligands will be elucidated soon.

Table 1.2: AhR ligands and AhR-mediated activity

Family	Molecules	Endogenous source	AhR-mediated physiological activity
Tryptophan metabolites	L-kynurenine	Kynurenine pathway	Suppresses cellular and humoral immune response and mediates primary endotoxemia resistance (10, 11).
	Xanthurenic acid	Kynurenine pathway	Not described (123).
	Kynurenic acid	Kynurenine pathway	Induces production of inflammatory cytokines (IL-6) (123).
	Triptamine	Triptophan metabolism	Weak activation. Only relevant in pathological conditions (179).
	ITE	Lung tissue (mucosal)	In DCs promote the differentiation of FoxP3$^+$ Treg in a RA-dependent manner (111).
	FICZ	UV-B photo derivate	Local activation of AhR in the skin after ultraviolet-B exposure mediates cellular response to UV-oxidative stress (180).
	IALD	Anaerobic intestinal bacteria (ex. lactobacilli)	In the gastrointestinal tract, promotes local IL-22 production by innate lymphoid cells, promoting antifungal resistance (181).
Heme-derived molecules	Biliverdin Bilirubin	Heme metabolism	Effects in liver or spleen (heme rich organs), activating canonical AhR signal transduction, with detoxification purposes (177).
Arachidonic acid metabolites	Prostaglandins Leukotriens	CYP1A1 and COX2 metabolism of arachidonic acid	Inflammatory responses after xenobiotic activation of AhR. This induces CYP1A1 and COX-2 expression and synthesis of the inflammatory arachidonic acid metabolites. Those amplifying AhR response (182).

ITE: 2-(1'Hindole-3'-carbonyl)-thiazole-4-carboxylic acid methyl ester
FICZ: 6-formylindolo[3,2-b]carbazole
IALD: Indole-3-aldehyde

1.3.1 Aryl Hydrocarbon Receptor activation

When inactive, AhR is located in the cytoplasm as part of a chaperone protein complex that includes the 90-kDa heat shock protein (HSP90), the c-src protein kinase and the AhR interacting protein Ara9 (also known as AIP1 or XAP-2) (183). It has been reported that specific ligands can trigger different AhR-mediated activities (178). The interaction of AhR with its specific ligands can lead to two different responses: genomic and non-genomic. Additionally, cell-dependent AhR protein interactions will also influence the final response (Figure 1.6).

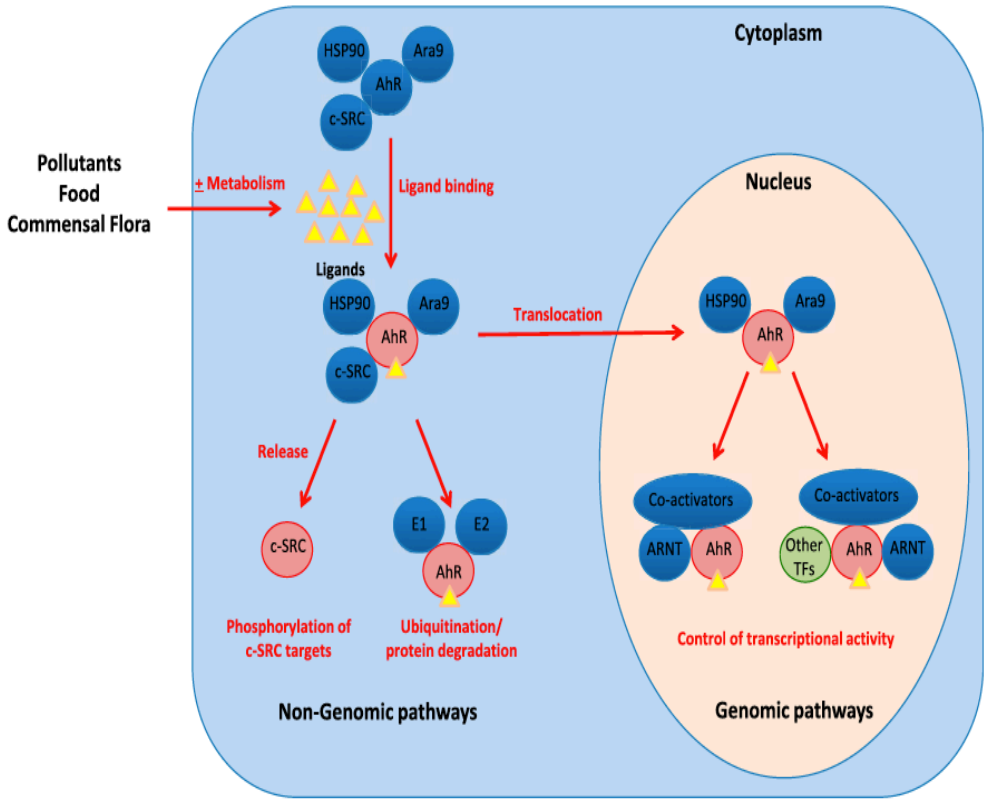

Figure 1.6: AhR activation can affect genomic and non-genomic pathways

Figure from Quintana et al. (184)

Genomic pathway

The interaction of AhR with its ligand allows its translocation to the nucleus, where AhR form a heterodimer with the AhR nuclear translocator (ARNT) and/or other transcription factors (183). The AhR:ARNT heterodimer interacts with a specific DNA sequence motif referred as canonical AhR binding site, Aryl hydrocarbon response element (AHRE) or Dioxin response element (DRE). This modulates the expression of detoxifying enzymes such as cytochrome P450 family. However, once bound to DNA, recruitment of different co-regulator proteins can result in variations of target gene expression (185).

Additionally, AhR can act via non-canonical AhR responsive sites (non-AHRE) as a dimer with ARNT. This phenomenon is mediated by ligand-specific mechanisms that result in altered DNA-binding specificity and/or recruitment of different co-activators. Moreover, overlapping binding profiles of ligand-activated AhR and ARNT, suggest that AhR can bind to non-AHRE DNA regions without requiring ARNT (186) and by interacting with other transcription factors. Additional mechanisms for AhR

activity include competition for co-factors with other transcription factors or receptors (187). Overall, AhR has shown to cross-talk or interact with several transcription factors, such as early growth response 1 (EGR-1), activator protein family (AP-1, AP-2), estrogen receptor, HIF, NRF2 (186) RelA and RelB (188) and various intracellular signalling pathways, including protein kinases, receptor tyrosine kinases, MAPK, c-src kinase, phosphodiesterase 2A, NF-κB signalling, and others; altogether leading to a wide range of transcription profiles (178) (Figure 1.7),

Differences on co-regulator proteins and co-factors among cell types will lead to cell-specific gene expression in response to AhR (described in more details below). The best-known interactions of AhR are with the nuclear hormone receptor signalling, mainly with estrogen receptor and with the cell cycle signalling pathways (for better description see review (189)). AhR can also interact with the NF-κB pathway, this, of particular interest in inflammatory responses. NF-κB includes five different transcription factors RelA (p65), RelB, c-Rel, p50 and p52, which are inactive when bound to their inhibitory IκB subunits. Once released from IκB subunits, the transcription factors forms homo-or hetero-dimers and translocates to the nuclei regulating target gene expression (190). Several points of interaction between AhR and NF-κB have been described.

Activation of the NF-κB under LPS inflammatory stimuli induces RelA-dependent activation of AhR expression and activity (191). Besides LPS, additional inflammatory insults have also shown to promote AhR expression, those including CD40 and CpG (192). Interestingly, AhR can directly interact with Rel A to form a transcriptionally inactive AhR:RelA dimer, which repress canonical NF-κB activation (193). This has been proposed as a mechanism that controls inflammatory response.

AhR can also interact with RelB, producing a AhR:RelB complex, which, in this case, can bind to a DNA recognition site and stimulate interleukine-8 transcription (188). Besides IL-8, other RelB:AhR responsive elements have been found in targets of the non-canonical NF- κB pathway, such as B-cell activating factor of the tumor necrosis factor family (BAFF), CC-chemokine ligand (CCL)-1 and the transcription factor IFR3 (194). Overall, AhR seems to have trans-repressive activity in the canonical NF-κB signalling.

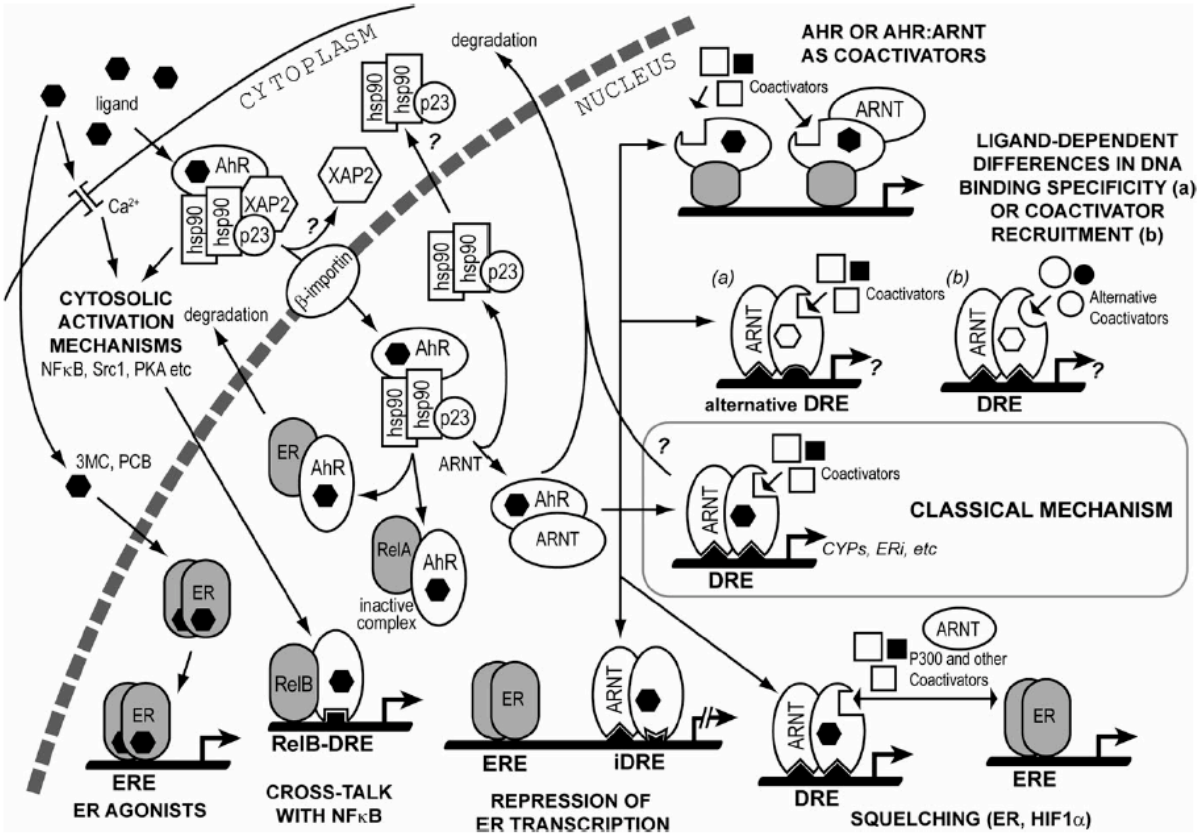

Figure 1.7: Mechanisms of action of the AhR and AhR ligands.

The AhR has been observed to bind to alternative DRE elements as a dimer with either ARNT or other transcription factors resulting in activation (i.e., with RelB) or repression (with ARNT at iDREs) of transcription. Ligand specific mechanisms have been described that result in altered AhR:ARNT DNA-binding specificity and/or recruitment of alternative co-activators. Independently of AhR binding to DNA, AhR (or AhR:ARNT) may act as a co-activator, and it may sequester other transcription factors (RelA) and/or target them for degradation. Additional mechanisms include AhR-dependent competition for ARNT or co-activators used by other transcription factors and receptors, resulting in squelching of their dependent transcription. Figure from Denison et al. (189).

Non-genomic pathway

In addition to its activity as a transcription factor, AhR can control different cellular processes through non-genomic signalling.

AhR has been shown to control the proteasome-dependent degradation of specific transcription factors. The *proteasome* system catalyses the degradation of ubiquitinylated proteins. Ubiquitin is covalently attached to target proteins through a series of reactions catalysed by ubiquitin activating enzyme (E1), ubiquitin conjugating enzyme (E2) and ubiquitin protein ligase (E3). E3 controls the specificity

of the ubiquitinylation reaction (195). AhR is a ligand dependent E3 ubiquitin ligase involved in the degradation of AhR interacting proteins as the estrogen receptor or androgen receptor (196). AhR is also involved in maintaining RelB expression (197) and lack of AhR results in accelerated degradation of RelB (198). Opposite to other NF-κB transcription factors basal polyubiquitinylation of RelB is not linked with its proteolysis. Not only that, but its polyubiquitinylation increases its transactivational potential, independently of the IKK complex (199). The ubiquitin E3 ligases involved in RelB polyubiquitinylation have not been identified. However, taking into account that (1) absence of AhR leads to accelerated RelB degradation (198) and (2) that AhR is a E3 ubiquitin ligase, AhR could be an E3 ubiquitin ligase for RelB.

Another AhR non-genomic activity involves c-src activation. Ligand-binding to AhR releases the c-src from the AhR/HSP90/c-src complex enabling c-src to then phosphorylate and activate different cellular targets (200). *Src kinase* is ubiquitously expressed and needs to be phosphorylated in order to be active. Because of its role in cell differentiation, proliferation, survival, cell adhesion, cell morphology, and motility, its activation is tightly regulated (201). While forming a complex with AhR, c-src remains inactive, but ligand activation of AhR induces c-src phosphorylation and activity (202). Therefore, AhR is necessary to maintain c-src inactive, but ligand-mediated AhR activation can induce c-src cascade. Release and auto-phosphorylation of c-src after AhR activation has been shown to phosphorylate IDO-1 (11). IDO-1 phosphorylation confers non-enzymatic properties to IDO-1. Once IDO-1 is phosphorylated, it can activate the non-canonical NF-κB pathway and induce TGF-β production (59). In addition, c-src can further participate in the TGF-β pathway through its interaction with the endopeptidase furin (203). Activation of furin is dependent of c-src, and this may have a potential role in the regulation of furin-mediated maturation of its substrates (204). TGF-β is synthesised as precursor polypeptide, which dimerises and needs to be proteolytically cleaved by furin prior to be secreted as a latent (inactive) TGF-β (205). c- src, together with other kinases, is also involved in the non-canonical Smad-TGF-β signalling, which involves the phosphorylation of the Smad linker region. This process can regulate the stability and transcriptional activity of Smads and is differently regulated depending on the type of kinase involved (206).

Cell-dependent AhR activation

AhR function has been mainly studied in immune cells. Its function can vary depending on the cell type. In regulatory T cells ($Foxp3^+/CD4^+$), AhR participates in both, the induction of Treg-specific genes (such as FoxP3 and SMAD1) (207) and the inhibition of genes associated with effector T cell function (such as IL-2) (208). AhR is also necessary for the differentiation of type 1 regulatory T cells (Tr1) ($CD4^+$/ Foxp3- / $IL\text{-}10^+$). It is functionally linked to several of the transcription factors reported to participate in Tr1 differentiation. AhR can physically interact with c-maf to cooperatively trans activate the IL-10 and IL-21 promoter (209) and IL-21 can further promote IL-10 production (184). In addition, AhR could also interact with the transcription factor STAT3 and favour the transcriptional activity of IL-10 promoter (184). In Th17 cells ($RORgammaT^+/CD4^+$) AhR increases the production of IL-21 and IL-22 (210). However, on those cells AhR does not directly activate the IL-17 promoter, but regulates the inhibitory effects of IL-2 on early stages of Th17 differentiation (211). AhR can supress the IL-2- mediated STAT5 activation (210) and also the TGF-β plus IL-6-mediated STAT1 activation (212). Both STATs inhibit Th17 differentiation. Further involvement of AhR in T cell activation is through its activity in dendritic cells (DCs). DCs play a central role in the control of T cell polarisation i*n vivo* and AhR can control the differentiation and function of DCs. Therefore AhR plays a direct and indirect role in T cell activation. AhR activation in DCs decreases the expression of class II major histocompatibility complex and co-stimulatory molecules as well as the production of Th1 and Th17 polarizing cytokines (58). In addition, AhR has shown to up regulate IDO-1 expression in DCs (58), resulting in an increase of kynurenines production. Activation of the KP in DC mediates immunosuppression by (1) tryptophan starvation–mediated T cell apoptosis and (2) kynurenines production inducing Tregs differentiation (111, 213). Recently, KYN was described as an endogenous ligand for AhR (11) creating a positive feedback loop.

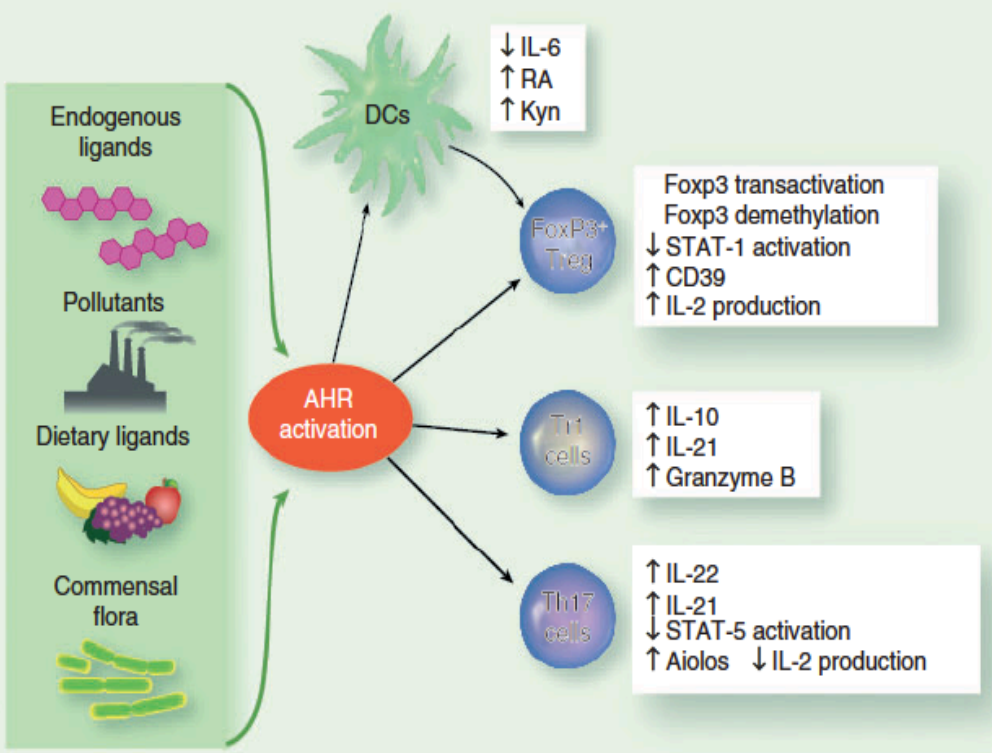

Figure 1.8: AhR activity is ligand and cell dependent

Activation of AhR induces different pathways depending on the T cell subset. Figure from Quintana et al. (214).

In contrast with the immune system, AhR role in the brain has not been extensively explored. However, AhR has shown to be expressed in neurons, astrocytes and probably resident microglia (if it is acceptable to compare them with monocytes as they both come from monocyte lineage).

In neurons, AhR have shown to play an important role in NMDA-mediated excitotoxicity. AhR can bind to the NR2A gene promoter inducing NMDA expression and activity (215). In addition, abnormal AhR activity by xenobiotic molecules or genetic depletion leads to impaired neurogenesis and cognitive function. This suggests that AhR can have functional implications in neuronal development, as well as, that activation with toxic ligands can affect its physiological role (216). Additional roles of AhR, include regulation of the circadian rhythm (217) and definition of the cell fate of GABAergic neurons (218).

AhR has also been shown to be expressed and active in mice foetal **astrocytes** (219). However, studies of its activity have only been done in glioblastoma cell lines, which

could differ considerably from primary astrocytes. The effects of the AhR agonist β-naphtoflavone (β-NF) have been studied in C6 cell line, a glioblastoma cell line used to study astrocyte differentiation mechanisms upon stimulation with cyclic AMP (cAMP). cAMP-mediated activation of protein kinase A (PKA) increases IL-6 secretion, which activates STAT3 translocation to the glial fibrillary acidic protein (GFAP) promoter and subsequently astrocyte differentiation (220). β-NF, probably through AhR activation, decreases cAMP induced IL-6 production (221). This could decrease astrocyte differentiation and astrogliosis, both processes related with IL-6 activity in astrocytes. In glioma cells, AhR has shown to mediate their malignant phenotype (10). Constitutive AhR is necessary for TGF- β production and its inhibition decrease both TGF- β production and signalling (222). The malignant phenotype of glioblastoma is dependent on TGF- β, indicating that AhR activation of those cells promotes proliferation, clonogenicity and invasiveness. However, in astrocyte cell line AhR has opposite function and its constitutive expression is necessary for negative control of TGF- β pathway (222). Therefore, abnormalities in AhR function in astrocytes would increase TGF- β signalling and its effects related with astroglial scar formation and fibrosis (223).

In macrophages (and maybe relevant for monocyte CNS infiltrate), AhR is necessary to negatively regulate inflammatory response. Some of its effects include interaction with STAT-1 with the consequent blockage of IL-6 promoter (224, 225) and inhibition of NLRP3 inflammasome under LPS activation (226).

1.4 Implication of the KP in neurodegenerative diseases

There is increasing evidence of altered KP metabolites in different neurological pathologies, showing a positive correlation between imbalance towards the KMO branch, excitotoxicity and oxidative stress. Table 1.3 summarise abnormalities of the KP found in some neurodegenerative diseases.

Table 1.3: KP alterations in different neurodegenerative diseases

Adapted from Vecsei et al. (3).

↑Glut ↑↑Mito ↑	Huntington's Disease
	- ↑ **IDO** activity in serum - ↓ **KYNA** levels in cortex, striatum and CSF - ↓ **KAT** activity in striatum - ↑ **3-HAO** activity in the brain - ↑ **3-HK** and **QUIN** levels in the brain - ↑ **KMO** and decreased **KYNU** activity in transgenic mice
↑Glut ↑↑Mito	Alzheimer's Disease
	- ↑ **IDO** activity in serum correlating with reduced cognitive performance - ↑ **KYNA** levels in hippocampus and striatum - ↑ **KAT** activity in striatum - ↓ **KYNA** in blood and CSF - ↑ **IDO** expression in regions with senile plaque formation - **QUIN** co-localisation with phosphorylated tau in the cortex and with senile plaques in hippocampus
Glut ↑↑Mito	Parkinson's Disease
	- ↑ **IDO** activity in serum and CSF correlating with disease severity - ↓ **KYNA** levels in the SNpc, frontal cortex and putamen - ↑ **3-HK** levels in SNpc and putamen - ↓ **KAT** activity in substantia nigra of MPP^+ treated mice
Glut Mito	Amyotrophic lateral sclerosis
	- ↑ **IDO** activity in serum and CSF - ↑ microglial and neuronal **IDO** expression in motor cortex and spinal cord - ↑ **KYNA** levels in CSF - ↓ **KYNA** levels in serum of patients with severe clinical status - ↑ **QUIN** levels in CSF
↑↑Immune	Multiple sclerosis
	- ↑ **IDO** activity in plasma and CSF - ↑ **KYNA** levels in CSF during acute relapse - ↓ **KYNA** levels in CSF during chronic remission - ↑ **3-HK** and **QUIN** levels in spinal cord of EAE mice

Neurotoxic insult characteristic from each disease:
Glut: glutamate excitotoxicity
Mito: mitochondria impairment
Immune: inflammation

1.4.1 Huntington Disease

Huntington Disease (HD) is a fatal inherited neurodegenerative disorder characterised by the progressive loss of neurons in the striatum and cortex affecting motor movements, personality and cognition (227). HD shows closer associations with metabolic KP disturbances within the brain compared to other neurodegenerative disorders due to excitotoxicity playing a central role in its pathogenesis. Neurotoxic effects of the mutant protein Huntingtin, can be further

potentiated when there is imbalance of glutamate homeostasis. Therefore, alterations of some of the endogenous NMDA agonists or antagonist through the KP could have an important role in its pathology. The first observation was a study showing that intra-striatal administration of quinolinic acid evokes HD-like pathology (228). Levels of 3-HK and QUIN are increased in the neostriatum and cortex of early stage HD patients (229). Recent studies showed increased KMO activity and lower Kynureninase in the brain of HD transgenic mice model (230). Exacerbating these effects, KAT activity and KYNA levels are significantly reduced in the striatum and cortex of HD patients (231). In addition, studies in yeast show higher toxicity by the mutant huntingtin protein when KAT was ablated whereas improvement when there is lack of KMO (232). Collectively, these findings support the hypothesis that the increased flux through the central neurotoxic branch of the KP may play an important role in HD pathology.

1.4.2 Alzheimer's Disease

Alzheimer's Disease (AD) is a progressive neurodegenerative disorder characterised by the accumulation of senile plaques in the brain consisting of misfolded β-Amyloid peptides (Aβ) and neurofibrillary tangles composed of phosphorylated tau aggregates (233).

Many studies have demonstrated that KP is directly or indirectly involved in AD. The most relevant evidence comes from observations of increased QUIN and IDO immunoreactivity in the hipocampus of AD brain sections (63). Interestingly, QUIN is remarkably increased in the surroundings of Aβ plaques and neurofibrilary tangles (63, 234). The involvement of QUIN in these pathological hallmarks has been further studied *in vitro*. $A\beta_{1-42}$, in both monomeric and aggregated forms, leads to significantly increased IDO activity and production of QUIN in human primary microglia and macrophages (138). Considering that amyloid plaques, which are closely associated with blood vessels, are surrounded by activated microglia and infiltrating macrophages (235), these cells could be responsible for the increased levels of QUIN in AD brain sections. Moreover, QUIN induces tau hyperphosphorylation in human primary neurons (236), which supports observations by Guillemin et al of QUIN co-localization with the neurofibrillary tangles (234). Therefore, it has been proposed that Aβ plaques induce QUIN production by microglia and infiltrate macrophages. Furthermore, the increase of

QUIN promotes tau hyperphosphorylation and neurofibrillary tangles (63, 234). QUIN can also potentiate neurotoxicity by promoting further oxidative stress, excitotoxicity, astrocyte activation and apoptosis (237).

Looking at the neuroprotective branch of the KP, KYNA concentrations in CSF and serum samples from AD patients are lower (238). However, elevated concentrations of KYNA have only been shown in caudate nucleus and putamen of AD patients, accompanied by increased KAT-1 activity (239). This indicates that KYNA-mediated excessive NMDA inhibition in these regions may be responsible for impaired memory, learning and cognition in AD patients. In addition, KYNA can non-competitively inhibit α-7 nicotinic acetylcholine receptors, which have a role in amyloid beta clearance in early stages of AD (240). Therefore, the lower KYNA levels in the CSF could shift the imbalance towards excitatory activity of increased QUIN or glutamate, but pathological KYNA concentrations in some regions of the brain could participate in the cognitive impairment of AD patients.

Finally, AD pathology is also associated with an increase of tryptophan catabolism by IDO activation in serum, which leads to a deficit of TRP in the brain. TRP is an essential amino acid and its content in the brain must be maintained in order to synthesize nerve growth factor (NGF) and brain derived neurotrophic factor (BDNF) (241). Low levels of these factors may impact AD pathology. TRP is also necessary for serotonin synthesis. Low levels of serotonin in the brain are associated with sleep disorders observed in AD patients (242).

1.4.3 Parkinson's Disease

Parkinson's Disease (PD) is a chronic progressive neurodegenerative disorder characterised by a loss of dopaminergic neurons in the midbrain and the presence of protein inclusions called Lewy bodies (243). Impaired KP metabolism has been reported in the brains of PD patients and in mouse models. Similar to AD and HD, IDO activity in the serum of PD patients is significantly increased, pointing to immune involvement (IDO activation) in the neurological disorder. Also, higher 3-HK levels and lower KYNA concentrations have been detected in the putamen, frontal cortex and substantia nigra of PD patients (244). While KAT-1 expression is decreased in the substantia nigra of MPTP treated mice (245), increased KAT-2 activity has been found in peripheral red blood cells of PD patients (243) associated with higher blood KYNA concentrations. However, as KYNA has limited abilities to cross the BBB (104), its concentration in the CNS remains lower. Imbalance towards the KMO branch of the

KP observed in the CNS of PD patients (high 3-HK and low KYNA), could potentiate excitotoxicity in the dopaminergic neurons. Indeed, it has been observed that activated microglial cells and $NMDAR^+$ dopaminergic neurons are increased in the substantia nigra of PD patients. This suggests that the NMDA receptor is likely to be activated by QUIN released by microglia (246) but the lower levels of KYNA would not counteract QUIN excitotoxicity. Accordingly, KYNA has shown to be neuroprotective in PD. This has been demonstrated by preclinical and clinical data (86) and in a PD mouse model, where KYNA exhibited partial protection against MPP^+ toxin on dopaminergic terminals of rat striatum (247). Since the highly selective NMDA antagonist, 7-chlorokynurenic acid, does not exert the same neuroprotective effects as KYNA, additional targets could account for its neuroprotection (86).

1.4.4 Amyotrophic Lateral Sclerosis

Amyotrophic Lateral Sclerosis (ALS) is a progressive neurodegenerative disease affecting motor neurons. There are a few studies that provide evidence of a link between tryptophan metabolism and ALS, and also involve SOD-1 . Aggregation of mutant SOD-1 is one of the causes of familial ALS. However, SOD-1 aggregation, in the non-familial ALS cases, can be reproduced by oxidation of the only aromatic residue found on the surface of SOD-1 protein, Trp-32, to KYN (248). The first enzyme of the KP - IDO1 - can catalyse this oxidation. Moreover, QUIN markedly increases SOD-1 expression (249), which may amplify SOD-1 pathology in ALS. A study of KP metabolites in patients with ALS with severe clinical status showed higher KYNA levels in CSF compared with controls; however, serum KYNA levels were lower (250). These results are in discordance with the protective role of KYNA in the CNS, but could be related to impaired degradation of KYNA and the subsequent decrease of KP metabolites, such as quinaldic acid. In fact, our group observed lower quinaldic acid in CSF of patients with ALS (Lee J.M., et al., unpublished data). Further findings by our group have shown elevated levels of QUIN and IDO activity in serum and CSF of ALS patients. This increase is also observed in brain and spinal cord tissue, and is attributed to microglia activation, which could potentiate neurotoxicity (66).

1.4.5 Multiple Sclerosis

Multiple sclerosis (MS) is a chronic, demyelinating autoimmune disease of the CNS characterised by the presence of peripheral immune cells within the sites of demyelination (251). TRP was the first metabolite found to be reduced in plasma and CSF of MS patients (252), indicating activation of the KP. The first enzyme of the KP, IDO-1 acts an endogenous negative regulator of the immune system to counteract inflammation (11). Moreover, its inhibition or activation can exacerbate (61, 62) the pathology of MS. Taking into account that MS pathology is a consequence of an imbalance in the immune system towards autoimmunity or inflammation, activation of IDO may be a concomitant self-protective response in MS. Although the net effect of IDO activation is thought to be beneficial in MS, its activation leads to an imbalance of KP neuroactive metabolites (253). Changes in other KP metabolites seem to be related to the progression of the disease. KYNA is significantly decreased in CSF of MS patients during chronic remission, but elevated in the CSF and plasma of MS patients undergoing acute clinical relapse (254). Therefore, the strong activation of KP during the acute phase leads to increased KYNA production. As the disease progress, the KP shifts towards the neurotoxic branch, decreasing KYNA production and increasing QUIN and 3-HK. Accordingly, QUIN and 3HK are higher in the spinal cord of the EAE mouse model (255), suggesting an increase in KMO activity. Degradation of KYN through the KMO branch decreases AA production, which has been shown to be protective in EAE (161) Therefore: IDO-1 activation could be a mechanism to overcome the pathology, but the abnormalities of the KP branch that degrades KYN, observed throughout the MS phases, could contribute to the progression of the pathology.

1.4.6 Psychiatric disorders: depression and schizophrenia

Depression has been linked with KP mainly through IDO. O'Connor et al found that chronic up-regulation of IDO after bacterial infection in mice is responsible for their depressive-like behaviours (256). Moreover, a polymorphism in IDO-1 increases the vulnerability to cytokine-induced depression (257). How systemic activation of IDO may lead to depression is likely to be related to a higher influx of KYN from the periphery to the CNS, increasing the activity of the KP neurotoxic branch. QUIN has been shown to be increased in post-mortem brains of patients with major depression

(258). It has also been found that 3-HK, with a region specific pattern, is increased in the striatum and amygdale, but reduced in cortex of a depression mouse model (259). Not only could increased KP neurotoxic metabolites play a role in depression pathology, but activation of KP reduces TRP available for the serotoninergic pathway. Decrease in serotonin due to acute TRP depletion can affect cognition and mood, which is characteristic of clinical depression (260).

Schizophrenia is a complex neuropsychiatric disorder characterised by different symptom clusters attributed to disturbances in dopaminergic, glutamatergic and GABAergic neurotransmission (261). It has been proposed that NMDAR hypofunction is a key mechanism of the pathology, as its pharmaceutical inhibition recreates schizophrenic symptoms in healthy subjects (262). Knowing that KYNA is an endogenous antagonist of NMDAR and that increased levels of NMDAR are found in CSF and post-mortem pre-frontal cortex of schizophrenic patients (263), it is plausible that KYNA plays a role in schizophrenia-related phenotypes. In fact, KYNA has been associated with the cognitive deficits of schizophrenic patients (264). Further characterisation of KP enzymes support the higher levels of KYNA observed in schizophrenic patients. This includes reduction of KMO combined with increased TDO in the frontal and anterior singulate cortices (265, 266). Moreover, no specific re-uptake processes for KYNA have been identified in the brain (267), indicating that pathological levels of KYNA could lead to its accumulation in the brain.

1.4.7 Infectious diseases

Human Immunodeficiency virus (HIV) infection is a chronic disease characterised by dramatic $CD4^+$ T cell depletion, resulting in immune response suppression and chronic inflammatory responses. Because HIV infection induces an immune response, there is activation of IDO, which likely favours HIV persistence through immune suppression. In relation to the neuropathology of this disease, QUIN is elevated in serum and CSF of patients with HIV. This is exacerbated in HIV-associated dementia (268). This implicates the potential involvement of QUIN in the neurodegenerative processes associated with HIV.

Infectious disease highly activates IDO in the periphery, which could lead to KP imbalance in the CNS. Consequently, the role of KP abnormalities in the

neuropathology associated with infection should not be discarded. In fact, KP involvement in neurodegeneration has been demonstrated in other infectious disease models, such as **cerebral malaria** or **trypanosomiasis** (269, 270). Disease-specific KP dysregulation within the brain may account for differences in the neurological dysfunction characteristic of the pathogen.

1.5 Conclusion

A large proportion of KP metabolites display neuroactive properties. However, only QUIN, 3-HK and KYNA have been shown to play key roles in several neurodegenerative diseases (section 1.4). This indicates the lack of validated techniques to detect emerging KP metabolites and the potentially more complex involvement of KP in neurological disorders has yet to be characterised.

The increase in 3-HK/QUIN levels occur in most of the diseases where glutamate excitotoxicity, oxidative stress and mitochondrial impairment play an important pathological role. This suggests that there is dysregulation of the KP towards the KMO branch in these diseases.

KAT and KMO activity require increased levels of KYN (78). However, KYN can only act as a positive regulator with KMO (69). In addition, inflammatory cytokines have been found to activate not only IDO, but also KMO, although this activation could be mediated by an increase in substrate availability (75-77). This suggests that KMO is the primary enzyme responsible for KYN degradation upon KP activation.

While the KMO branch appears to be controlled solely by bioprecursor availability (271), variations in the cellular metabolic and energetic state can modulate the KAT branch, subsequently affecting KP balance. Glucose depravation (99), and energy impairment (97) have been shown to reduce KAT activity. The implication of cellular metabolism in KP regulation could not only explain KP abnormalities under pathological conditions (ii), but also the segregation of the two KP branches in healthy brain (i) (Figure 1.9).

(i) Divergence of metabolic regulation between neural cells has previously been described (272). Astrocytes rely on glycolysis (273) and this could favour the KAT branch.

(ii) Changes in cellular metabolism have been described in innate and adaptive immune responses (274). This suggests that differences in KP metabolites during MS progression (254) could account for metabolic changes due to the switch from innate to adaptive immune responses in the acute and remission phase, respectively.

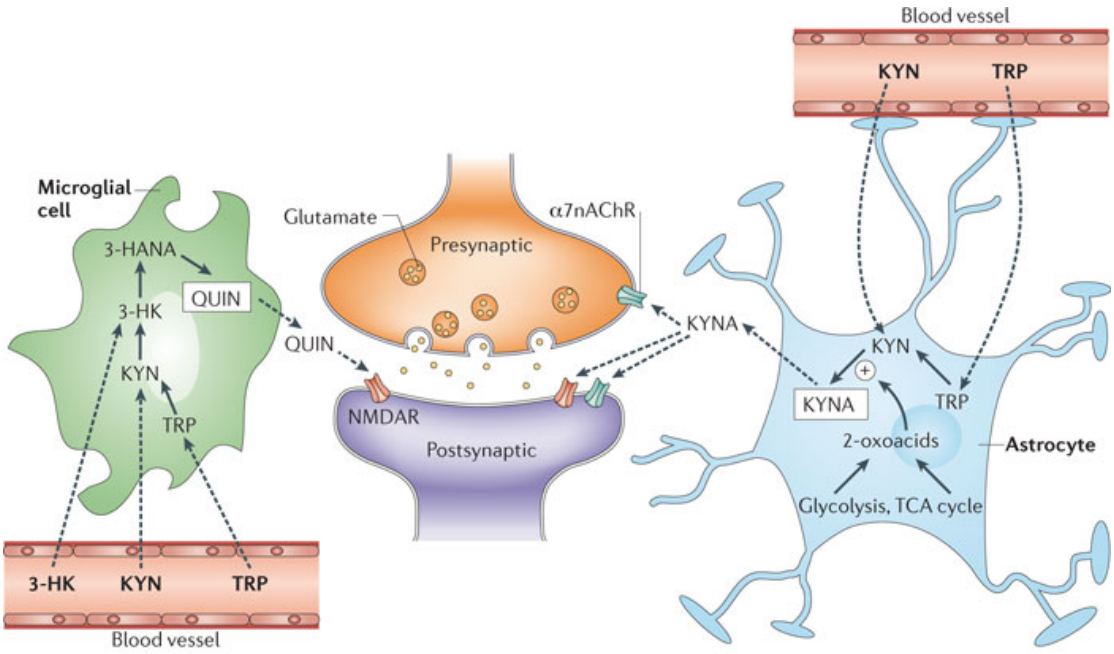

Figure 1.9: Segregation of the two KP branches in the brain

Astrocytes account for KYNA biosynthesis, while microglia account for QUIN. Figure from Schwartz et al. (67).

In conclusion, due to the neuroinflammatory component of several neurological diseases, IDO is activated and KYN levels increase in the CNS. This has been shown to mediate tolerance in the periphery, and could be a protective physiological response to neuroinflammation. However, other disease-specific aetiological factors, such as mitochondria dysfunction and metabolic changes, contribute to the pathogenesis of neurological diseases. These factors could also affect KP metabolite homeostasis and potentiate neurodegeneration.

Chapter 2

Research objectives

2.1 Problem statement

KP activation is a common feature in a large proportion of neurodegenerative diseases. KP activation is reflected by higher KYN levels in blood and CNS. In the CNS, the enzyme (KMO or KAT) that predominantly degrades KYN can vary depending on the disease, thus, altering the production of specific KP metabolites. In neurodegenerative diseases where excitotoxicity and mitochondrial dysfunction play important roles in their pathology, it is common to see higher QUIN and 3-HK levels in the affected areas, as a consequence of increased KMO activity. In contrast, increased levels of KYNA due to KAT hyperactivity is characteristic of diseases involving cognitive dysfunction. Whether these abnormalities in KP regulation are a consequence of the disease or one of the causes still remains unclear. In order to better understand the roles of the KP in physiology and pathology it is necessary to further elucidate the following questions: (1) Is CNS KP activation a response from the host to help overcome the disease?; (2) Does CNS KP activation promote the disease? If the response is affirmative in both cases, then, (3) when does KP activation cease being a mechanism of defence to become a trigger? and (4) what are the stimuli causing the pathologic KP imbalance? The answer to these questions is necessary to determine the appropriate pharmacological treatment targeting the KP.

2.2 Main Hypothesis

In response to the questions raised in the problem statement, we hypothesize that acute KP activation is necessary to overcome the pathological hallmark of the disease, however chronic KP up regulation or dysregulation contributes to the pathogenesis and progressive neurodegeneration through neuroinflammation, mitochondrial dysfunction, excitotoxicity and oxidative stress. These effects have shown to contribute to the vast majority of neurodegenerative diseases.

2.3 Specific aims

Among all the KP metabolites, we first focused on **KYN** and its contribution to acute neuroinflammation. We then studied **KMO** and its involvement in oxidative stress and mitochondrial dysfunction. Finally, we studied a possible **treatment strategy** that could restore the neuronal energy status and indirectly regulate the KP.

AIM 1: Is an increase in KYN levels in the CNS a mechanism to regulate neuroinflammation? If so, how?

KYN is able to cross the BBB; therefore activation of KP in the periphery will be reflected in the CNS by a rise in KYN levels. Our aim was to study the physiological or pathological roles of increased KYN levels in neuroinflammation. A target for KYN is AhR, and its activation participates in the control of inflammation. We have used astrocytes to determine how activation of AhR by KYN can mediate their inflammatory response to LPS.

AIM 2: How does KMO contribute to neurotoxicity and why is it up regulated?

KMO activity is increased in neuropathologies involving mitochondria dysfunction and excitotoxicity, ultimately leading to an increase in QUIN and 3-HK levels in the CNS. Although the mechanisms involved in QUIN neurotoxicity are well established, the role played by 3-HK is controversial. Our aim was to study the possible neurotoxic roles of constitutive KMO hyperactivation in mitochondrial function and oxidative stress. This will aid in elucidating differences between autonomous and extracellular 3-HK effects. To study this aim, we used a cell line stably expressing KMO. This

allowed us to extrapolate how this could affect neurons, which express active KMO. The second aim was to evaluate whether mitochondrial impairment can affect the direction the KP is taking (KMO versus KAT). It is known that mitochondrial inhibition decreases KAT activity; our question is whether it could be activating KMO instead.

AIM 3: To search for natural candidates that could protect against mitochondrial impairment and additionally, prevent neurotoxic effects of KMO hyperactivation.

Mitochondrial dysfunction and the resulting energy impairment have been identified as features of many neurodegenerative diseases. Whether this energy impairment is the cause of the disease or the consequence of preceding impairment(s) is still under discussion, however a recovery of cellular bioenergetics would plausibly prevent or improve the pathology.

Our aim was to screen various natural molecules for their ability to increase intracellular ATP and then elucidate the mechanism of action, through assessing different metabolic routes involved in cellular energy status.

We showed with the completion of the previous aim that mitochondrial dysfunction induces KMO activation, resulting in an exacerbation of the mitochondrial damage. Therefore, a possible therapeutic approach to decrease KMO-mediated neurotoxic activity would be to restore mitochondria activity, with the additional advantage of promoting the KAT branch of the KP. Our second aim is to determine whether increased cellular energy status can favour KYNA turnover and therefore identify new therapeutic targets to pharmacologically regulate the KP.

2.4 Research approach

To achieve the aim of the thesis the chapters are as outlined:

Chapter 1 summarises the literature regarding endogenous regulatory mechanism of KP, KP metabolites activity and abnormalities of KP in relation with different neurodegenerative diseases. Thus giving a better understanding on how KP

abnormalities can contribute to the pathology and what could be causing the dysregulation.

Chapter 3 describes the general methods used on this study.

Chapter 4 studies how KYN contributes to neuroinflammation by targeting astrocytes and AhR.

Chapter 5 studies how KMO is activated and the effects of its over activation.

Chapter 6 studies the mechanism of action of a natural molecule as an energy booster and its implications in KP regulation.

Chapter 7 states the overall conclusions.

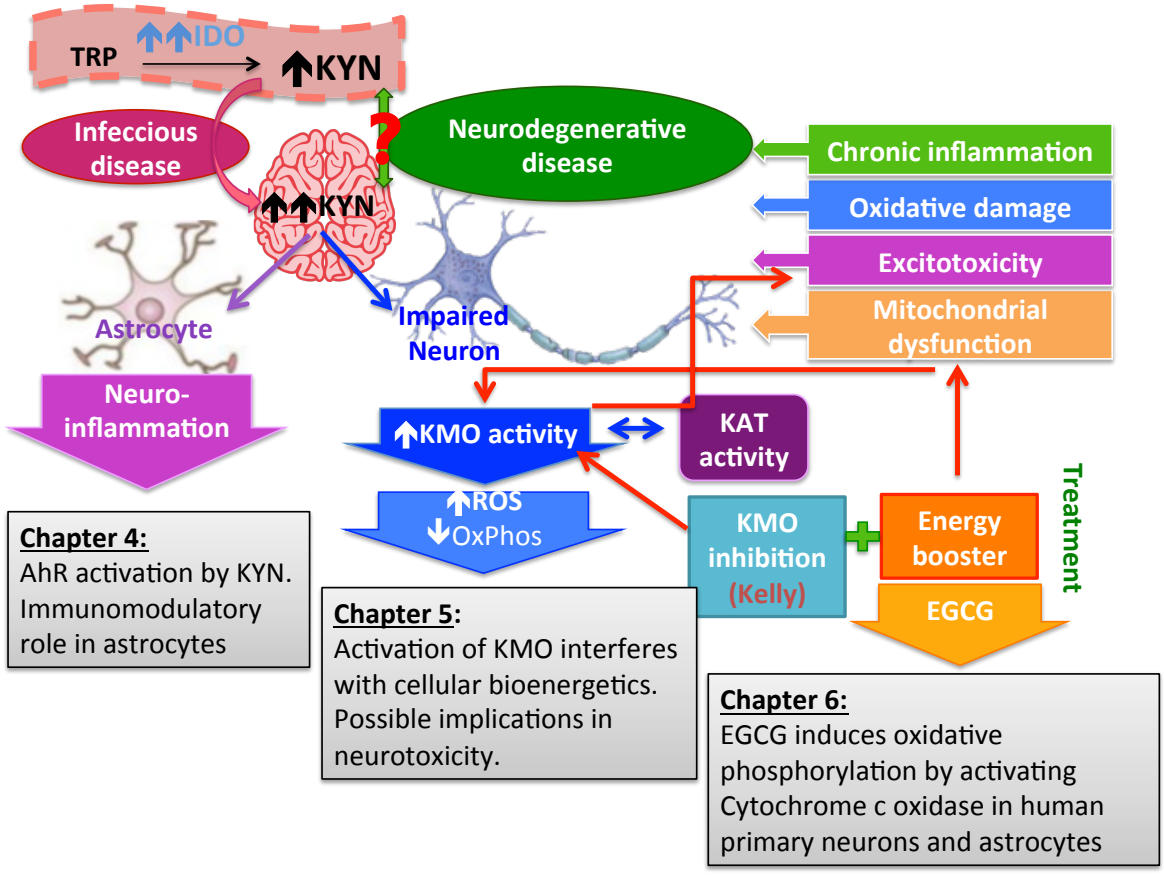

Figure 2.1: Research approach

Neurological diseases (involving chronic inflammation, oxidative stress, excitotoxicity and mitochondrial dysfunction) are associated with high KYN levels in the CNS. We will study; (1) KYN role in neuroinflammation, (2) the KMO branch and implications in oxidative stress, and (3) possible treatments targeting mitochondria dysfunction and the KP. Red arrows indicate negative regulation and show what we hypothesise to happen with the treatments.

Chapter 3
Materials and Methods

3.1 Human primary neural cell cultures

This protocol has been approved by the Human Ethics Committees of Macquarie University (Ethic approval 5201300330). Human foetal brains were obtained from 16–19 week-old foetuses, collected following therapeutic termination with informed consent. Mixed brain cell suspensions were prepared using protocols previously described by Guillemin et al. (136, 275). Cerebral portions of foetal brains were washed thoroughly with PBS to remove visible meningeal tissue and blood vessels. The neural dissociation kit (Miltenyi Biotec) was used to obtain single cell suspensions, following manufacturer's instructions. Briefly, 1 gram of tissue was weighed and manually dissociated in cold Hanks buffered saline solution. Tissue suspensions were pelleted, resuspended in pre-heated enzyme mix 1 (containing Papain), and incubated under rotation for 15 minutes at 37°C. Enzyme mix 2 was then added and incubated under the same conditions for a further 10 minutes. The tissue was dissociated mechanically using a glass pipette, applied to a 40µm cell strainer and washed with PBS. The cell suspension was centrifuged at 300 *g* for 10 minutes and pellet re-suspended in Neurobasal medium (Invitrogen,) for neuronal culture or Roswell Park Memorial Institute (RPMI) medium (Invitrogen) for astrocyte cell culture.

3.1.1 Human primary neurons

Neurons were cultured by plating the mixed cell suspension in culture dishes or glass

coverslips coated with Matrigel (1:20 in Neurobasal) and maintained in Neurobasal medium supplemented with 1% B-27 supplement, Glutamax (2 mM), 1X Antibiotic-Antimycotic, Hepes (5 mM) and Glucose (2 mM) for 7-10 days at 37°C in a humidified atmosphere containing 5% CO_2 (275). Medium was subsequently changed 2 days after plating and then every 3 days thereafter.

3.1.2 Human primary astrocytes

Astrocytes were obtained by seeding high density mixed brain cell suspension in cell culture flasks. Astrocytes were maintained in RPMI medium supplemented with 10% FBS, Glutamax (2mM) and 1X Antibiotic-Antimycotic at 37°C in humidified atmosphere containing 5% CO_2 (136). Attached cells were washed with PBS and new medium added twice per week. When the desired confluence was achieved, cells were trypsinised and expanded. 95% purity was achieved within three passages.

3.2 Western blot

3.2.1 Whole cell lysate extract

Cell cultures were washed once with warmed PBS and lysed in ice-cold radioimmunoprecipitationassay (RIPA) buffer, containing 50 mM Tris pH 8.0, 150 mM NaCl, 1% NP40, 5 mM EDTA, 0.5% sodium deoxycholate and 0.1% sodium dodecyl sulphate (SDS) (Sigma-Aldrich) in the presence of Complete Protease Inhibitor Cocktails (Roche). Cells were harvested and kept on ice for 30 minutes. Samples were then centrifuged at 12,000 g for 20 minutes at 4 °C and supernatant stored at -80 °C.

3.2.2 Immunoblotting

First, protein concentrations of the lysate were determined using Pierce BCA protein assay Kit (Thermo Scientific), following manufacturer's instructions.

Equal amounts of protein samples (15-20 µg) in total volumes of 15µL of RIPA were denatured in 4X Laemmli buffer (Bio-Rad) by heating samples for 5 minutes at 95 °C. Protein samples were then loaded into Mini-Protean TGX precast PAGE gels (Bio-Rad) and separated at 120-150V for 1 h in an electrophoresis chamber (Bio-Rad)

submerged in Tris/glycine/SDS buffer (Bio-Rad). A molecular weight (MW) marker ladder was used to identify target protein bands (Dual Colour Pre-Stained Standard, 10-250 kDa, BioRad). Proteins were electrophoretically transferred to a nitrocellulose membrane (Bio-Rad) equilibrated in blotting buffer (Bio-Rad), using the Trans-Blot Turbo system (Bio-Rad) at 25 V for 7 minutes. To block non-specific binding sites, nitrocellulose membranes were incubated in 5% non-fat milk powder dissolved in TBS containing 0.1% Tween 20 (TBS-T) at room temperature (RT) for 1 h on a shaking platform. Membranes were incubated with primary antibodies (Table 3.1) in TBS-T overnight at 4°C on a shaking platform, followed by three 10 min washes in TBS-T and incubated with alkaline phosphatase-coupled secondary antibodies (Table 3.1) for 45 minutes at RT on a shaking platform. Membranes were washed three times for 10 minutes in TBS-T and incubated for 5 minutes with Clarity Western ECL substrate (Bio-Rad). Protein bands were detected in a ChemiDoc XRS detection system (Bio-Rad) driven by Quantity One software. For re-use, membranes were stripped by washing in ddH_2O for 5-10 minutes in 0.2 M NaOH and a further 5 minutes in ddH_2O at RT. Membranes were blocked again before antibody reprobing. For analysis of target protein bands, band densities of the appropriate MW size were measured using Image Lab software (Bio-Rad). Background intensity was subtracted and bands normalised to individual GAPDH (cytosol) or Fibrillarin (nuclei) loading controls. Averages and Standard Errors of the Mean (s.e.m.) for each treatment condition were determined and results presented as a fold increase of control band intensities.

Table 3.1: Summary of antibodies used for Immunoblotting

Antibody	*Host*	*Manufacturer*	*Specificity*	*Dilution*
KMO	rabbit	LSbio	Human	1:500
IDO [cv152]	rabbit	Reference (*3*)	Mice	1:500
AhR [RPT9]	mouse	Abcam	Mice	1:500
RelB [C-19]	rabbit	Santa Cruz	Mice	1:500
p100/p52	rabbit	Cell Signalling	Mice	1:1000
p65 [C-20]	rabbit	Santa Cruz	Mice	1:1000
Fibrillarin	mouse	Abcam	Mice	1:1000
GAPDH	rabbit	Cell Signalling	Mice/Human	1:1000
Immunoglobulins/HRP	goat	Dako	Mice	1:10000
Immunoglobulins/HRP	goat	Dako	Rabbit	1:10000

3.3 Quantitative real-time polymerase chain reaction

3.3.1 Total RNA extraction

Trizol extraction

Total RNA from cells were prepared using Trizol reagent (Invitrogen), unless otherwise specified. RNA extraction was performed following the manufacturer's instructions. Briefly, cells were seeded at $100x10^3$ cells per 22 mm well. After treatment, the cell supernatant was partially removed, leaving 100-200 µL. Trizol reagent was added into the well (1 ml total volume) and cells allowed to lyse for 5 minutes. The whole content of the well was then placed in an RNAse-free Eppendorf and 200 µL of chloroform (Sigma-Aldrich) was added. The Eppendorf was vigorously mixed and incubated for 5 minutes at RT before proceeding with the gradient centrifugation at 8000 g for 15 minutes. The upper layer of the gradient (removed without touching the adjacent layer) was placed in a new RNAse-free Eppendorf and 500 µL of isopropanol (Sigma-Aldrich) was added. Tubes were vigorously agitated and incubated for 10 minutes at RT, allowing for the RNA to precipitate. RNA was then pelleted by centrifugation at 12,000 *g* for 15 minutes at 4°C, washed with 1 mL of 75% ethanol (Sigma), air dried for 10 minutes and resuspended in 20 µL RNAse free water. Complete solubilisation of RNA in water was achieved by incubating in a 55°C water bath for 5 minutes.

RNeasy on-column extraction

Total RNA from cells and tissue was also prepared from RNeasy mini kits (Qiagen) according to manufacturer's instructions. Samples were lysed and homogenised with lysis buffer with added β-Mercaptoethanol, which immediately inactivated RNases and denatured unwanted proteins. The samples were then transferred into an RNA miniprep column, where the total RNA binds to the membrane and contaminants are washed away through a series of washes and centrifugations. Ethanol was added according to manufacturer instructions to provide appropriate binding conditions. DNA contamination was removed by treating the RNA sample with on-column RNase-free DNaseI included in the kit. High-quality RNA was then eluted in 30 µL of UltraPure water.

RNA quantification and quality

RNA quantity and purity was evaluated spectrophotometrically by determination of absorbance readings at 260 nm, 230 nm and 280 nm using a NanoDrop (Thermo Scientific). A260 is used to quantify RNA and ratio of A260/A280 and A260/A230 assess RNA purity, ratios lower than 1.7 indicates protein, Trizol or guanidine HCl contamination. RNA integrity was assessed with denaturing RNA agarose gel. RNA Integrity Number (RIN) was calculated by the Agilent 2100 electrophoresis Bioanalyzer by the Ramaciotti Centre (UNSW). RIN assesses the presence or absence of RNA degradation products being 10 the most intact RNA. Figure 3.1 displays two different RNA samples extracted with on-column (Figure 3.1*a*) and Trizol (Figure 3.1b) procedures and analysed for the RIN. RIN≥9.8 in both samples demonstrates that both RNA extraction methods are adequate, and therefore repeatability of experiments is ensured. The RNA was then stored at -80°C until cDNA synthesis.

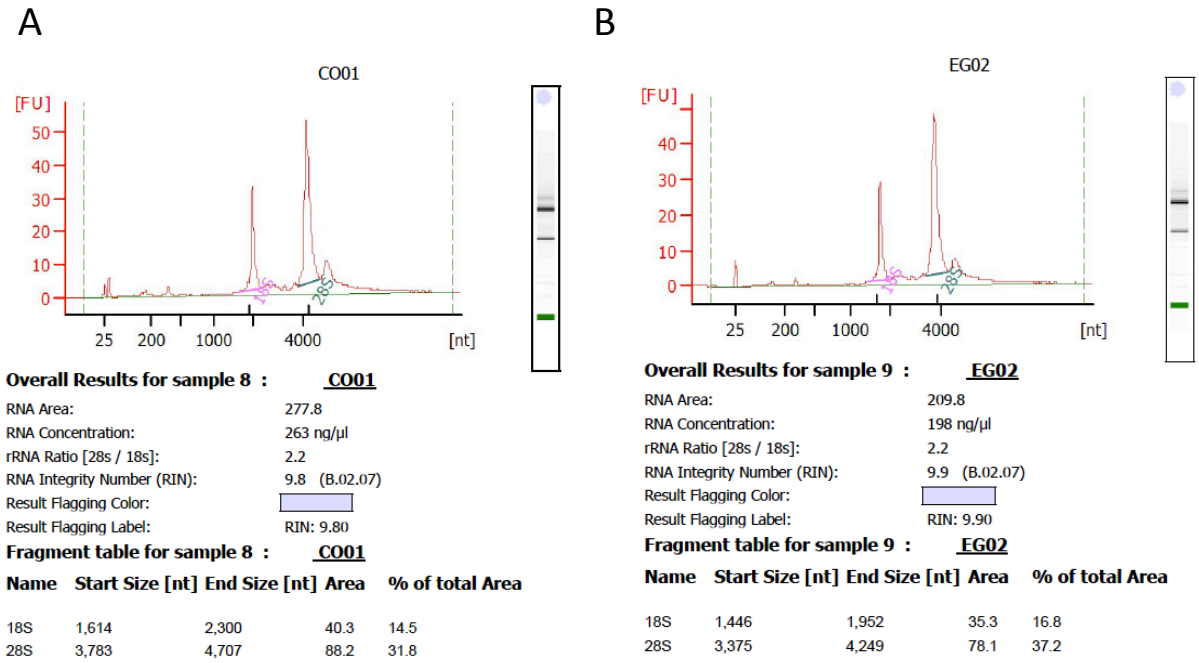

Figure 3.1: Electropherograms of intact total RNA

3.3.2 cDNA synthesis

Standard reverse transcription (RT) was performed with 1.5 µg of total RNA in a final volume of 20 µl using the Superscript Vilo cDNA Synthesis Kit in accordance with the

manufacturer's recommendations. The protocol for cDNA synthesis has been optimised for generating first-strand cDNA for use in two-step qRT-PCR. Briefly, for a single reaction, the following components were combined: 4 µl of 5X VILO Reaction Mix, 2 µl of 10X SuperScript Enzyme Mix, x µl (1.5 µg) of RNA and DEPC-treated water to a final volume of 20 µl. A separate tube, which was the No-RT reaction tube, consisted of all of the above components but with omission of the Enzyme Mix. This was used as a control to confirm that no genomic DNA was present in the sample. The tube was gently mixed and then placed on a Mastercycler gradient PCR machine for the cDNA synthesis reaction with the following parameters: (1) incubation at 25°C for 10 minutes (2) incubation at 42°C for 60 minutes, and (3) termination of the reaction at 85°C at 5 minutes. The resulting cDNA was then stored at -80°C until further use.

3.3.3 Quantitative real-time polymerase chain reaction

cDNA was diluted to a concentration of 2.5ng/ul with RNase-free water. Briefly, 4 µl of the diluted synthesised cDNA together with the appropriate primers and 5 µL SYBR® Select Master Mix (Applied Biosciences) was added to a total volume of 10 µl. Primers were used at 250 nM final concentration and quantity of cDNA was 10 ng per reaction. A PCR reaction mastermix was prepared for each primer before dispensing into 96x or 384x PCR plate cells. No-template control (NTC) reactions were also prepared for each gene. These consisted of all reaction components except for cDNA, which was replaced by 4 ul of DNase-free water. The cDNA of the No-RT reaction samples were also used to confirm that no genomic DNA was present in the samples. This was only performed in initial pilot studies where only 3-6 samples were initially tested for the presence of genomic DNA after on-column DNase treatment of the samples or Trizol extraction. qRT-PCR was carried out using a Viia7 Real-Time PCR system (Applied Biosciences, NSW, Australia). The cycling parameters for all genes were the following: initial denaturation at 95˚C for 3 minutes, then 40 cycles of 95˚C for 20 s, and 60˚C for 20 s. The annealing temperatures were optimised for each primer, being 60˚C adequate for all the primers used. All transcripts were measured in each unknown sample in triplicates. Target gene expression values were normalised to two endogenous reference genes: β-2 microglobulin (β2M), glyceraldehyde 3-phosphate dehydrogenase (GAPDH), hypoxanthine phosphoribosyltransferase (HPRT), phosphoglycerokinase (PGK)-1 or TATA-binding protein (TBP). After normalisation, each sample was expressed relative to a control

sample (non-treated control), according to Vandesompele guideline (276). Quantification of RNA expression was calculated following the equations below. The equation uses geometric mean (GM) of the two reference genes and Efficiency (E) calculated for each of the primer sets as described below.

(1) ΔCt = Ct (Target -treated) – GM (Ct (Reference -treated))

(2) ΔCt = Ct (Target -control) – GM (Ct (Reference -control))

(3) ΔΔ Ct = ΔCt (treated) – ΔCt (control)

(4) $E^{(-\Delta\Delta Ct)}$

Primer description and efficiency

The oligonucleotide primers for qRT-PCR amplification were obtained from several sources: designed by Dr Benjamin Heng, a gift from a collaborating laboratory (Department of Experimental Medicine, University of Perugia), or designed by using the Primer BLAST (web-based NCBI primer designing tool: http://www.ncbi.nlm.nih.gov/tools/primer-blast/). All obtained sequences were blasted with BLAST for determination of exon/intron boundaries and evaluating the best potential outcome based on relative scores and secondary structures. The following parameters were used during the design: melting temperatures 58-61°C, primer lengths 20-24bp and amplicon lengths 90-200 bp. Primer pairs were directed to locate on different exons or directly spanning exon-exon junctions of each cDNA. For each primer pair, reaction efficiency estimates were derived from a standard curve generated from a serial dilution of selected cDNA highly expressing the gene of interest. Specificity was verified by a single peak in melting curve analysis (Figure 3.2.a). The reaction efficiency was derived from the standard curve (Figure 3.2.c) where the mean Ct values (of each dilution point) were plotted against the logarithm of the cDNA dilution factor. Each dilution was assayed in triplicates.

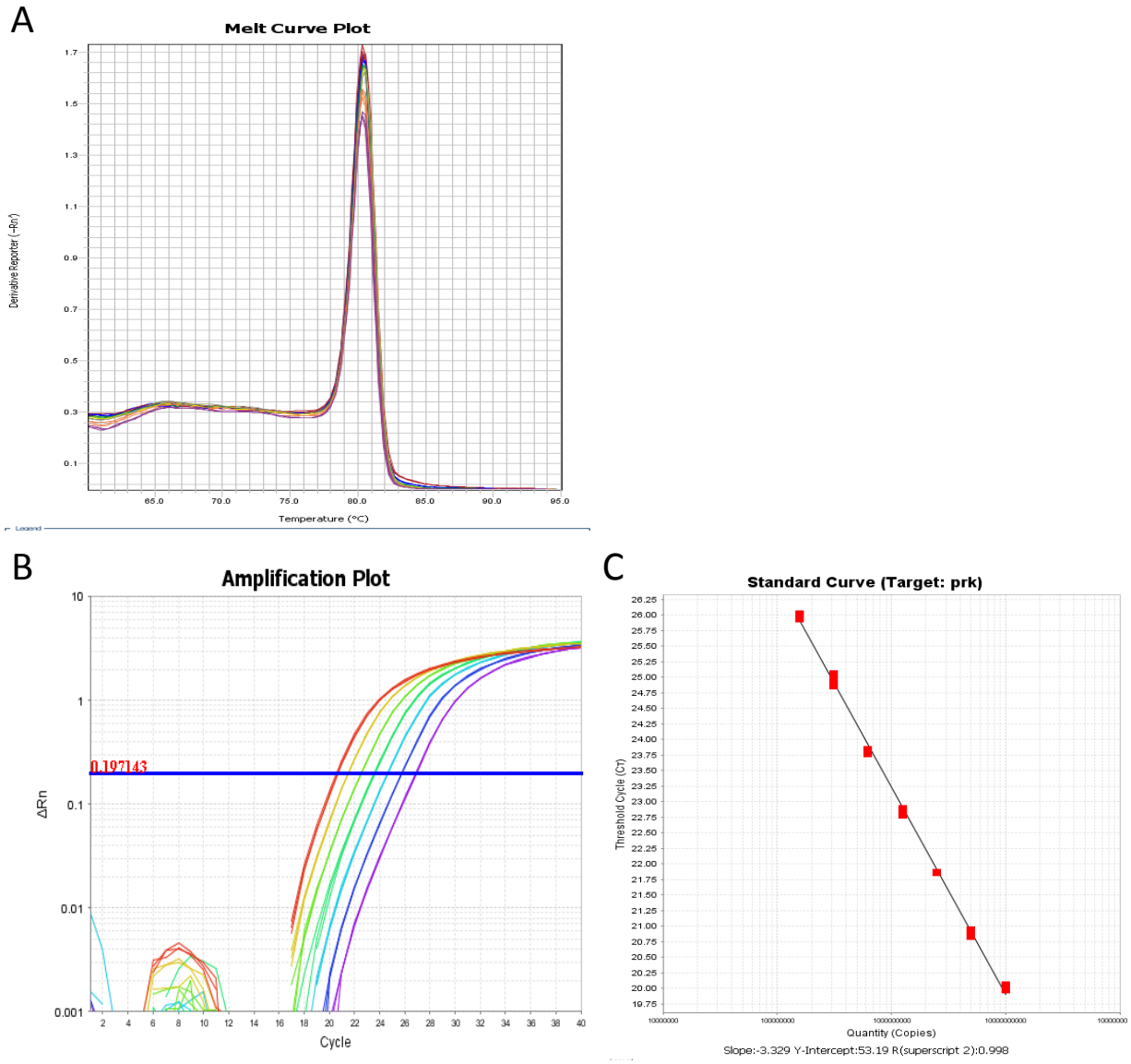

Figure 3.2: qRT-PCR plots obtained during primer optimization

(**a**) Melting curve plot, (**b**) amplification plot from serial cDNA dilutions and (**c**) standard curve to determine primer efficiency.

3.4 KP metabolite quantification

High performance liquid chromatography (HPLC) or ultra high performance liquid chromatography (UHPLC) was performed to determine the levels of 3-HK, KYN and KYNA in the supernatant of growing cells in culture. Cell culture supernatants were deproteinised diluting the sample 1:4 with 20% trichloroacetic acid (Sigma-Aldrich) and vortexed for protein precipitation. The samples were then centrifuged at 13, 000 *g* for 10 minutes at 4^{o}C, after which the supernatant was filtered through a 0.45 µm, 4 mm, hydrophobic PTFE filter (Merck Millipore, Darmstadt, Germany), and transferred

into a volume insert and placed into a 2 ml vial (Agilent Technologies; CA, US). The vial was capped and set onto a HPLC/UHPLC auto sampling device. Background values from traces in medium were subtracted for each metabolite to represent net cellular production. Read outs of the standards, 3-HK, KYNA and KYN (Sigma-Aldrich), were expressed as peak area, which is used to plot the linear standard curve against the known concentration of the standards used (only acceptable if $R^2 \geq 0.99$). Peak areas from samples were then interpolated from the standard curve to calculate the actual concentrations of 3-HK, KYNA and KYN and expressed as μM or nM. The intra- and inter-assay coefficient of variations ranged from 5% to 7% for all the metabolites detected using the UHPLC/HPLC. Each experiment was performed in triplicate using supernatants from primary cultures derived from three different cell culture preparations. All results are expressed as the mean ± s.e.m.

3.4.1 Ultra high performance liquid chromatography

3-HK and KYN were concurrently measured using an Agilent Technologies 1290 Infinity UHPLC system (Agilent Technologies) as previously described with slight modifications (275). Briefly, the standards and samples were separated using Agilent Eclipse Plus C18 RRHD (1.8 μM, 2.1 X 150 mm) reverse phase column at an injection volume of 10 μL. The mobile phase consists of 0.1 M sodium acetate (Sigma-Aldrich) at pH 4.65 filtered through 47 mm, pore size 0.45 μm cellulose membrane filter (Agilent Technologies). It was pumped isocratically with a flow rate of 0.75 mL/min and with column temperature at 38°C. KYN and 3-HK were detected using multi-wavelength detection at 365 nm KYN.

3.4.2 High performance liquid chromatography

KYNA was assayed by the Agilent 1200 series HPLC system (Agilent Technologies), as outlined in (275) with minor changes. Briefly, 30 μl of the standards and samples were applied to an Agilent Zorbax Eclipse XDB-C18 (5 μm, 150 X 4.6mm i.d.) column with column temperature at 38°C. KYNA was eluted isocratically at a flow rate of 0.75 ml/min with a mobile phase consisting of 50 mM sodium acetate (Sigma-Aldrich) with 0.25 M of zinc acetate (Sigma-Aldrich) and 2.25% (v/v) acetonitrile (Ajax Finechem). The mobile phase was prepared freshly and filtered through a 0.45 μm pore size cellulose membrane filter (Agilent Technologies) prior to use. KYNA is

detected using a fluorescence detector at an excitation wavelength of 344 nm and an emission wavelength of 388 nm. The final concentrations of unknowns were calculated by interpolation of the standard curve (only acceptable if $R^2 \geq 0.99$).

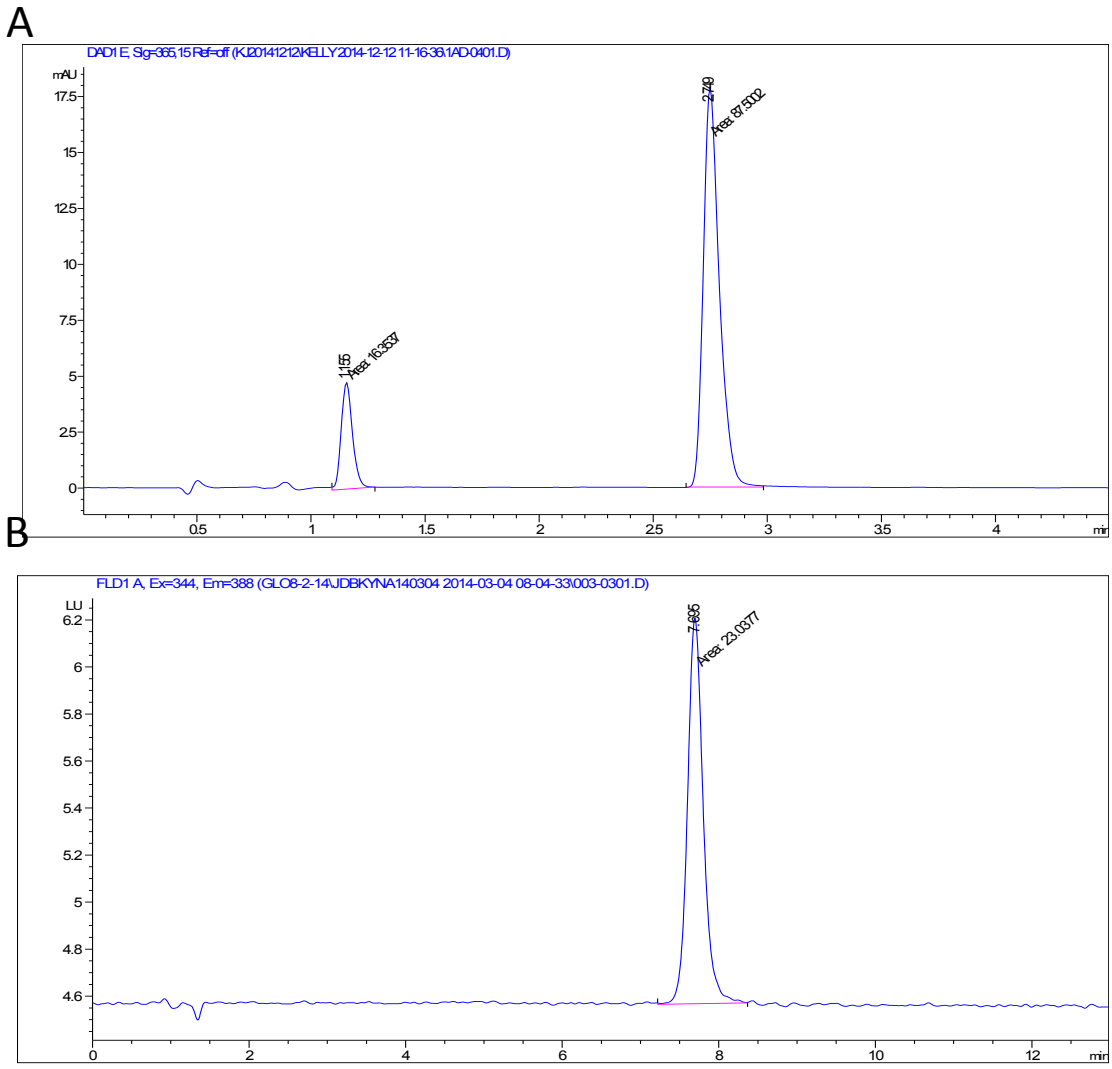

Figure 3.3: Chromatograph display

(**a**) UHPLC chromatograph display for 20 µM 3-HK and 50 µM KYN standards (left to right). (**b**) HPLC chromatograph display for 50 nM KYNA standard.

3.5 Immunocytochemistry

Cells were cultured on glass Coverslips (Menzel; Lower Saxony, DE) in 24-well tissue culture plates accordingly with each cell type procedure. When ready for immunostaining, cells were washed once with PBS pre-warmed to 37 ºC and fixed with 4% paraformaldehyde (PFA; Electron Microscopy (EM)-grade; Electron Microscopy Sciences (16% solution)) in fresh PBS at RT for 15 minutes. Cells were

washed three times with PBS and permeabilised for 90 sec with 0.05% Triton X-100 (Sigma-Aldrich). Cells were then blocked for 45 minutes in 5% heat-inactivated goat serum (60 ºC for 30 minutes; Invitrogen) in PBS and incubated with primary antibody (Table 3.2) for 2h at RT or overnight at 4ºC, diluted in 5% goat serum. For co-labelling studies, primary antibodies were applied sequentially with several gentle PBS washes in between. Secondary antibodies were diluted (1:400) in 5% goat serum and applied for 45 minutes at RT. Following three PBS washes, coverslips were mounted with ProLong Gold reagent containing 4´,6-diamidino-2-phenylindole (DAPI) (Invitrogen) on glass slides (Menzel-Gläser). Epifluorescence images were obtained on a Olympus FV1000 confocal microscope (Olympus; Middlesex) and captured with a CCD camera. Images were analysed and processed using ImageJ software (available at http://rsbweb.nih.gov/ij/).

Table 3.2: Summary of antibodies used for Immunocytochemistry

Antibody	*Host*	*Manufacturer*	*Specificity*	*Dilution*
KMO	rabbit	LSbio	Human	1:500
IDO [cv152]	rabbit	Reference (*3*)	Mice	1:500
AhR [RPT9]	mouse	Abcam	Mice	1:500
RelB [C-19]	rabbit	Santa Cruz	Mice	1:500
p100/p52	rabbit	Cell Signalling	Mice	1:1000
p65 [C-20]	rabbit	Santa Cruz	Mice	1:1000
Fibrillarin	mouse	Abcam	Mice	1:1000
GAPDH	rabbit	Cell Signalling	Mice/Human	1:1000
Immunoglobulins/HRP	goat	Dako	Mice	1:10000
Immunoglobulins/HRP	goat	Dako	Rabbit	1:10000

3.6 Mitochondrial respiration in intact cells

Oxygen consumption in intact cells was measured using the high-resolution respirometer Oxygraph-2K (Oroboros instruments). Zero oxygen measurements were taken after injection of sodium dithionite and polarographic oxygen sensors were calibrated with air-saturated culture medium at 37°C. Intact cells were removed from the tissue culture dish and re-suspended in normal culture medium. Cell suspension was immediately placed in the oxygraph chamber at 37°C under

continuous stirring at 300rpm. After monitoring Routine respiration (R), sequential injections of the following chemicals were performed to evaluate different mitochondrial respiration rates: oligomycin (5 μM) to inhibit ATP synthase and measure the proton leak (L); FCCP (4 μM) is a protonophore that uncouples ATP synthesis from the electron transport system (ETS) to evaluate the ETS maximum capacity; and rotenone (1 μM) and antimycin A (2.5 μM) to inhibit complex I and complex III respectively and to measure the residual oxygen consumption (ROX) (Figure 3.4). Each experiment was repeated three times with different cell preparations and results were expressed as pmol O_2 consumed per minutes per million cells or oxygen consumption rate (OCR).

3.7 Statistical analysis

All *in vitro* determinations are presented as means ± the standard error of the mean (s.e.m.) or standard deviation (s.d.) from at least three independent experiments, unless otherwise indicated. Student's t-test (two-sided and paired) was used for two-group analysis, performing separate Student's t-test in multi-group analysis. All analyses were conducted using GraphPad Prism software (version 3.0; GraphPad Software). Statistical significance was accepted at $p<0.05$.

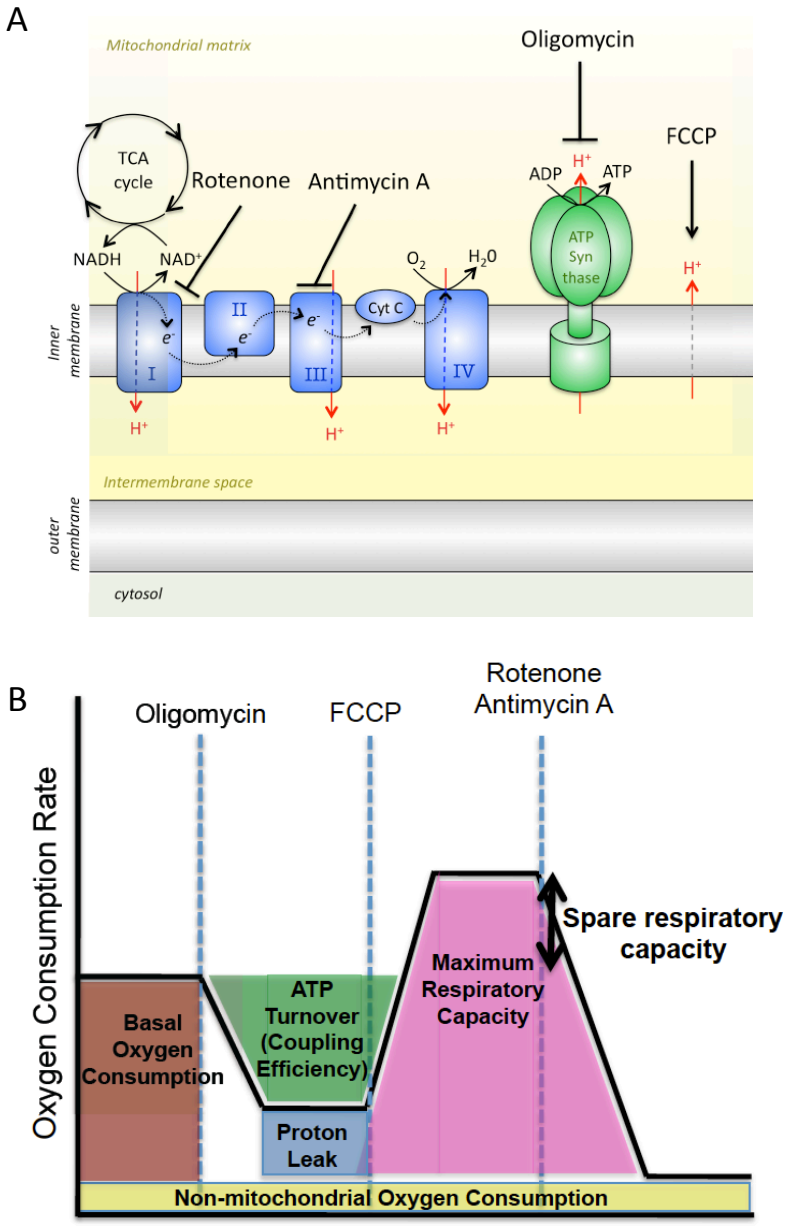

Figure 3.4: Bioenergetics profile

(**a**) Shows a schematic overview of the effects of mitochondrial inhibitors on the electron transport system. (**b**) Shows in detail the different parameters that can be studied using the high-resolution respirometer Oxygraph-2K: *OCR* measured prior to the addition of drugs (Routine respiration; R) and then following the addition of the indicated drugs. Reduction of ORC after *oligomycin* indicates the amount of O2 consumed for mitochondrial ATP generation and the *proton leak (L)*. *FCCP* allows H+ back into the matrix independent of the ATP synthase; cells attempt to maintain the chemiosmosis gradient after FCCP by moving H^+ back out to the intermembrane space, which requires the use of the ETS and the consumption of O_2 as the final electron acceptor. After FCCP the *maximum capacity (MR)* of the mitochondria to use OXPHOS is revealed. *Spare respiratory capacity (SRC)* is the difference between maximal OCR and R and as such is an indicator of how close to its bioenergetic limit the cell is functioning. *Rotenone* and *antimycin A* together render a complete shutdown of the ETS. Figure from van der Windt et al. (274).

Chapter 4

Immunoregulatory function of astrocytes. A role for Kynurenines

4.1 Introduction

Reactive astrocytes have complex functions and overcome gradated continuum changes during the course of CNS injury. These changes can be reversible, such as alteration in gene expression or cell morphology, to long-lasting scar formation with re-arrangement of physiological functions (277). Reversible changes in activated astrocytes occurring during an acute or fast resolving insult have shown to be protective for the CNS (278). However severe reactive astrogliosis caused by a long lasting non-resolved trigger exacerbates the pathology (279), promoting inflammation, excitotoxicity, inhibiting axonal growth and compromising the BBB (277).

The KP is activated in an extensive number of neurodegenerative pathologies, leading to increased KYN concentration in serum (3). This increase will rapidly be reflected in the CNS, as KYN can cross the BBB through the large neutral amino acid carrier (L-

system) (104). KYN has widely been studied for its function as a mediator of a tolerogenic inflammatory response in immune cells (see section 1.2.1). Recently, it has been demonstrated that AhR activation by KYN may be responsible for this activity (11). Therefore, increase of KYN in the CNS is presumed to be an endogenous immunosuppressive response to counteract neuroinflammation. However, both the immunoregulatory role of KYN and AhR presence in the CNS has not been characterised so far. Here we reported for the first time that mice primary adult astrocytes express AhR, being a possible target for KYN and a mechanism for neuroinflamatory control in response to acute CNS damage.

Degradation of KYN in the CNS leads to the production of neuroactive compounds. Concentrations of KYN metabolites are altered in an extensive number of neurodegenerative pathologies (see section 1.4). Considering that (1) several KP metabolites have shown to activate AhR (see Table 1.2) and (2) specific ligands can trigger different transcriptional partners for AhR and mediate different responses (178), abnormalities on KP concentrations could affect AhR activity and astrocyte response in neuroinflammation. Here, we reported that, under inflammatory trigger, binding of the KP ligands, KYN or KYNA, to AhR leads to a different cytokine profile expression in astrocytes. While KYN promotes *Il-10* expression (anti-inflammatory), KYNA favours *Il-6* expression (pro-inflammatory). Cytokine imbalance towards inflammation may affect astrocyte function during the course of the CNS pathology. Because astrocytes are the most active cells producing KYNA in the CNS (67), impairment of their activity will provoke KP abnormalities, further affecting ligand-mediated AhR responses and neuroinflammation.

In conclusion, astrocyte response to an acute insult in the CNS, could contribute to resolving the damage. However, as the pathology progress, neuroactive KP metabolites will increase in the CNS. Sustained KP imbalance, through abnormal AhR activation in astrocytes, may promote neuroinflammation and contribute to the severe reactive astrogliosis observed in chronic neurological diseases (Figure 4.11 summarise the mechanisms discussed in the following sections).

4.2 Methods

4.2.1 Mice primary cell cultures

CD4⁺ naïve T cell purification

Spleens were obtained from adult C57BL/6 WT mice (8-9 weeks) (AEC No.08/24). Naive $CD4^+$ T cells from pooled lymph nodes were purified as described (48, 107). Briefly, $CD4^+$ T cells were obtained from collagenase-treated spleens (collagenase type IV; Sigma-Aldrich). Total spleen cells were washed with 2 mM EDTA in PBS to disrupt DC-T cell complexes, and EDTA was also present in subsequent steps involving the use of positive selection columns. Cells were resuspended in RPMI and placed in a 15mL tube containing Ficoll Plaque-Plus (GE Healthcare Life Sciences) without disturbing the interface, and centrifuged at 2000 rpm for 25 minutes at 4°C for gradient isolation of lymphocytes. The low-density fraction at the interface was collected and washed several times. The recovered cells were separated using MACS beads (Miltenyi Biotec, Auburn, California, USA) according to the manufacturer's recommendation. Briefly, cells were resuspended at 10^7 cells/ml of MACS buffer (0.5% human serum and 2 mM EDTA in PBS) and incubated with anti-CD4 magnetic beads at 4°C for 15 minutes. The cell suspension was applied to lymphocyte separation column, and $CD4^+$ cells were separated using positive selection.

Adult primary mice astrocytes and brain monocyte-derived cells

This protocol has been approved by the Garvan/St Vincent's Animal Ethics Committees (Approval No. 13/42). Brains from adult C57BL/6 WT mice (8-9 weeks) were stripped of their meninges and minced in Ca^{2+}-free Hank's balanced salt solution (HBSS). Neural tissue was digested with the Neural Tissue Dissociation Kit (P) (Miltenyi Biotec) following the manufacturer's instructions.

The cell suspension was washed with Ca^{2+}-HBSS and centrifuged at 500 *g* for 25 minutes at 19°C over a 0%/30%/70% isotonic Percoll gradient to remove myelin debris, and most neuronal cells, oligodendrocytes and erythrocytes as previously described (280, 281). Briefly, the gradient was set up re-suspending the cell pellet from 2 brains in 2 mL of 70% Percoll in a 15 mL falcon tube. Next, 4 mL of 30% Percoll solution and 3mL of PBS were added on top to form a three-layer gradient.

Mixture of the three layers should be avoided during the process. Using a transfer pipette, the interphase between the 30 and 70 % Percoll layers was collected into a new tube and washed with PBS. The cells obtained were sorted using $CD11b^+$ beads (Miltenyi Biotec) according to manufacture's instructions. The negative and positive fraction were washed with PBS and re-suspended in astrocyte cell culture medium (RPMI medium with 10% foetal bovine serum, penicillin- streptomycin (50 U/ml), 2-mercaptoethanol (50 μM) and L-glutamine (2 mM)) or murine cell culture medium (IMDM medium with 10% foetal bovine serum, penicillin- streptomycin (50 U/ml), 2-mercaptoethanol (50 μM) and L-glutamine (2 mM)) respectively. The positive fraction containing the monocytic CNS infiltrate and microglia were plated and incubated at 37°C in a humidified atmosphere containing 5% CO_2 for 24h to remove the magnetic beads until treatment. The negative fraction containing the remaining brain cell mixture was plated in a 30mm dish and incubated at 37°C in a humidified atmosphere containing 5% CO_2 for 24-48h. Non-adherent cells were washed out, in order to eliminate lymphoid cells, non-monocyte myeloid cells, stem cells, platelets and red blood cells. The remaining adherent cells after having removed $CD11b^+$ cells were mainly astrocytes. Astrocyte-enriched cell cultures were expanded twice using TrypLE (Invitrogen), and further selected by removing non-adherent cells 3h after dissociation and plating. This eliminates most endothelial cells (282). Fresh medium was added to the culture every 2 days and astrocytes were used within 10 days after first plating to avoid expansion of unlikely fibroblast contamination (283). Purity of astrocyte preparations was checked with a GFAP antibody (BD Biosciences), showing 84.2±5.1% astrocytes (Figure 4.1a, b) with less than 0.2% of CD11b contamination when $CD11b^+$ cells have been previously removed (Figure 4.1c). Astrocytes for ex-vivo experiments were isolated using ACSA-2 (Astrocyte Cell Surface Antigen-2) MicroBead Kit (Miltenyi Biotec) from the whole brain cell suspension, plated and incubated at 37°C in a humidified atmosphere containing 5% CO_2 for 24h to remove the magnetic beads prior treatment.

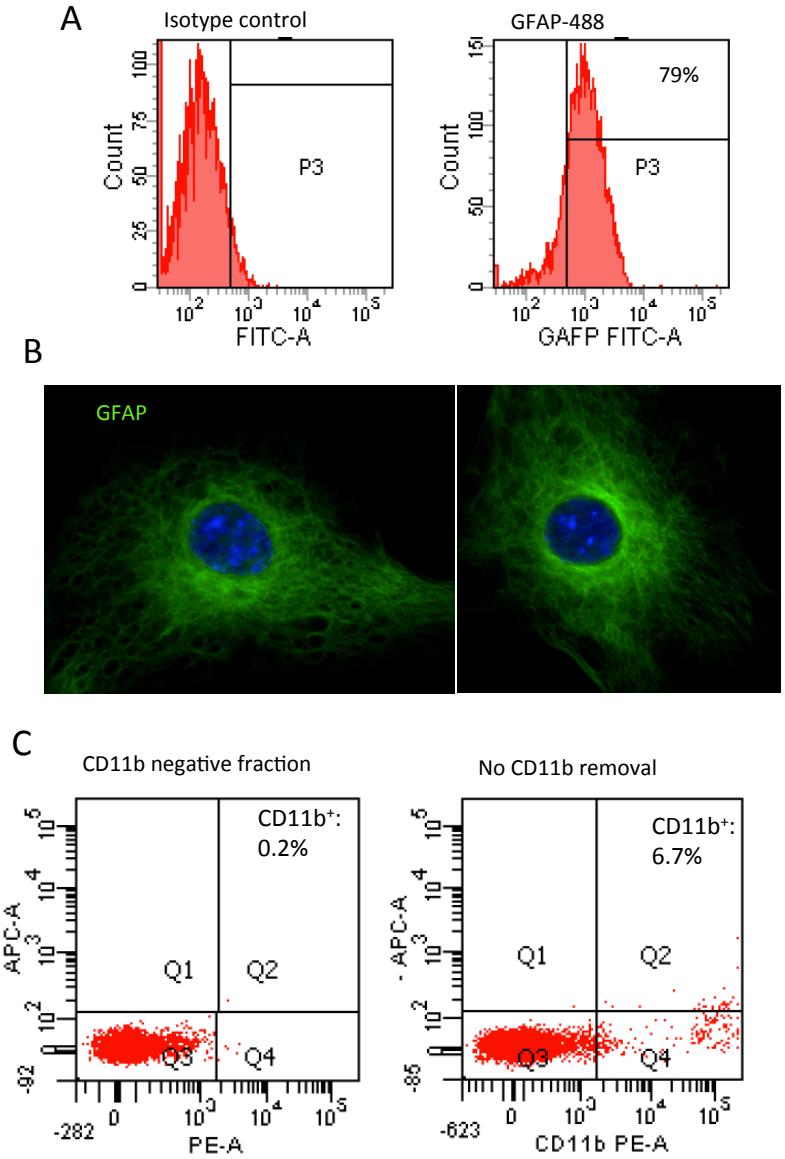

Figure 4.1: Isolation of adult astrocytes from CNS

(**a**) GFAP expression in the astrocyte cultures assessed by FACS analysis. Data is representative of two experiments and in the quadrants is shown the mean of GFAP expression versus isotope control. (**b**) Intracellular immunofluorescence showing GFAP positive astrocytes. Representative data of four independent experiments. (**c**) CD11b expression in the astrocyte cultures using or not CD11b magnetic beads negative selection and assessed by flow cytofluorometry. Data is representative of two experiments and in the right quadrant is shown the percent of $CD11b^+$ cell in the total astrocyte preparation.

Co-culture of T cells with astrocytes

Astrocytes were previously seeded at 40×10^3 cells per well in a 24 well plate and incubated overnight at 37°C in a humidified atmosphere containing 5% CO_2. For neutralization of TGF-β, astrocytes were washed with PBS and incubated in murine

cell culture medium (IMDM medium with 10% foetal bovine serum, penicillin-streptomycin (50 U/ml), 2-mercaptoethanol (50 μM) and L-glutamine (2 mM)) with an affinity-purified monoclonal antibody to TGF-β (40 μg/ml; 1D11) for 1h previously to proceed with the co-culture. Naive CD4+ cells (3×10^5) were added directly to the astrocyte culture or using transwell inserts (Corning) to evaluate changes in T cell differentiation, in the absence of cell contact. Co-cultures, in the presence of soluble anti-CD3 (1 μg/ml; affinity-purified clone 2C11) (48), were maintained overnight for RNA extraction or, alternatively, for 3 days for evaluating protein expression. Addition of soluble anti-CD28 was not necessary in co-cultures involving cell-contact, as astrocytes express in their membrane the co-stimulatory molecules CD80 and CD86 (Figure 4.2a). In co-culture conditions where there is no cell contact $CD4^+$ T cell viability and proliferation in the absence of anti-CD28 was confirmed using Click-it EdU (Invitrogen), following manufacturer's instructions. Briefly, $CD4^+$ T cells were cultured in the presence of soluble anti-CD3 (1 μg/ml) or its corresponding isotype control, as well as in the astrocyte co-culture conditions previously described. 2X EdU working solution in culture medium was prepared and added to equal volume of cell supernatant to have a final concentration of 10 μM EdU. After overnight incubation at 37°C in a humidified atmosphere containing 5% CO_2, cells were harvested, fixed, permeabilised and processed for EdU detection by flow cytometry with FACSCalibur flow cytometer (BD Bioscience). Figure 4.2b shows proliferation of $CD4^+$ T cells with soluble anti-CD3 in the culture conditions used for our studies (one representative of two conditions), but no proliferation in the absence of anti-CD3, indicating that the absence of anti-CD28 does not affect the survival of our $CD4^+$ T cells cultures in the conditions tested.

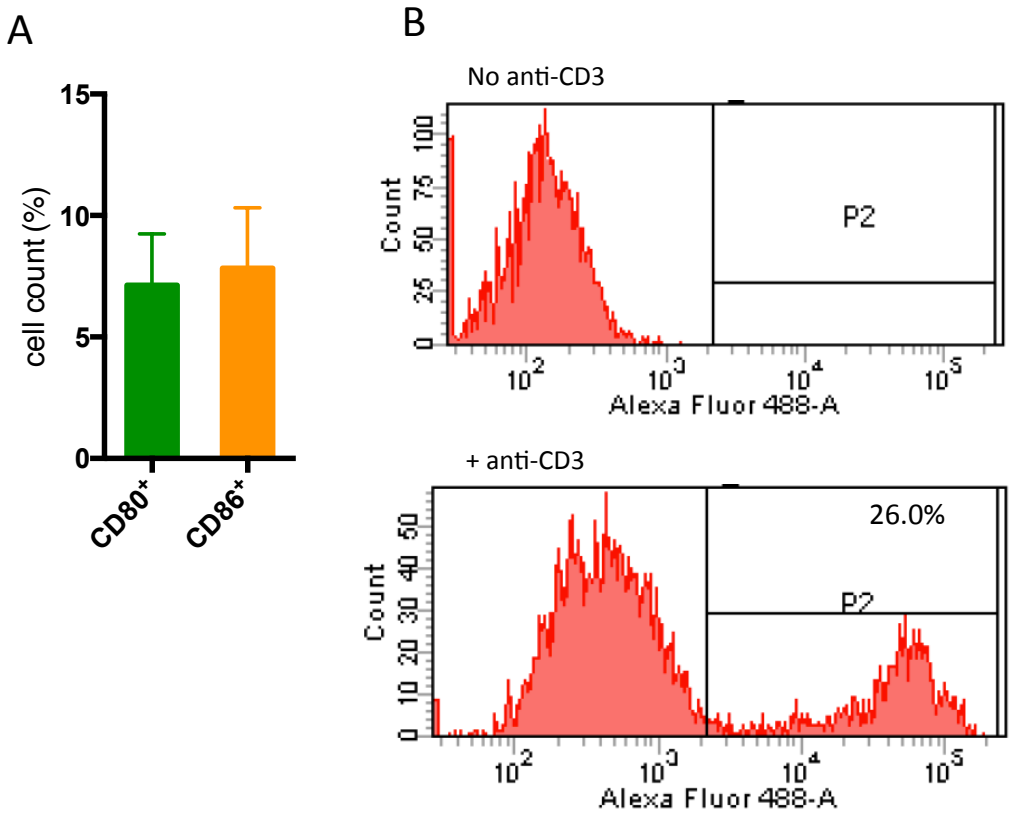

Figure 4.2: CD4⁺ T cells co-culture optimisation

(**a**) Cell surface CD80 and CD86 expression in astrocyte assessed by cytofluorometric analysis. Data (means ± s.e.m.) are from two experiments and shown as frequency of CD80⁺ or CD86⁺ in total astrocyte population versus isotype control. (**b**) Proliferation of CD4⁺ T cells, activated or not with anti-CD3, for 4 days was assessed by flow cytofluorometry as the frequency of cells positive for the thymidine analog EdU. Data is from one experiment representative of four.

4.2.2 Flow cytometry

After treatment, accutase (Invitrogen) was used to obtain a single cell suspension of astrocytes. Alternatively, non-adherent cells (T cells) were mechanically dissociated. Single cell suspension was washed once with FACS buffer (0.2% BSA, 0.05% sodium azide in PBS) and transferred into a FACS tube (Falcon) in a total volume of 80 µL of FACS buffer).

In all FACS analyses, cells were treated with rat anti-CD16/32 (2.4G2) (Biolegend) for 15 minutes at 4°C for blockade of Fc receptors before assaying on a FACSCalibur flow cytometer (BD Bioscience) using FlowJo 7.1 software (FLOWJO LLC). Cell surface staining was done by incubating the cell suspension with the corresponding labelled

antibodies (Table 4.1) for 30 minutes at 4°C. Cells were washed with 2 mL of FACS buffer and resuspended in 0.5 mL of FACS buffer for immediate analysis or fixed for intracellular staining. Cells requiring intracellular staining were fixed for 5 min with 2% paraformaldehyde in PBS (PFA; Electron Microscopy (EM)-grade; Electron Microscopy Sciences, USA (16% solution) at RT, permeabilised by washing with permeabilization buffer (0.5% Saponin (Sigma) in PBS) and incubated for 30 minutes with the corresponding labelled antibody in permeabilization buffer. Finally, cells were washed with FACS buffer and resuspended in 1% PFA in FACS buffer for analysis. All FACS analyses included the use of isotype control antibodies.

Table 4.1: Summary of antibodies used for Flow Cytometry analysis

Antigen	*Label*	*Clone*	*Manufacturer*	*Specificity*	*Isotype*
CD4	PE	GK1.5	BD Pharmingen	Mice	Rat IgG2a, kappa
LAP	PE	TW7-16B4	eBioscience	Mice	Mouse IgG1, kappa
GARP	APC	YGIC86	eBioscience	Mice	Rat IgG2a, kappa
Foxp3	FITC	FJK-16s	eBioscience	Mice	Rat IgG2a, kappa
GFAP	Alexa488	4A11	BD Pharmingen	Mice Human	Mouse IgG2b

4.2.3 Enzyme-Linked Immuno Assay

Cytokine quantification was kindly done by Dr. Carmine Vacca (Department of Experimental Medicine, University of Perugia). Briefly, mouse cytokines (IL-6, IL-10, IL-27 p28, TNF-α, IFN-β and IFN-γ) were measured in culture supernatants by enzyme-like immuno assay (ELISA) with specific kits (R&D Systems and ebioscience) following manufacturer's instructions and according to published procedures (43, 120). TGF-β1 was measured in serum free culture supernatants with TGF-β1 immunoassay system (Promega) following manufacturer's instructions. Supernatants were processed with and without acid treatment to detect bioactive and latent TGF-β1 respectively.

4.2.4 Nuclear extract for Immunoblotting

Astrocytes in 30-100 mm dishes were washed once with warmed PBS and harvested using the mild-trypsin ”like” reagent TripLE (Invitrogen). Then, $300x10^3$ cells were transferred into an Eppendorf, washed with fresh culture medium and resuspended in a final volume of 1mL with culture medium. Treatment for fast kinetic translocation studies (up to 2h) was directly done in the Eppendorf containing the cell suspension, which was incubated at 37°C in a humidified atmosphere containing 5% CO_2 for the time required for treatment. After cells were immediately placed on ice and pelleted at 3000 rpm for 5 minutes at 4°C using the Microcentrifuge (Eppendorf). Cells were washed once with cold PBS in the presence of phosphatase inhibitor complex (Roche) and the nuclear extraction performed using the Nuclear extract kit (Active Motif) following the manufacturer’s instructions. Briefly, cells were re-suspended in 150 µL of hypotonic buffer and incubated on ice for 15 minutes. Afterwards, NP40 was added to a final concentration of 5% and cells were vortexed for 10 seconds and spun down at 12,000 g for 30 seconds at 4°C. The supernatant containing the cytosol fraction was kept for validation of the method. The pellet containing the nuclear fraction was lysed with 40 µL of lysis buffer and incubated on ice for 30 minutes under 150 rpm agitation. The nuclear lysate was then centrifuged at 12000 rpm for 10 minutes at 4°C to remove nuclear debris and the supernatant containing the nuclear extract stored at -80°C. Purity of the nuclear extract was verified by immunoblotting at varying concentrations (5-20 µg) of the nuclear lysate versus the cytosolic component and analysed using as control GAPDH for the cytoplasm and fibrillarin as a nuclear marker. Figure 4.3 shows no presence of GAPDH in the nuclear lysate, as well as, no fibrillarin in the cytosol, indicating that there is no cross contamination between the nuclei and cytosol.

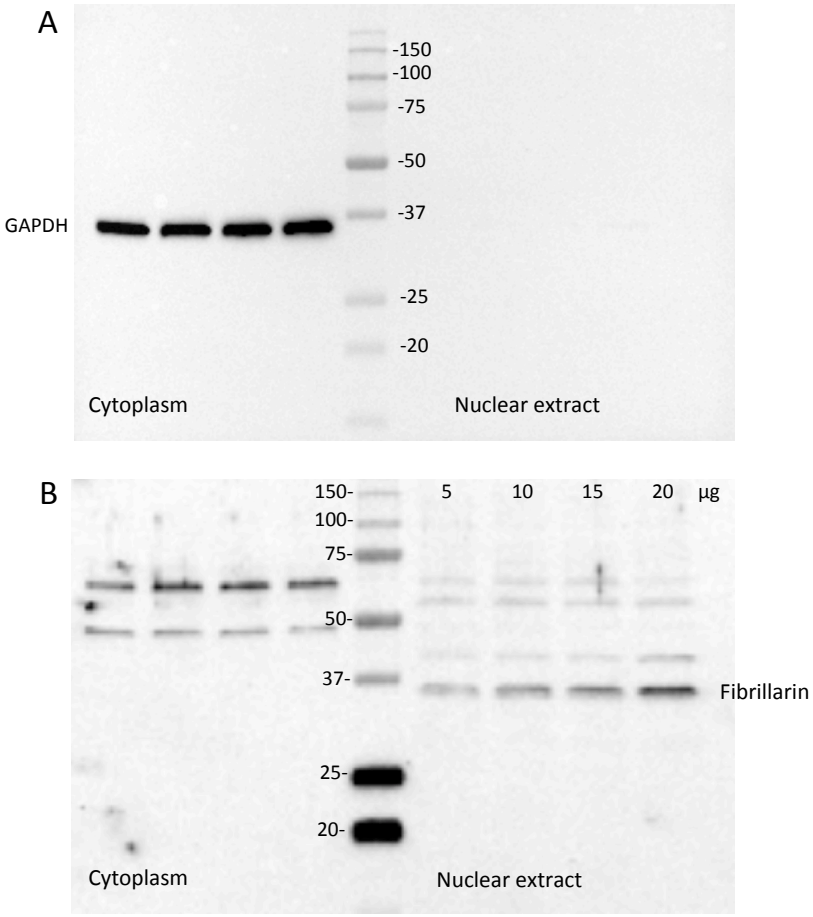

Figure 4.3: Validation of the nuclear extraction method

Cytoplasm and nuclear extract (5-20 µg) from astrocytes was analysed by immunoblot using specific antibodies for GAPDH (**a**) and Fibrillarin (**b**).

4.2.5 Quantitative real-time polymerase chain reaction

After treatment, RNA extraction from astrocytes or microglia was performed following the method described in section 3.3.1 (Trizol). In co-culture studies CD4 T cells where washed out with medium from the transwell and processed for Trizol RNA extraction. qRT-PCR procedures can be found in section 3.3.3 . Table 4.2 lists the primers used in this study.

Table 4.2: Primer sequences used in Chapter 4

Gene	*Forward sequence*	*Reverse Sequence*
Il-10	5'-GGCGCTGTCATCGATTTCTC -3'	5'-ATGGCCTTGTAGACACCTTGG -3'
Tnf-α	5'-TCTACTGAACTTCGGGGTGA -3'	5'-CACTTGGTGGTTTGCTACGA -3'
Tgf-β	5'- GCCTGAGTGGCTGTCTTTTG-3'	5'-TGGGGCTGATCCCGTTGATT -3'
Il-6	5'-CCGGAGAGGAGACTTCACAG -3'	5'- TCCACGATTTCCCAGAGAAC-3'
Igf-1	5'- ATCTGCCTCTGTGACTTCTTGA -3'	5'- GCCTGTGGGCTTGTTGAAGT -3'
Inf-γ	5'- ATA TCTGGAGGAACTGGCAA -3'	5'- CATGAATGCATCCTTTTTCG -3'
Il-23a	5'- CTTCACACCTCCCTACTA-3'	5'- CACTGCTGACTAGAACTC -3'
Il-12b	5'- CATCAAGAGCAGTAGCAGTTC -3'	5'- GTCCCTTTGGTCCAGTGT -3'
Ahr	5'- CCACTGACGGATGAAGAAGGA-3'	5'- ATCTCGTACAACACAGCCTCTC -3'
Cyp1a1	5'- GACACAGTGATTGGCAGAG-3'	5'- GAAGGTCTCCAGAATGAAGG-3'
Foxp3	5'- CCCAGGAAAGACAGCAACCTTTT-3'	5'- TTCTCACAACCAGGCCACTTG -3'
Rorγ	5'- ACAACAGCAGCAAGTGATGG -3'	5'- CCTGGATTTATCCCTGCTGA -3'
Tbp	5'- CCTGCCACACCAGCTTCTGA-3'	5'- GACTGCAGCAAATCGCTTGGG -3'
Gapdh	5'- GCCTTCCGTGTTCCTACCC -3'	5'- CAGTGGGCCCTCAGATGC -3'

4.3 Results

4.3.1 Adult astrocytes express AhR and this can be activated by KYN

Increased KYN levels in the CNS, found in several neurodegenerative diseases (3), could represent a mechanism to down regulate neuroinflammation associated to those diseases. We found that treatment of astrocytes with 100UI of IFN-γ for 48h resulted in IDO-1 induction (Figure 4.4a). However, we found that astrocytes could also uptake KYN produced by other cells and then degrade it through the KP without necessarily activate IDO-1 (284). Additionally we found that astrocytes constitutively express AhR as shown by mRNA (Figure 4.4b) and protein (Figure 4.4a). Of interest, KYN was able to activate AhR as shown by the induction of *Cyp1a1* after 6h treatment in both ex-vivo isolated astrocytes (Figure 4.4d) and cultured astrocytes (Figure 4.4c). Even though AhR has different DNA-binding sites, AhR:ARNT recruitment to the AHRE clusters in the promoter of cytochrome P450 (CYP)1 family genes remains one of the best predictor of AhR interaction with chromatin (186). Therefore, induction of *Cyp1a1* can be used as a marker of both canonical AhR activation and non-canonical AhR activation since a slight increase can be observed in the activation of genes that

do not necessarily require the AhR/ARNT complex. CYP1A1 activity increases oxidative stress and this can activate NF-κB and AP-1 transcriptional activity, increasing expression of pro-inflammatory cytokines. IL-6 is one of the best-known pro-inflammatory cytokine, its promoter contains binding sites for both AP-1 and NF-κB. It has been shown that *Il-6* expression can be induced by KYN-mediated activation of AhR in glioblastoma (10). In our study, we did not observe any increase of *Il-6* expression or cytokine release in astrocytes treated with 50 µM of KYN for 6 or 24h, respectively (Figure 4.4e,f). These results indicate that KYN-mediated AhR activation in astrocytes, under non-inflammatory conditions, does not primarily activate non canonical AhR pathway.

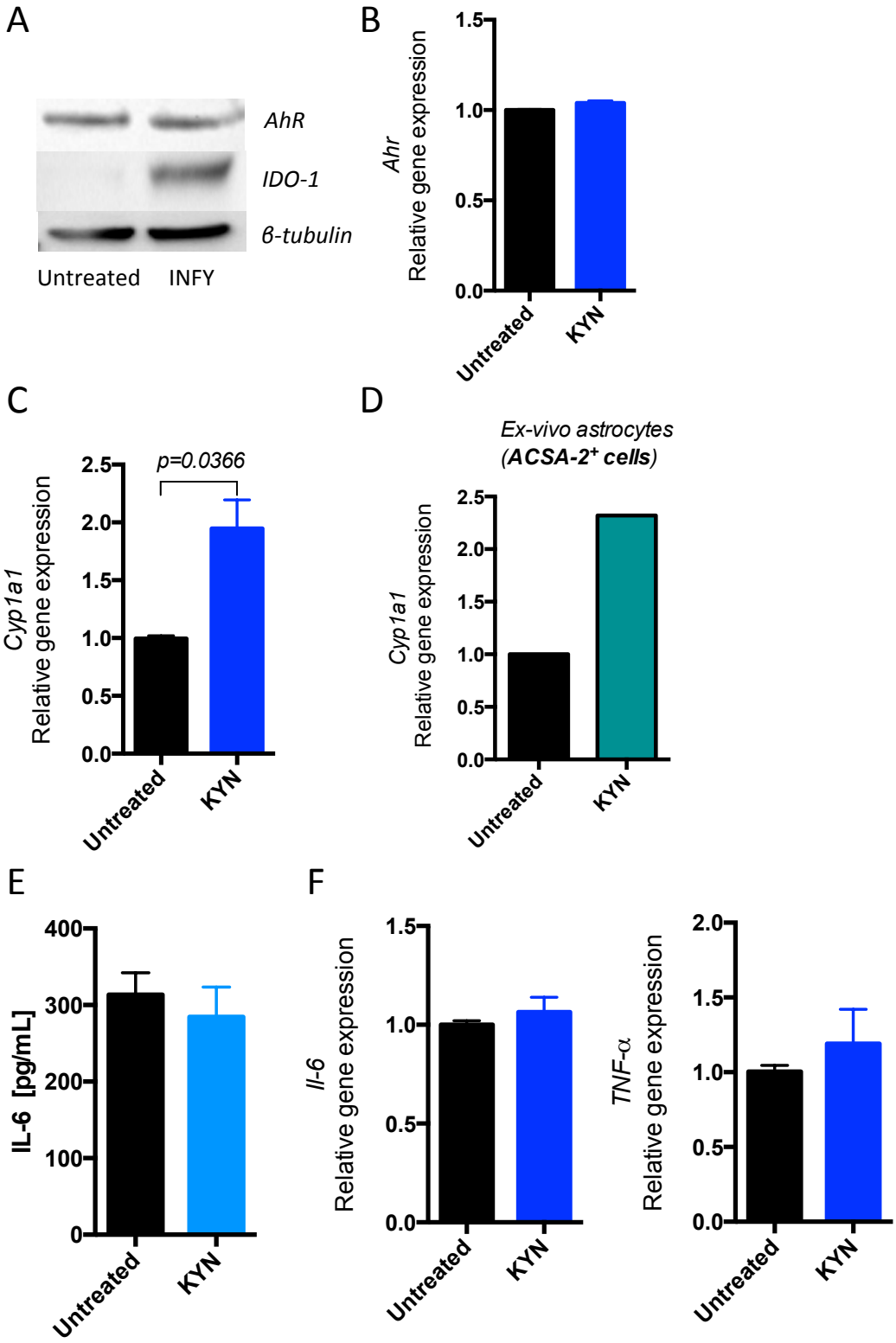

Figure 4.4: KYN is an endogenous ligand of AhR in astrocytes

(**a**) Astrocytes were treated with 100 UI of IFN-γ and qualitatively analysed by immunoblot by the use of specific antibodies. (**b**) Gene transcript expression of astrocytes after 16h treatment with 50 µM of KYN. Data (means ± s.e.m. of three experiments) are presented as normalised transcript expression in the samples relative to normalised transcript expression in untreated sample and show no induction of *Ahr* expression by KYN (Student's t-test). Gene transcript expression of

in-vitro cultured astrocytes (**c**,**f**) and ex-vivo isolated astrocytes (**d**) after 6h treatment with 50 μM of KYN. Data (means ± s.e.m. of three experiments) are presented as normalised transcript expression in the samples relative to normalised transcript expression in untreated sample (Student's t-test). (**e**) Cytokine measurement in supernatants of astrocytes treated with 50 μM of KYN for 24h. Data are means (± s.e.m.) from three experiments (treatment versus none; Student's t-test).

4.3.2 Astrocytes promote an immunoregulatory environment dependent on TGF-β and AhR

Microglia are the tissue-resident macrophages in the CNS and the only resident immune cells. They are essential in brain homeostasis from development through aging and, as tissue-resident macrophages, also participate in innate immunity (285). Astrocytes have previously shown to regulate microglia or CNS-infiltrating monocytes inflammatory response in EAE, activating them towards different phenotypes (279, 286) (Phenotype classification for macrophage is described in Figure 4.5). We studied the immune role of astrocytes by analysing, first in physiological conditions, the response that they provoke in microglia. The supernatant of 24h astrocyte cell culture was added to $1x10^6$ freshly isolated $CD11b^+$ cells from adult mice brain (section 4.2.1). We observed that microglia or CNS-infiltrating monocytes cultured for 16h in astrocyte media have higher *Il-10* expression and maintain basal levels of *Tnf-α*, *Il-6* and *Tgf-β* compared with non-astrocyte conditioned $CD11b^+$ cells (Figure 4.6a). This profile could be classified as alternative M2 polarisation, according to the macrophage classification (287). M2 microglia/monocyte activation is involved in immunoregulation, and tissue remodelling (288) and in the CNS plays an important role in synapse maintenance and plasticity because of its phagocytic capacity (289-291). Those are characteristic functions of the microglial homeostatic signature (292). Therefore, astrocyte normal function could be necessary to maintain the physiological signature of microglia and aberrant microglia could be a consequence of homeostatic astrocyte loss of function.

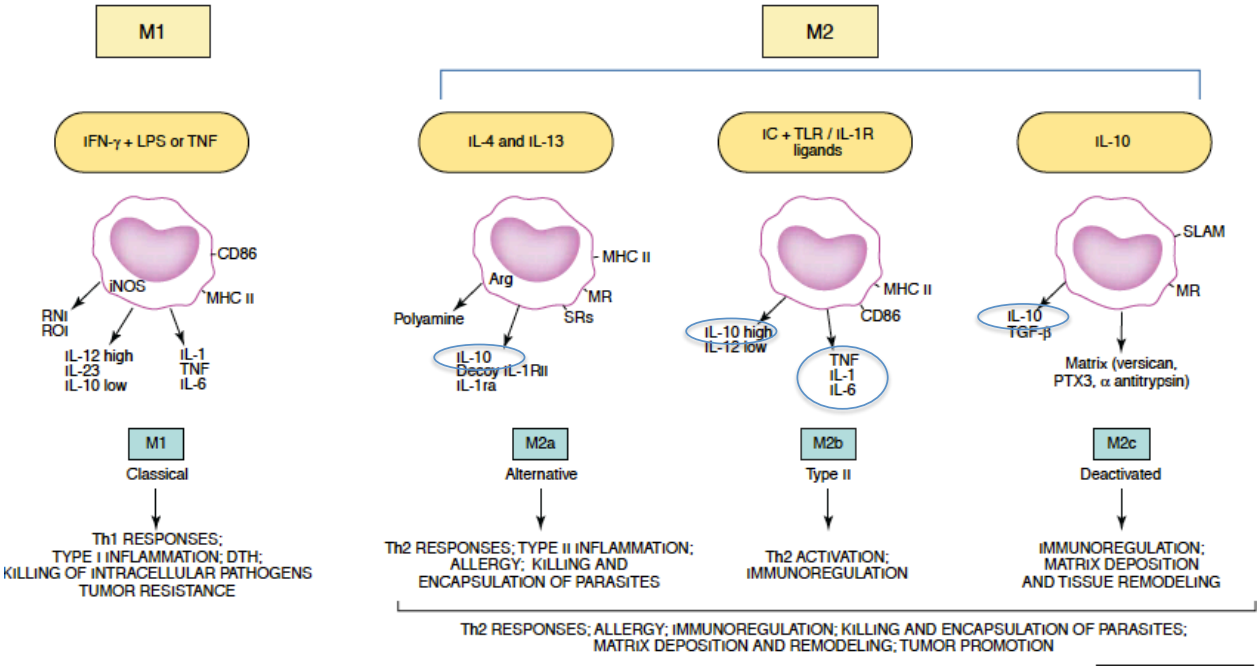

Figure 4.5: Macrophage (microglia?) classification

Microglia has been proposed to follow similar activation patterns to those observed in macrophages (290) and can be classified into two different phenotypes, commonly named as pro-inflammatory (M1) and alternative activated/anti-inflammatory (M2)(293). Differently to macrophages and characteristic of microglia, a specific microglial signature has been defined in freshly isolated adult microglia named microglial homeostatic signature (M0), which is dependent on TGF-β and can be differentiated from aberrant microglia (294). Figure adapted from Mantovani et al. (288).

Based on such results our next approach was to identify alterations in astrocytes normal function that could affect its activity in maintaining microglia physiological signature. However, due to the difficulty in isolating pure microglia and the lack of well-established available markers for M0/M1/M2 cell subsets, we continued our studies using $CD4^+$ T cells as a tool to further characterize the regulatory activity of astrocytes in immune cells. Naïve $CD4^+$ T cells, upon activation, can differentiate into several subsets. The environment provided by other cellular sources influence the differentiation of naïve $CD4^+$ T cells into their subsets (295). In order to determine which environment astrocytes provide we co-cultured naïve $CD4^+$ T cells with astrocytes and analysed the subset predominantly induced. Different transcription factors have been shown to be essential and specific for the different $CD4^+$ T cell subsets. The transcription factors *Tbet*, *Gata3*, *Rorγ* and *Foxp3* can be used as a markers for Th1 (296), Th2 (297), Th17 (298) and Treg (299) subsets respectively. We found that naïve $CD4^+$ T cells showed an increase in differentiation towards Treg

and Th2 cell subsets when co-cultured with astrocytes for 16 h in a transwell system and in the presence of anti-CD3 (Figure 4.6b). No changes in Th1 and Th17 were observed in the same conditions. The mechanisms underlying astrocyte-mediated differentiation of naïve $CD4^+$ T cells towards Treg subset was further characterised. Increase of $CD4^+$ $Foxp3^+$ cells was also observed when naïve $CD4^+$ T cells were co-cultured with astrocytes for 72h, in the same conditions as before (Figure 4.6c). Treg can be generated *in vitro* with TGF-β (300), therefore we evaluated possible implication of astrocytic TGF-β on Treg differentiation. Using the previous conditions (Figure 4.6c), blockage of TGF-β with an affinity-purified monoclonal antibody to TGF-β (40 μg/ml; 1D11), decreased the astrocyte-mediated differentiation of naïve $CD4^+$ T cells towards Treg (Figure 4.6d). AhR is constitutively expressed in astrocytes (Figure 4.4a), moreover the defects observed in AhR deficient mice (214) suggest that it could be playing a role in astrocyte normal physiology. To further study its immune role in astrocyte function we analysed the cytokine profile of WT astrocytes compared with AhR-/- over 48h. AhR null astrocytes showed increased production of the inflammatory cytokines IL-6 and IL-1β (Figure 4.6e), together with lower expression of *Tnf-α* (Figure 4.6f). Therefore, AhR could be required for astrocyte immunoregulatory function. In order to assess that, we co-cultured naïve $CD4^+$ T cells with WT and AhR-/- astrocytes for 72h. Astrocyte-mediated induction of Treg was lower in AhR null astrocytes compared with WT (Figure 4.6g). This indicates that AhR and TGF-β expression in astrocytes could be necessary for their immuneregulatory function and to control neuroinflammation. Preliminary data studying the role of TGF-β in astrocyte function is shown in the Appendix.

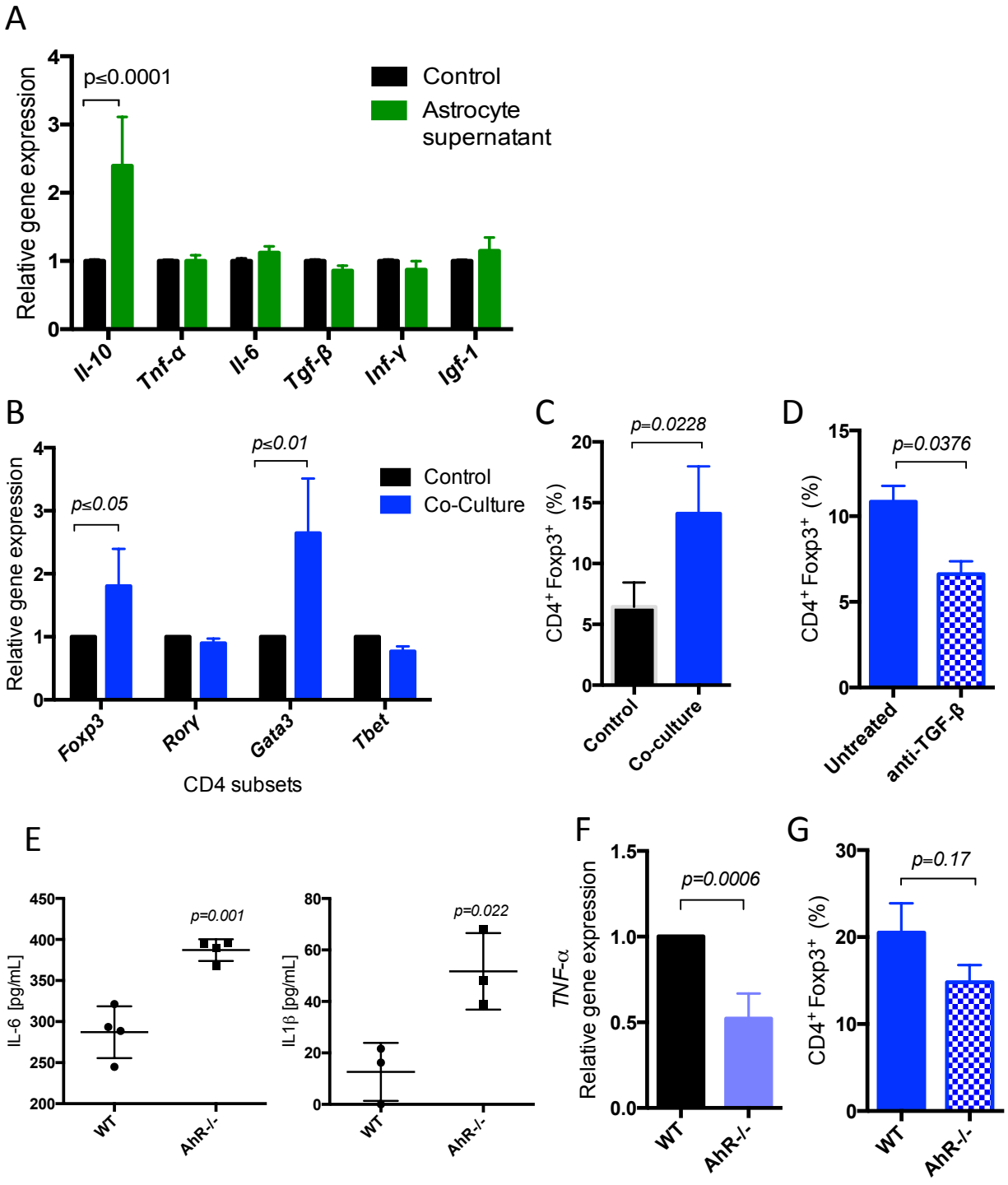

Figure 4.6: Astrocytes promote an immunoregulatory environment in the CNS. Role for TGF- β and AhR

(**a**) Gene transcript expression of microglia/CNS monocytes after treatment for 6h with 24h astrocyte supernatant. Data (means ± s.e.m. of three experiments) are presented as normalised transcript expression in the samples relative to normalised transcript expression in untreated sample (Student's t-test). (**b**) Gene transcript expression of $CD4^+$ T cells after co-culture with astrocytes in a transwell system for 16h. Data (means ± s.e.m. of three experiments) are presented as normalised transcript expression in the samples relative to normalised transcript expression in

non-cocultured sample (Student's t-test). (**c**, **d**, **g**) Foxp3 in $CD4^+$ T cells assessed by flow cytofluorometry as the frequency of $CD4^+Foxp3^+$. $CD4^+$ T cells where activated with anti-CD3. $CD4^+Foxp3^+$ frequency after 4 days co-culture of naïve $CD4^+$ T cells **(c)** in transwell system with astrocytes, (**d**) in transwell system with astrocytes where TGF-β was blocked and (**g**) with WT and AhR KO astrocytes. Data (means ± s.e.m.) are from two or three experiments. (Student's t-test). (**e**) IL-6 and IL-1β were measured in 24h supernatants of AhR KO and WT astrocytes. Data (means ± s.e.m.) are from three or four independent experiments (Student's t-test). (**f**) Basal gene transcript expression in WT and AhR KO astrocytes. Data (means ± s.e.m. of three experiments) are presented as normalised transcript expression in AhR KO sample relative to normalised transcript expression in WT sample (Student's t-test).

4.3.3 Activation of AhR by KYN promotes transactivation of RelB

We showed that AhR could be activated by KYN in astrocytes (Figure 4.4c). Additionally, AhR is involved in the immunoregulatory function of astrocytes (Figure 4.6g). However, the (1) AhR-dependent mechanisms involved in astrocytes immunoregulatory function and (2) KYN-mediated AhR genomic activity (targeting cytokines expression) in astrocytes needs to be clarified. Among different transcription factors that can interact with AhR, NF-kB has well characterised functions in the immune system (189) and it has previously shown to be inducible in astrocytes (301). Therefore, our first approach was to evaluate KYN-mediated AhR activity in the transactivation of several transcription factors of the NF-kB pathway. We observed that KYN induces translocation of RelB into the nuclei after 15 minutes of treatment (Figure 4.7a). KYN-mediated RelB translocation to the nuclei is dependent on AhR, as shown by the decrease of RelB translocation when AhR is inhibited with CH223191 (Figure 4.7b). In addition, KYN does not induce RelB translocation in AhR null astrocytes. Not only that, but AhR-/- showed considerably lower RelB basal levels compared with the WT (Figure 4.7c). To determine whether KYN can also induce RelB transcriptional activity, we evaluated mRNA expression of several cytokines involved in astrocyte inflammatory response and RelB transcriptional activity (279, 302). No changes in *Il-6*, *Tgf-β*, *Tnf-α* and *Igf-1* were induced after 6h treatment with KYN (Figure 4.7d). This indicates that inflammatory co-stimulus may be necessary in order to observe changes in KYN-mediated RelB transcriptional activity.

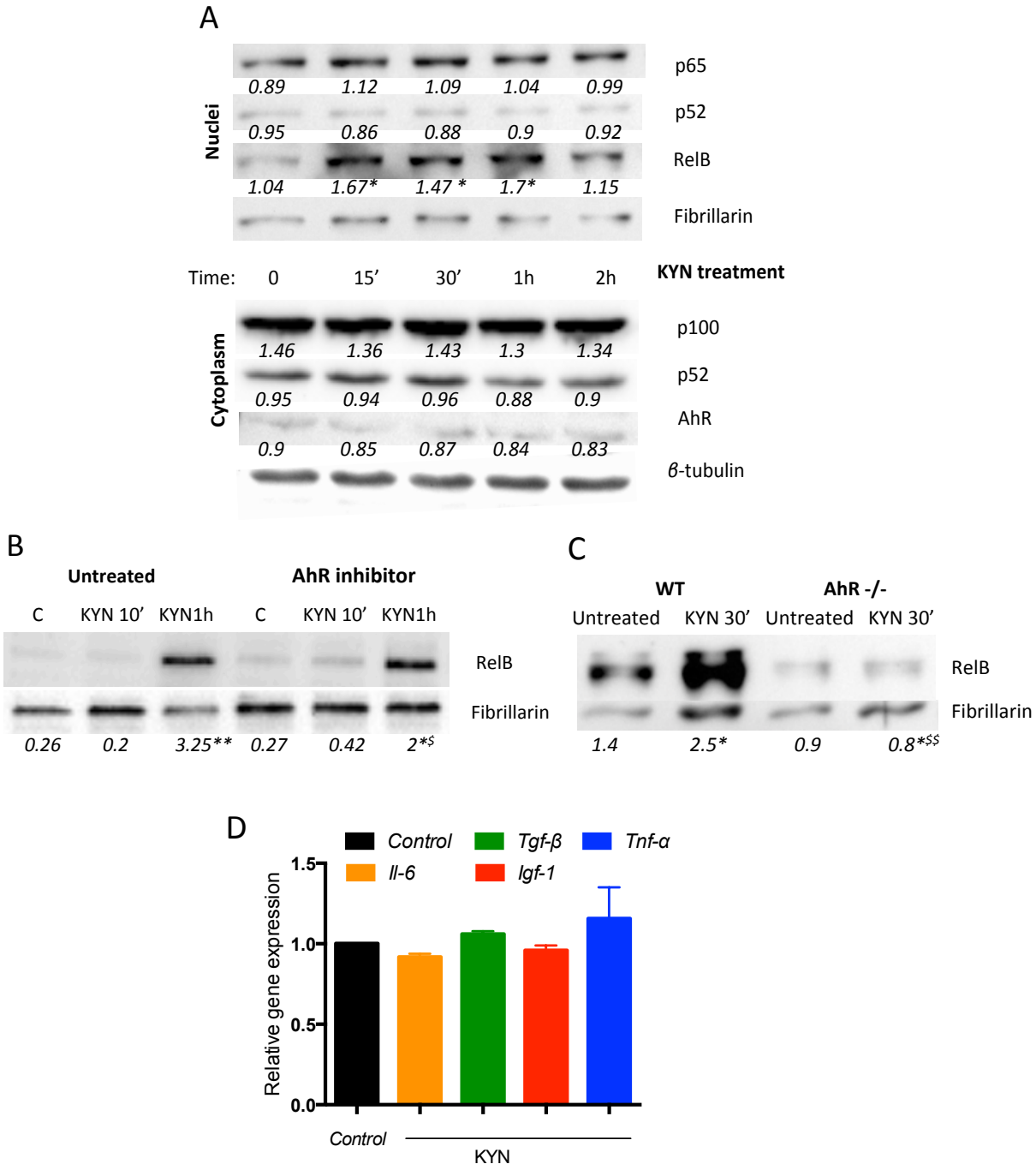

Figure 4.7: Activation of AhR by KYN promotes transactivation of RelB

(**a**) Immunoblot analysis of NF-κB from nuclear extract of astrocytes treated at different time points with 50 µM of KYN. Ratios are means of two experiments. *p≤0.01 (treatment versus none; Student's t-test). Immunoblot analysis of RelB from nuclear extracts (**b**) of astrocytes treated with KYN in the presence or not of CH223191 or (**c**) of WT and AhR KO astrocytes treated with KYN. Ratios are means of two or three experiments. *p≤0.01, **p≤0.005 (treatment versus none; Student's t-test), $p≤0.05 (AhR inhibitor versus no inhibitor; Student's t-test) and $$p≤0.001 (AhR KO versus WT; Student's t-test). (**d**) Gene transcript expression of astrocytes treated with 50 µM of KYN for 6h. Data (means ± s.e.m. of three experiments) are presented as normalised transcript expression in the samples relative to normalised transcript expression in untreated sample (Student's t-test).

4.3.4 Characterization of astrocyte inflammatory response to LPS

Astrocytes express toll-like receptors, including TLR-4 (279), which is activated by LPS. Activation of TLR-4 in astrocytes initiates a signalling through NF-kB, MAPK and JAK1/STAT1 pathways, which in turn induce the expression of pro-inflammatory cytokines (301) modulating immune responses (303). Therefore, we used LPS to trigger astrocyte inflammatory response and to study how activation of AhR by KYN could modulate this response. In order to address this issue, we first characterised the response of primary astrocytes cultures to LPS. We found that LPS activated NF-κB in astrocytes, as evidenced by nuclear translocation of the p65 NF-κB subunit 30 minutes after treatment with 10 ng/mL of LPS (Figure 4.8a). LPS induces the expression of specific NF-κB target genes (301, 304, 305) such as IL-27, TNF-α, IL-6 and IL-1β. We observed that LPS rapidly increased IL-6 and IL1- β production in astrocytes after 2h and TNF-α and IL-27 after 24 and 48h respectively (Figure 4.8b). Then we further analysed the modulation of mRNA for *Tnf-α*, *Il-6* and *Il-10* in astrocytes after treatment with LPS. We found the maximal induction after 6h of treatment (Figure 4.8c), and therefore, we took this time point for the following LPS treatments.

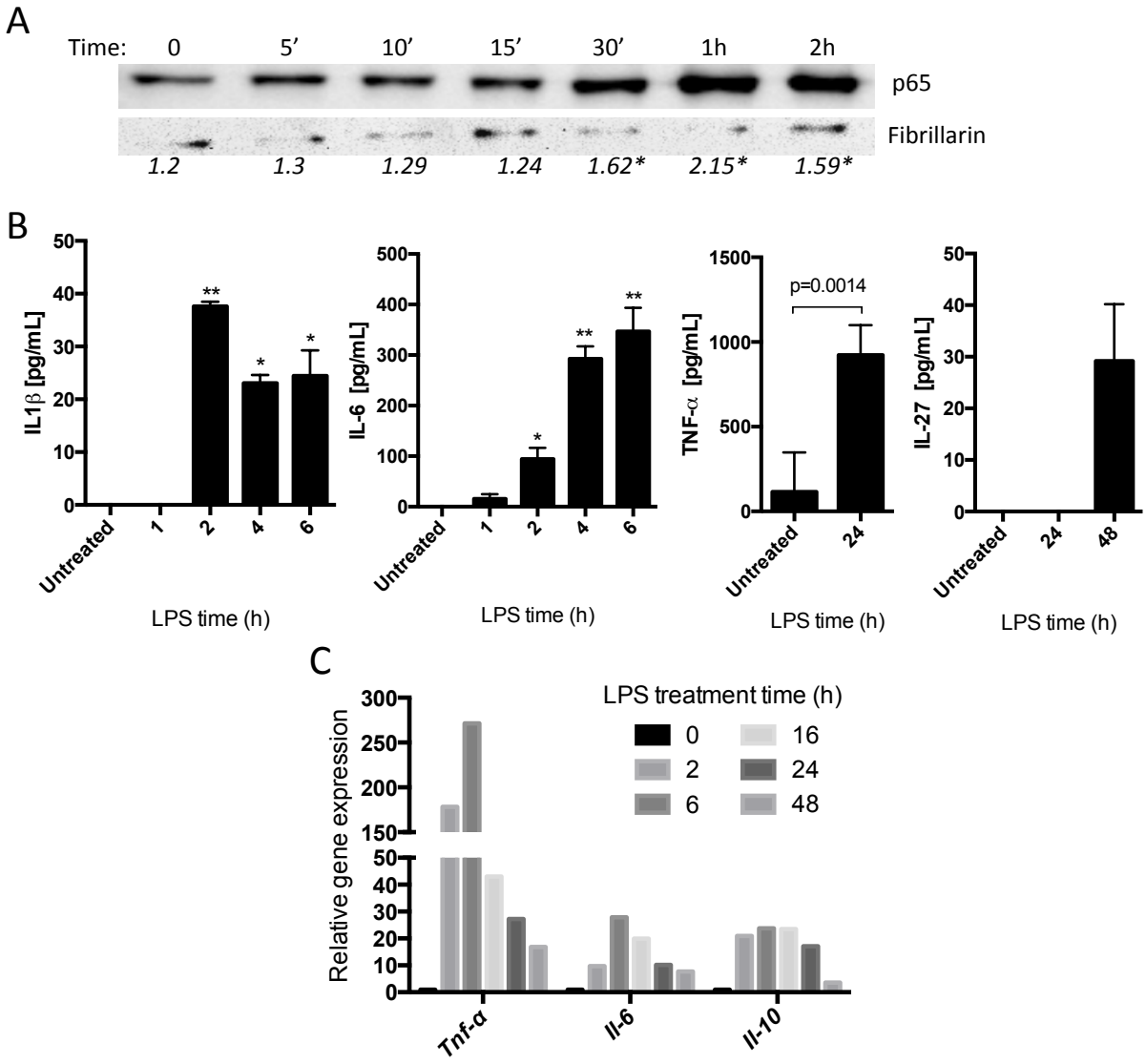

Figure 4.8: Characterization of astrocyte response to LPS

(**a**) Immunoblot analysis of p65 in nuclear extracts of astrocytes treated or not with 10ng/mL of LPS at different time points. Ratios are means of two experiments. *p≤0.05 (treatment versus none; Student's t-test) (**b**) Cytokine measurements in supernatants of astrocytes, treated with 10 ng/mL of LPS at different time points. Data (means ± s.e.m.) are from two or three experiments. *p≤0.05, **p≤0.01 (treatment versus none; Student's t-test). (**c**) Gene transcripts expression in astrocytes treated with 10ng/mL of LPS at different time points. Data (means ± s.e.m. of two experiments) are presented as normalised transcript expression in the samples relative to normalised transcript expression in untreated sample.

4.3.5 KYNA/KYN ratio modulates inflammatory response to LPS in astrocytes

To evaluate the immunomodulatory activity of KYN-activated AhR in response to an inflammatory insult, we pretreated astrocytes for 2h with 50 μM of KYN, followed by LPS for 6h. Expression of *Il-6*, *Il-10*, *Tgf-β1*, *Igf-1*, *Tnf-α*, *Il-23a* and *Il-12b* was evaluated by qRT-PCR (Figure 4.9a). LPS-mediated expression of *Il-6* was increased when astrocytes had been previously exposed to KYN, but no changes were observed in the other cytokines. IL-6 is a pro-inflammatory cytokine and activation of AhR by KYN, under inflammatory conditions, has been previously showed to decrease its production rather than increase it in other cell subsets (11). Therefore we questioned whether astrocytes could rapidly metabolise KYN to KYNA, being *Il-6* induction the result of KYNA activity instead of KYN. HPLC analysis of the astrocytes supernatant showed 4-fold increase of KYNA after 2h treatment with KYN (Figure 4.9b). Astrocytes can metabolise KYN to KYNA through the KATs. However, KAT-2 is the principal isoform responsible for KYNA synthesis in the brain (88, 89) and therefore, we used the selective and irreversible inhibitor for KAT-2, PF-04859989 (IC_{50}=263 nM) (306) to decrease KYNA synthesis. We treated astrocytes with KYN in the presence of 0.5 μM of PF-04859989. Expression levels of *Il-6*, *Il-10* and *Tnf-α* were determined after 6h stimulation with 10ng/mL of LPS. Inhibition of KAT-2 prevented the increase of *Il-6* expression observed in KYN pretreated astrocytes in response to LPS. In addition, when KAT-2 was inhibited, KYN pretreatment increased *Il-10* expression after LPS treatment (Figure 4.9c). No differences were observed in *Tnf-α* expression.

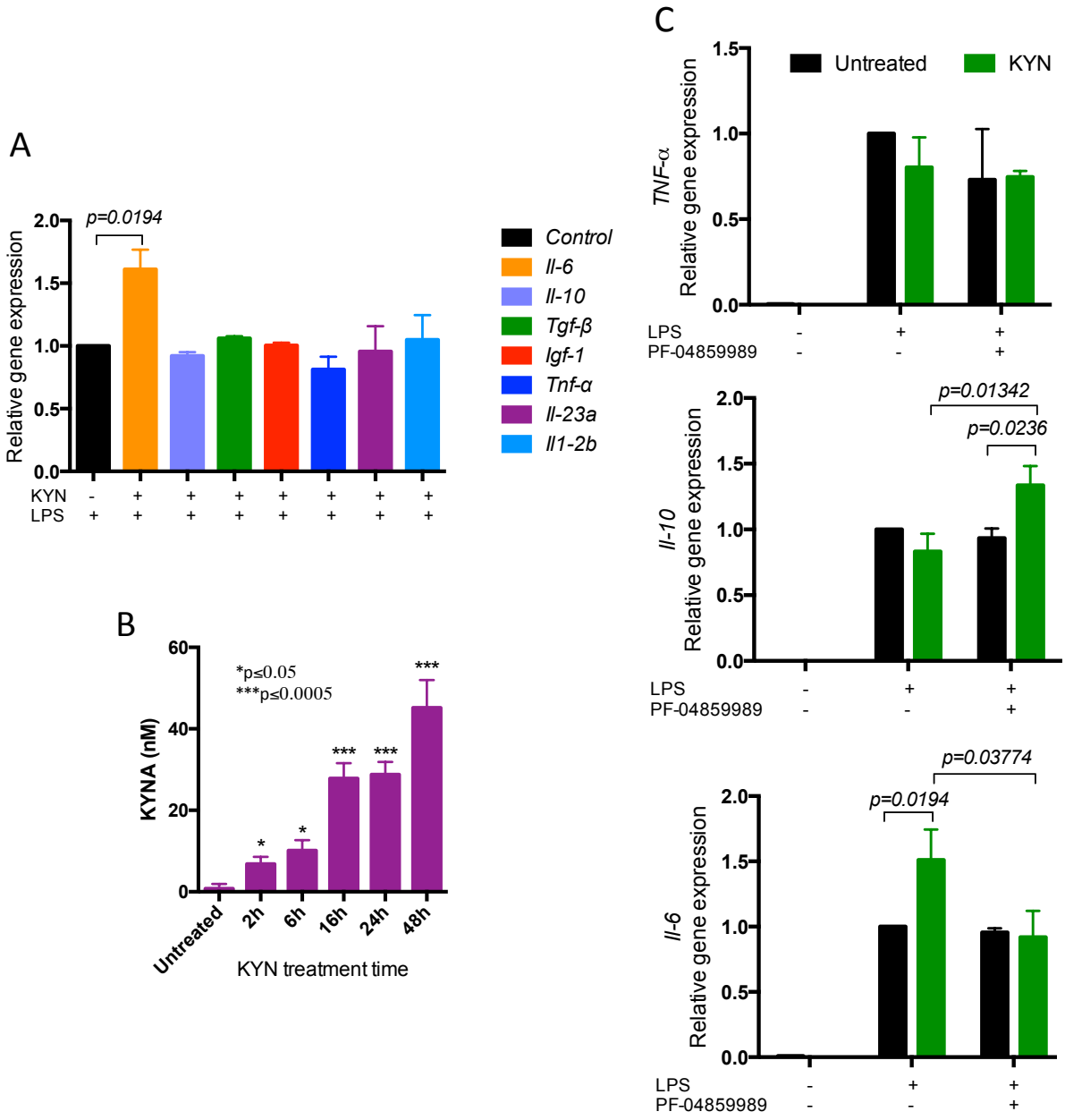

Figure 4.9: KYN modulate astrocyte's inflammatory response to LPS

(**a**) Gene transcript expression of astrocytes pretreated or not with 50 µM of KYN for 2h prior treatment with 10ng/mL of LPS for 6h. Data (means ± s.e.m. of three experiments) are presented as normalised transcript expression in the samples relative to normalised transcript expression in non-pretreated sample (Student's t-test). (**b**) KYNA quantification in astrocyte supernatant treated with 50 µM of KYN at different time points. Data (means ± s.e.m.) are from three experiments. *p≤0.05, ***p≤0.0005 (treated versus untreated; Student's t-test). (**c**) Gene transcript expression of astrocytes pretreated for 2h with 50 µM of KYN in the presence or not of PF-04859989, prior treatment with 10ng/mL of LPS for 6h. Data (means ± s.e.m. of three experiments) are presented as normalised transcript expression in the samples relative to normalised transcript expression in non-pretreated sample (Student's t-test).

4.3.6 KYN and de-novo synthesised KYNA, differently activate AhR

KYNA has also shown to activate AhR (123) and under inflammatory conditions to synergistically potentiate *Il-6* expression. Therefore KYNA could be competing with KYN for AhR activation, promoting *Il-6* expression. Activation of AhR by KYNA has only been described in hepatocellular carcinoma cell line and it could be different in astrocytes. We determined AhR activation by KYNA in astrocytes, shown as increase of *Cyp1a1* expression, at different time points and using 1 μM (higher concentration than the KYNA produced by astrocytes after treatment with 50 μM of KYN for up to 48h). KYNA did not increase AhR-mediated *Cyp1a1* expression at any time point, whereas KYN did increase *Cyp1a1* expression after 6h and after 48h (Figure 4.10a). However, KYNA, despite being able to activate AhR, could be showing no activity because is unable to cross the cell membrane and bind to AhR (267). Supporting this, we observed that *Cyp1a1* expression is higher in astrocytes treated with KYN for 6h when KYNA synthesis is not inhibited with 500 nM of PF-04859989 (Figure 4.10b). In addition, the higher *Cyp1a1* expression after 48h treatment with KYN is likely to be mediated by KYNA, as after 48h most of the KYN is metabolised to produce KYNA. This indicates that KYNA needs to be intracellularly synthetised in order to better activate AhR in astrocytes and that KYNA can poorly be taken up by astrocytes. Note that higher concentrations of PF-04859989 could not be used to completely block KYNA production as it has shown to activate cytochrome P450-mediated metabolism (306), probably by inducing AhR-mediated xenobiotic activation. In fact, we observed increase of *Cyp1a1* expression when using 5 μM of PF-04859989 and therefore we did our treatments at not higher dose than 500 nM. 500 nM of PF-04859989 did not activate *Cyp1a1* expression, but also did not completely blocked KYNA synthesis (data not shown). Knowing that KYNA can activate AhR in astrocytes, next we studied whether $KYNA^{high}KYN^{low}$-mediated activity in response to inflammatory trigger was dependent of AhR. AhR inhibition with 5 μM of CH223191 prevented the increase of *Il-6* expression observed in astrocytes pretreated with KYN in response to LPS (Figure 4.10c). Thus supporting the possibility of different ligand-mediated responses of AhR in astrocytes. The involvement of CH223191 and PF-04859989 themselves on *Il-6* and *Tnf-α* induction was discarded (Figure 4.10d).

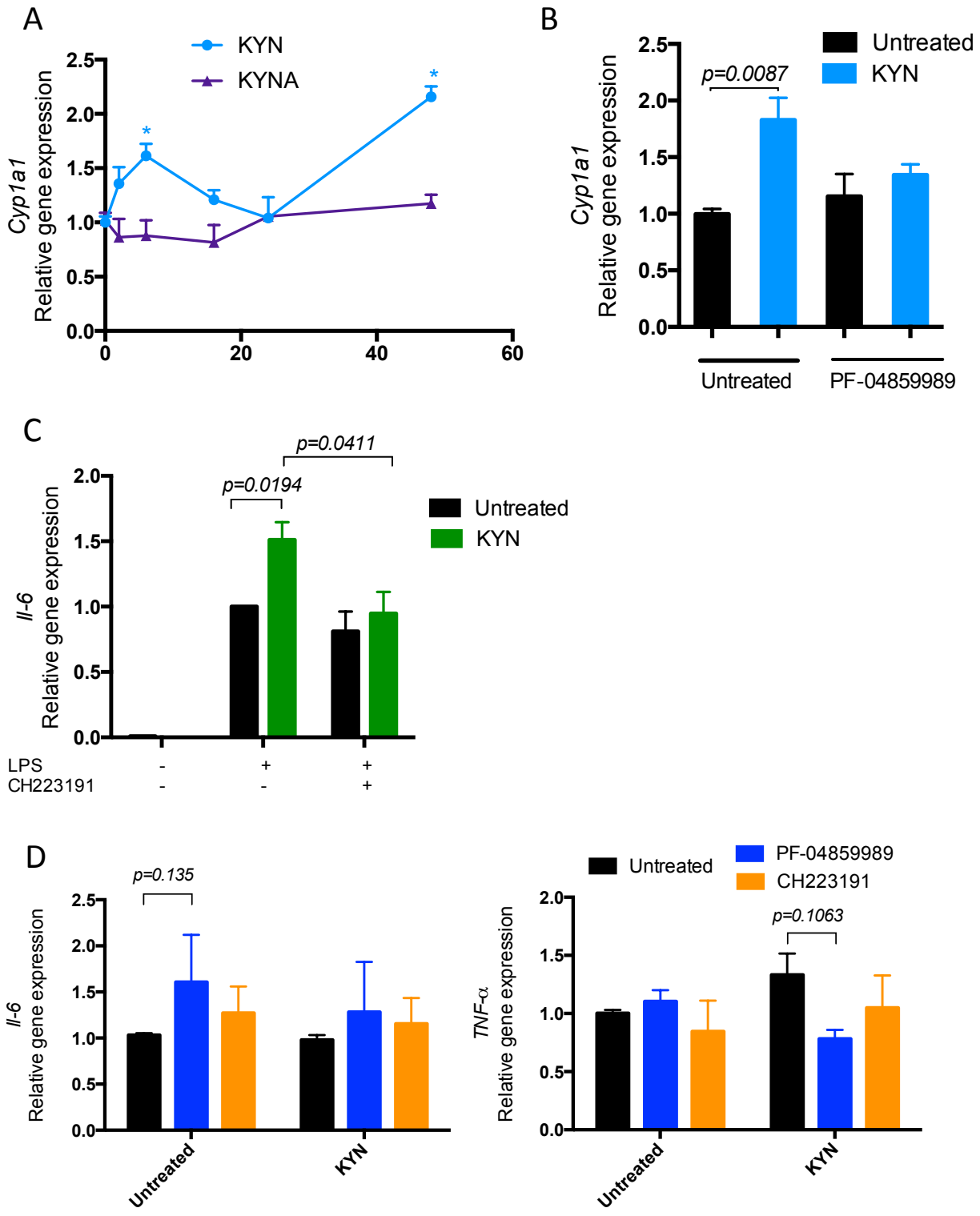

Figure 4.10: KYN and de-novo synthesised KYNA, by binding to AhR, promote different cytokine profile expression in response to LPS

(**a**) Gene transcript expression of astrocytes treated with 1 µM of KYNA or 50 µM of KYN at different time points. Data (means ± s.e.m. of three experiments) are presented as normalised transcript expression in the samples relative to normalised transcript expression in untreated sample. *p≤0.05 (Student's t-test). (**b**) Gene transcript expression of astrocytes treated for 6h with 50 µM of KYN in the presence or not of PF-04859989. Data (means ± s.e.m. of two experiments) are presented as

normalised transcript expression in the samples relative to normalised transcript expression in untreated sample (Student's t-test). (**c**) Gene transcript expression of astrocytes pretreated for 6h with 50 µM of KYN in the presence or not of CH223191 before treatment with 10ng/mL of LPS for 6h. Data (means ± s.e.m. of three experiments) are presented as normalised transcript expression in the samples relative to normalised transcript expression in non-pretreated sample (Student's t-test). (**d**) Gene transcript expression of astrocytes treated for 8h with 50 µM of KYN in the presence or not of CH223191 or PF-04859989. Data (means ± s.e.m. of two experiments) are presented as normalised transcript expression in the samples relative to normalised transcript expression in untreated sample (Student's t-test).

4.4 Discussion

Astrocytes are the most abundant cells in the CNS. Under physiological conditions they modulate synaptic activity and provide nutrients and support for neuronal survival (277). In accordance with their supportive role, our results show that the physiological function of astrocytes is necessary to maintain inflammatory balance towards tolerance and probably the homeostatic signature of microglia. We firstly showed that under physiological conditions astrocytes promote M2-like microglia/CNS monocyte phenotype, characterised by high *Il-10* expression (288). This phenotype further supports neuronal survival by participating in CNS remodelling and synapse maintenance (289). The physiological immunoregulatory function of astrocytes was shown in our co-culture studies with $CD4^+$ T cells. Astrocytes create an environment that drive activated naïve $CD4^+$ T cells, towards Treg differentiation. Even though this fact may not be relevant under healthy conditions, due to minimal $CD4^+$ T cells and astrocytes interaction, it shows that astrocytes participate in the anti-inflammatory or immune privileged CNS microenvironment. In contrast, under pathological conditions, such as inflammation or aging, astrocytes have shown to alter their activities and function leading to beneficial or detrimental effects on the surrounding cells depending on the stage or the type of pathology (277). Accordingly, reactive astrocytes have been shown to control or exacerbate neuroinflammation in the acute or chronic phase of EAE, respectively (279).

Most neuroinflammatory diseases show increased levels of KYN in the CNS (67). We observed that KYN induces the translocation of RelB into the nuclei, which requires AhR. RelB preferably forms heterodimers with p52 and p50, although an inhibitory interaction with RelA and homodimerisation has also been described (307). RelB-p50

interacts with DNA sequences similarly to RelA-p50 and activates *Tnf-α* expression (308). However, we showed that KYN did not induce translocation of the RelB heterodimer partner, p52 or increase *Tnf-α* expression (Figure 4.7d). This indicates that KYN may be increasing the compartmentalisation of RelB into the nuclei without activating its transcriptional partners, p50 or p52, and therefore explaining the lack of transcriptional activity we observed.

The RelB monomer is extremely unstable and quickly degraded. (307). The KYN-induced RelB translocation to the nuclei may be affecting the cellular location of the transcription factor, therefore making it less prone to its target promoters or degradation. Higher availability of RelB in the nuclei could promote its anti-inflammatory transcriptional activity when astrocytes are triggered with an inflammatory stimulus, such as LPS. We and others, have shown that LPS induces the translocation of RelA (p65) into the nuclei of astrocytes (301). By interacting with RelA, RelB can antagonize RelA-mediated transcription of pro-inflammatory cytokines (307) or compete for transcription factors, such as p50, modifying the final response to LPS (309). Binding of KYN to AhR not only induces RelB translocation into the nuclei (when high concentrations of KYN), but may be necessary to prevent RelB degradation (at physiological concentrations of KYN), as shown by decreased total RelB in AhR null astrocytes. We proposed that AhR could be acting as an E3 ubiquitin ligase for RelB. RelB poly-ubiquitinization prevents its degradation and increases its transactivational potential (199). Therefore, the physiological availability of KYN, by maintaining AhR activity and preserving RelB, could be necessary to assure the regulatory function of astrocytes in healthy CNS. In contrast, the translocation of RelB into the nuclei, induced by high KYN levels, may prevent an exacerbated inflammatory response against an inflammatory trigger (LPS). In support of this, we showed that KYN increases *Il-10* expression in response to LPS and this could be a consequence of its activity in RelB. Accordingly, RelB-mediated *Il-10* expression has previously been described in bone marrow DCs and has been shown to require functional AhR (310). Moreover, activation of AhR by KYN in cDC showed to increase *Il-10* expression (11).

Nevertheless, we showed that the effects of AhR activation by KYN in astrocytes can be disguised by its rapid KAT-mediated degradation to KYNA, and can only be

observed when KAT-2 is inhibited. Both, KYN and KYNA have been shown to be ligands for AhR (11, 123) and thus could be competing or interfering with each other. Additionally, we observed that KYN and KYNA can induce a different AhR-mediated response. We demonstrated that while a high KYNA/KYN ratio promotes *Il-6* expression in response to LPS, increasing the ratio towards KYN favours *Il-10* expression. This is in accordance with previous studies showing that under inflammatory conditions KYNA synergistically potentiates *Il-6* expression through AhR activation (123). Nevertheless, the relative affinity of KYN or KYNA for AhR is not clear. In hepatic cells, KYNA is a more potent AhR agonist (123), while in glioblastoma cells, KYN is the most potent AhR agonist (10). In our mouse primary astrocyte cultures, KYN-mediated *Cyp1a1* expression, which is almost entirely dependent on AhR activity, was lower in the presence of KAT-2 inhibitor. This would indicate that, in astrocytes, KYNA is a more potent activator of AhR. However, it should be taken into account that *Cyp1a1* is induced through AHRE driven response (canonical), and in a lower extent, through non-canonical AhR activation (186). AhR has an extremely promiscuous binding pocket, containing different binding sites (311, 312). Radioligand competition assays with TCCD showed that KYNA binds to the AhR TCCD-binding pocket with an IC_{50} of 1.4 μM. Therefore, activation of AhR by KYNA could activate AHRE, similarly to TCCD (123). In contrast, the KYN binding site in AhR differs from TCCD (11). This indicates that while KYNA better induces an AhR-mediated AHRE driven response and *Cyp1a1* expression, KYN favours the non-canonical or the non-genomic AhR activation, with the final outcome of a different gene transcription profile or activity. Therefore, increased *Il-6* expression by a high KYNA/KYN ratio under an inflammatory trigger could be a consequence of increased oxidative stress mediated by CYP1A1 activity. We demonstrated that $KYNA^{high}KYN^{low}$-mediated *Il-6* expression required AhR, as inhibition of AhR with CH223191 restored *Il-6* expression. Even though we observed that CH223191 only slightly reduced KYN-mediated RelB translocation into the nuclei, its activity blocking KYNA-mediated *Il-6* induction was stronger. The antagonist CH223191 is a ligand-selective antagonist of the AhR TCDD binding site (313), which will therefore preferably block KYNA -mediated AhR activation.

IL-6 is important in the initiation of inflammation and recruitment of innate immune cells in the CNS (314, 315). The main function of IL-10 is to suppress pro-inflammatory cytokine production in order to limit tissue damage and to support

neuronal survival by activating anti-apoptotic gene expression (316). Importantly, it should be considered that the increase in *Il-6* expression attributed to KYNA does not necessarily imply that KYNA induces inflammatory responses in astrocytes. In fact, we only observed an increase in *Il-6* expression with *Tnf-α* expression being unaffected. Moreover, an increase in astrocyte IL-6 release could have a beneficial role as an initial response towards an inflammatory event in the CNS. IL-6 can target neural cells inducing neurite outgrowth, neurogenesis, synaptic plasticity and transmission, which has shown to be beneficial under acute neurodegenerative stimuli, such as stroke or trauma (317). It is also involved in the activation of astrocytes and astroglial scar formation in injured CNS (318), which prevents exaggerated immune cell infiltration to the CNS. Moreover, IL-6 is also important as a mediator of astrocyte differentiation from undifferentiated precursor cells (221). However its over-production, upon chronic release, is associated not only with increased pro-inflammatory events, but also with neuronal dysfunction (317). Therefore, a physiological increase in KYNA concentration could be important in enhancing astrocyte and neuronal activity, favouring recovery of neural function, but detrimental upon accumulation or exaggerated concentrations.

Overall, KP activation could be a mechanism to effectively control an overwhelming acute inflammatory insult, by inducing a non canonical NF-kB response and IL-10 production. However, prolonged KP activation, in chronic diseases, will lead to an increased KYNA/KYN ratio and long-term IL-6 production, which will affect astrocyte's physiology. In agreement with our results, Mayo et al. showed that in mice with EAE, astrocytes have lower *Il-10* and higher *Il-6* expression during the chronic or progressive phase of the disease (279). Thus, maintained high levels of IL-6 in conjunction with other abnormalities caused by a long-lasting insult could exacerbate chronic neuroinflammation and contribute to a severe reactive astrogliosis state (Figure 4.11).

4.5 Conclusions

In summary, our results demonstrated that ligand-dependent activation of AhR in astrocytes is necessary to control inflammatory responses under acute pathological conditions, by (1) promoting RelB translocation into the nuclei, which decreases transcription of pro-inflammatory cytokines and (2) increasing *Il-6* expression, which mediates astrocyte activation and glial scar formation and prevents immune cell infiltration into the brain.

Moreover, we provided evidence indicating that the type of response mediated by astrocytes varies depending upon the KP metabolite balance, as they each differently activate AhR, promoting particular transcriptional activity. Therefore, long-term KP metabolite imbalance in activated or aged astrocytes, could promote severe reactive astrogliosis by modifying their normal response to inflammation, promoting sustained IL-6 production.

Supporting the important role of astrocytes in physiological conditions, we observed that their interaction with brain resident cells or with immune cells, could be necessary to maintain an anti-inflammatory environment and to assure clearance and plasticity in the CNS, both being activities essential in preventing neurodegeneration in the aged brain.

In conclusion, physiological levels of KP metabolites could be necessary to assure the essential protective function of astrocytes in the healthy brain, whereas abnormalities in KP metabolites, due to a pathological condition, could help to resolve an acute insult, but when the repair is not possible, worsen the disease. In addition, the activity of KP metabolites in neuroinflammation seems to be closely mediated by AhR in astrocytes.

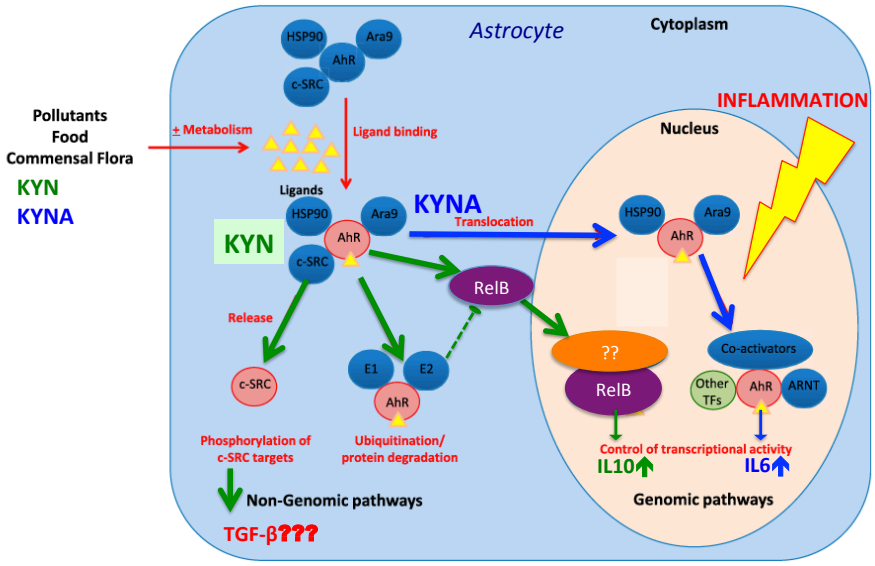

Figure 4.11: Scheme representing the involvement of KP metabolites in neuroinflammation

AhR can be activated differently by KYN and KYNA. KYN induces translocation of RelB into the nuclei, promoting a non-canonical NF-κB response and *Il-10* expression under inflammatory conditions. The fast degradation of KYN into KYNA can diminish this effect by the ability of KYNA to also bind to AhR. Thus, inducing a different response against inflammation, with the final outcome of increased *Il-6* expression. Adapted from Quintana et al. (214).

4.6 Future directions

4.6.1 In order to better mimic neurodegenerative diseases, using an insult other than LPS would be more appropriate to study kynurenines-dependent activation of AhR in response to inflammation

Even though LPS is a good mediator of inflammation, its relevance to study neurodegenerative diseases is debatable. Despite its isolation from the peripheral immune activity, the CNS cells are equipped with recognition tools allowing them to become aware of infectious agents and to build up immune responses (291). Astrocytes express TLR and respond to TLR agonists by releasing pro-inflammatory molecules (301). However, the inflammatory cascade induced by LPS is probably disproportioned and far stronger than the inflammation found in a neurodegenerative environment. Additionally, even though astrocytes can modulate immune responses (303), it is not their main role and the severe activation induced by LPS could cover up or diminish the effects of our treatments.

More relevant inflammatory triggers (such as amyloid beta, prion or miss-folded proteins characteristic of specific neurodegenerative diseases) will need to be used to further elucidate how KP metabolite imbalance (by binding to AhR) mediates inflammatory responses in neurodegeneration. Although we observed differences in IL-10 and IL-6 regulation, different inflammatory stimuli will activate different pathways and therefore the final outcome of AhR activity could be different (Figure 4.12).

4.6.2 KAT branch of the KP in astrocytes

In the CNS, astrocytes are the predominant cells expressing the KAT enzymes (67). They express four different isoforms, although KAT-2 has been shown to be the principal isoform responsible for KYNA synthesis in the brain (described in section 1.1.3). All KATs isoforms have several metabolic activities other than KYNA synthesis and alteration in their activity can not only affect KYNA/KYN ratio, but also other substrates concentrations.

Accordingly, KAT-2 inhibition not only decreases KYNA levels, but can also increase its other substrate, aminoadipate, which can only be degraded by KAT-2 and can have activity in glial cells (80, 86). The selective irreversible KAT-2 inhibitor, PF-04859989, did not completely block KYNA synthesis at 1 μM. This indicates that upon KAT-2 inhibition, the other KATs can degrade the increased levels of KYN to produce KYNA. All KATs have high Km values for KYN (78) and therefore, increase in KYN (upon KAT-2 inhibition) will displace KAT-1, 3 and 4 activities for their main substrates and also affect some α-ketoacids concentrations (amine acceptors of the reaction). Among those α-ketoacids, some have shown immunoregulatory activity, such as phenylpyruvate (319), and changes in their concentrations could also influence the overall immune response of astrocytes.

Summarizing, in addition to the high KYNA/KYN-mediated AhR activity, increase in other KAT substrates concentrations (as a consequence of KAT-2 inhibition) could also be mediating the inflammatory response of astrocytes to LPS. Therefore, future studies should done to be addressed that (Figure 4.12).

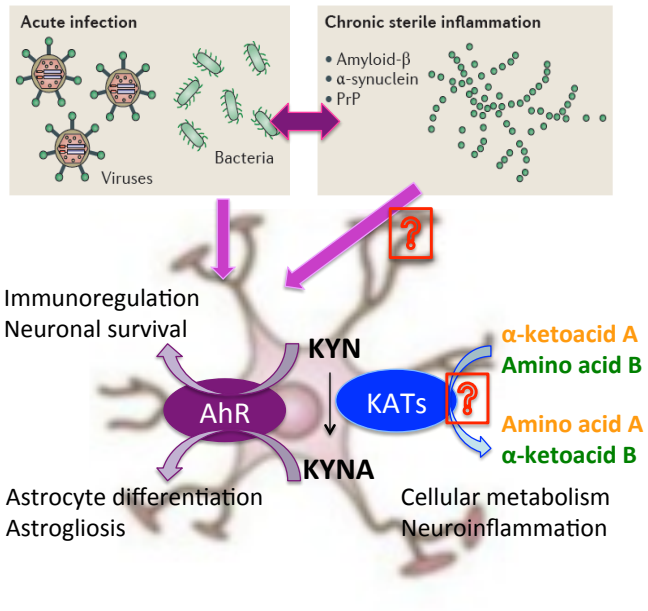

Figure 4.12: Scheme representing the two points that need to be further investigated

First how KP metabolites abnormalities affect AhR-mediated response to chronic sterile inflammation. Second whether, additionally to variations in KYNA/KYN ratio, abnormalities in KATs substrates, other than KYN, could also be affecting the inflammatory response of astrocytes.

Chapter 5

Interaction between Kynurenine 3-monooxygenase and cellular bioenergetics

5.1 Introduction

The KP represents the main route for the catabolism of TRP that ultimately leads to the formation of the essential co-factor NAD+ (Figure 1.1). TDO or IDO-1 and IDO-2 (18) (5), which are oxidation catalysts of KYN (320), catalyse the first and rate limiting step of TRP catabolism. KYN is then further metabolised by two branches of the KP. The first branch utilizes the enzyme KAT to produce the neuroprotective KYNA while the second branch uses KMO that leads to production of the neurotoxic metabolites 3-HK and QUIN. Under pathological conditions, the KP is over-activated and as KMO has higher affinity for KYN than KAT (321), KYN will be driven through the KMO branch.

KMO is an oligomeric protein that contains non-covalently bound flavin adenine dinucleotide (FAD) co-factor. It belongs to the monooxygenase family and is located in the outer mitochondrial membrane where it converts KYN to 3-HK. KMO catalyse

the incorporation of one atom of molecular oygen into KYN in the presence of NADPH as an electron donor. The reaction takes place in two half-reactions: (1) During the reductive reaction, the prosthetic group FAD is reduced to $FADH_2$ by NADPH and (2) during the oxidative reaction, $FADH_2$ acts as an electron donor and it is oxidised by oxygen to FAD, with the subsequent hydroxylation of KYN (68). The aromatic substrate, KYN, acts as an effector for NADPH by stimulating the rate at which NADPH reduces FAD. This prevents the reduction of FAD in the absence of aromatic substrates that ordinarily, would result in the loss of reducing equivalents and in the formation of hydrogen peroxide during FAD re-oxidation (68). However, the product of the reaction (3-HK), can also act as an effector for NADPH, but as 3-HK is not the substrate of the reaction, the following $FADH_2$ re-oxidation leads to the formation of H_2O_2 (70). Consequently, 3-HK has been described as a powerful generator of ROS and potential endogenous neurotoxin. Studies in neuronal cultures *in-vitro* showed that 3-HK induces ROS-dependent apoptosis through hydrogen peroxide production (143-145) potentially involving reduction of the redox-active metal ions copper (Cu) and iron (Fe) (322). Further studies demonstrated sodium-dependent neutral amino acid transporters take up 3-HK (147). Nevertheless, it should be acknowledged that 3-HK pro-oxidant activity has only been shown at non-physiological concentrations. At physiological or pathological concentrations, 3-HK seems to be responsible for maintaining cellular redox homeostasis (148) (154).

Activation of the KMO branch of the KP can affect the intracellular redox balance, potentially impairing cellular bioenergetics. ROS induction by 3-HK can promote mitochondrial dysfunction by several mechanisms involving Ca^{2+} release from ER reservoirs (144), decrease in activity of electron transport system (ETS) complexes (323), damage to mtDNA, decrease of e^- donor substrates (324) and mitochondrial membrane lipid peroxidation (325). Prolonged exposure to QUIN also induces excitotoxicity. QUIN stimulates NMDA receptors causing Ca^{2+} overload, which can result in the collapse of the mitochondrial proton gradient, inducing a bioenergetic crisis (326).

Although acute and chronic exposure to 3-HK and/or QUIN, resulting from increased KMO activity can lead to oxidative damage and potentially apoptosis (327), activation of KP is necessary for *de novo* synthesis of NAD^+. NAD^+ is required for ATP production

through glycolysis and to generate the substrates (e^- donors) necessary for ETS function. This emphasises the importance of understanding KMO function and regulatory mechanisms, particularly in neurons, which are highly sensitive to oxidative stress and energy deprivation (273).

As activation of KMO may induce the production of neurotoxic metabolites, its inhibition may increase the neuroprotective KYNA, which makes KMO an interesting potential target in neurodegenerative disease therapy. Indeed, it has been observed that ischemic brain damage can be reduced by KMO inhibition, possibly by shifting KYN metabolism to KYNA production thereby reducing NMDA activity (328). KMO inhibition also prevents ataxia and death in mice infected with the malaria parasite *Plasmodium*, correlating with higher levels of KYNA (329). More recent studies have shown that KMO inhibition has beneficial effects in animal models of Huntington's and Alzheimer's Disease (330). In addition, KMO inhibition can protect against mutant Huntingtin protein in yeast. This effect is linked with a reduction of 3-HK, QUIN and ROS production. However, it is believed that these events occur independently of the NMDA receptor (232), confirming other studies that have shown multiple mechanisms of KMO-mediated neurodegeneration other than QUIN-dependent NMDA excitotoxicity for review see Guillemin: *Quinolinic acid, the inescapable neurotoxin* (139).

Even though neurons express KMO they cannot produce QUIN, but they are known to produce 3-HK (275). 3-HK has shown to be pro-oxidant and synergistically potentiate QUIN toxicity (150) as *in vivo* studies suggest that 3-HK could be neurotoxic at lower concentrations when co-injected with QUIN, indicating a synergistic potentiation of QUIN toxicity (150). Therefore, we hypothesised that neuronal KMO and cell-autonomous 3-HK may be the co-stimulatory signal needed for excitotoxicity.

In order to further study the mechanisms of neurotoxicity induced by KMO activation, we used a mammalian cell line to overexpress KMO. We observed that increased KMO activity decreases mitochondrial spare respiratory capacity (SRC) and increase ROS production. This effect could not be reproduced by extracellular addition of 3-HK, implying low transport of 3-HK across the membrane and in agreement with previous studies showing that supra-physiological concentrations of 3-HK are needed

to induce toxicity (154). We conclude that when cellular energy turnover is compromised, the KP is redirected through the KMO branch in order to increase NAD^+ production, but with the long-term outcome of mitochondrial dysfunction. Accordingly, we describe KMO as a double edge sword for neurons. Its moderate activation can promote cellular bioenergetic state, but chronic activation will not only deplete energy stores but also induce oxidative damage.

5.2 Methods

5.2.1 Cell cultures

Human primary neurons

Human primary neurons were prepared and maintained as described in section 3.1.1

HEK293

Maintenance

HEK293, human embryonic cancer cells, were cultured in 100mm tissue culture dishes for up to 25 passages and maintained in Dulbecco's Modified Eagle's medium (DMEM) culture medium (Invitrogen) supplemented with 10 % FCS and 1X Antibiotic-Antimycotic at 37°C in a humidified atmosphere containing 5% CO_2.

HEK-pEZ[-] and HEK-pEZ[KMO] were cultured as HEK293 but using selection medium (complete DMEM culture medium with 300 μg/mL of G418).

Splitting cell lines

When 80-90 % confluence, cell lines were split by mechanically dissociating them with the pipette. The cell culture medium was first replaced with 10 mL of fresh culture medium and the harvested cells were then diluted 10 times in complete DMEM culture medium or selection medium. 10mL of the diluted cell suspension was plated in 100mm tissue culture dishes for 3-4 days at 37°C in a humidified atmosphere containing 5% CO_2 prior to use or splitting.

Freezing down and Recovery of Frozen Cell Lines

The cells were harvested, as previously described, and pelleted by centrifugation for 6 minutes at 300 *g* at room temperature. The cell pellet was resuspended in

3 mL of freeze down media (DMEM medium, 20% FBS, 10% DMSO). After aliquoting 1 mL into 2 mL cryogenic vials, the cells were first transferred to the cryogenic 1°C freezing container (Nalgene) and then into the -80°C freezer. For long term storage, the frozen cells were placed in liquid nitrogen. When the cells were required, the vials were collected from the liquid nitrogen container and placed at room temperature. Before the cells were completely thawed, they were washed with 10mL of PBS, resuspended in 10 mL of complete DMEM culture medium and platted in 100mm tissue culture dishes at 37°C in a humidified atmosphere containing 5% CO_2.

5.2.2 Plasmid constructs

An expression clone containing cDNA encoding human KMO (hKMO) (NM_003679) was purchased from Genecopeia (Genecopeia, United Bioresearch). Figure 5.1 shows information about the clone, which is referred to as pEZ[KMO] (Also available at: *file:///Users/gloriacastellanogonzalez/Library/Mail%20Downloads/EX-I0187-M02.map.html*).

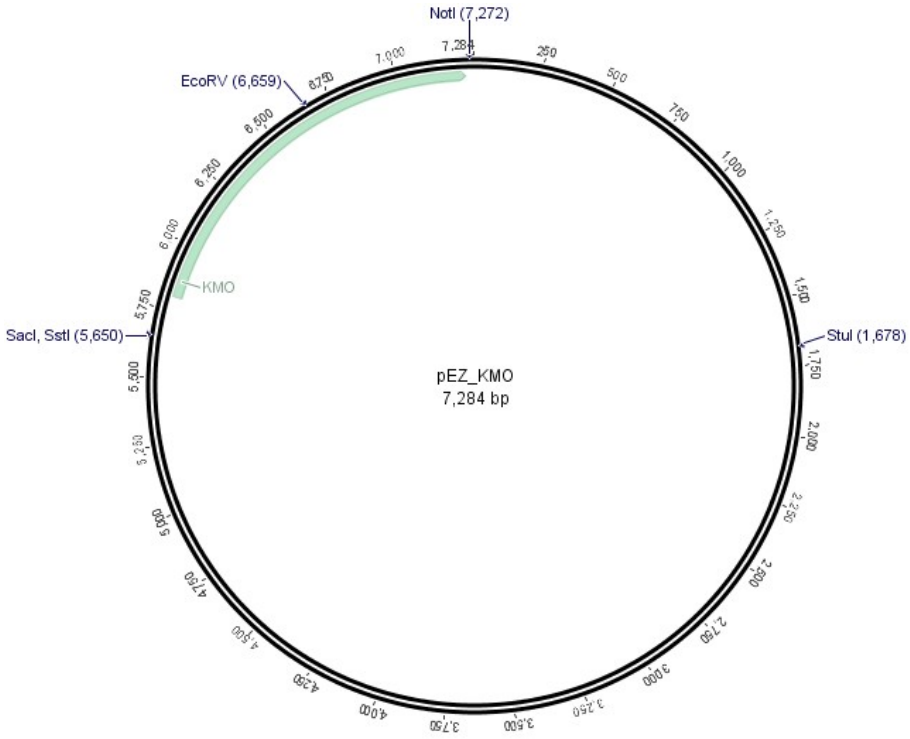

Figure 5.1: Map of the pEZ[KMO] construct

The cleave locus for the restriction enzymes used are shown in the construct map.

Blunt-end cloning to obtain the empty vector

Blunt-end cloning was used in order to remove the KMO cDNA from pEZ[KMO] construct. This plasmid will be transfected in parallel with pEZ[KMO] and used as a control in non-KMO expressing cells. First, pEZ[KMO] construct was cleaved by SacI and NotI restriction enzymes (New England BioLabs) following manufacturer's instructions. This leads to complete removal of the hKMO cDNA from the pEZ vector backbone (Figure 5.1). Briefly, a double digest was performed with 5 µg of pEZ[KMO], 1U of Sac1 and Not1 in NEB buffer 4, supplemented with 1 % BSA for 3h at 37°C. After the digest, the reaction was subjected to agarose gel electrophoresis to separate the linearised vector backbone from the hKMO cDNA, using the undigested template as a control. The agarose gel showed two digestion products, the lower band (~1627bp) corresponding to the digested hKMO cDNA while the upper band (~5802bp) corresponding to the digested pEZ empty vector backbone. The digested vector backbone was obtained by excising the appropriate bands in the gel followed by DNA gel extraction, using QUIAquick gel extraction kit (Qiagen), according to manufacturer's instructions. Subsequently, the purified pEZ empty vector backbone was re-ligated by blunt end cloning to obtain the pEZ empty control plasmid. The

purified pEZ empty vector backbone was eluted in 43.5 µL MilliQ water and added to a PCR tube with 5 µL of buffer 2, 0.5 µL of dNTPs and 1 U of DNA polymerase 1, large (Knenow) fragment (New England Biolabs) for blunting. Blunt-ends were achieved by incubating the reaction mixture for 15 minutes at 25°C followed by enzyme heat-inactivation for 20 minutes at 75°C. The reaction was cleaned up from enzymatic reaction products by column with a QIAquick Gel Extraction Kit (Qiagen) following manufacturer's instructions with slight modifications. Five times the reaction volume of buffer QC was added to the reaction tube and then the protocol was strictly followed. Products were eluted into 15 µL MilliQ water. Quantification and purity of the DNA was verified spectrophotometrically with the Nanodrop (Thermo scientific). For the blunt-ends ligation to occur, 5' phosphate was added to the linear construct, using 75ng of DNA, 0.5U of polynucleotide kinase enzyme and 1 µL of ligation buffer (New England Biolabs) in a final volume of 10 µL. Phosphorylation was done at 37°C for 20 minutes and the enzyme was heat inactivated at 65°C for 10 minutes. Finally, 1 U of ligase enzyme (New England Biolabs) was added to the above reaction and incubated overnight for 16h allowing ligation of the blunt ends. The product of the ligation reaction (2µL) was transformed into competent E. Coli cells (OneShot TOP10 Cells, Invitrogen) as indicated below.

E. Coli transformation with vector constructs

To generate large quantities of each vector construct used in this project, competent E. Coli cells were first transformed with the DNA constructs. 10-20 pg of DNA construct was added to a vial containing 25 µl of competent E. Coli cells (OneShot TOP10 Cells, Invitrogen) and incubated on ice for 30 minutes. E. coli were then heat-shocked for 30 seconds at 42°C and 125 µl of warm SOC Medium (a modified lysogeny broth (LB), Invitrogen) added. Vials were incubated for 1 h at 37°C in a shaker set to 225 rpm LB agar plates (LB broth + 1 % Agar) containing 100 µg/ml Ampicillin (Invitrogen) were inoculated with 100µl of transformed cells and incubated (inverted) overnight at 37°C. Since the vectors used in this project contain an Ampicillin-resistant gene, only those E. coli cells that have taken up the DNA construct will grow overnight.

Verification of new construct (empty vector)

Following overnight incubation, five single E. coli colonies were selected and inoculated in 15 ml tubes containing 2 ml of LB medium and 100 µg/ml Ampicillin (selection LB). E. Coli were incubated for 6h at 37°C with 200 rpm agitation (preculture). 2 µL of the preculture was added to 2 ml of selection LB (for Mini-prep) and 500 µL of the preculture to 25 mL of selection LB (for Midi-prep) and incubated overnight at 37°C with 200 rpm agitation. First, quick plasmid extraction from E. Coli was performed via mini-prep, in order to verify the success of the cloning before proceeding with the large quantity Midi-prep plasmid extraction. After isolating the plasmid from the 5 different colonies using Miniprep (Qiagen) a 30 minutes quick digestion at 37°C was done with the restriction enzymes EcoRV (only present in KMO) or StuI (present in the plasmid bone) in buffer 2 or buffer 4 respectively. The pEZ[KMO] plasmid was digested, as well, and used as a positive control for digestion with both enzymes. The products of the digestion for the different colonies were separated in 1% agarose gel. Figure 5.2 shows that all the colonies incorporated only the empty vector, as the only enzyme digesting the plasmid is StuI (present only in the plasmid bone) but not EcoRV, which only digested the positive control pEZ[KMO]. After verifying that the selected colonies had incorporated only the empty vector, we proceed to isolate the plasmid from the E. Coli suspension previously prepared for Midi-prep DNA extraction. This is necessary to obtain higher yields of endotoxin-free empty vector, which is required for cell transfection studies.

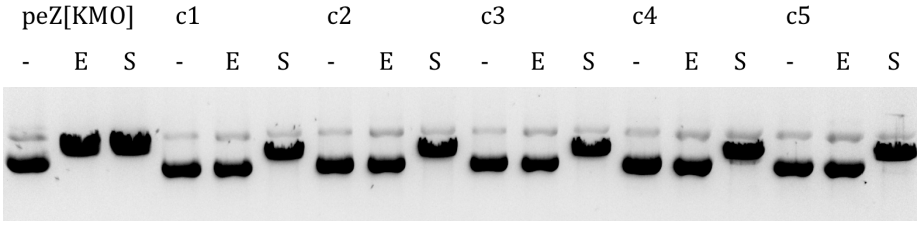

Figure 5.2: Empty vector construct verification

Product of the digestion with EcoRV (E) and StuI (S) of the plasmid isolated from 5 different colonies (c1-c5) assessed by electrophoresis and compared with the original construct.

Midi-prep extraction of DNA from E. coli

Single E. coli colonies grown on LB agar plates were selected and inoculated in 50 ml

flasks containing 25 ml LB medium and 100 µg/ml Ampicillin as described above. E. Coli were incubated overnight at 37°C at 200 rpm. E. Coli suspension was transferred to a 50 ml tube and centrifuged for 15 minutes at 4°C at 4800 g. The Qiagen midiprep kit (Qiagen) was used to extract plasmid from bacterial cells, following manufacturers protocol. Briefly, the supernatant was discarded and the pellet re-suspended in Buffer P1. Buffer P2 was added, gently mixed and incubated for 5 minutes at RT. Buffer P3 was added, gently mixed and incubated on ice for 15 minutes. The lysate was centrifuged at ≥20,000 *g* for 30 minutes at 4°C. The supernatant containing the plasmid DNA was re-centrifuged to completely remove bacteria debris and then transferred to a Qiagen tip pre-equilibrated with buffer and the supernatant drained by gravity. The tip was washed twice with buffer and the flow through discarded. Filtered DNA was eluted, precipitated by addition of isopropanol and centrifuged at 12,000 *g* for 60 minutes at 4C°. The supernatant was discarded and the DNA pellet washed with 70% ethanol and centrifuged at 15,000 *g* for a further 30 minutes at 4°C. The supernatant was discarded and the pellet air-dried for 10 minutes. DNA was resolved in 300 µl freshly prepared 1x Tris-EDTA (TE; 10 mM, Tris-HCl pH 8, 1 mM EDTA) buffer, quantified by UV spectrophotometry at 260nm using the Nanodrop 2000c (Thermo Scientific) and stored at -20°C.

5.2.3 Transfection of HEK293

For each individual well, 2 µg DNA were diluted in 100 µL Opti-MEM (Gibco, Invitrogen) and 0.5 µL PLUS reagent (Invitrogen) was added to the mixture. After 5 minutes of incubation, 1.25 µL Lipofectamine LTX (Invitrogen) were added and incubate for 30 minutes. Then, the cells (80 % confluent) in 500 µL culture media (without antibiotics) were transfected by adding the mixture drop wise to cells. All transfected cells were maintained in the 37°C incubator for 2 days, to allow expression of the transfected DNA. In the first set up experiment, cells were transfected with Actin-GFP (gift from Ariel Seaton) and incubated for 48h until they were fixed and transfection efficiency assessed under microscopy (as number of cells positive for GFP staining). Figure 5.3 shows ≥50 % positive transfected cells using the conditions previously described.

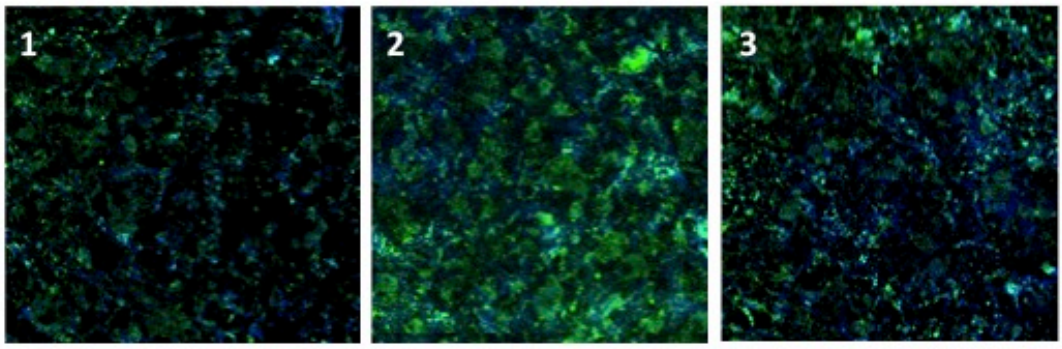

Figure 5.3: Transfection efficiency

Qualitative mosaic image showing three different wells containing HEK293 transfected with GFP plasmid.

5.2.4 Generation of stable HEK293 expressing pEZ[-] and pEZ[KMO]

Before stably transfect HEK293, the constructs used were sequenced by the Ramaciotti Centre (UNSW), to verify the identity of the purchased construct and to discard any mutations during cloning the empty vector.

Both constructs have Neomycin as stable transfection marker. An initial pilot study was done in order to determine the minimum concentration of G418 (for neomycin selection) necessary to prevent cell growth in non-transfected cells. Briefly, $50x10^3$ cells were plated in a 24 well plate, after 24h, cells feed with medium containing increasing concentrations (0.1-1.5mg/mL) of G418. New selection medium was added every 2-3 days and after 10 days cell viability was quantified by MTT assay. Figure 5.4a shows complete cell death at 600 mg/mL of G418, being this concentration used to select the cells that have incorporated the plasmid. Cells were transfected with pEZ[-] or pEZ[KMO] as previously described (section 5.2.3) and 48h after transfection the selection medium was added. Medium containing G418 was changed every 2-3 days and cells were maintained under standard conditions for 4 weeks. Negative control with non-transfected cells showed complete cell death after 3 weeks, indicating that proliferating cells in the transfected conditions have incorporated the plasmid. Mixed population of drug resistant cells were analysed for RNA expression and hKMO expression was only detectable by PCR in pEZ[KMO] transfected cells, but not in pEZ [-](Figure 5.4b). KMO activity was determined in HEK293, HEK-pEZ[-] and HEK-pEZ[KMO] cells with or without adding 50 µM of KYN

in complete culture medium for 24h. 3-HK concentration was measured in the cell supernatants and HEK-pEZ[KMO] showed higher production of 3-HK than HEK-pEZ[-] or HEK293. Moreover, addition of KYN, showed 20-fold increase of 3-HK turnover after 24h in HEK-pEZ[KMO], indicating expression of active KMO (Figure 5.4c). Due to the fact that the transfected plasmid have not been incorporated into the genome of the cell, sustained antibiotic selection will be required to eliminate the cells that lose the plasmid. HEK293 transfected cells with pEZ[-] or pEZ[KMO] were named HEK-pEZ[-] and HEK-pEZ[KMO] respectively.

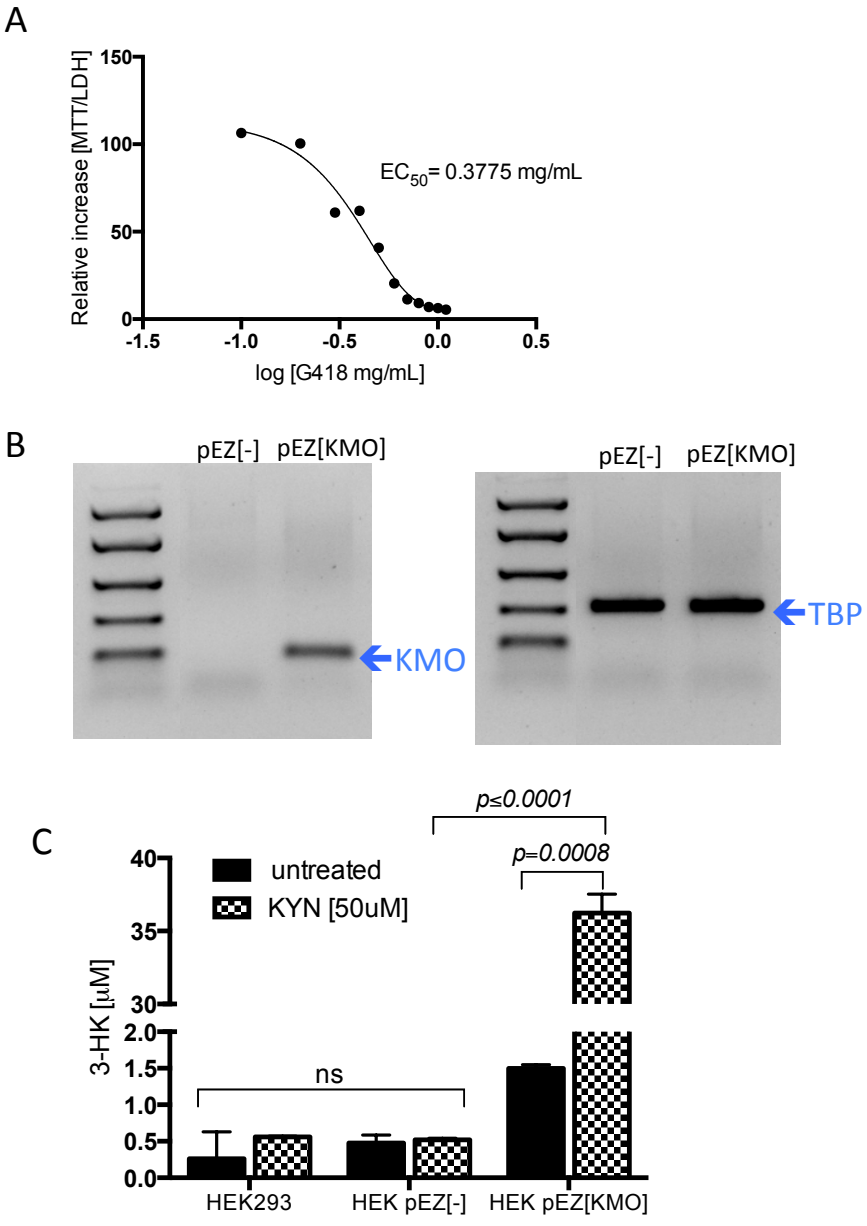

Figure 5.4: Stable HEK293 overexpressing pEZ[-] and pEZ[KMO]

(**a**) Viability of HEK293 after treatment with increasing concentrations of G418 assessed by MTT assay. Data are representative of two experiments. (**b**) Qualitative

KMO gene expression of HEK-pEZ[KMO] and HEK-pEZ[-] assessed by PCR. (**c**) 3-HK measured in cell culture supernatants of HEK293, HEK-pEZ[-] and HEK-pEZ[KMO] after treatment with 50 μM of KYN for 24h. Data (means ± s.e.m.) are from three experiments (Student's t-test).

5.2.5 Mammalian cell model for KMO activity studies

HEK-pEZ[KMO] cells could be used as a tool to study KMO activity, with applications in screening of pharmacological inhibitors or studying regulatory mechanisms of KMO activity. We previously showed that HEK-pEZ[KMO] cells express active KMO (Figure 5.4**c**) and quantification of 3-HK and KYN by UHPLC can be used to determine KMO activity (3-HK/KYN ratio).

HEK-pEZ[KMO] were washed and treatments were always done in serum free DMEM for up to 90 minutes. Inhibition of KMO activity was tested by adding increasing concentrations of the inhibitor (0.5-500 μM) for 15 minutes, followed by addition of 50 μM of KYN. This allows the drug to arrive to its site of action before adding the substrate KYN. Accordingly, mitochondrial inhibitors were also added 15 minutes prior to add KYN. Supernatants were collected after 1h incubation with 50 μM of L-KYN at 37°C in a humidified atmosphere containing 5% CO_2. Cell supernatants were collected for 3-HK and KYN quantification by UHPLC. Cells were lysed in RIPA buffer for protein quantification. Total 3-HK and KYN concentrations were normalised against total protein to account for any difference in cell density.

5.2.6 Ultra high performance liquid chromatography

3-HK and KYN were concurrently measured using an Agilent 1200 series UHPLC system as previously described in section 3.4.1 . Each experiment was performed in triplicate using supernatants from primary cultures derived from three different human foetal brains and from HEK cultures. All results are expressed as the mean ± s.e.m.

5.2.7 Immunoblotting

Human primary neurons were harvested and immunoblotted as described in section 3.2 using anti-human KMO (LSBio) or anti-human GAPDH (Cell Signalling).

5.2.8 Immunocytochemistry

Immunocytochemistry using anti-human KMO (LSBio) and anti-MAP2 (BD), as neuronal marker, was performed following section 3.5 procedures.

5.2.9 Oxidative stress determination

Intracellular oxidative stress was assessed by monitoring H_2O_2 (indicative of ROS generation). The amount of intracellular H_2O_2 can be estimated by the cell-permanent 2′,7′-dichlorofluorescein (DCF)-H_2 dye (Invitrogen), which oxidizes in the presence of H_2O_2 to its fluorescent product DCF (331).

To examine the potential of 3-HK to exhibit pro-oxidant activity, HEK-pEZ [-] cells and neurons were treated with varying concentrations of 3-HK (10 nM to 10 μM) for 24h in complete medium.

To examine how KMO overexpression may modulate intracellular ROS, 2 million HEK-pEZ[-] or HEK-pEZ[KMO] cells were plated in 100mm cell culture dishes and grown over 2 days in complete medium. Parallel experiments assessing the effect of KMO inhibition were performed using HEK-pEZ[KMO] cells treated with 5 to 100 μM of the well-described KMO inhibitor Ro-61-8048 (Calbiochem; Merck Millipore) in complete medium for 48h, adding new inhibitor every 24h.

After treatment, cells were washed and incubated with 10 μM DCF-H_2 in Leivovitz's (L-15) medium (Invitrogen) for 30 minutes, cells were then washed twice with PBS, and HEK cells were resuspended in L-15 medium and placed in a 96 well plate or L-15 medium was added directly to the neuron culture plate. Fluorescence intensity was monitored using the PHERAstar FS plate reader (BMG labtech) with excitation and emission wavelengths of 485 nm and 530 nm, respectively.

5.2.10 ATP- Luminescent measurements

Assessment of cellular ATP in KMO overexpressing cells required platting 2 million cells of HEK-pEZ[-] or HEK-pEZ[KMO] in 100mm cell culture dishes, which were grown over 2 days in complete medium.

Human primary neurons were treated with varying concentrations of 3-HK (10 nM to 10 μM) for 24h in complete medium. Controls were treated with equal amount of the solvent used for treatment.

Intracellular total ATP production was immediately assessed, after the cells were washed and harvested in PBS, using a commercially available luciferase-luciferin system (ATPlite, Perkin Elmer), as described in section 6.2.2 .

5.2.11 Assessment of mitochondrial membrane potential

Mitochondrial membrane potential was determined with Rhodamine 123 (R123), as described in section 6.2.4 . Briefly, HEK-pEZ[-] or HEK-pEZ[KMO] cells were incubated with 10 μM R123 (quenching mode) under normal incubation conditions for 30 minutes. The R123-containing medium was removed and cells were placed in L-15 medium and incubated at 37°C for 15 minutes. Cells were harvested in L-15 medium, placed in a 96 well plate and fluorescence was measured in the PHERAstar plate reader with excitation and emission set at 560 and 645 nm respectively.

5.2.12 Mitochondrial respiration in intact cells

Oxygen consumption in intact cells was measured using the high-resolution respirometer Oxygraph-2K (Oroboros instruments) as described in section 3.6 . Intact cells, from HEK-pEZ[-] and HEK-pEZ[KMO] cultures, were detached and concentrated in normal culture medium to 3 x10^6 cells/mL. Cell suspensions were immediately placed in the oxygraph chamber at 37°C under continuous stirring at 300 rpm for respiration analysis. Each experiment was repeated three times with different cell preparations and results were expressed as pmol O_2 consumed per min per million cells.

5.2.13 Quantitative real-time polymerase chain reaction

Total RNA from cells was prepared from RNeasy mini kits (Absolutely RNA Miniprep Kit) and processed as described in general methods. The relative expression of KMO was normalised against the housekeeping genes *Tbp* and *Pgk-1*. Data were analysed

with the ΔCt values and expressed as fold change compared to controls. Primer sequences used for qRT-PCR are shown in Table 5.1.

Table 5.1: Primer sequences used in Chapter 5

Gene	*Forward sequence*	*Reverse Sequence*
Kmo	5'-TAGCCCTTTCTCATAGAGGACG-3'	5'-CTCTCATGGGAATACCTTGGGA-3'
Pgk-1	5'-TCACTCGGGGCTAAGCAGATT-3'	5'-CAGTGCTCACATGGCTGACT-3'
Tbp	5'-GGGAGCTGTGATGTGAAGT-3'	5'-GGAGGCAAGGGTACATGAGA-3'

5.3 Results

5.3.1 Neurons express functional KMO

Previous research from our group has shown that human primary neurons express KMO, which can degrade KYN to produce KYNA and 3-HK. However, neurons do not breakdown 3-HK to form QUIN, but produce PIC instead (275). Hence, before assessing the effect of KMO over activation (see section 5.6) and neurotoxicity mediated by intracellular 3-HK in human primary neurons, we characterised the KMO branch under physiological conditions. We used new and more sensitive techniques in addition to quantifying KMO protein by WB.

Human primary neurons were isolated as previously described in methods section. Protein was collected from 4 different neuronal cultures and analysed for KMO protein. All neuronal cultures showed expression of KMO (Figure 5.5a), which was confirmed by co-localization of KMO with the neuronal marker Map2 (Figure 5.5b). We further characterised the KP in human primary neurons by quantification of KYNA, 3HK and KYN in cell culture supernatants (Figure 5.5c). Neurons consumed KYN through the two main branches of the KP, as both KYNA and 3-HK were found in increased concentrations (through the activity of the enzymes KAT and KMO, respectively). However, KMO has higher specificity and affinity for KYN than KAT, suggesting that it would metabolise most of the KYN available (321). Further confirmed by the results as the concentration of 3-HK produced at the 24h time-point were 10 times higher than the concentration of KYNA produced (Figure 5.5c).

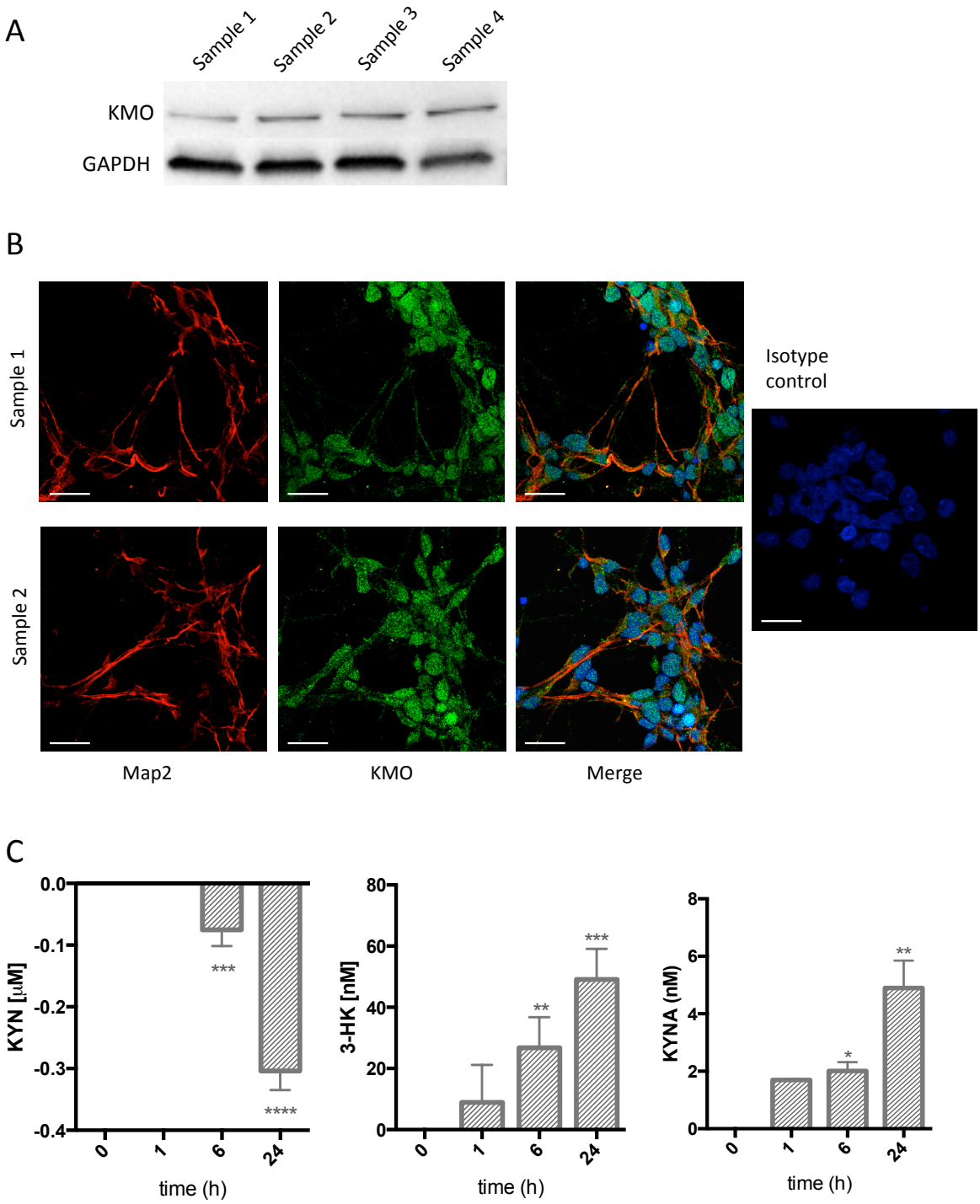

Figure 5.5: KMO characterization in human primary neurons

(**a**) Immunoblot qualitative analysis in human primary neurons from four different samples for KMO. (**b**) Intracellular immunofluorescence of human primary neurons showing co-expression of the neuronal marker, Map2 with KMO. Representative data of four independent experiments. Scale bar: 25µm. (**c**) KYN, KYNA and 3-HK was measured in human primary neurons supernatant. Data (means ± s.e.m.) are from three experiments. ****p≤0.001, ***p≤0.005, **p≤0.01, *p≤0.05 (time point versus time 0; Student's t-test).

5.3.2 Increased KMO expression induces ROS production and mitochondrial dysfunction

Cytokines such as IFN-γ (75) and IL-1β have been shown to induce KMO (76, 77), however these are not specific for KMO and modulate other KP enzymes and inflammatory pathways. In order to study the effects of pathological KMO overexpression, without the interfering effects of an unspecific KMO inducer, we generated HEK293 stably expressing hKMO (HEK-pEZ[KMO]) cells.

3-HK has been previously described as a powerful generator of ROS and potential endogenous neurotoxin (143-145). Therefore, KMO overexpression might increase 3-HK synthesis and ROS downstream. We found that HEK-pEZ[KMO] cells showed a two-fold increase in DCF fluorescence, a well-described marker of ROS production, compared with HEK-pEZ[-] cells (Figure 5.6a). As ROS can affect mitochondrial function, we quantified mitochondrial membrane potential, finding increased ΔΨm values (Figure 5.6b). This does not necessarily indicate ETS activation, as hyperpolarisation of ΔΨm does not always mirror changes on mitochondrial proton gradient (pH)(332). Further, respiratory status also needs to be analysed in order to fully interpret the results. In fact, an increase in cytosolic [Ca^{2+}], due to release of ER stores, which is also responsible for ΔΨm hyperpolarisation (333), has been described in neural cells treated with 3-HK (144).

To establish how mitochondrial function is affected when KMO is overexpressed, we measured the bioenergetics profile in a basal state and after the addition of oligomycin, FCCP, and rotenone and antimycin A (Figure 3.4). We found no significant change in the OCR at the basal state (R), an indicator of cellular oxidative phosphorylation (OXPHOS) in HEK-pEZ[KMO] cells compared with HEK-pEZ[-]. However, cells overexpressing KMO demonstrated a substantially lower SRC when compared to HEK-pEZ[-]. Thus, this indicates that, mitochondrial respiration in HEK pez[KMO] operates closer to its maximum capacity (MR) (Figure 5.6d). Mitochondrial respiratory status of HEK-pEZ[-] was in accordance with previous studies in HEK293 (334). Optimal conditions for maximal OCR was determined empirically by 0.025 μM of FCCP titration steps in HEK-pEZ[-] and HEK-pEZ[KMO] (Figure 5.6c). SRC could decrease due to higher ATP demands, reduced oxidative capacity caused by partial uncoupling of mitochondrial complexes or by defects in substrate oxidation.

However, we did not observe uncoupling changes (L), being reduced substrate availability (NADH) the most likely cause of decrease in MR. In addition, intracellular ATP levels did not change or where slightly increased (Figure 5.6e), indicating that, even though there is impaired mitochondrial capacity, the cell can still meet normal ATP demands.

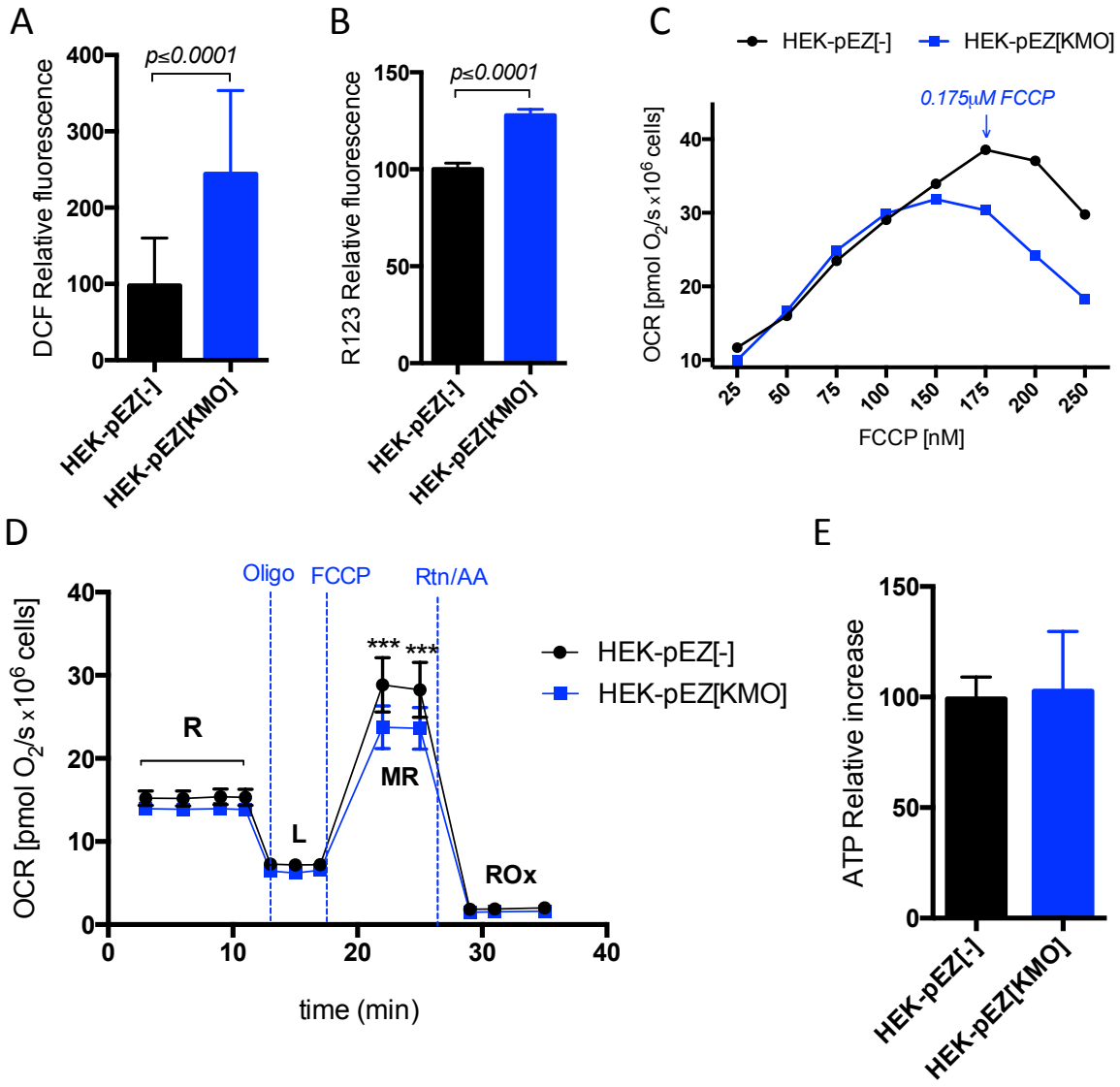

Figure 5.6: Effect of KMO overexpression in ROS production, mitochondria function and ATP turnover

ROS (**a**), mitochondrial membrane potential (**b**) and intracellular ATP (**e**) of HEK-pEZ[KMO] and HEK-pEZ[-] after 48-72h was assessed by DCF fluorescence, R123 florescence or luminescence intensity, respectively. Data (means ± s.e.m. of three experiments) are presented as normalised mean intensity in HEK-pEZ[KMO] relative to normalised mean intensity in HEK-pEZ[-] (Student's t-test). (**c**,**d**) O_2 consumption rate of intact HEK-pEZ[-] and HEK-pEZ[KMO] showed by superimposed oxygraph traces from parallel measurements in two chambers. (**c**) FCCP titrations were added

in both chambers for the study of the maximal respiratory capacity (MR). (**d**) Mitochondrial inhibitors were added, at the time points indicated, in both chambers for the study of respiratory states. Data (means ± s.e.m. of three experiments) are presented as cell number-specific oxygen flux. ***p≤0.001 (HEK-pEZ[KMO]versus HEK-pEZ[-]; Student's t-test).

5.3.3 Extracellular 3-HK only induces mild oxidative stress. A role for autonomous KMO activation

We hypothesize that, in neurons, cell-endogenously produced 3-HK could directly induce ROS production, mitochondrial dysfunction and neurotoxicity, compared with, extracellular 3-HK produced by glial cells. We showed that HEK-pEZ[KMO] in the absence of additional KYN had significant increase of ROS production (Figure 5.6a). 3-HK concentration in the cell culture supernatant of those cells ranged between 1.5±0.5 μM after 24h (Figure 5.4c). In order to study whether the metabolic effects observed in cells overexpressing KMO were due to 3-HK, we treated HEK-pEZ[-] with up-to 10 μM of 3-HK (which is 10 times higher than 3-HK concentration in supernatant of HEK-pEZ[KMO] for 24h. However, extracellular 3-HK did not increase ROS production at the concentrations used (Figure 5.7a). Although we could not detect QUIN in HEK-pEZ[KMO] supernatants (data not shown), in order to discard the QUIN-mediated ROS induction hypothesis, HEK-pEZ[-] cells were treated with increasing concentrations (0.3-100 μM) of QUIN for 24h. No change in ROS production was observed (Figure 5.7b).

Human primary neurons treated with 3-HK, as in Figure 5.7a, were assessed for ROS production and showed similar results than HEK (Figure 5.7c). However, intracellular ATP levels were affected in human primary neurons treated for 24h with 10 μM of 3-HK (Figure 5.7d), revealing metabolic differences between primary neurons and cell lines. Different to neurons, HEK can overcome mitochondrial defects caused by oxidative stress by using excess of NAD^+ (increased through KMO activation) as a metabolic substrate for glycolysis and even raise ATP turnover despite mitochondria impairment (Figure 5.6e).

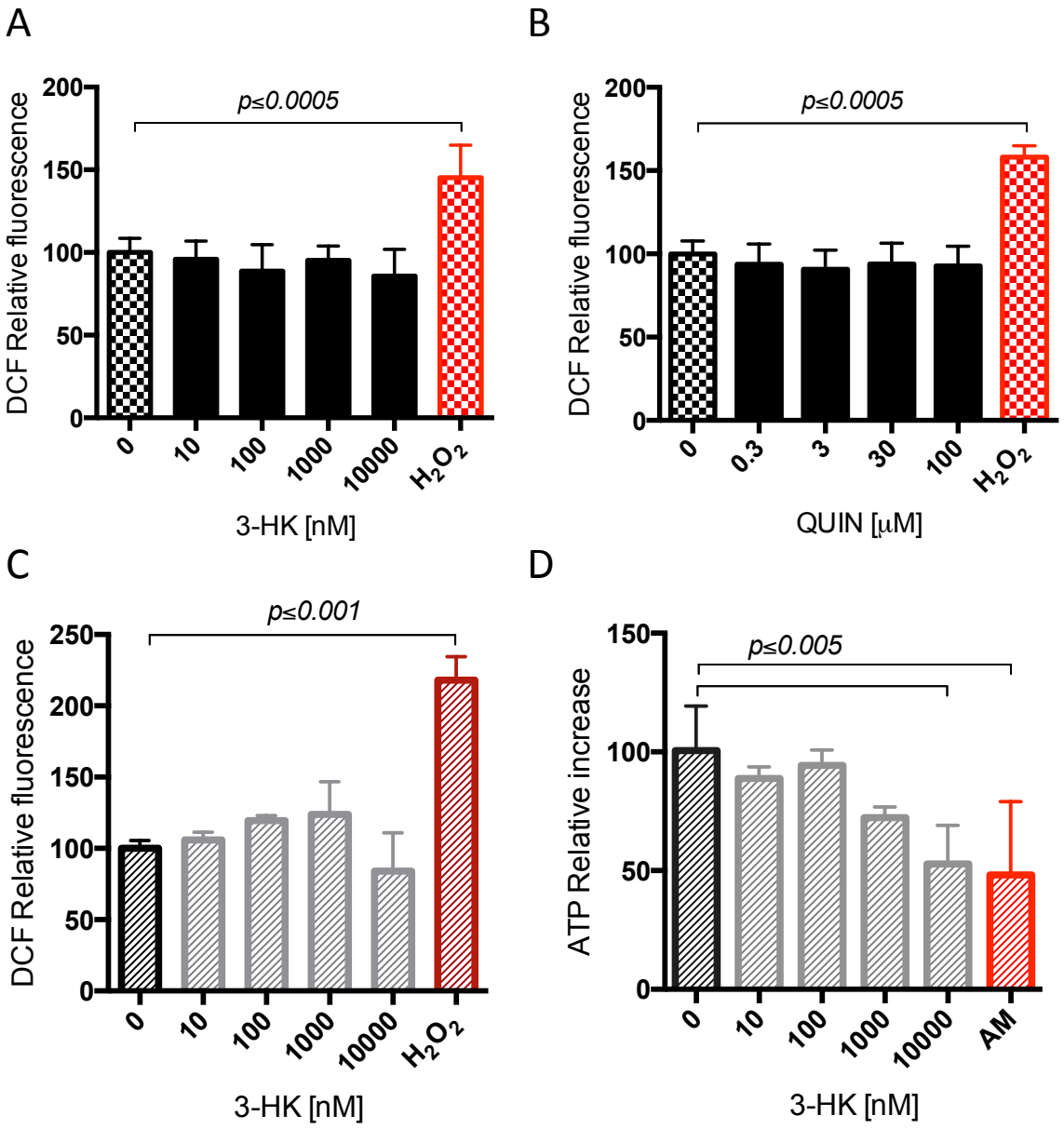

Figure 5.7: Effects of extracellular 3-HK in HEK-pEZ[-] and human primary neurons

ROS of HEK-pEZ[-] (**a**,**b**) and human primary neurons (**c**) after treatment with increasing concentrations of 3-HK (**a**,**c**) or QUIN (**b**) (and H_2O_2 as a positive control) for 24h and assessed by DCF fluorescence intensity. Data (means ± s.e.m. of three experiments) are presented as normalised mean intensity in sample relative to normalised mean intensity in untreated sample (Student's t-test). (**d**) ATP of human primary neurons after treatment with increasing concentrations of 3-HK (or AM as a positive control) for 24h and assessed by luminescence intensity. Data (means ± s.e.m. of three experiments) are presented as normalised mean intensity in sample relative to normalised mean intensity in untreated sample (Student's t-test).

5.3.4 KMO inhibition does not block ROS production induced by KMO overexpression

We hypothesise that ROS production observed in HEK-pEZ[KMO] could be pharmacologically reversed by using the synthetic KMO inhibitor Ro-61-8048. KMO inhibition would reduce 3-HK production and ameliorate mitochondrial dysfunction. Ro-61-8048 in our HEK-pEZ[KMO] model showed IC_{50} of 48±6 µM (Figure 5.8a). Experimental procedure is described in section 5.2.5 . We then used Ro-61-8048 at concentrations that effectively decreased 3-HK and analysed ROS production. Ro-61-8048 not only did not decrease ROS production in our *in-vitro* model but it induced oxidative stress at higher concentrations (100 µM) (Figure 5.8b). This could indicate that 3-HK is not the main source of ROS production in our overexpressing model or/and that at higher concentrations Ro-61-8048 could induce ROS.

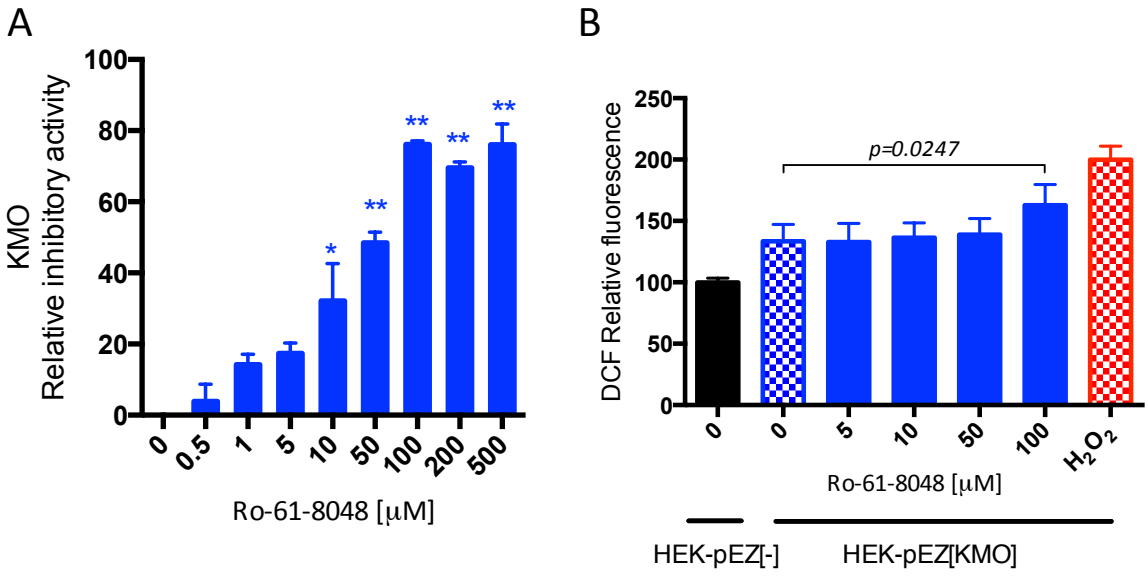

Figure 5.8: ROS production after pharmacological inhibition of KMO in HEK-pEZ[KMO]

(**a**) KMO activity of HEK-pEZ[KMO] after treatment with increasing concentrations of Ro-621-8048 (0.5-500 µM) and supplemented with 50 µM of KYN for 1h assessed by the ratio of 3-HK and KYN concentration measured in serum free cell culture supernatants. Data (means ± s.e.m. from three experiments) are presented as normalised mean inhibitory activity in sample relative to normalised mean inhibitory activity in untreated sample. *p≤0.001, **p≤0.0001 (treatment versus none; Student's t-test). (**b**) ROS of HEK-pEZ[KMO] after treatment with increasing concentrations of Ro-621-8048 (5-100 µM) (or H_2O_2 as a positive control) for 48h and assessed by DCF fluorescence intensity. Data (means ± s.e.m. of three experiments) are presented as normalised mean intensity in HEK-pEZ[KMO] relative to normalised mean intensity in HEK-pEZ[-] (Student's t-test).

5.3.5 Mitochondrial dysfunction favour the KMO branch

Mitochondrial activity has previously been shown to be involved in the regulation of the KP. For instance, inhibition of mitochondrial respiration decreases KAT-1 and KAT-2 activity (98), increasing substrate availability for KMO thereby redirecting the KP through the KMO branch.

In order to evaluate the effect of mitochondrial impairment on KMO activity, we blocked the different complexes of the ETS and analysed KMO activity using the HEK-pEZ[KMO] model. When complex IV was inhibited with sodium azide, 3-HK increased, indicating significantly higher KMO activity (Figure 5.9a) Inhibiting complex III and ATP synthase (with antimycin A and oligomycin respectively also resulted in slightly higher 3-HK production (Figure 5.9a). In order to determine whether increase of KMO activity could be mediated by increase of KMO expression, human primary neurons were treated with oligomycin (5 μM), FCCP (0.2 μM), rotenone (1 μM) and antimycin A (2.5 μM) and KMO mRNA was determined. Human primary neurons were treated with the mitochondrial inhibitors for 6h and KMO mRNA was determined by qRT-PCR. Mitochondria inhibition showed no effect on KMO expression in human primary neurons (Figure 5.9b). This suggests that, under mitochondrial impairment, agonistic regulation of KMO is inducing its activity.

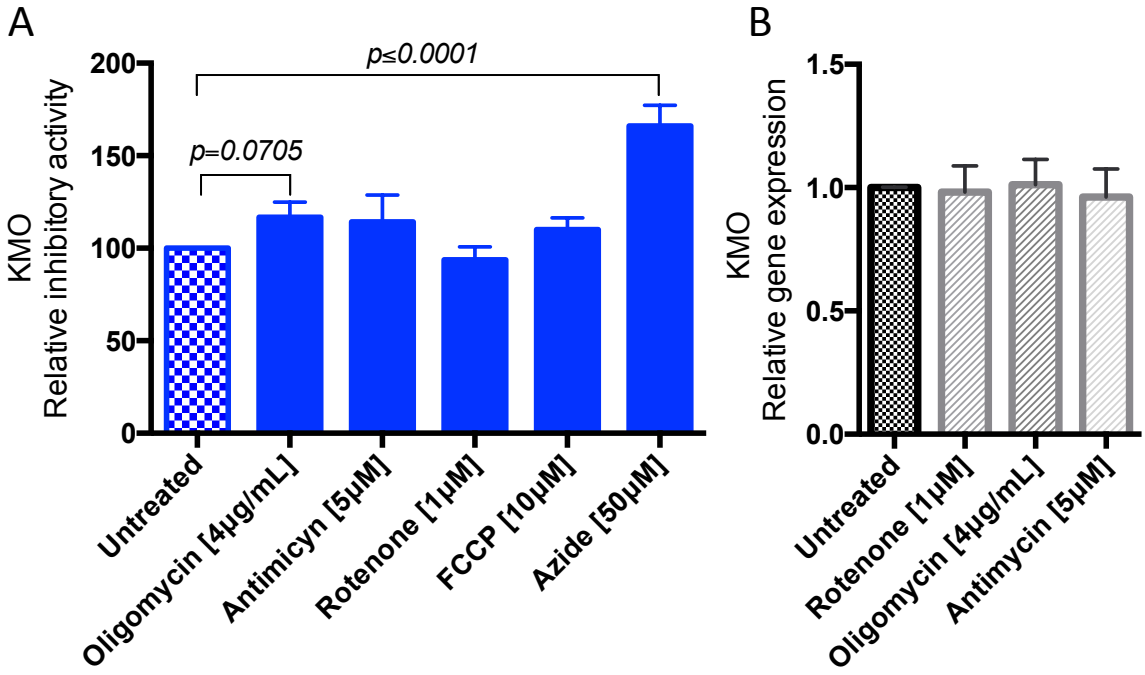

Figure 5.9: Mitochondria inhibition drives the KP through the KMO branch

(**a**) KMO activity of HEK-pEZ[KMO] after treatment with specific mitochondrial complexes inhibitors and supplemented with 50 µM of KYN for 1h assessed by the ratio of 3-HK and KYN measured in serum free cell culture supernatants. Data (means ± s.e.m. from three experiments) are presented as normalised mean activity in sample relative to normalised mean activity in untreated sample (Student's t-test). (**b**) Gene transcript expression of human primary neurons after treatment with specific mitochondrial complexes inhibitors for 6h. Data (means ± s.e.m. of three experiments) are presented as normalised transcript expression in the samples relative to normalised transcript expression in untreated sample (Student's t-test).

5.4 Discussion

Under physiological conditions, mitochondrial oxidative phosphorylation carries more than 90% of the neuronal ATP production. Because neurons rely on mitochondrial respiration as a main source of energy, they are highly vulnerable to oxidative stress and mitochondrial impairment (324). The two main metabolites of the KMO branch in the KP (3-HK and QUIN) have been shown to play an important role in redox imbalance (113). By activating the NMDAR, QUIN can induce excitotoxicity through increasing intracellular Ca^{2+} levels, and 3-HK at high concentrations can act as a pro-oxidant (145). Therefore, inhibition of KMO would be a good strategy to decrease neurotoxicity. In fact, some studies have already shown that KMO inhibition in the *Saccharomyces cerevisiae* model of HD (232) and the transgenic *Drosophila melanogaster* HD model (335) can decrease

neurodegeneration. In the current study, a reduction of 3-HK has been proposed as the mechanism of neuroprotection. However, it has to be taken into account that, *in vitro*, 3-HK pro-oxidant activity has only been shown at non-physiological or pathological concentrations and once it is up-taken by the cell (145). This supports our hypothesis that neuronal cell-autonomous 3-HK has higher neurotoxic activity than 3-HK released by glia. Our group has previously shown that human primary neurons express KMO (275) and we have further confirmed this data and showed that it is active and can synthetise 3-HK. However, neurons cannot synthetise QUIN (275). This should be taken into consideration, as the *in vitro* effects seen in pure human primary neurons treated with 3-HK may not be a secondary effect of endogenous QUIN production.

Cells overexpressing KMO showed a three-fold increase in 3-HK production. It has been previously demonstrated that 3-HK induces oxidative stress through an increase in hydrogen peroxide production (145, 336). In accordance with this study, our ROS quantification results showed that cells overexpressing KMO were twice as prone to oxidative stress. An increase in ROS production leads to redox imbalance that will affect mitochondrial function (323). In fact, the bioenergetics profile of cells overexpressing KMO showed substantially lower SRC when compared with wt. A limitation of oxidative capacity observed by a decrease of SRC in our cell model, could have different causes, mainly related with defects in mitochondrial complexes or substrate availability (337). Three possible reasons for higher KMO activity affecting SRC may be: (1) Increase on ROS production observed in cells overexpressing KMO can induce NO production (338). NO has been shown to inhibit mitochondrial respiration by decreasing the affinity of Cytochrome c oxidase for oxygen (334), this would decrease complex IV maximal capacity. (2) Due to the fact that KMO is localised in the outer mitochondria membrane, ROS can be locally produced by 3-HK. Hydrogen peroxide can rapidly diffuse across the inner membrane of the mitochondria affecting mitochondrial DNA (mtDNA). mtDNA is particularly susceptible to ROS as its repair capacity is less robust than that from nuclear DNA and the outcome of mtDNA mutations can lead to alteration on mitochondria encoded proteins (339). Approximately 5% of the proteins in the ETS are coded by mtDNA, those belonging to the NADH-dehydrogenase, cytochrome c oxidase, ATP synthase and cytochrome b complexes (340). Impaired synthesis of those proteins would lead to decrease on the mitochondrial capacity to produce ATP and increase of free radical

production, being both events observed in cells overexpressing KMO. (3) KMO uses NADPH as a substrate. Whether glucose enters glycolysis or the pentose phosphate pathway in part depends on the concentration of NADPH (83). When the cell is rapidly converting NADPH to $NADP^+$. Raise of $NADP^+$ allosterically activates the first enzyme of the pentose phosphate pathway (glucose 6-phosphate dehydrogenase). Therefore, decreasing the availability of glucose 6-phosphate to fuel glycolysis, the citric acid cycle and, consequently, decreasing the substrates for oxidative phosphorylation: NADH and succinate (for complex I and complex II respectively). Due to reduced substrate availability (of reduced e- carriers), the maximal mitochondria capacity will accordingly decrease. In support of this, our group showed that high levels of 3-HK, which would activate NADPH consumption through KMO, decreased NADH levels in human primary neurons and astrocytes (149).

Not only 3-HK-induced ROS production contribute to the redox imbalance observed in KMO overexpressing cells, but also decreases on NADPH availability due to activation of KMO-mediated FAD reduction (68). This indicates that as important as having high 3-HK concentration is to have increased KMO expression or activity, to induce oxidative stress. In fact, those two act together, as 3-HK can activate KMO-mediated FAD reduction (70). In addition, KMO activation, independently of 3-HK production, will decrease antioxidant cell potential as it decreases NADPH availability for GSH (341) and catalase (342), which are essential for the cellular antioxidant capacity. According with that, we could not reproduce the ROS production observed in cells overexpressing KMO by addition of 3-HK in the supernatant of HEK-pEZ[-].

Previous studies have shown that 3-HK can induce ROS-mediated neurotoxicity at 10 μM in hippocampal and cortical neurons, however its up-take through sodium-dependent neutral amino acid transporters is needed (147). HEK 293 may not have the 3-HK transporter; therefore higher concentrations (250-500 μM, as described in literature) would be needed to induce ROS-mediated downstream toxicity (144). On the other hand, human primary neurons are more likely to express the sodium-dependent neutral amino acid transporter. However, 10 μM of 3-HK did not induce ROS production, but it decreased intracellular ATP. Indicating that lower concentrations of 3-HK than those required for HEK are needed to induce neurotoxicity.

Reduction of intracellular 3-HK levels by pharmacological inhibition of KMO would be expected to decrease ROS production in KMO overexpressing cells. However, the well-known KMO inhibitor, 3,4-dimethoxy-N-[4-(3-nitrophenyl)thiazole-2-yl] benzenesulfonamide (Ro-61-8048), did not decrease ROS production, but increased it at higher concentrations. The NADPH-dependent reduction of FAD in KMO, is not specific on recognition of the native substrate, but also can recognize substrate-like molecules (68), and Ro-61-8048 is structurally analogous to KYN (343). This indicates, that Ro-61-8048 can block 3-HK synthesis, but also be recognised by KMO and induce the NADPH-dependent reduction of FAD, and consequent production of H_2O_2. This should be taken into account when designing KMO inhibitors because, depending on their structure, they could inhibit 3-HK production but at expenses of increase hydrogen peroxide formation. Supporting our findings, this effect has been previously described with other synthetic KMO inhibitors analogues of KYN, such as, benzoylalanine and m-nitrobenzoylalanine (69).

In mammals, the KP through the KMO branch represents the *de novo* synthesis of NAD^+ from dietary tryptophan (344). NAD^+ is a key component in glycolysis, as well as in the catabolism of fatty acids and some amino acids. It is also essential in the citric acid cycle, which provides substrates for the ETS with the final outcome of ATP production. Therefore, when cellular energy status is triggered, activation of KP through KMO is likely to happen in order to increase NAD^+ and favour aerobic oxidation and ATP turnover. Moreover, it has previously been reported that pharmacological inhibition of oxidative phosphorylation with 3-nitropropionic acid (complex II inhibitor) results in reduced KAT-1 and KAT-2 activity (98). This indicates that: (1) KMO branch activation favours ATP production, and (2) when there is low ATP/ADP ratio the KAT branch of the KP is switched down (probably to potentiate NAD^+ production). This correlates with our results, where inhibition of ETS complex III, IV and V (antimycin A, sodium azide and oligomycin, respectively) showed an increase on KMO activity (even though only was highly significant for complex IV). Complex I inhibition (with rotenone) did not induce KMO activity, probably because electrons can still enter in the ETS through complex II at expenses of higher ROS production.

In conclusion, KMO should be given further consideration in neurodegeneration not only because is the door that controls the production of KP neurotoxic metabolites (3-HK and QUIN), but more importantly; (1) for its expression in neurons and possible role in mitochondrial dysfunction observed in most of the neurodegenerative diseases (2) for its capacity to generate redox imbalance, independently of metabolite production, and (3) for its participation in cellular energy control. Thus suggesting the need for development of new KMO inhibitors that not only decrease 3-HK synthesis but also ROS production.

5.5 Conclusion

As an acute response, KMO activation in neurons could restore ATP decline induced by mitochondrial inhibition by providing NAD^+ substrate to glycolytic source of ATP. However, KMO activation is not sustainable for long period of time as it would (1) lead to depletion of NADPH reservoir (68) decreasing aerobic respiratory capacity (as observed in KMO overexpressing cells) (2) induce oxidative stress affecting neuronal survival (145) and (3) exacerbate neurotoxicity caused by glutamate excitotoxicity. Additional considerations involving KMO neurotoxicity should be taken *in vivo,* as other cell types are involved. For example, QUIN produced by KMO activation in glia cells could potentiate neurotoxicity started by neuronal 3-HK (345). Also KMO activation in peripheral cells could decrease KYN availability in the brain necessary to produce the neuroprotective KYNA. Supporting that, inhibition of KMO in the periphery has shown to ameliorate neurodegeneration in AD and HD mice model. This independently of 3-HK and QUIN levels on the brain, but related to a raise of KYNA (330). This suggests that the neuroprotective mechanism underlying KMO inhibition is different depending on the cell type. Therefore, when designing KMO inhibitors, the cell target should also be considered. Not only that, but development of new KMO inhibitors, that can also decrease KMO-mediated ROS production, is needed in order to target neurons.

In this study we also propose a potentiation mechanism for KMO neurotoxicity. We showed that, under mitochondrial dysfunction, the KP is driven through the KMO branch in order to promote synthesis of the glycolytic co-factor NAD^+. But we have also shown that activation of KMO induces ROS production and mitochondrial impairment. Therefore, KMO becomes part of a loop where mitochondrial damage

exacerbation is the final outcome. This fact is especially relevant on neurons, which are highly sensible to mitochondria impairment.

In conclusion, activation of the KMO branch in the KP, as an acute response to energy deficit, could be necessary to quickly restore ATP levels. However, long-lasting KMO activation, due to pathological KMO overexpression or chronic mitochondrial impairment, will exhaust the antioxidant cell potential and promote mitochondrial dysfunction (Figure 5.10).

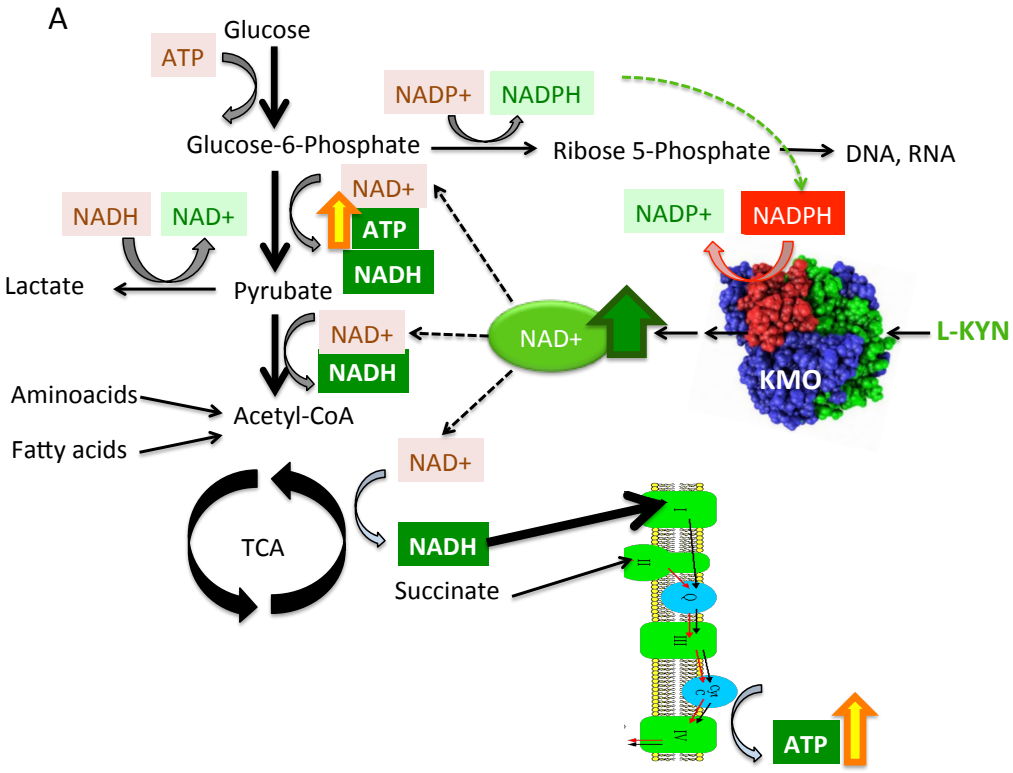

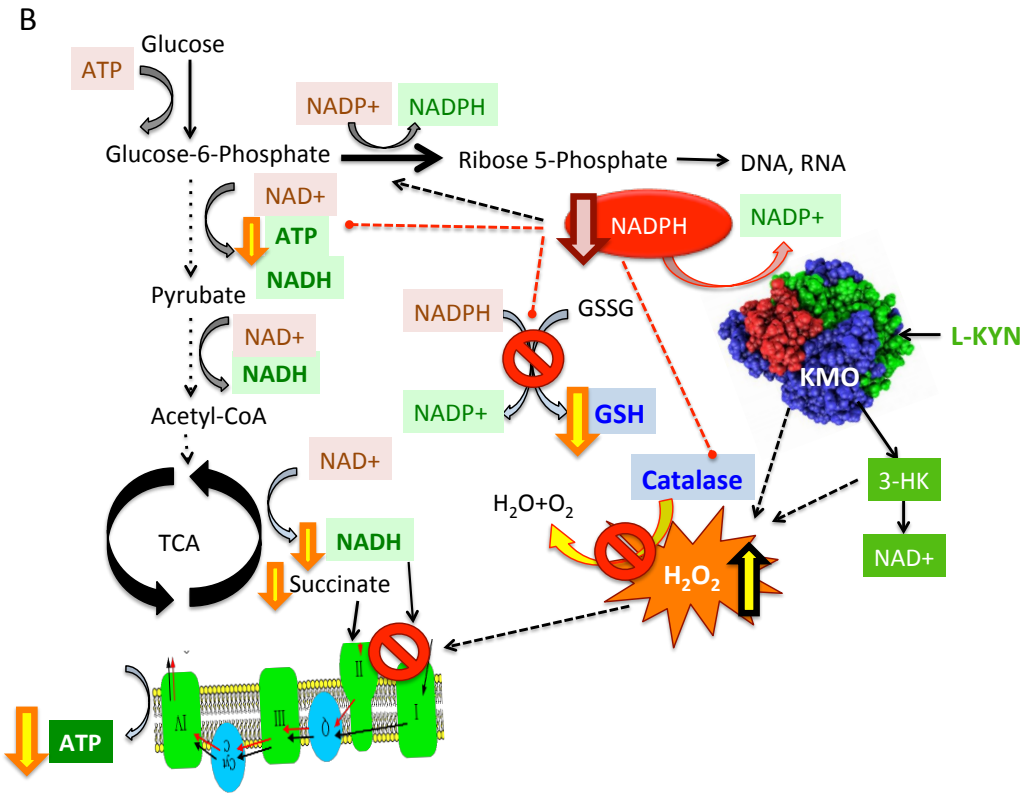

Figure 5.10: Proposed effects of KMO under acute or chronic activation in neurons

(**a**) Acute activation of KMO leads to increased NAD^+ levels, which is incorporated in glycolysis and tricarboxylic acid (TCA) cycle. Thus, provide the substrates necessary for oxidative phosphorylation and promote ATP turnover. (**b**) Long term or chronic KMO activation exhaust NADPH reservoir. Thus, inhibits glycolysis to favour de novo synthesis of NADPH through the pentose 5-phosphate pathway and decrease cellular antioxidant capacity, leading to increased ROS production and mitochondrial dysfunction.

5.6 Future directions

When interpreting our results, we should take into consideration that KMO was overexpressed in a non-neuronal cell line, which is metabolically different to primary neurons. The bioenergetics profile of HEK overexpressing KMO showed substantially lower SRC when compared with wt. This indicates that an increase in KMO activity may decrease the ability to produce energy through oxidative phosphorylation. However, we did not observe a decrease in ATP levels, which indicates that under normal conditions, those cells could cope with energy requirements, most likely by relying on glycolysis. Primary neurons constantly require energy to sustain glutamatergic neurotransmission, and they are the most energy demanding cells in the brain and the most sensitive to energy stress. In order to maintain the antioxidant

redox status, neurons mainly degrade glucose through the pentose phosphate pathway at the expense of decreasing the glucose available for energy turnover through glycolysis. Neurons rely on mitochondrial oxidation as the main source of ATP and use the pyruvate provided by astrocytes as a substrate for the TCA cycle (272). Therefore mitochondrial impairment caused by KMO hyperactivity would affect their survival.

Our initial aim was to create a KMO-stable transfected neuroblastoma cell line (using SH-SH5Y; ATC CRL-2266) in order to study the role of KMO activity in neurons. However, due to cell death induction by hKMO overexpression we had to conduct our experiments in HEK293. Another approach to that problem, would be to stable transfect SH-SH5Y with a plasmid where KMO expression is under the control of an inducible promoter. This would allow to successfully expanding the SH-SH5Y cells that incorporated the plasmid and induce KMO overexpression only at the time of the experiment, avoiding cell death during the selection steps.

In order to study how an increase of KMO activity would specifically affect energy metabolism in human primary neurons, our next approach will be transfect our primary cultures with pEZ[KMO]. Real time measurements of mitochondrial function and glycolysis can be done in neuronal cell cultures using Seahorse Bioscience technology. This would allow us to observe whether KMO activity induces a metabolic switch in neurons from mitochondrial respiration to glycolysis. This is not only interesting in neurons, but could also be relevant as a regulatory mechanism of the immune response. Differences in glycolysis and mitochondrial respiration have previously been described in effector and memory $CD8^+$ T cells (274).

Chapter 6

Epigallocatechin-3-gallate induces oxidative phosphorylation in human primary neurons and astrocytes. New insight to modulate the kynurenine pathway

This research chapter is adapted and modified from the following publication:

Gloria Castellano-González, Nicolas Pichaud, J. William O. Ballard, Alban Bessede, Helder Marcal and Gilles J. Guillemin (2014)

"*Epigallocatechin-3-gallate induces oxidative phosphorylation by activating cytochrome c oxidase in human primary neurons and astrocytes*"

6.1 Introduction

Epigallocatechin-3-gallate (EGCG) is the main polyphenol component of green tea, representing more than 10% extract in dry weight. This naturally occurring molecule is a flavonoid that belongs to the catechin subgroup. The strongest bioactivity of flavonoids is anti-oxidant which is potentiated by the catechol structure. This functional group can chemically scavenge ROS at relatively low concentrations but has pro-oxidative/pro-apoptotic properties at higher concentrations (346). Moreover, it can modulate protein functions through interactions within their hydroxyl group and the amino and carbonyl groups in proteins (347). These properties have conferred multiple physiological and therapeutic benefits to EGCG. For example, it has been used in cancer therapy for its apoptotic and anti-proliferative properties and its activity on immune response (348-352). EGCG has also been shown to be beneficial in autoimmune diabetes due to its anti-inflammatory activity in different cell types (353). Finally, it has important protective effects in neurodegenerative diseases involving different molecular mechanisms and signalling pathways (for review (354)).

Although many studies attribute the neuroprotective role of EGCG to its properties as a radical scavenger (Zhuang et al. 2003), other pharmacological properties may further contribute to its therapeutic benefits. Neurodegenerative diseases are usually accompanied by fuel restrictions in neurons and mitochondrial impairment. EGCG has been previously shown to target energy metabolism in several cell types, mainly as an agonist of the main cellular energy sensor, AMP-Activated protein kinase (AMPK) (355, 356). Studies in mice demonstrated that EGCG can cross the blood barrier and reach the brain (357) and it has been shown to accumulate in neuronal mitochondria (358). Of interest, it has also been shown to restore mitochondrial membrane potential, mitochondrial function as well as ATP synthesis in Alzheimer's Disease mice model (359).

Lower ATP production and increased formation of ROS in mitochondria are commonly observed alongside cytochrome c oxidase (CcO) impairment (323), which has have been shown to occur in AD pathology and other neurodegenerative diseases. CcO or mitochondrial complex IV is the terminal oxidase of the mitochondrial ETS and catalyses the final step of the electron transfer from reduced cytochrome c to oxygen.

It is also one of the proton pumps that generates the proton gradient across the inner mitochondrial membrane to power ATP synthesis (360).

Natural occurring molecules with antioxidant capacity have been studied for their potential capacity to restore impaired mitochondrial function under neurodegenerative conditions. In this study, we screened different natural compounds for their ability to increase neuronal ATP-turnover. Our aim was to find candidates that can alleviate the mitochondrial impairment observed in neurodegenerative diseases and to identify their underlying mechanisms of action.

Our results showed that EGCG induces CcO activity in human primary neurons and astrocytes. It suggests that in addition to its antioxidant properties EGCG can induce mitochondrial respiration by activating CcO in human primary neurons, increasing ATP production without altering redox balance. Therefore using EGCG because of its poly-pharmacological activities, its bioavailability properties and its restoring effect on mitochondrial function makes it a promising candidate for treating several neurodegenerative diseases with mitochondrial impairment as a common feature.

6.2 Methods

6.2.1 Cell culture

Human primary neurons and astrocytes were prepared and maintained as described in section 3.1 .

6.2.2 ATP- Luminescent measurements

Several natural compounds were screened for their ability to induce ATP-turnover. Treatment with KYNA (10 µM), P. Emblica (30 µg/mL), Pomegranate (30 µg/mL), Curcumin L. (30 µg/mL), Berberine (30 µM) or EGCG (30 µM) was done for 2 and 24h in human primary neurons. Among the different natural compounds tested, EGCG showed the most significant increase in intracellular ATP production in human primary neurons (Figure 6.1) and was therefore selected for further analysis. For EGCG-ATP kinetics induction studies, cells were treated with 10 µM of EGCG in the appropriate culture media at different time points. For dose–dependent studies

increasing concentrations of EGCG in the appropriate culture media were added for 24h in neurons and 3h in astrocytes. For ATP depletion studies, cells were treated with 2.5μM antimycin A, 1 μM of rotenone, 5 μM of oligomycin, 10 mM of sodium azide, 10 μM of Compound C and 5 mM of 2-deoxy-D-glucose (2-DG). Treatment with the mitochondrial inhibitors was performed 2h before treatment with EGCG. 2-DG or Compound C was added with EGCG for 24h. Controls were treated with equal amount of the solvent used for each treatment. After treatments the cells were immediately harvested in PBS and assessed for intracellular total ATP production using a commercially available luciferase-luciferin system (ATPlite, Perkin Elmer) in a PHERAstar plate reader. Cells were lysed by repeated freeze and thaw cycles and centrifuged at 10,000 g for 10 minutes; the supernatant was used for ATP measurements and protein quantification. All experiments were performed using a minimum of 1 mg/mL of cell protein lysate. Protein measurements were determined using Pierce BCA protein assay Kit (Thermo scientific). Total ATP was normalised against total protein to account for any difference in cell density.

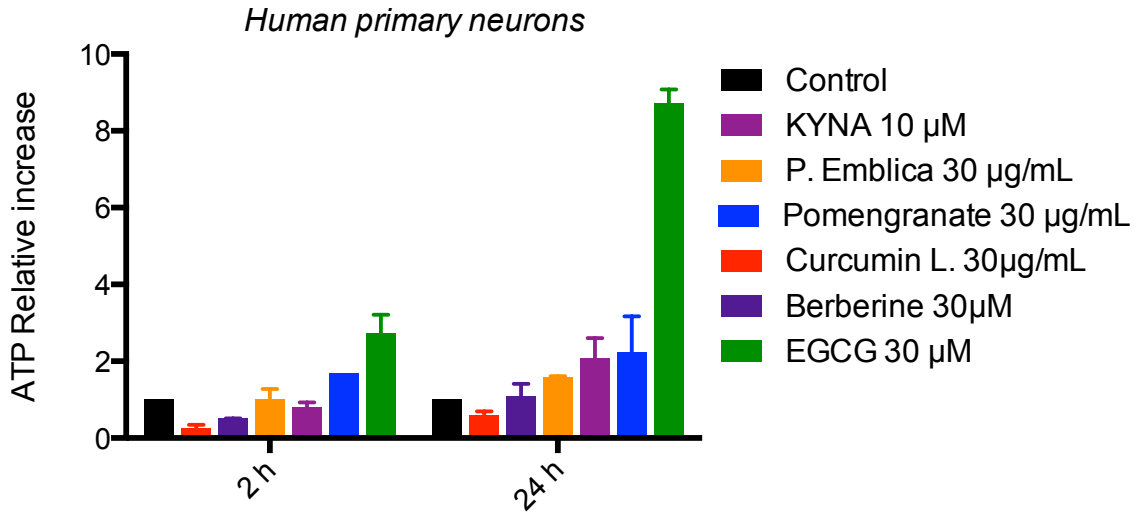

Figure 6.1: Screening of natural occurring molecules for its ability to increase ATP turn over in human primary neurons

ATP production of neurons after treatment with natural compounds assessed by luminescent intensity. Data (means ± s.e.m. of two experiments) are presented as normalised mean intensity in sample relative to normalised mean intensity in untreated sample. ***p≤0.001 (EGCG treatment versus none after 24h; Student's t-test).

6.2.3 Cytotoxicity

The release of LDH in the cell culture supernatant correlates with the amount of cell death and membrane damage, providing an accurate measure of cellular toxicity (361). LDH activity was measured in parallel with the ATP. It was assayed using the commercial CytoTox 96 cytotoxicity assay (Promega) following the manufacturer's specifications. LDH activity in the supernatants was normalized against total protein to account for any difference in cell density.

6.2.4 Assessment of mitochondrial membrane potential

Quantitative mitochondrial membrane potential (ΔΨm) was determined using R123, as previously described (362) with slight modifications. Neurons or astrocytes cultures in 12 well plates were treated at different time points with 10 µM of EGCG in culture medium. Then, cells were washed with warm PBS and incubated with 10 µM of R123 (quenching mode) in L-15 medium supplemented with 5 mM of glucose for 20 minutes at 37°C in a humidified atmosphere containing 5% CO_2. The R123-containing medium was removed and cells were washed with PBS and further incubated in warm L-15 medium supplemented with 5 mM of glucose at 37°C for 15 minutes. The sample was immediately placed in the fluorescence spectrophotometer (PHERAstar plate reader) at 37°C with excitation and emission set at 560 and 645 nm respectively and mean fluorescence intensity was measured using orbital averaging to account for uneven cell distribution across the well. In quenching mode the probe accumulates within the mitochondria forming aggregates that quench some of the fluorescent emission of the dye. Mitochondrial depolarization (higher ΔΨm) results in the release of the dye, thus unquenching the dye and increasing the fluorescence signal.

Quantitative ΔΨm was also determined using CMXRosamine (CMXRos) probe (MitoTracker, Invitrogen Life technologies) according to previous studies showing that an increase in ΔΨm lead to an increase of CMXRos fluorescence intensity (363). Briefly, neurons cultured in glass coverslips were treated at different time points with 10 µM of EGCG in culture medium. Then cells were washed with warm PBS prior to add 50 nM of CMXRos in L-15 medium supplemented with 5 mM of glucose. Cells were incubated for 30 minutes at 37°C in a humidified atmosphere containing 5%

CO_2, then washed with warm PBS and immediately fixed with 4% paraformaldehyde for 15 minutes at room temperature. Nuclear staining was performed by incubating the cells with 4,6-diamidino-2-phenylindole (DAPI) at 1 mg/mL for 2 minutes at room temperature. Then, after washing with PBS, the coverslips were mounted on glass slides with Fluoromount-G. Epifluorescence images were obtained on an Olympus FV1000 confocal microscope captured with a CCD camera. For each coverslip, ten randomly selected fields were acquired using the same settings along each experiment. After background correction, fluorescence intensity for CMXRos was measured for each condition using ImageJ software (364). Mean fluorescence intensity was normalized against the total number of cells.

6.2.5 Mitochondrial respiration in intact cells

Oxygen consumption in intact cells was measured using the high-resolution respirometer Oxygraph-2K (Oroboros instruments), as described in section 3.6 . Briefly, intact cells were removed from the tissue culture dish with TripE (Invitrogen) and after one wash with PBS, 5 $x10^6$ cells were added to normal culture medium. Cell suspension was immediately placed in the oxygraph chamber at 37°C under continuous stirring at 300 rpm for respiration analysis. Each experiment was repeated three times with cell preparations from different samples and results were expressed as pmol O_2 consumed per min per million cells or OCR relative to OCR during routine respiration.

6.2.6 Quantitative real-time polymerase chain reaction

Total RNA from cells was prepared from RNeasy mini kits (Absolutely RNA Miniprep Kit) and processed as described in general methods. The relative expression of peroxisome proliferator-activated receptor Ɣ coactivator 1α (Pgk-1α), mitochondrial transcription factor A (Tfam) and Mitofusin2 was normalised against the house-keeping genes Tbp and Pgk-1. Data were analysed with the ΔCt values and expressed as fold change compared to controls. Primer sequences used for qRT-PCR are shown in Table 6.1.

Table 6.1: Primer sequences used in Chapter 6

Gene	*Forward sequence*	*Reverse Sequence*
Tfam	5'-CCTGCTCGGAGCTTCTCAAA-3'	5'-ACCCTTGGGGTCATTTGGTG-3'
Pgc-1α	5'-AGAACAGCTAACTCCAAGTCAGATT-3'	5'-CTTCAGCTTTTCCTGCGGTGAAT-3'
Pgk-1	5'-TCACTCGGGGCTAAGCAGATT-3'	5'-CAGTGCTCACATGGCTGACT-3'
Tbp	5'-GGGAGCTGTGATGTGAAGT-3'	5'-GGAGGCAAGGGTACATGAGA-3'
Mitofusin2	5'-ACCCTGATGCAGACGGAAAA-3'	5'-ACCAGGAAGCTGGTACAACG-3'

6.2.7 Mitochondrial complex IV content and activity

The activity of complex IV (cytochrome c oxidase) was measured by using Human complex IV activity microplate assay Kit from Mitosciences (Abcam) according to the manufacturer's instructions. Briefly, cells were lysed and BCA assay was used to measure total protein content. The same amount of protein was loaded in each condition (≈100 µg). Complex IV was immunocaptured with CcO antibody and the activity was measured by the oxidation rate of reduced cytochrome *c* at 550 nm, using PHERAstar plate reader (BMG labtech).

6.2.8 Oxidative stress determination

Intracellular oxidative stress was assessed using the DCF-H_2 dye (Invitrogen) as in section 5.2.9 . Astrocytes and neurons were pretreated with varying concentrations of EGCG (1-100 µM) for 2h (astrocytes) and 24h (neurons). After washing twice with PBS, cells were incubated with 10 µM DCF-H_2 in L-15 medium supplemented with 5 mM of glucose for 30 minutes at 37°C in a humidified atmosphere containing 5% CO_2. Then, cells were washed twice with PBS and pre-warmed L-15 medium supplemented with 5 mM of glucose and 1% FCS was added. The fluorescence intensity was immediately measured at 37°C using orbital averaging in the PHERAstar plate reader with excitation and emission wavelengths set at 485 nm and 530 nm respectively.

6.2.9 Apoptosis

Apoptosis was measured quantitatively using Annexin-V FITC (BD Biosciences) and propidium iodide. This protocol numerates early apoptotic cells by probing for cell surface exposed phosphatidylserine with FITC labelled annexin V and for plasma membrane integrity by propidium iodide (PI). Cells were treated with EGCG at different concentrations for 24h and with TNF-α as an apoptotic positive control for 48h. Recovered cells were suspended in 1X binding buffer and Annexin-V FITC and propidium iodide were added prior to flow cytometry analysis.

6.3 Results

6.3.1 EGCG induces ATP production in human primary neurons and astrocytes with different kinetics and dose-response patterns.

After EGCG was selected for its capacity to increase ATP production in human primary neurons (Figure 6.1), we investigated the mechanism of action of the ATP production induced by EGCG by performing dose-response and kinetic studies in the two main cell types present in the brain: neurons and astrocytes.

Both neurons and astrocytes showed a 2-fold increase in ATP production after 1h treatment with 10 μM EGCG. In neurons, the ATP production is maintained and increased over 48h (Figure 6.2a) whereas in astrocytes the ATP is restored to basal levels after 16h (Figure 6.2c). Neurons and astrocytes were treated with different dose of EGCG (1 to 100 μM) for 3h in astrocytes and 24h in neurons. Increasing concentrations of EGCG (up to 60 μM) correlate with increasing production of ATP in neurons (Figure 6.2b). In astrocytes however, ATP production was maximal at 1-10 μM, and dropped at higher concentrations (Figure 6.2d). Cytotoxicity studies were done in parallel to verify that the treatments used were not causing cell death and that the increase of ATP observed was not due to induction of apoptotic pathways. LDH was measured in the supernatant of each condition, showing no cytotoxicity over 72h in neurons and astrocytes treated with 10 μM of EGCG (Figure 6.2e). However, cell death was induced in neurons and astrocytes when treated for 24h with more than 40 μM of EGCG (Figure 6.2f). These results correlate with the decrease in ATP production observed in neurons (Figure 6.2b) at more than 60 μM.

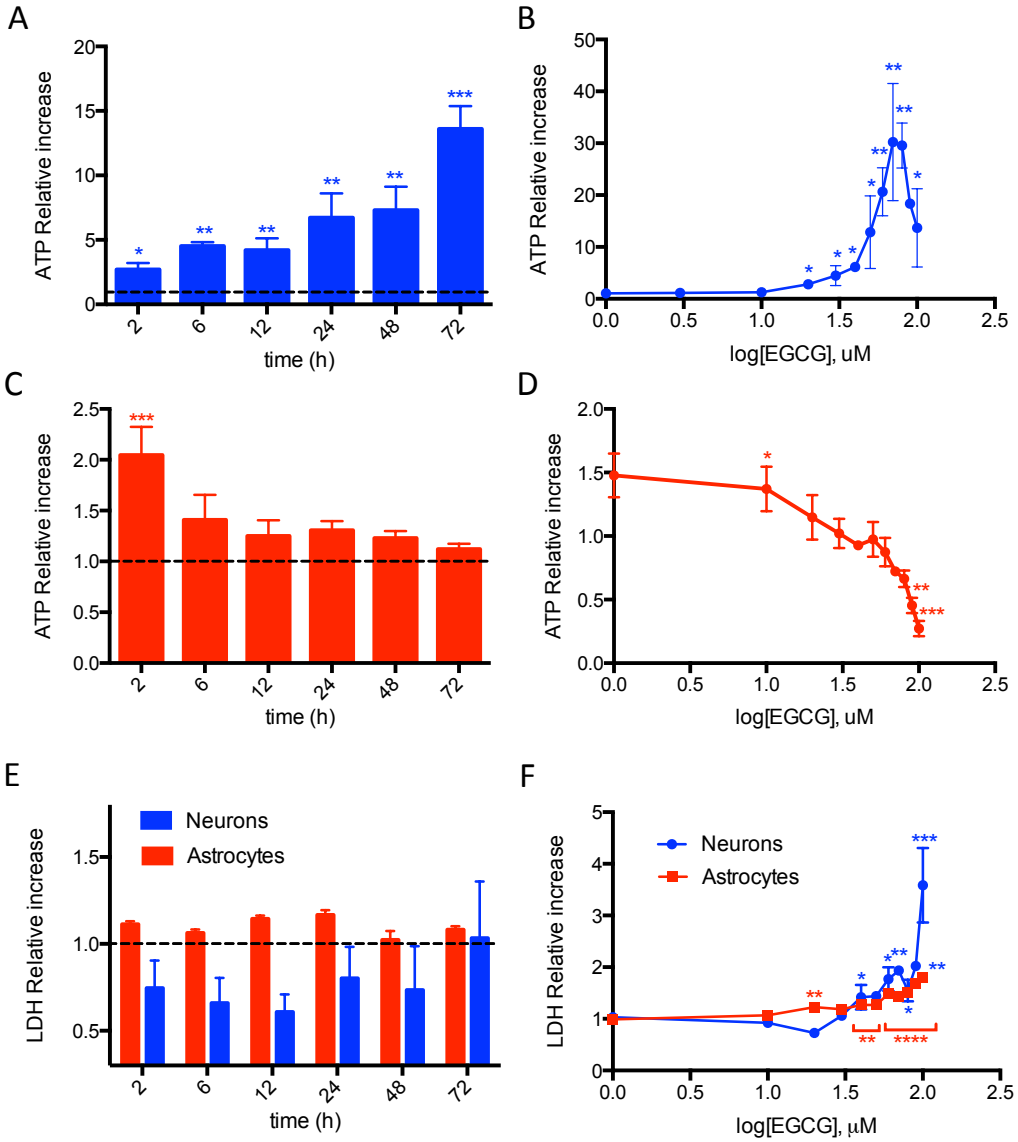

Figure 6.2: ATP modulation in neuron and astrocytes by EGCG treatment

ATP production of neurons (**a,b**) and astrocytes (**c,d**) after treatment with 10 µM EGCG at different time points (**a,c**) and with increasing concentrations (1-100 µM) for 24h (**b**) or 2h (**d**) was assessed by luminescent intensity. Data (means ± s.e.m. of three or six experiments) are presented as normalised mean intensity in sample relative to normalised mean intensity in untreated sample for each time point. *p≤0.05, **p≤0.01, ***p≤0.005 (treatment versus none; Student's t-test). Cell death of neurons and astrocytes after treatment with 10 µM EGCG at different time points (**e**) and with increasing concentrations (1-100 µM) for 24h neurons or 2h astrocytes (**f**) assessed by LDH activity in cell. Data (means ± s.e.m. of three experiments) are presented as normalised mean activity in sample relative to normalised mean activity in untreated sample. *p≤0.05, **p≤0.01, ***p≤0.005, ****p≤0.001 (treatment versus none; Student's t-test).

6.3.2 EGCG increases mitochondrial membrane potential in both astrocytes and neurons

Mitochondrial membrane potential relates to cells' capacity to generate ATP by oxidative phosphorylation. Mitochondria produce ATP via the electrochemical proton motive force (Δp), which is due to the transfer of electrons through the complexes of the ETS and provides the energy to drive the protons against their concentration gradient across the inner mitochondrial membrane (332).

Due to the increase in ATP production observed after 1h treatment (Figure 6.2 a,c), we hypothesised that EGCG may be acting directly in one of the two main sources of ATP production in the cell: oxidative phosphorylation or glycolysis. Taking into account that the main source of ATP in neurons is mitochondrial oxidative phosphorylation (273) and that the effect of EGCG on ATP production is significantly higher in neurons than in astrocytes (Figure 6.2a,c), we therefore looked at the effect of EGCG on mitochondrial function. We examined changes on the mitochondrial membrane potential ($\Delta\psi_m$), which can be used as an indicator of the Δp. Increase in ATP due to an activation of the ETS would co-occur with an increase of Δp and $\Delta\psi_m$. In this study, $\Delta\psi_m$ is measured with two different probes: R123 and CMXRos. Treatment with EGCG showed an increase in $\Delta\psi_m$ by R123 fluorescence in both cell types, reaching its maximum after 10 minutes in astrocytes and 1h in neurons (Figure 6.3a). The experimental time was limited to 1h, because quenching is a non linear event that can only be appropriate for monitoring acute effects of experimental treatments (365). Study of relative changes of $\Delta\psi_m$ was also performed by IF using CMXRos in human primary neurons (363). We observed an increase on the relative fluorescence intensity of CMXRos within the mitochondria after 10 minutes treatment with EGCG (Figure 6.3b). Thus, the induction of R123 and CMXRos fluorescence by EGCG indicates that $\Delta\psi_m$ is increasing. Moreover, it suggests that EGCG effect on ATP production could be mediated by induction of the ETS.

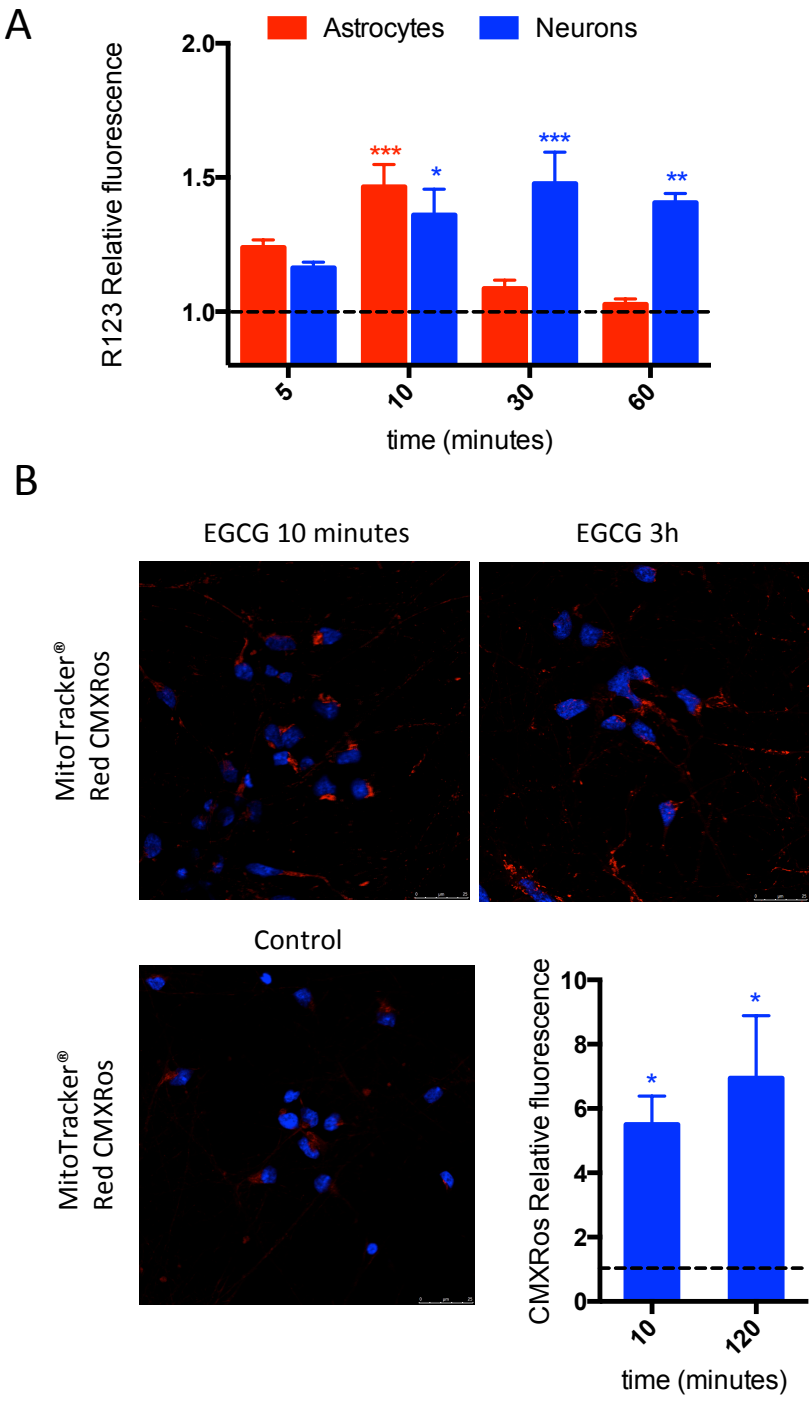

Figure 6.3: EGCG increases mitochondrial membrane potential

(**a**) Mitochondrial membrane potential of astrocytes and neurons assessed by R123 fluorescence intensity measured at different time points after 10 µM of EGCG treatment. Data (means ± s.e.m. from three experiments) are presented as mean fluorescence in sample relative to mean fluorescence in untreated sample for each time point. ***p≤0.001, **p≤0.005, *p≤0.01 (treatment time point versus time 0; Student's t-test), (**b**) Mitochondrial membrane potential of neurons assessed by Mitotracker CMXRos fluorescence intensity after treatment with 10 µM of EGCG. Data (means ± s.e.m. of two experiments) are presented as normalised mean fluorescence in sample relative to normalised mean intensity in untreated sample for each time point. *p≤0.01 (treatment versus none; Student's t-test).

6.3.3 EGCG increases neuron and astrocytes mitochondrial respiration but does not induce mitochondrial biogenesis

Δp is dependent of $\Delta\psi_m$ and the mitochondrial pH gradient (ΔpH) and can be represented at 37°C by the equation: $\Delta p(mV) = \Delta\psi_m - 60\Delta pH_m$. However, $\Delta\psi_m$ does not necessarily follow the proton gradient (ΔpH_m), which is directly related to ATP production. During cellular stress, $\Delta\psi_m$ could be altered by dysregulation of intracellular ionic charges (ie. Ca^{2+} or K^+), independently of ETS induction (366). In order to assure that the changes observed in $\Delta\psi_m$ are mediated by ETS induction, we monitored cell oxygen consumption using high-resolution respirometry.

Considering that EGCG increases $\Delta\psi_m$ within 10 minutes, the O_2 rate was monitored before and after EGCG addition. We found that addition of 10 µM EGCG immediately increased routine O_2 consumption rate (R) in neurons (Figure 6.4b) and astrocytes (Figure 6.4a). No significant differences were observed in proton leak or ETS capacity. Cellular routine respiration is supported by exogenous substrates in the culture medium. Only physiological energy demand, energy turnover and the degree of coupling (intrinsic uncoupling and pathological dyscoupling) control the levels of respiration and phosphorylation in the physiological R of intact cells (337, 367). Knowing that EGCG does not increase energy demand and that there are no changes on intrinsic uncoupling (L), the increase in O_2 consumption is probably linked to an increase in energy turnover.

Measuring mitochondrial respiration in intact cells allows the integration of mitochondrial quality (function) and quantity (density). To determine whether the changes observed in routine respiration were due to an increase in mitochondrial density, we measured expression of two key genes involved in mitochondrial biogenesis, *Pgc-1α* and *Tfam* as well as a marker of mitochondrial mass, *mitofusin 2* (368). Our results showed that EGCG did not influence mitochondrial biogenesis. It therefore suggests that the observed changes in mitochondrial respiration were due to an increase of the mitochondrial functional properties induced by EGCG (Figure 6.4c).

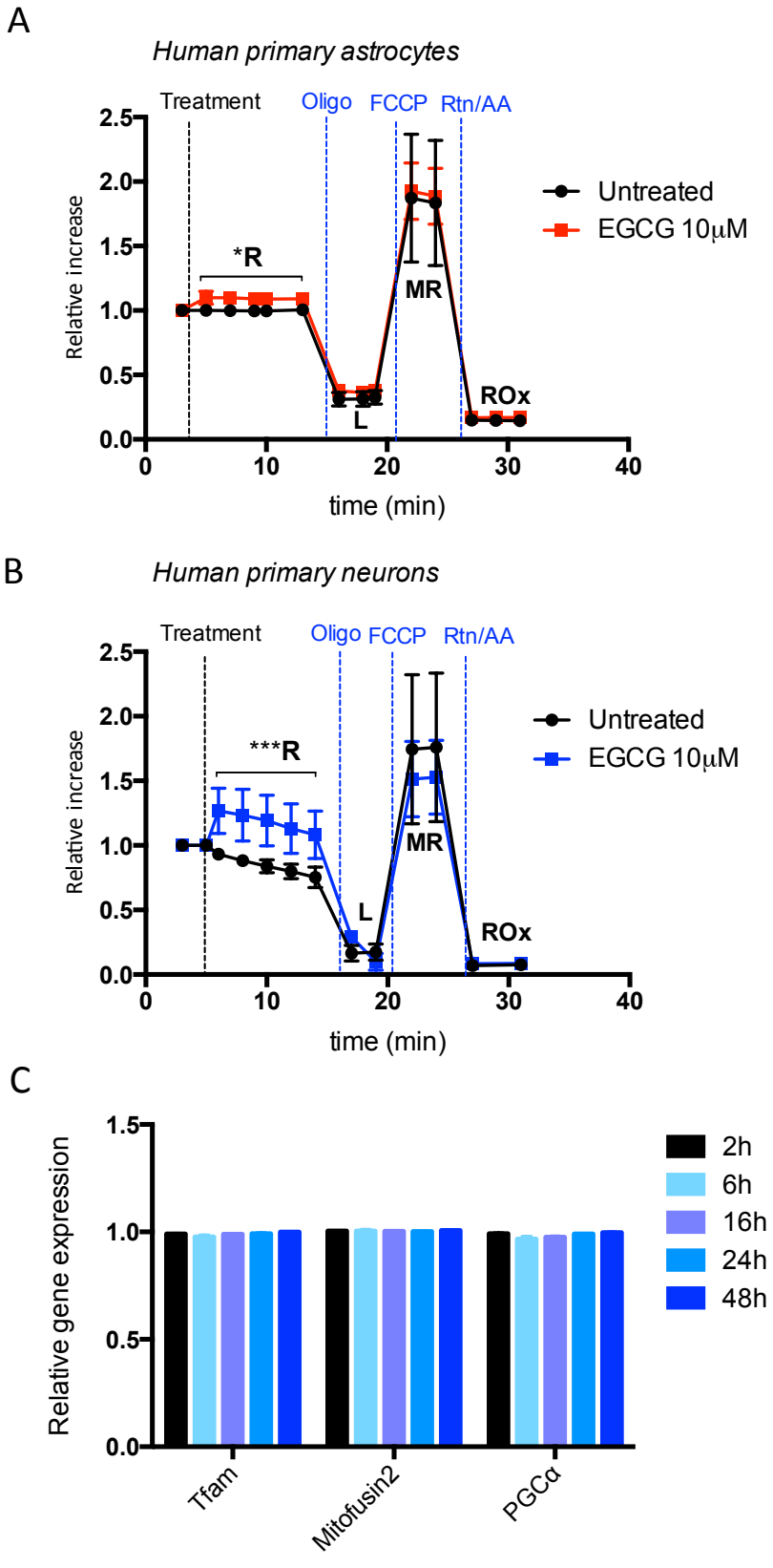

Figure 6.4: EGCG increases neuron and astrocytes routine respiration without altering mitochondrial biogenesis

O_2 consumption rate [pmol O_2/min] of intact astrocytes after treatment with 10 µM of EGCG for 2h (**a**) and neurons before treatment with 10 µM of EGCG (**b**) showed by superimposed oxygraph traces from parallel measurements in two chambers.

Mitochondrial inhibitors (and treatment in b) were added, at the time points indicated, in both chambers for the study of respiratory states. Data (means ± s.e.m. of three experiments) are presented as cell number-specific oxygen flux in sample relative to cell number-specific oxygen flux in control sample during routine respiration. *p≤0.05 ***p≤0.005 (Treatment versus none; Student's t-test). (**c**) Mitochondrial biogenesis markers (*Tfam* and *PGC-α*) and mitochondrial mass marker (Mitofusin2) gene transcript expression of human primary neurons after treatment with 10 μM of EGCG at different time points. Data (means ± s.e.m. of three experiments) are presented as normalised transcript expression in the samples relative to normalised transcript expression in untreated sample (Student's t-test).

6.3.4 EGCG-dependent ATP increase is inhibited when complex IV is blocked in neurons and astrocytes, but not when glycolysis is inhibited

To establish whether EGCG enhances oxidative phosphorylation by directly activating a mitochondrial complex, we measured changes in EGCG-dependent intracellular ATP increase in the presence of different complexes inhibitors. The time of treatments were chosen based on the previous kinetics studies, i.e. 16 h in neurons and 2 h in astrocytes. Sodium azide, a reversible inhibitor of complex IV, decreased the EGCG-dependent ATP production in neurons and astrocytes (Figure 6.5a,b). Moreover, when ATP synthase was irreversibly inhibited with oligomycin, a decrease in EGCG-dependent ATP production was also observed. Although neither sodium azide nor oligomycin completely blocked the effect of EGCG on ATP production in neurons, they did so in astrocytes. This could be due to differences in time of treatment, as longer treatment time in neurons could allow EGCG to activate secondary targets of other cellular metabolic pathways.

We also tested whether EGCG-dependent ATP production could be mediated by induction of the glycolysis pathway or by AMPK. We used 2-Deoxy-D-Glucose (2-DG), which competitively inhibits the production of glucose-6-phospahate from glucose at the hexokinase level, the rate-limiting enzyme of the glycolysis pathway (369) and 10 μM of Compound C (AMPK pharmacological inhibitor). Neither 2-DG nor Compound C inhibited the EGCG-induced ATP production in neurons (Figure 6.5c, d).

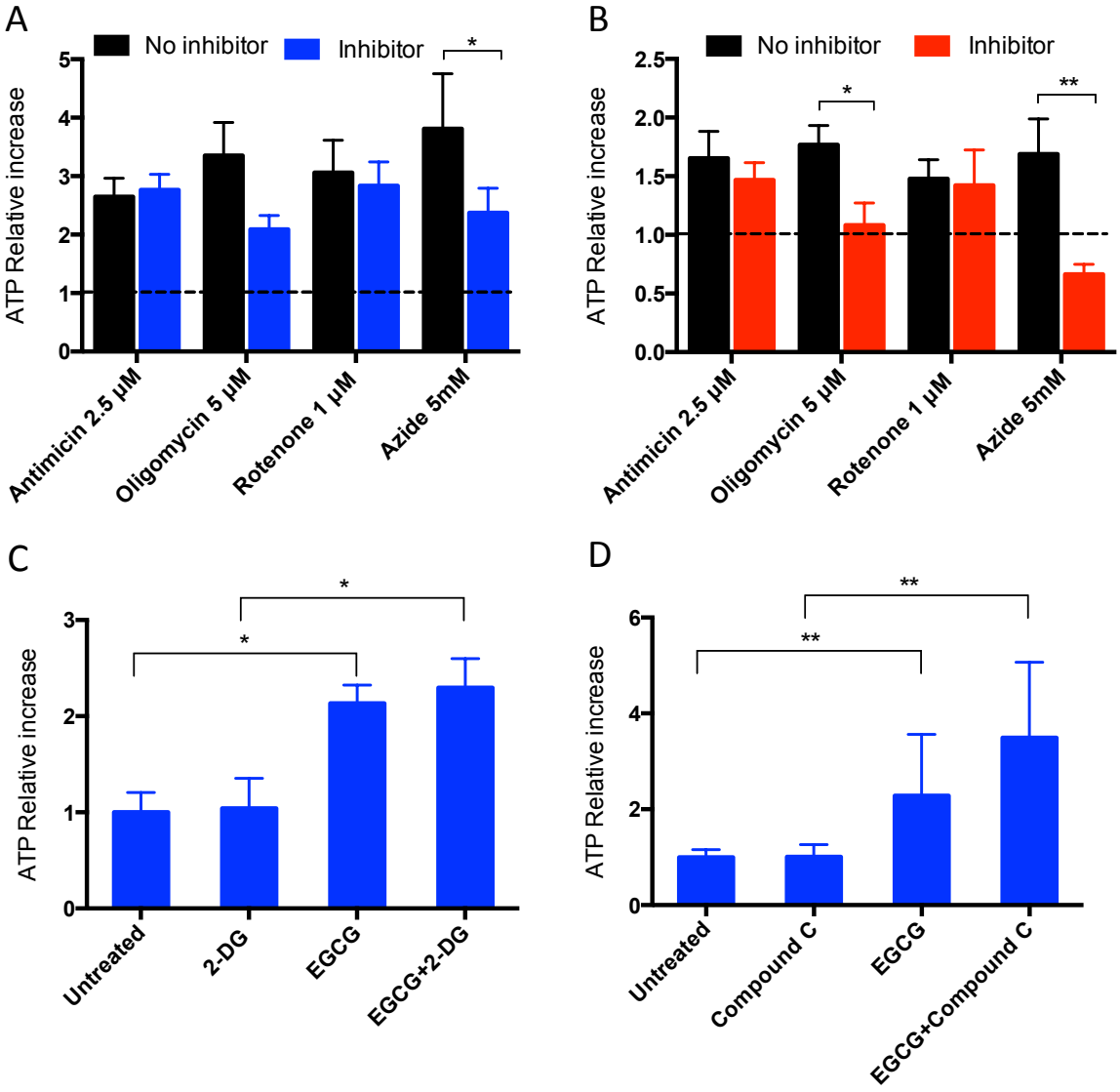

Figure 6.5: EGCG-dependent ATP increase is inhibited when complex IV is blocked in neurons and astrocytes.

ATP production of neurons (**a**) and astrocytes (**b**) after treatment with 10 µM EGCG with or without specific mitochondrial complexes inhibitors for 16 and 2h, respectively and assessed by luminescent intensity. Data (means ± s.e.m. of three experiments) are presented as normalised mean intensity in sample relative to normalised mean intensity in non-EGCG treated sample from each condition (no inhibitor and inhibitor), in which fold change=1. *p≤0.01, **p≤0.005 (Student's t-test). ATP quantification of neurons after treatment with 10 µM EGCG with or without Compound C (**c**) or 2-DG (**d**) for 16h and assessed by luminescent intensity. Data (means ± s.e.m. of three experiments) are presented as normalised mean intensity in sample relative to normalised mean intensity in untreated sample. *p≤0.01, **p≤0.005 (Student's t-test).

6.3.5 EGCG activates complex IV activity in neurons and astrocytes without concomitant increase of ROS production

In order to confirm the direct effect of EGCG in cytochrome c oxidase activity, we immunocaptured its cellular content and measured its activity by following the degradation rate of cytochrome c in cell cultures exposed to 10 μM EGCG. We observed higher cytochrome c activity in neurons and astrocytes treated with EGCG compared with the controls (Figure 6.6a,b), therefore confirming that EGCG is activating complex IV activity. Interestingly, we observed an increase of O_2 consumption in intact cells after complete inhibition of the mitochondrial complexes I, III and V when 10 μM of EGCG was added in the culture medium (data not shown). This observation supports that EGCG is increasing complex IV activity.

Molecular oxygen is reduced to water in the complex IV by a sequential four-electron transfer, however a minor proportion can be reduced by a $1e^-$ addition that occurs predominantly in the complex III but also in the complex I (370). High $\Delta\psi_m$ enhances the reduction of molecular oxygen to superoxide anion O_2^- by complex I and III. Since EGCG is increasing complex IV activity, the concomitant increase in $\Delta\psi_m$ is expected to promote higher rates of mitochondrial superoxide. In order to verify this hypothesis, we therefore measured ROS production in EGCG treated neurons and astrocytes. Treatment with EGCG up to 50 μM in both cell types did not increase ROS production, whereas 100 μM increased their production in neurons (Figure 6.6c). Excessive ROS production is associated with induction of apoptosis. We therefore measured activation of apoptosis with AnnexinV$^+$/PI$^-$ FACs analysis in astrocytes treated for 48h with increasing concentrations of EGCG. We did not observed increased apoptosis (AnnexinV$^+$/PI$^-$) or necrosis (AnnexinV$^+$/PI$^+$) in astrocytes treated with up to 30 μM of EGCG compared with the control. However, both necrotic and apoptotic cells were increased in 100 μM treatment with EGCG (Figure 6.6d). These results indicate that the induction of complex IV by EGCG does not increase ROS production at the concentrations used in our study. Nonetheless, at higher doses the increase of $\Delta\psi_m$ by complex IV activation could be increasing superoxide production by complex I and III, which ultimately induces apoptosis and cell death.

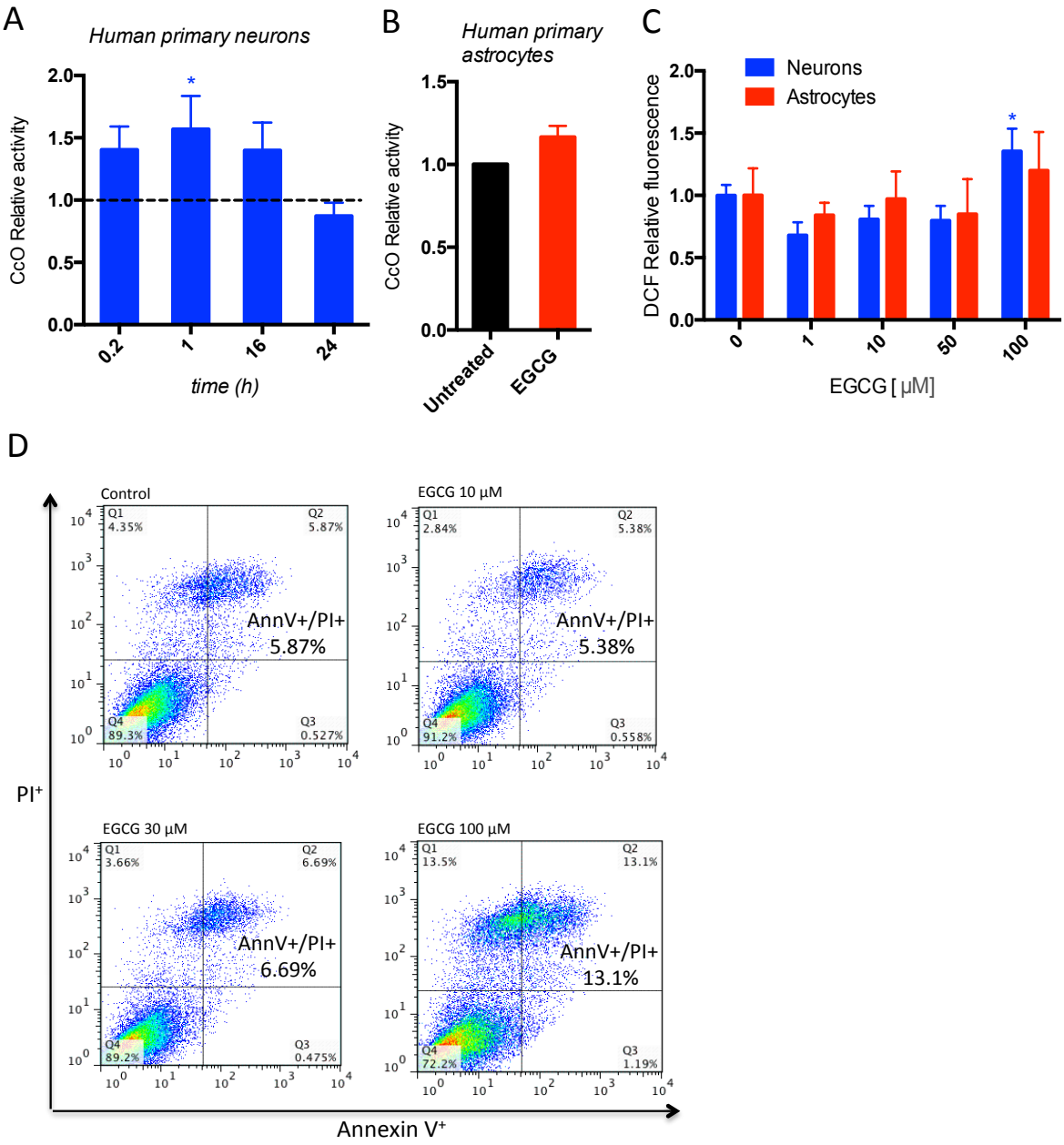

Figure 6.6: EGCG activates complex IV activity without increasing oxidative stress or apoptosis

Cytochrome c oxidase activity of neurons and astrocytes after treatment with 10 µM of EGCG at different time points (**a, b**) assessed by the enzymatic degradation rate of cytochrome c and showed as relative increase of untreated. Data (means ± s.e.m. of three experiments) are presented as normalised mean activity in sample relative to normalised mean activity in untreated sample for each time point. *p≤0.01 (Student's t-test). (**c**) ROS production of neurons after treatment with different concentrations of EGCG (1-100 µM) and assessed by DCF fluorescence intensity. Data (means ± s.e.m. of three experiments) are presented as mean intensity in sample relative to mean intensity in untreated sample. *p≤0.01 (Treatment versus none; Student's t-test). (**d**) Apoptosis of astrocytes after treatment with 10-100 µM of EGCG for 48h and assessed by cytofluorometry as the frequency of cells positive for AnnexinV and PI. Data are from one experiment representative of three.

6.3.6 Increase of mitochondrial ATP turnover favours KP activation through KAT

We have described in the previous chapter that decrease on mitochondrial function, accompanied by triggered cellular energy status activates the KMO branch of the KP. Moreover, KAT-1 and -2 activity has shown to be decreased when mitochondrial complex II is inhibited (98). Therefore, increase of mitochondrial ATP turnover induced by EGCG could promote the KAT branch of the KP. Human primary astrocytes were treated with 50 µM of KYN in the presence or absence of 10 µM of EGCG. After 24h, supernatants were collected for KYNA quantification. Upon KP activation KYN increases, and we reproduced that by adding KYN to the cell cultures, this can be further metabolised through KMO or KAT. We observed an increase of KYN metabolised by KAT in astrocytes treated with EGCG compared with the untreated, as shown by increased KYNA production (Figure 6.7). Thus indicating that EGCG, probably by increasing cellular energy status, can indirectly modulate the KP promoting its neuroprotective branch.

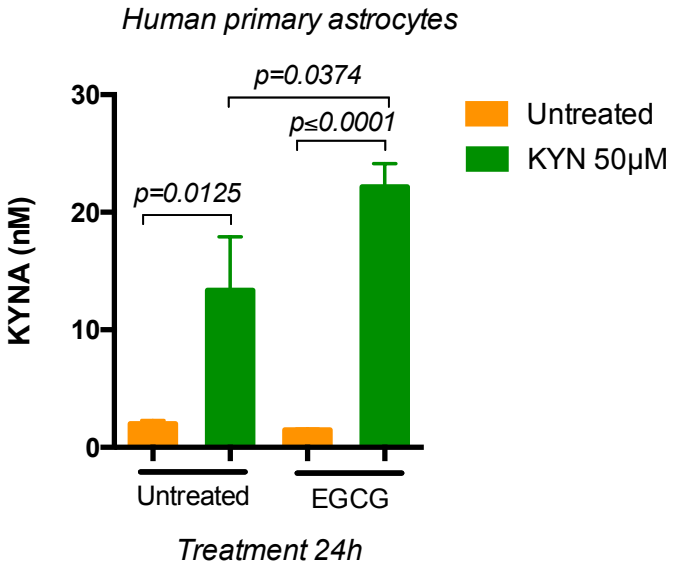

Figure 6.7: Increase of ATP favours KP activation through the KAT branch

KYNA was measured in cell culture supernatants of human primary astrocytes after treatment with 10 µM of EGCG in the presence of 50 µM KYN for 24h. Data (means ± s.e.m.) are from three experiments (Student's t-test).

6.4 Discussion

The brain is highly vulnerable to energy and oxidative damage, which are the main contributing factors in the etiology of neurological disorders and ageing (371). Therefore, restoring energy balance in the brain could be of paramount importance to improve several neurodegenerative diseases. In the current study, we demonstrated that EGCG induces energy turnover (ATP) by directly activating complex IV in the mitochondria of human primary neurons and astrocytes. Several studies have suggested that EGCG can counteract mitochondrial dysfunction and oxidative stress mainly because of its antioxidant activity (358, 372), but to our knowledge our study is the first to show the direct effect of EGCG on complex IV activity.

EGCG can specifically accumulate in the mitochondria of neurons and protect against oxidative stress, by acting as a natural free radical scavenger (358). Accordingly, we observed that EGCG targets the mitochondria of two different neural cell types, inducing mitochondrial respiration. Our results are also consistent with previous studies showing that EGCG can rescue inflammatory cytokine-mediated reduction of ATP and $\Delta\psi_m$ in insulin–producing β cells (373) and can restore oligomeric Aβ peptides-dependent impaired ATP levels, $\Delta\psi_m$ and respiratory rates in neuroblastoma cell line and brain of AD mice model (359). All these responses were attributed to its antioxidant properties. Our data show that EGCG can not only stabilize the ETS (specifically at the level of complex IV) under pathological conditions, but can also potentiate its activity without inducing toxicity under physiological conditions in human primary neurons and astrocytes. Furthermore, we demonstrated here that these effects are not due to the antioxidant properties of this natural molecule.

Some studies have already linked the role of EGCG to energy metabolism as an agonist of AMPK. AMPK is a crucial cellular energy sensor, which promotes ATP production when activated by switching on catabolic pathways while switching off anabolic or biosynthetic pathways (For reviews:(374, 375)). For example, EGCG has been shown to inhibit gluconeogenesis (biosynthesis) in hepatocytes by activating CaMKKβ-AMPK (376), improve insulin signalling pathway, and inhibit lipogenic enzymes through AMPK activation (377, 378). Moreover, it can suppress cell growth

and migration by AMPK-mediated activation of tumor suppressor p53 in cancer cells (379-382).

AMPK can be activated by metabolic stresses that decrease ATP, but also through phosphorylation by LKB-1 complex or calmodium-dependent protein kinase kinase β (CaMKKβ). CaMKKβ is important in the neural tissue because it senses increase in cytosolic Ca^{2+}, which usually trigger ATP-consuming processes (383) and could therefore be a possible target for EGCG activity. Our results show that pharmacological inhibition of AMPK in human primary neurons with Compound C, which inhibits both LKB-1 and CaMKKβ –mediated AMPK activation, did not block EGCG-dependent ATP production. Moreover, inhibition of the glycolysis pathway, which can be activated by AMPK and is the alternative source of ATP, did not affect EGCG-induced ATP production in neurons. We also looked at the markers used to study changes in mitochondrial mass (mitofusin2) and biogenesis (PGC-1α and Tfam), which have also been found to be up regulated by AMPK (384). AMPK phosphorylates PGC-1α, which activates its own transcription (374). We found that EGCG did not affect mRNA levels of any of those genes, indicating that the increase in ATP production is not due to activation of AMPK-mediated mitochondrial biogenesis. However, we cannot discard that EGCG acts on AMPK and activates PGC-1α (376). It is indeed possible that the fastest and first notable effect of EGCG is on ETS-ATP production resulting in an increase of ATP/ADP ratio that would be sensed by AMPK and would subsequently block its activation. In fact, when mitochondrial complex IV and V in the ETS are respectively inhibited by sodium azide and oligomycin, EGCG-mediated ATP production, even though significantly reduced, is not completely blocked in human primary neurons. It suggests that AMPK-mediated ATP production can be activated by EGCG only when mitochondrial ATP turnover is blocked, thus maintaining the higher levels of ATP observed in neurons. Although EGCG-mediated ATP production is completely blocked by oligomycin and sodium azide in human primary astrocytes, the variations observed between neurons and astrocytes could be due to longer EGCG treatment time in neurons. Of interest, it also points out the divergence of metabolic regulation between neurons and astrocytes (272). Neurons main source of ATP is oxidative phosphorylation, whereas astrocytes rely on glycolysis (273). This might explain why the EGCG-mediated ATP production via the ETS had a greater impact in neurons than in astrocytes under the same treatment conditions. We also observed different kinetic properties for ATP production in

neurons and astrocytes, which could also be explained by differences in cytochrome c oxidase regulation in the two cell types. CcO is composed of 13 different subunits in mammals, which are encoded by both mitochondrial and genomic DNA (385). Many of the nuclear subunits have different isoforms, which are differently induced and expressed according to the energy requirement of the tissue (For complete review see:(360)). Among them, subunit IV is a key regulator of CcO, as it inhibits CcO when senses high ATP/ADP ratios (386). Two isoforms of subunit IV (IV-1 and IV-2) have been described. CcO IV-1 is ubiquitously expressed in all tissues, whereas CcO IV-2 showed only high expression levels in adult lung and neurons, but not in astrocytes (387). Neuronal CcO IV-2 abrogates allosteric inhibition of CcO by ATP, supporting a constantly high neuronal activity, whereas in astrocytes, which express CcO IV-1, ATP increase can block CcO (388, 389). Our results show that EGCG induces an early increase of ATP in astrocytes (which resumes after 6h) as well as an exponential ATP increase in neurons (which raises over 48h). We believe that it could be explained by the ATP-mediated allosteric inhibition of CcO in astrocytes, but not in neurons, driven by the different isoforms of CcO subunit IV occurring in the two cell types. This also supports that EGCG-induced ATP increase in both cell types is mediated by an increase in ETS activity.

Another explanation for our results would be that EGCG could prevent inflammatory-induced iNOS overexpression and NO generation. It has been reported that NO can bind to the heme of CcO subunit II and inhibit its activity by competing with O_2 (373, 390). Therefore, EGCG could activate complex IV by reducing NO-mediated inhibition of CcO. However, the induction of CcO activity by EGCG was observed under physiological conditions when there is no increase of inflammatory stress, decreased oxygen levels or alteration on CcO affinity for oxygen. It is therefore unlikely that NO inhibition participates to the EGCG mechanisms of action for CcO activation. Other important regulators, which bind to different subunits of cytochrome c oxidase, such as the hormone sub-product 3,5-diiodothyronine (391), hypoxia-inducible factor (392) or cardiolipin (393) are known to modulate CcO activity. Alternatively, processes such as phosphorylation (394), allosteric inhibition by proton gradient (395) or availability of substrates, ADP and oxygen also participate in CcO regulation. We believe that EGCG could influence these physiological regulators and interact with them, leading to an increase of CcO activity. Another possible mechanism to take into consideration is that EGCG could act as an electron (e^-) donor to cytochrome c. EGCG

has a reduction energy (E_R) of +0.43 eV and has previously been shown to be able to transfer e^- to the nucleotide dGMP (396). EGCG would act similarly to *N*,*N*,*N*′,*N*′-Tetramethyl-*p*-phenylenediamine (TMPD) (E_R =+0.23eV), which is the artificial substrate used to reduce cytochrome c in respirometry assays for measuring CcO activity. EGCG is quite stable in aqueous solution under air (396), and would not easily go under auto-oxidation, as TMPD does, therefore making unnecessary the addition of ascorbate to maintain the reduced state of the e^- donor. However, further studies need to be done to elucidate the mechanistic basis of EGCG effect on the activation of complex IV.

Pharmacokinetic studies in mice demonstrated that EGCG could cross the BBB and reach the brain (357). It has been shown in mice that a dose of 1.5 -3 mg/ kg of EGCG, which is 1.5 times more the daily consumption in humans, administrated orally reach the brain at a concentration of 2-3 nmol/g of tissue (397). Taking into account that EGCG accumulates in neuronal mitochondria (357, 358), it is likely that sufficient concentration of EGCG arrive to its site of action (CcO), showing pharmacological activity. On the other hand, it should be considered that EGCG has a narrow therapeutic window and its accumulation in the mitochondria could lead to high concentrations and neurotoxic effects. Therefore, further bioavailability and pharmacokinetic studies *in vivo* need to be done to determine the appropriate clinical dosing in order to consider EGCG in neurodegenerative diseases therapeutics.

EGCG has been shown to act as an antioxidant, reducing ROS induced by neurotoxic compounds. In this study, we also show that used at low concentrations, it increases CcO activity, ATP production and $\Delta\psi_m$ without inducing ROS production, cytotoxicity or apoptosis. Specifically, our results provide compelling evidences that EGCG targets mitochondria of human primary neurons and astrocytes, activating CcO and increasing ATP turnover without affecting the redox state of the cell. Moreover, increase of ATP could regulate the KP, synergistically promoting neuroprotection through activation of the KAT branch of the KP (see section 6.6). This natural compound may therefore be a potential interesting candidate to counteract mitochondrial dysfunction and oxidative stress observed in many neurodegenerative diseases.

6.5 Conclusions

In summary, our results demonstrate that EGCG can potentiate the activity of CcO in cultured neurons and astrocytes, increasing the proton gradient across the inner mitochondrial membrane to power ATP synthesis. Nevertheless, CcO regulation, assembly and structure are complex and tissue specific (360) and how EGCG acts as an agonist of CcO needs to be further characterised (Figure 6.8). We observed stronger activity of EGCG in neurons than in astrocytes due to bioenergetics metabolic differences between the two cell types (272) and higher affinity of EGCG for neuronal mitochondria (358). Overall, the activity of EGCG as a cell energy booster could have therapeutical applications in neurodegenerative diseases by: (1) restoring mitochondrial function in neurons and (2) activating KAT in astrocytes and the synthesis of neuroprotective KP metabolites.

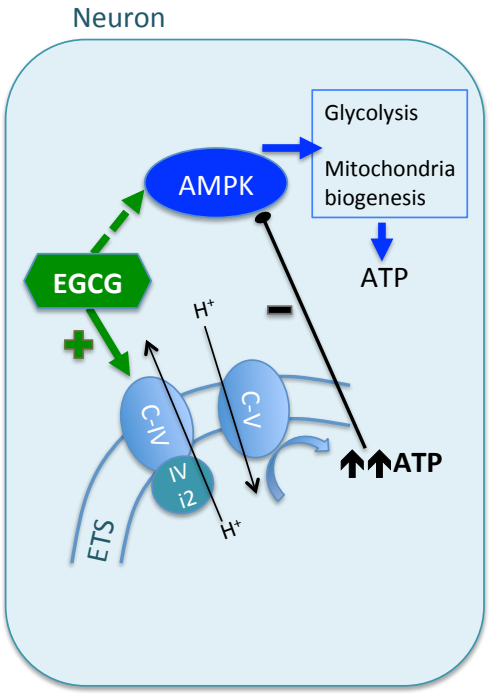

Figure 6.8: Proposed mechanism of EGCG activity in neurons

EGCG can cross the BBB and reach neuronal cytoplasm, where targets mitochondrial complex IV (CcO). EGCG increases CcO activity by interacting with its physiological regulators or directly acting as an electron donor. Overall, activation of CcO leads to increase of ATP turnover by ATP synthase. High levels of ATP are sensed by the subunit IV of CcO, allosterically inhibiting its activity. However, neurons express the isoform 2 of the subunit IV, which is not sensible to ATP increase. EGCG can also activate AMPK, but the rapid raise of mitochondrial ATP, decreases ADP:ATP ratio, which is an inhibitory signal for AMPK activity.

6.6 Future directions

Mitochondrial dysfunction is a common feature of many neurodegenerative disorders, notably Parkinson's Disease. Thus, contributing to the neurotoxic events characteristic of the disease. Taking into account our results from the previous chapter, mitochondrial dysfunction could be the cause of KP dysregulation towards the KMO branch, characteristic of most neurodegenerative diseases (3). Increase of mitochondria activity by EGCG would not only counteract mitochondrial dysfunction, but could also restore the KP normal metabolism. Thus, reducing the production of excitotoxic and pro-oxidant KP metabolites, which would ameliorate the pathology.

The next approach would be to elucidate (1) whether KP abnormalities occur as a consequence of mitochondrial impairment and (2) how treatment with an energy booster (EGCG) could restore KP regulation and ameliorate the pathology, by using a mice model. In this case, we propose using MPTP mouse model for Parkinson's disease because it combines impairment in oxidative phosphorylation (398), accompanied by decreased KYNA concentrations in the CNS (244, 245). Therefore, being this the most suitable to evaluate both, improvements in mitochondrial capacity and restore of KP metabolites physiological levels, in regard to amelioration of the pathological hallmarks. Treatment in parallel with a KMO inhibitor, sharing similar pharmacokinetic and pharmacodynamics properties to those of EGCG, could be used to determine whether the hypothetical protective activity of EGCG is a consequence of reduction in KMO activity, restore of mitochondrial activity or both. Moreover, potential new targets for PD treatment could emerge.

Chapter 7
Final conclusions

7.1 Final conclusions

Detailed conclusions have been inserted in each chapter, and are summarised as follow:

1. Increased KYN level in the CNS is likely to be a mechanism to promote CNS defence against pathogens when activating the AhR in astrocytes (**Chapter 4**).
2. The type of astroglial anti-inflammation response can be modulated through alterations of the KP metabolites, as those differently activate the AhR (**Chapter 4**).
3. Physiological concentrations of KYN, constitutive expression of the AhR and membrane bound TGF-β are important in astrocyte functions in healthy CNS (**Chapter 4**).
4. Not only KMO activity can promote oxidative stress and a decrease in mitochondrial capacity, but KMO activation is also a cellular mechanism able to overcome deficient energetic status (**Chapter 5**).
5. Autonomous KMO activity could play a role in neurotoxicity, as 3-HK shows to be toxic only when produced endogenously (**Chapter 5**).
6. EGCG target CcO in the mitochondria, increasing ATP turnover (**Chapter 6**).
7. Increase of cellular bioenergetic status by EGCG drives the KP through the neuroprotective KAT branch. Therefore could be a good candidate to treat some specific neurodegenerative diseases involving mitochondria dysfunction and glutamate excitotoxicity (**Chapter 6**).

"The art of medicine consists in amusing the patient while nature cures the disease" ~Voltaire

It is important to learn how the body regulates itself before approaching unnecessary treatments. This would reveal what drugs should target, focusing on the cause and not the consequence, which in most cases are just a defence mechanism from our body. Drugs only "help" when the body can't cope with the insult, does it abnormally or the response does not end when the trigger has been resolved. Therefore, we need to know when and how activation of some pathways, including the KP, stop helping resolve the insult to contribute or exacerbate the pathology, then act.

To the question: Is up regulation of the KP the cause or a consequence of the disease? We could conclude that it is likely to be a consequence, as it is common in most of the neurological diseases. Its up regulation could be a mechanism of defence in response to an acute insult. However, aging and other chronic-related factors, such as exhaustion of compensatory mechanisms, contribute to extended and disease-specific alterations in the KP. Thus, leading to long-lasting variance in the subsequent metabolites and contributing to the disease. Localization and type of the alterations, is specific of the disease, which explains the different manifestations characteristic of each pathology.

Appendix

TGF-β in Astrocytes

The studies showed in this section are a continuation of results in Chapter 4 (section 4.3.2). This research chapter is attached as an appendix because the preliminary results did not fit with the main aims of this thesis.

Literature review

Understanding the regulation of TGF-β

Transforming growth factor-β (TGF-β) is a pleiotropic cytokine involved in embryogenesis and has the most prominent role in the immune system by controlling several aspects of inflammatory responses, T cell differentiation, B cell isotype switching and tolerance (399). This essential role has been demonstrated in mice lacking TGF-β1, which develop an early and fatal multifocal inflammatory disease (400). However, alterations in specific components of the TGF-β signalling pathway, leading to increase of its activity, have also shown to contribute to a broad range of pathologies. Some of those pathologies include cardiovascular and developmental diseases, fibrosis and cancer (399). The TGF-β subfamily has three isoforms expressed in mammals, TGF-β1, 2, 3 (401). TGF-β 1, 2 and 3 are initially synthesised as an inactive protein dimer (pre-pro-TGF-β) that undergoes a multistep maturation process. Pre-pro-TGF-β is proteolytically cleaved by furin to yield the latent TGF-β complex composed of homodimeric latency-associated peptide (LAP) that wraps around homodimeric mature TGF-β and this can be released associated or not to a binding protein (402). Three different forms of latent TGF-β complex have been described: (1) the small latent form (SLC) composed of TGF-β bound to LAP; (2) a large soluble latent form (LLC) that consists of SLC covalently linked to latent TGF-β-binding protein-1 (LTBP-1); (3) and a membrane latent form composed of SLC-TGF-β associated with the membrane glycoprotein-A repetitions predominant protein (GARP or LRRC32) (403) (Appendix Figure 1). While LTBP-1 targets latent TGF-β to the extracellular matrix (ECM) (404), GARP associates latent TGF-β to the cell surface (405). LTBPs are large proteins, which can co-assemble with fibrillin, collagen and fibronectin in the ECM, where latent TGF-β is stored until activation (406). The role of LTBPs in TGF-β assembly and activation is well established, however, that is not the case with GARP. Some studies support that GARP is a new latent TGF-β-binding protein that regulates the bioavailability of TGF-β in an autocrine or paracrine mode (403). In contrast to broad expression of LTBPs among different cell types, GARP has only been detected in activated ($Foxp3^+$) Tregs, platelets and mesenchymal stromal cells (405).

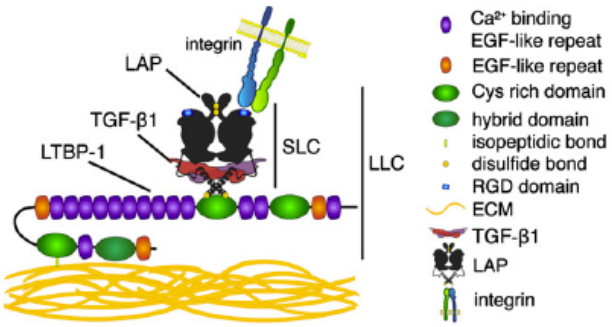

Appendix figure 1: Latent TGF- β

TGF- β 1 is secreted into the ECM as a LLC, consisting of the SLC (LAP-TGF- β 1) bound to LTBP-1 (407).

Active TGF-β can be released from its latent complex by different mechanisms; including plasmin, matrix metalloproteinases (MMP-2 and MMP-9) (205), trombospondin-1 (408), reactive oxygen species (409), acidic pH and microorganism-secreted proteases (205). Plasmin needs to be produced from plasminogen by the enzymatic action of urokinase plasminogen activator (uPA), and for this to occur, uPA needs to be bound to uPA receptor (uPAR). Some molecules have shown to activate uPA, such as parathyroid hormone (410). On the other hand, some cells can produce plasminogen activator inhibitor (PAI), which inhibits uPA activity (205). Therefore expression of positive regulators of uPA, uPAR and PAI will modulate active TGF-β availability in the cell target surroundings. However those mechanisms have not shown to be necessary for the physiological function of TGF-β, as null mice for uPA and uPAR do not have the lesions characteristics of TGF-β null mice (411, 412). This suggests that those regulatory mechanisms become important under pathological circumstances, but they are not implicated in homeostasis and development. More relevant for physiological TGF-β function and activation are integrins. Mice carrying a mutation that impairs association of latent TGF-β with integrin develop defects identical to those observed in mice lacking TGF-β1 (400). Integrins are a large family of cell adhesion and signalling receptors, consisting on a α and β subunits that form a heterodimeric type I transmembrane receptor. There are 24 integrin receptors in mammals and four can bind and liberate active TGF- β: $\alpha_V\beta_3$, $\alpha_V\beta_5$, $\alpha_V\beta_6$ and $\alpha_V\beta_8$. TGF-β activation by the different integrins is further described by Worthington (413). Of all the integrins, $\alpha_V\beta_8$ is the most relevant in the brain. It is expressed in astrocytes (414) and $\alpha_V\beta_8$-mediated activation of TGF-β by astrocytes is important in controlling

brain angiogenesis (415) and neurovascular homeostasis (416). Activation of TGF-β by integrins can be independent of proteolysis and involves transmission of cell traction forces to the LAP moiety of LLC. For this to occur, it is important (1) the incorporation of TGF-β into the extracellular matrix by association with LTBP (417), (2) integrin binding affinity and strength through association of the β cytoplasmic domain with the actin cytoskeleton (characteristic of $\alpha_V\beta_6$), and (3) ECM stiffness and resistance to integrin pulling (407). As $\alpha_V\beta_8$ has short cytoplasmic tail, it does not interact with the actin in the cytoplasm and it requires the co-expression of MMP to process latent TGF-β (418). The mechanisms of SLC activation in GARP are less explored than in LLC, however, they seem to work similarly. Two integrins could bind to GARP-SLC-TGF-β, $\alpha_V\beta_6$ and $\alpha_V\beta_8$ and activate the release of active TGF-β. This can occur within the same cell or involving nearby cells interaction (419). Similarly to LLC with the ECM, GARP must be at the cell membrane to promote TGF-β secretion (403). Into the cell, GARP competes with LTBP for latent TGF-β, therefore, the cells that can produce GARP will preferably keep TGF-β in cell membrane instead of secrete into the ECM (403). Supporting that, mesenchymal stromal cells (MSC) lacking of GARP, have reduced SLC expression in the membrane, but higher secretion of active TGF-β. However, TGF-β in the GARP complex has shown to be released from the membrane by two different mechanisms. It has been reported that T cells but not other cells, can secrete latent TGF-β bound to GARP, those complexes are shed from the cell membrane by proteases, but its function needs to be determined (420). In addition, active TGF-β can be released from GARP/ SLC in T cells membrane by integrin $\alpha_V\beta_8$ in autocrine or paracrine mode. Depletion of integrin $\alpha_V\beta_8$ increases GARP/ SLC in the membrane and decrease active TGF-β (419).

Introduction

In the brain, TGF-β is necessary for neurodevelopment, modulation of the immune response (421) and most importantly for microglia development and homeostatic signature (294). However, under pathological conditions, it has also been associated with astrogliosis, astrocytic scar tissue (422) and the production of ECM components such as collagen, fibronectin and condrotin sulphate proteoglycans (CSPGs) (314). ECM is crucial for TGF-β and other growth factors storage, for example latent TGF-β associated to LTBP remains bound to the ECM proteins, being this essential for tissue remodelling (423). ECM composition determines its stiffness, being this altered in

fibrosis or glial scar and aging and therefore losing its physiological functions (423). ECM stiffness also favours the release of active TGF-β from the LTBP, which in turn will potentiate synthesis of ECM proteins that favour scar formation (424).

Overall, under an acute inflammatory event in the CNS, TGF-β would be necessary to control the inflammatory response and to reduce immune cell recruitment to the CNS by promoting glia scar barrier. On the other hand, under chronic degenerative conditions, TGF-β promotes fibrosis, exacerbating aging processes and impairing the BBB function (399). In the CNS astrocytes contribute to both, the synthesis of ECM proteins (423) and the BBB formation (425), moreover they can produce and respond to TGF-β (314). This makes them an interesting target to study the effects of TGF-β in the CNS. We observed that astrocytes have a novel regulatory mechanism in TGF-β signalling, involving the localization of latent TGF-β in their membrane bound to GARP. This opens up new possibilities to understand how TGF-β might favour or protect against neuroinflammation and the role of astrocytes on these processes.

Methods

Methods used in these studies are described in section 4.2 .

Results

Astrocyte express latent TGF-β in their membrane bound to GARP and LPS can increase its expression.

We previously showed the involvement of TGF-β in astrocyte immunoregulatory function (Figure 4.6d). Surprisingly, despite the high expression levels of TGF-β in astrocytes we could not detect TGF-β in the cell culture supernatant after treatment for several time points with LPS, IFN-γ and KYN and with and without acid-treating the supernatant (detection level limit for the ELISA guaranteed by manufacturer is 5pg/mL). This led us to think that TGF-β could be either sequestered in the cytoplasm or bound in the membrane. We discard the first option as if it was sequestered in the cytoplasm it would have not affected astrocyte-mediated T cell differentiation. Then we measured LAP in the membrane of astrocytes harvested with accutase and 30.57±9.47% of the astrocyte population showed presence of LAP in their membranes (Appendix Figure 2 a,b). LAP antibody had been previously tested for specificity using Treg as positive control. LAP-TGF-β (or SLC) is released by the cells

associated to LTBP and remains in the ECM (404). However, if that was the case, TGF-β would be detected in the supernatant after acid-treatment. We therefore hypothesised that latent TGF-β could be synthetised by astrocytes associated to GARP targeting the cell surface. We showed co-expression of GARP and LAP in astrocyte cell membrane under normal conditions (Appendix Figure 2c). Blocking intracellular protein transport processes with monensin (GolgiStop; BD Biosciences), which blocks the final processes necessary to localise GARP in the cell surface, decreased the number of $GARP^+$ and LAP^+ cells (Appendix figure 3b). This and the lack of GARP expression in the microglia cell line, BV2, provide evidence for the specificity of the antibody used in astrocytes. Moreover, expression of GARP and LAP is up regulated under inflammatory stimuli with 10ng/mL of LPS treatment for 16h (Appendix Figure 2c).

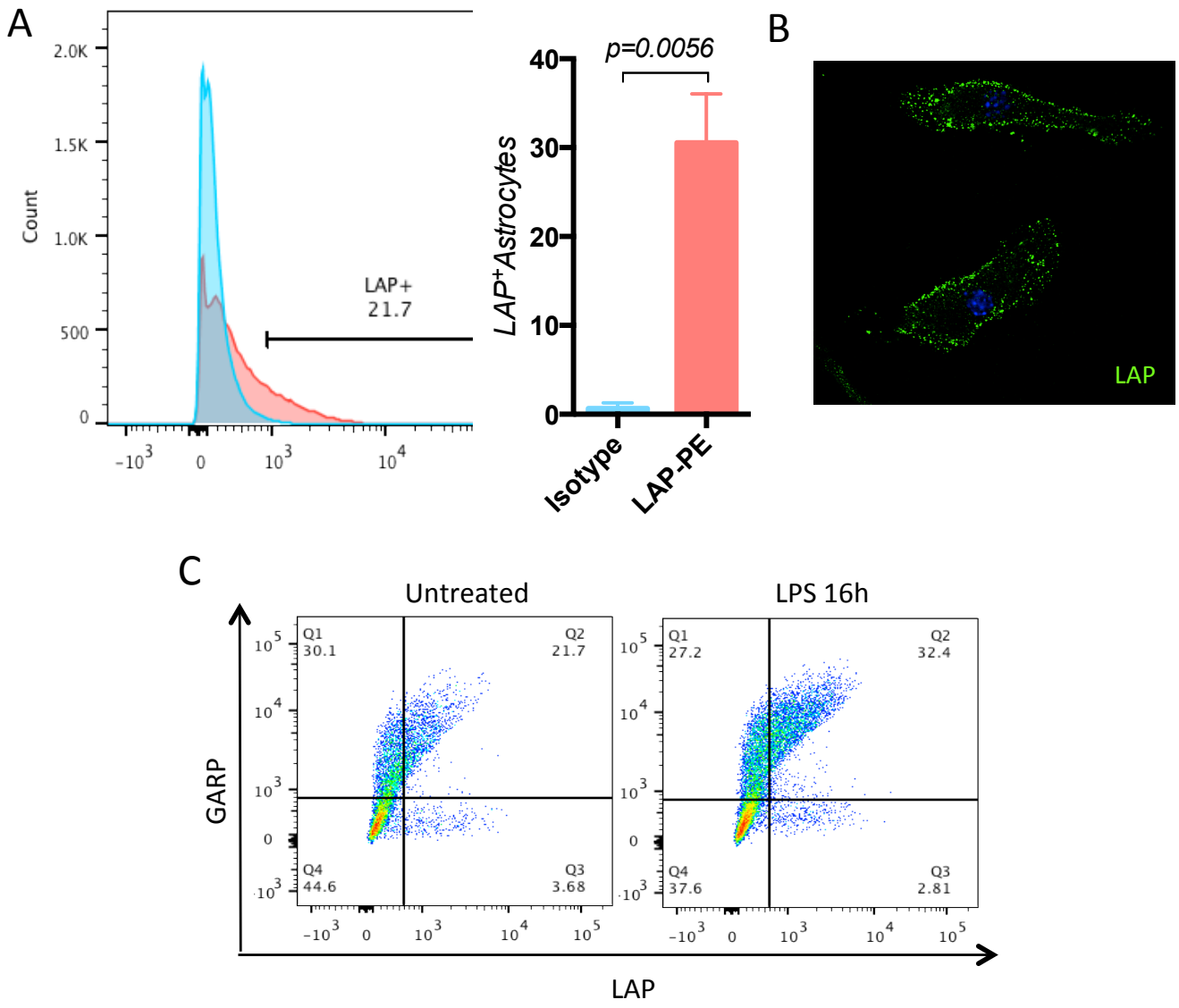

Appendix figure 2: Astrocyte constitutively express LAP-TGF-β in their membranes bound to GARP

(**a**) Cell surface LAP expression in astrocyte assessed by cytofluorometric analysis. Data (means ± s.e.m.) are from three experiments and shown as frequency of LAP$^+$ in total astrocyte population (Student's t-test; anti-LAP versus isotype control). (**b**) Extracellular immunofluorescence showing the expression of LAP in astrocyte's cell surface. Representative data of two independent experiments. (**c**) Cell surface LAP and GARP expression in astrocyte stimulated with 10 ng/mL of LPS for 16h and assessed by cytofluorometric analysis. Data are representative of three experiments and shown in the top right quadrant as frequency of LAP$^+$GARP$^+$ cells in total astrocyte population. Compiled results (mean ± s.e.m.): untreated, 69.99±6.7; LPS, 76.08 ± 5.76 (p=0.0186, *Student's* t-test; treatment versus none).

AhR could be necessary to maintain TGF-β homeostasis in astrocytes

The possible interaction between AhR and TGF-β, has been discussed by Gomez-Duran (426). However, AhR modulation has shown to affect TGF-β synthesis differently depending on the cell type (222). Our aim was to study how AhR could modulate TGF-β in mouse primary astrocytes under KYN-mediated activation or inhibition with CH223191.

Activation of AhR with 50 μM of KYN at different time points (2h-24h) had no effect on LAP and GARP expression (data not shown). However, it could be possible that KYN is not the best ligand to activate AhR-mediated TGF-β modulation. c-src activity has previously shown to be involved in latent TGF-β intracellular processing (204) and ligand binding to AhR has shown to promote c-src activation (11). Therefore we hypothesise that activation of AhR could induce c-src mediated latent TGF-β processing and increase LAP-TGF-β (or SLC) availability in the cell surface. We observed that inhibition of c-src with 5 μM of PP2 for 16h decreased both LAP and GARP constitutive expression in astrocyte membrane (Appendix Figure 3b) and reduced TGF-β mRNA levels, similarly to monensin (Appendix Figure 3a). Taking into account that Smad TGF-β signalling can activate a positive feed-back loop leading to increase of its own expression (54), reduction of LAP in the membrane by monensin and PP2 treatment, would therefore explain the decrease of TGF-β expression. To demonstrate the involvement of AhR in c-src activity, we inhibit AhR with CH223191 and analysed GARP/LAP expression. Surprisingly, AhR inhibition showed opposite effects to those observed with c-src inhibition. GARP/LAP expression increased after AhR inhibition with 5 μM CH-223191 for 72h (Appendix Figure 3c).

This suggests that (1) physiological activation of AhR by its endogenous ligands may be necessary to down regulate TGF-β signalling in astrocytes and (2) c-src activity is necessary for either: latent TGF-β processing or TGF-β signalling, independently of AhR activity.

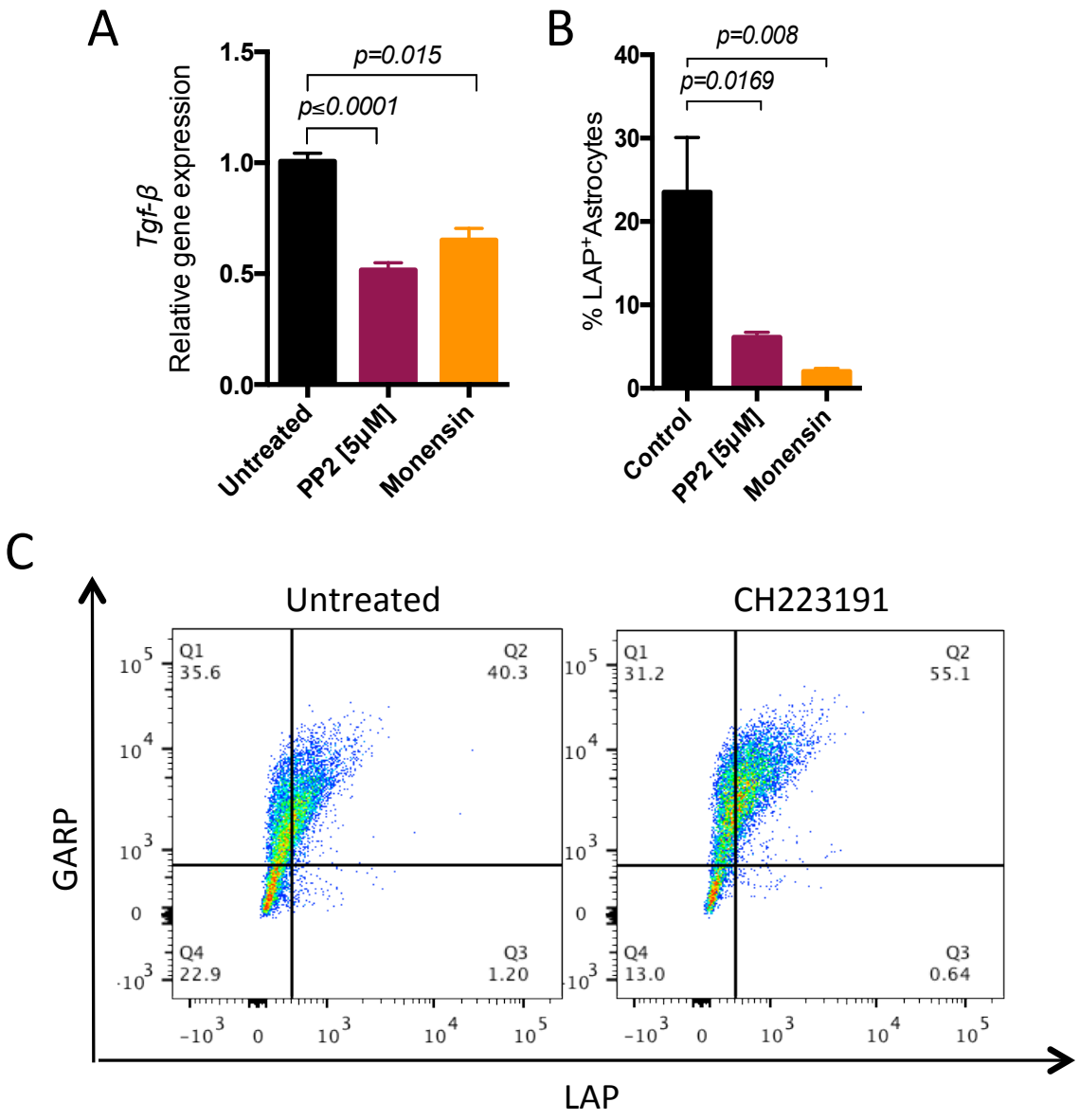

Appendix figure 3: GARP/LAP-TGF-β expression in astrocyte's cell surface can be regulated by c-src and AhR

(**a**) Gene transcript expression of astrocytes treated with 5 μM of PP2 or monensin for 4h. Data (means ± s.e.m. of three experiments) are presented as normalised transcript expression in the samples relative to normalised transcript expression in untreated sample (Student's t-test). (**b**) Cell surface LAP expression in astrocytes treated with 5 μM of PP2 or monensin for 4h and assessed by cytofluorometric analysis. Data (means ± s.e.m.) are from three experiments and shown as frequency of LAP^+ in total astrocyte population (Student's t-test; anti-LAP versus isotype control). (**c**) Cell surface LAP and GARP expression in astrocyte treated with 5 μM of CH223191 for 72h and assessed by cytofluorometric analysis. Data is representative of three experiments and shown in the quadrants as frequency of LAP^+, $GARP^+$ or LAP^+GARP^+ cells in total astrocyte population. Compiled results of LAP^+GARP^+ (mean ± s.e.m.): untreated, 38.43±4.75; CH223191, 45.58 ± 5.67 (p=0.0187, *Student's* t-test; treatment versus none).

Discussion

TGF-β has concentrated much attention due to its role in many crucial physiological processes (427). Most cell types can express TGF-β, however, release and response to TGF-β largely depends on the microenvironment and the cell type (421). Therefore, determining the cell-specific up-stream pathways regulating TGF-β expression and the downstream mechanisms of signalling propagation would be essential to understand the role of this cytokine in astrocytes. Our findings show, for the first time, that astrocytes express LAP-TGF-β in their membrane bound to GARP. This is different to most cell types, which release LAP-TGF-β, mainly bound to LTBP, targeting LAP-TGF-β to the ECM. However, those findings were only obtained towards the end of my PhD and results on AhR involvement on the TGF-β signalling are only on the initial stages. Therefore we can just hypothesise in order to address future experiments. Our data suggests that AhR inhibition increases the constitutively expressed GARP-bound LAP-TGF-β in the cell surface. This is in accordance with several studies in different cell types showing TGF-β overexpression when AhR is absent (222, 428). However, all of those studies showed increase of LTBP bound LAP-TGF-β and to our knowledge this is the first study showing AhR and GARP cross-talk. On the same way that prolonged inhibition of AhR increases GARP expression, physiological activation of AhR by endogenous ligands (probably KYN and KYNA) could be necessary to maintain TGF-β homeostasis (at physiological concentrations). TGF-β promotes glia scar formation after injury (223) and physiological activity of AhR, by controlling TGF-β availability in astrocyte surface, could be necessary for limiting tissue scaring in CNS pathologies. Additionally, TGF-β is important in controlling inflammation. Inflammatory stimuli also increased GARP expression in astrocytes, thus indicating that GARP/ LAP-TGF-β up regulation under inflammatory trigger (such as LPS) could help resolving inflammation. Nevertheless, chronic up regulation of GARP and LAP-TGF-β available in the cell surface would promote scar-regenerating phenotype of astrocytes and BBB abnormalities. This could happen as a consequence of (1) competitive inhibition of AhR physiological activation by its endogenous ligands (as shown with the AhR inhibitor, CH223191) or (2) un-resolved inflammatory status.

Taking into account results from Chapter 4, we can conclude that physiological activation of AhR is necessary to prevent astrogliosis, and maintain healthy CNS. This

based on; (1) AhR null astrocytes showed increase of basal *Il-6* production (Figure 4.6e), which would potentiate astrogliosis, (2) inhibition of AhR increases basal TGF-β (Appendix Figure 3c), which at pathological concentrations would also potentiate astrogliosis and (3) AhR null astrocytes showed a decrease in constitutive *Tnf-α* expression (Figure 4.6f). TNF-α together with IFN-Ɣ promotes trafficking through the choroid plexus between the blood stream and the brain, this allowing CNS repair and maintenance (429). We hypothesise that the lost of AhR physiological activity in astrocytes would decrease immune trafficking to the CNS (by promoting scar tissue and decreasing BBB permeability) and affect CNS maintenance and functional plasticity (430).

Conclusions

In conclusion, we observed that astrocytes express **LAP- TGF-β** in their cell surface and this is increased when physiological activation of **AhR** by its endogenous ligands is displaced and under inflammatory conditions. Reversible changes in activated astrocytes occurring during an acute or fast resolving insult have shown to be protective for the CNS (278). However severe reactive astrogliosis caused by a long lasting non-resolved trigger exacerbates the pathology (279). In agreement with that, GARP/ LAP-TGF-β up regulation in astrocytes could help resolving acute inflammation, because of its role in immune tolerance (399). Nevertheless, chronic up regulation of TGF-β available in their cell surface would promote scar-regenerating phenotype of astrocytes (223) and BBB abnormalities, exacerbating neurodegeneration.

Future directions

First, the expression of LAP-TGF-β in the cell surface of astrocytes bound to GARP, which has never been described before, needs to be further validated and characterised. Immunoblot analysis of LAP and GARP from membrane extract of astrocytes by using different antibodies would be necessary to support our findings. Additionally, immunohistochemistry analysis of brain tissue sections co-labelled with an astrocyte marker and LAP and/or GARP would discard LAP-TGF-β presence in the cell surface as a consequence of *in vitro* cell culturing. Finally, the expression of LAP-

TGF-β in the cell surface of mice astrocytes bound to GARP could be estimated in humans by using human primary astrocytes cell culture.

Once the previous studies have confirmed the presence of TGF-β in astrocyte's membrane, further characterisation of its regulation by AhR needs to be done (Appendix Figure 4). Our results suggest that inhibition of physiological AhR activation up regulates membrane GARP/LAP expression in astrocytes. The metabolic pathways involved in AhR-mediated TGF-β regulation could be studied *in vitro* by analysing astrocyte's transcriptomes after AhR inhibition. Differences in mRNA expression profiles of TGF-β-related pathways between the two conditions could give hints on the mechanisms undelaying AhR activity in regulation of TGF-β.

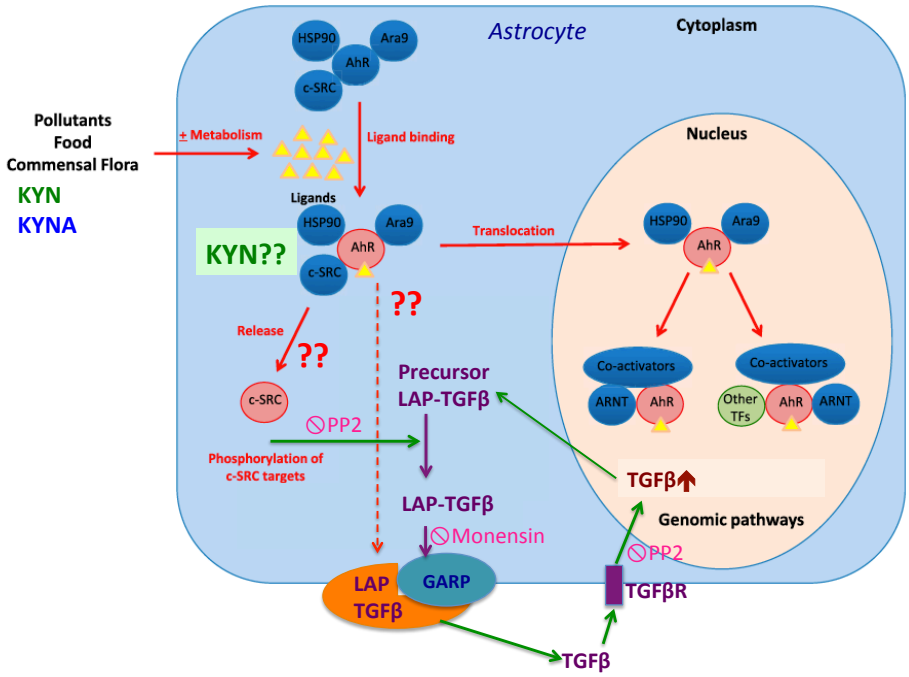

Appendix figure 4: TGF-β regulation in relation with AhR

Under physiological conditions, KYN could act as an endogenous ligand of AhR being necessary for TGF-β homeostasis (to avoid overexpression). C-src activity is necessary for GARP/LAP-TGF-β availability in astrocyte's membrane, however the role of AhR in this process remains unknown. Adapted from Quintana et al. (214).

Further studies to determine the role of AhR in physiological and pathological astrocyte function could be studied *in vivo* using an astrocyte-specific conditional AhR KO mice model. This model would allow us to observe differences in the BBB integrity or in the CNS inflammatory profile associated with the physiological activity of

astrocytic-AhR. Not only that, but inducing EAE in this mice model would also provide further understanding in whether AhR activity in astrocytes is necessary to ameliorate the progression or onset of a neurodegenerative disease. All those studies would take into consideration changes of TGF-β as a mechanism for the astrocyte-specific conditional AhR KO mice model phenotype in physiological and pathological conditions.

References

Reference list

1. Hargreaves KM, Pardridge WM. Neutral amino acid transport at the human blood-brain barrier. Journal of Biological Chemistry. 1988;263(36):19392-7.
2. Moffett JR, Namboodiri MA. Tryptophan and the immune response. Immunology and Cell Biology. 2003;81(4):247-65.
3. Vecsei L, Szalardy L, Fulop F, Toldi J. Kynurenines in the CNS: recent advances and new questions. Nature reviews Drug discovery. 2013;12(1):64-82.
4. Ball HJ, Sanchez-Perez A, Weiser S, Austin CJ, Astelbauer F, Miu J, et al. Characterization of an indoleamine 2,3-dioxygenase-like protein found in humans and mice. Gene. 2007;396(1):203-13.
5. Metz R, DuHadaway JB, Kamasani U, Laury-Kleintop L, Muller AJ, Prendergast GC. Novel Tryptophan Catabolic Enzyme IDO2 Is the Preferred Biochemical Target of the Antitumor Indoleamine 2,3-Dioxygenase Inhibitory Compound d-1-Methyl-Tryptophan. Cancer Research. 2007;67(15):7082-7.
6. Thackray SJ, Mowat CG, Chapman SK. Exploring the mechanism of tryptophan 2,3-dioxygenase. Biochem Soc Trans. 2008;36(Pt 6):1120-3.
7. Shimizu T, Nomiyama S, Hirata F, Hayaishi O. Indoleamine 2,3-dioxygenase. Purification and some properties. The Journal of biological chemistry. 1978;253(13):4700-6.
8. Katz JB, Muller AJ, Prendergast GC. Indoleamine 2,3-dioxygenase in T-cell tolerance and tumoral immune escape. Immunological Reviews. 2008;222(1):206-21.
9. Meng B, Wu D, Gu J, Ouyang S, Ding W, Liu ZJ. Structural and functional analyses of human tryptophan 2,3-dioxygenase. Proteins. 2014.
10. Opitz CA, Litzenburger UM, Sahm F, Ott M, Tritschler I, Trump S, et al. An endogenous tumour-promoting ligand of the human aryl hydrocarbon receptor. Nature. 2011;478(7368):197-203.
11. Bessede A, Gargaro M, Pallotta MT, Matino D, Servillo G, Brunacci C, et al. Aryl hydrocarbon receptor control of a disease tolerance defence pathway. Nature. 2014;511(7508):184-90.

12. Knox WE, Auerbach VH. The hormonal control of tryptophan peroxidase in the rat. The Journal of biological chemistry. 1955;214(1):307-13.
13. Kanai M, Funakoshi H, Takahashi H, Hayakawa T, Mizuno S, Matsumoto K, et al. Tryptophan 2,3-dioxygenase is a key modulator of physiological neurogenesis and anxiety-related behavior in mice. Molecular brain. 2009;2:8.
14. Werner-Felmayer G, Werner ER, Fuchs D, Hausen A, Reibnegger G, Wachter H. Characteristics of interferon induced tryptophan metabolism in human cells in vitro. Biochimica et Biophysica Acta - Molecular Cell Research. 1989;1012(2):140-7.
15. Dai W, Gupta SL. Regulation of indoleamine 2,3-dioxygenase gene expression in human fibroblasts by interferon-Œ≥. Upstream control region discriminates between interferon-Œ≥ and interferon-Œ±. Journal of Biological Chemistry. 1990;265(32):19871-7.
16. Ball HJ, Yuasa HJ, Austin CJD, Weiser S, Hunt NH. Indoleamine 2,3-dioxygenase-2; a new enzyme in the kynurenine pathway. The international journal of biochemistry & cell biology. 2009;41(3):467-71.
17. Yuasa HJ, Ball HJ, Austin CJD, Hunt NH. 1-l-methyltryptophan is a more effective inhibitor of vertebrate IDO2 enzymes than 1-d-methyltryptophan. Comparative Biochemistry and Physiology Part B: Biochemistry and Molecular Biology. 2010;157(1):10-5.
18. Ball HJ, Sanchez-Perez A, Weiser S, Austin CJD, Astelbauer F, Miu J, et al. Characterization of an indoleamine 2,3-dioxygenase-like protein found in humans and mice. Gene. 2007;396(1):203-13.
19. Lob S, Konigsrainer A, Zieker D, Brucher BL, Rammensee HG, Opelz G, et al. IDO1 and IDO2 are expressed in human tumors: levo- but not dextro-1-methyl tryptophan inhibits tryptophan catabolism. Cancer immunology, immunotherapy : CII. 2009;58(1):153-7.
20. Sono M, Taniguchi T, Watanabe Y, Hayaishi O. Indoleamine 2,3-dioxygenase. Equilibrium studies of the tryptophan binding to the ferric, ferrous, and CO-bound enzymes. Journal of Biological Chemistry. 1980;255(4):1339-45.
21. Hayaishi O, Hirata F, Ohnishi T, Henry JP, Rosenthal I, Katoh A. Indoleamine 2,3-dioxygenase: incorporation of 18O2-- and 18O2 into the reaction products. Journal of Biological Chemistry. 1977;252(10):3548-50.
22. Ozaki Y, Reinhard Jr JF, Nichol CA. Cofactor activity of dihydroflavin mononucleotide and tetrahydrobiopterin for murine epididymal indoleamine 2,3-dioxygenase. Biochemical and Biophysical Research Communications. 1986;137(3):1106-11.
23. Maghzal GJ, Thomas SR, Hunt NH, Stocker R. Cytochrome b5, not superoxide anion radical, is a major reductant of indoleamine 2,3-dioxygenase in human cells. The Journal of biological chemistry. 2008;283(18):12014-25.
24. Rosell FI, Kuo HH, Mauk AG. NADH Oxidase Activity of Indoleamine 2,3-Dioxygenase. Journal of Biological Chemistry. 2011;286(33):29273-83.
25. Thomas SR, Mohr D, Stocker R. Nitric oxide inhibits indoleamine 2,3-dioxygenase activity in interferon-gamma primed mononuclear phagocytes. The Journal of biological chemistry. 1994;269(20):14457-64.
26. Thomas SR, Terentis AC, Cai H, Takikawa O, Levina A, Lay PA, et al. Post-translational Regulation of Human Indoleamine 2,3-Dioxygenase Activity by Nitric Oxide. Journal of Biological Chemistry. 2007;282(33):23778-87.
27. Fujigaki H, Saito K, Lin F, Fujigaki S, Takahashi K, Martin BM, et al. Nitration and inactivation of IDO by peroxynitrite. J Immunol. 2006;176(1):372-9.
28. Volpi C, Fallarino F, Pallotta MT, Bianchi R, Vacca C, Belladonna ML, et al. High doses of CpG oligodeoxynucleotides stimulate a tolerogenic TLR9,ÄìTRIF pathway. Nat Commun. 2013;4:1852.
29. Takikawa O. Biochemical and medical aspects of the indoleamine 2,3-dioxygenase-initiated L-tryptophan metabolism. Biochem Biophys Res Commun. 2005;338(1):12-9.
30. Robinson CM, Shirey KA, Carlin JM. Synergistic transcriptional activation of indoleamine dioxygenase by IFN-Œ≥ and tumor necrosis factor-Œ±. Journal of Interferon and Cytokine Research. 2003;23(8):413-21.

31. Carlin J, Borden E, Sondel P, Byrne G. Biologic-response-modifier-induced indoleamine 2,3-dioxygenase activity in human peripheral blood mononuclear cell cultures. The Journal of Immunology. 1987;139(7):2414-8.
32. Fujigaki H, Saito K, Fujigaki S, Takemura M, Sudo K, Ishiguro H, et al. The Signal Transducer and Activator of Transcription 1Œ± and Interferon Regulatory Factor 1 Are Not Essential for the Induction of Indoleamine 2,3-Dioxygenase by Lipopolysaccharide: Involvement of p38 Mitogen-Activated Protein Kinase and Nuclear Factor-ŒʃB Pathways, and Synergistic Effect of Several Proinflammatory Cytokines. Journal of Biochemistry. 2006;139(4):655-62.
33. Jung ID, Lee C-M, Jeong Y-I, Lee JS, Park WS, Han J, et al. Differential regulation of indoleamine 2,3-dioxygenase by lipopolysaccharide and interferon gamma in murine bone marrow derived dendritic cells. FEBS Letters. 2007;581(7):1449-56.
34. Suh HS, Zhao ML, Rivieccio M, Choi S, Connolly E, Zhao Y, et al. Astrocyte indoleamine 2,3-dioxygenase is induced by the TLR3 ligand poly(I:C): mechanism of induction and role in antiviral response. Journal of virology. 2007;81(18):9838-50.
35. Wang B, Koga K, Osuga Y, Cardenas I, Izumi G, Takamura M, et al. Toll-like receptor-3 ligation-induced indoleamine 2, 3-dioxygenase expression in human trophoblasts. Endocrinology. 2011;152(12):4984-92.
36. Iwasaki A, Medzhitov R. Toll-like receptor control of the adaptive immune responses. Nat Immunol. 2004;5(10):987-95.
37. Volpi C, Fallarino F, Bianchi R, Orabona C, De Luca A, Vacca C, et al. A GpC-Rich Oligonucleotide Acts on Plasmacytoid Dendritic Cells To Promote Immune Suppression. The Journal of Immunology. 2012;189(5):2283-9.
38. Mellor AL, Baban B, Chandler PR, Manlapat A, Kahler DJ, Munn DH. Cutting Edge: CpG Oligonucleotides Induce Splenic CD19+ Dendritic Cells to Acquire Potent Indoleamine 2,3-Dioxygenase-Dependent T Cell Regulatory Functions via IFN Type 1 Signaling. The Journal of Immunology. 2005;175(9):5601-5.
39. Romani L, Bistoni F, Perruccio K, Montagnoli C, Gaziano R, Bozza S, et al. Thymosin alpha1 activates dendritic cell tryptophan catabolism and establishes a regulatory environment for balance of inflammation and tolerance. Blood. 2006;108(7):2265-74.
40. Mahanonda R, Sa-Ard-Iam N, Montreekachon P, Pimkhaokham A, Yongvanichit K, Fukuda MM, et al. IL-8 and IDO expression by human gingival fibroblasts via TLRs. J Immunol. 2007;178(2):1151-7.
41. Munn DH, Sharma MD, Mellor AL. Ligation of B7-1/B7-2 by Human CD4+ T Cells Triggers Indoleamine 2,3-Dioxygenase Activity in Dendritic Cells. The Journal of Immunology. 2004;172(7):4100-10.
42. Baban B, Hansen AM, Chandler PR, Manlapat A, Bingaman A, Kahler DJ, et al. A minor population of splenic dendritic cells expressing CD19 mediates IDO-dependent T cell suppression via type I IFN signaling following B7 ligation. International Immunology. 2005;17(7):909-19.
43. Grohmann U, Orabona C, Fallarino F, Vacca C, Calcinaro F, Falorni A, et al. CTLA-4-Ig regulates tryptophan catabolism in vivo. Nature Immunology. 2002;3(11):1097-101.
44. Fallarino F, Grohmann U, Hwang KW, Orabona C, Vacca C, Bianchi R, et al. Modulation of tryptophan catabolism by regulatory T cells. Nature Immunology. 2003;4(12):1206-12.
45. Grohmann U, Fallarino F, Bianchi R, Belladonna ML, Vacca C, Orabona C, et al. IL-6 inhibits the tolerogenic function of CD8 alpha+ dendritic cells expressing indoleamine 2,3-dioxygenase. J Immunol. 2001;167(2):708-14.
46. Fallarino F, Asselin-Paturel C, Vacca C, Bianchi R, Gizzi S, Fioretti MC, et al. Murine Plasmacytoid Dendritic Cells Initiate the Immunosuppressive Pathway of Tryptophan Catabolism in Response to CD200 Receptor Engagement. The Journal of Immunology. 2004;173(6):3748-54.
47. von Bubnoff D, Matz H, Frahnert C, Rao ML, Hanau D, de la Salle H, et al. FcŒµRI Induces the Tryptophan Degradation Pathway Involved in Regulating T Cell Responses. The Journal of Immunology. 2002;169(4):1810-6.
48. Grohmann U, Volpi C, Fallarino F, Bozza S, Bianchi R, Vacca C, et al. Reverse signaling through GITR ligand enables dexamethasone to activate IDO in allergy. Nat Med. 2007;13(5):579-86.

49. von Bergwelt-Baildon MS, Popov A, Saric T, Chemnitz J, Classen S, Stoffel MS, et al. CD25 and indoleamine 2,3-dioxygenase are up-regulated by prostaglandin E2 and expressed by tumor-associated dendritic cells in vivo: additional mechanisms of T-cell inhibition. Blood. 2006;108(1):228-37.
50. Iachininoto MG, Nuzzolo ER, Bonanno G, Mariotti A, Procoli A, Locatelli F, et al. Cyclooxygenase-2 (COX-2) inhibition constrains indoleamine 2,3-dioxygenase 1 (IDO1) activity in acute myeloid leukaemia cells. Molecules. 2013;18(9):10132-45.
51. Jung ID, Lee JS, Lee C-M, Noh KT, Jeong Y-I, Park WS, et al. Induction of indoleamine 2,3-dioxygenase expression via heme oxygenase-1-dependant pathway during murine dendritic cell maturation. Biochemical Pharmacology. 2010;80(4):491-505.
52. Marteau F, Gonzalez NS, Communi D, Goldman M, Boeynaems JM, Communi D. Thrombospondin-1 and indoleamine 2,3-dioxygenase are major targets of extracellular ATP in human dendritic cells. Blood. 2005;106(12):3860-6.
53. Ogasawara N, Oguro T, Sakabe T, Matsushima M, Takikawa O, Isobe K-i, et al. Hemoglobin induces the expression of indoleamine 2,3-dioxygenase in dendritic cells through the activation of PI3K, PKC, and NF-κB and the generation of reactive oxygen species. Journal of Cellular Biochemistry. 2009;108(3):716-25.
54. Pallotta MT, Orabona C, Volpi C, Vacca C, Belladonna ML, Bianchi R, et al. Indoleamine 2,3-dioxygenase is a signaling protein in long-term tolerance by dendritic cells. Nature Immunology. 2011;12(9):870-8.
55. Orabona C, Pallotta MT, Volpi C, Fallarino F, Vacca C, Bianchi R, et al. SOCS3 drives proteasomal degradation of indoleamine 2,3-dioxygenase (IDO) and antagonizes IDO-dependent tolerogenesis. Proceedings of the National Academy of Sciences of the United States of America. 2008;105(52):20828-33.
56. Musso T, Gusella G, Brooks A, Longo D, Varesio L. Interleukin-4 inhibits indoleamine 2,3-dioxygenase expression in human monocytes. Blood. 1994;83(5):1408-11.
57. Fallarino F, Grohmann U, Puccetti P. Indoleamine 2,3-dioxygenase: from catalyst to signaling function. Eur J Immunol. 2012;42(8):1932-7.
58. Nguyen NT, Kimura A, Nakahama T, Chinen I, Masuda K, Nohara K, et al. Aryl hydrocarbon receptor negatively regulates dendritic cell immunogenicity via a kynurenine-dependent mechanism. Proceedings of the National Academy of Sciences of the United States of America. 2010;107(46):19961-6.
59. Pallotta MT, Orabona C, Volpi C, Vacca C, Belladonna ML, Bianchi R, et al. Indoleamine 2,3-dioxygenase is a signaling protein in long-term tolerance by dendritic cells. Nat Immunol. 2011;12(9):870-8.
60. Munn DH, Zhou M, Attwood JT, Bondarev I, Conway SJ, Marshall B, et al. Prevention of allogeneic fetal rejection by tryptophan catabolism. Science. 1998;281(5380):1191-3.
61. Yan Y, Zhang GX, Gran B, Fallarino F, Yu S, Li H, et al. IDO upregulates regulatory T cells via tryptophan catabolite and suppresses encephalitogenic T cell responses in experimental autoimmune encephalomyelitis. J Immunol. 2010;185(10):5953-61.
62. Kwidzinski E, Bunse J, Aktas O, Richter D, Mutlu L, Zipp F, et al. Indolamine 2,3-dioxygenase is expressed in the CNS and down-regulates autoimmune inflammation. FASEB journal : official publication of the Federation of American Societies for Experimental Biology. 2005;19(10):1347-9.
63. Guillemin GJ, Smythe GA, Veas LA, Takikawa O, Brew BJ. A beta 1-42 induces production of quinolinic acid by human macrophages and microglia. NeuroReport. 2003;14(18):2311-5.
64. Widner B, Leblhuber F, Walli J, Tilz GP, Demel U, Fuchs D. Degradation of tryptophan in neurodegenerative disorders. Advances in experimental medicine and biology. 1999;467:133-8.
65. Widner B, Leblhuber F, Fuchs D. Increased neopterin production and tryptophan degradation in advanced Parkinson's disease. J Neural Transm. 2002;109(2):181-9.
66. Chen Y, Stankovic R, Cullen KM, Meininger V, Garner B, Coggan S, et al. The kynurenine pathway and inflammation in amyotrophic lateral sclerosis. Neurotox Res. 2010;18(2):132-42.
67. Schwarcz R, Bruno JP, Muchowski PJ, Wu H-Q. Kynurenines in the mammalian brain: when physiology meets pathology. Nat Rev Neurosci. 2012;13(7):465-77.

68. Crozier-Reabe KR, Phillips RS, Moran GR. Kynurenine 3-Monooxygenase from Pseudomonas fluorescens: Substrate-like Inhibitors both Stimulate Flavin Reduction and Stabilize the Flavin,àíPeroxo Intermediate yet Result in the Production of Hydrogen Peroxide. Biochemistry. 2008;47(47):12420-33.
69. Palfey BA, McDonald CA. Control of catalysis in flavin-dependent monooxygenases. Archives of Biochemistry and Biophysics. 2010;493(1):26-36.
70. Breton J, Avanzi N, Magagnin S, Covini N, Magistrelli G, Cozzi L, et al. Functional characterization and mechanism of action of recombinant human kynurenine 3-hydroxylase. European Journal of Biochemistry. 2000;267(4):1092-9.
71. Halford S, Freedman MS, Bellingham J, Inglis SL, Poopalasundaram S, Soni BG, et al. Characterization of a novel human opsin gene with wide tissue expression and identification of embedded and flanking genes on chromosome 1q43. Genomics. 2001;72(2):203-8.
72. Alberati-Giani D, Cesura AM, Broger C, Warren WD, Rover S, Malherbe P. Cloning and functional expression of human kynurenine 3-monooxygenase. FEBS Lett. 1997;410(2-3):407-12.
73. Hirai K, Kuroyanagi H, Tatebayashi Y, Hayashi Y, Hirabayashi-Takahashi K, Saito K, et al. Dual role of the carboxyl-terminal region of pig liver L-kynurenine 3-monooxygenase: mitochondrial-targeting signal and enzymatic activity. J Biochem. 2010;148(6):639-50.
74. Erickson JB, Flanagan EM, Russo S, Reinhard Jr JF. A radiometric assay for kynurenine 3-hydroxylase based on the release of 3H2O during hydroxylation of l-[3,5-3H]kynurenine. Analytical Biochemistry. 1992;205(2):257-62.
75. Guillemin GJ, Kerr SJ, Smythe GA, Smith DG, Kapoor V, Armati PJ, et al. Kynurenine pathway metabolism in human astrocytes: A paradox for neuronal protection. Journal of Neurochemistry. 2001;78(4):842-53.
76. Connor TJ, Starr N, O'Sullivan JB, Harkin A. Induction of indolamine 2,3-dioxygenase and kynurenine 3-monooxygenase in rat brain following a systemic inflammatory challenge: A role for IFN-Œ≥? Neuroscience Letters. 2008;441(1):29-34.
77. Zunszain PA, Anacker C, Cattaneo A, Choudhury S, Musaelyan K, Myint AM, et al. Interleukin-1[beta]: A New Regulator of the Kynurenine Pathway Affecting Human Hippocampal Neurogenesis. Neuropsychopharmacology. 2011.
78. Han Q, Cai T, Tagle DA, Li J. Structure, expression, and function of kynurenine aminotransferases in human and rodent brains. Cellular and molecular life sciences : CMLS. 2010;67(3):353-68.
79. Han Q, Li J, Li J. pH dependence, substrate specificity and inhibition of human kynurenine aminotransferase I. European journal of biochemistry / FEBS. 2004;271(23-24):4804-14.
80. Han Q, Robinson H, Li J. Crystal structure of human kynurenine aminotransferase II. The Journal of biological chemistry. 2008;283(6):3567-73.
81. Cooper AJ. The role of glutamine transaminase K (GTK) in sulfur and alpha-keto acid metabolism in the brain, and in the possible bioactivation of neurotoxicants. Neurochemistry international. 2004;44(8):557-77.
82. Hodgkins PS, Wu HQ, Zielke HR, Schwarcz R. 2-Oxoacids regulate kynurenic acid production in the rat brain: studies in vitro and in vivo. J Neurochem. 1999;72(2):643-51.
83. Lehninger A, Nelson D, Cox M. Lehninger Principles of Biochemistry: W. H. Freeman; 2008.
84. Guidetti P, Okuno E, Schwarcz R. Characterization of rat brain kynurenine aminotransferases I and II. J Neurosci Res. 1997;50(3):457-65.
85. Spencer JP, Whiteman M, Jenner P, Halliwell B. 5-s-Cysteinyl-conjugates of catecholamines induce cell damage, extensive DNA base modification and increases in caspase-3 activity in neurons. J Neurochem. 2002;81(1):122-9.
86. Nemeth H, Toldi J, Vecsei L. Kynurenines, Parkinson's disease and other neurodegenerative disorders: preclinical and clinical studies. Journal of neural transmission Supplementum. 2006(70):285-304.
87. Buchli R, Alberati-Giani D, Malherbe P, Kohler C, Broger C, Cesura AM. Cloning and functional expression of a soluble form of kynurenine/alpha-aminoadipate aminotransferase from rat kidney. The Journal of biological chemistry. 1995;270(49):29330-5.

88. Passera E, Campanini B, Rossi F, Casazza V, Rizzi M, Pellicciari R, et al. Human kynurenine aminotransferase II--reactivity with substrates and inhibitors. The FEBS journal. 2011;278(11):1882-900.
89. Guidetti P, Amori L, Sapko MT, Okuno E, Schwarcz R. Mitochondrial aspartate aminotransferase: a third kynurenate-producing enzyme in the mammalian brain. J Neurochem. 2007;102(1):103-11.
90. Guidetti P, Hoffman GE, Melendez-Ferro M, Albuquerque EX, Schwarcz R. Astrocytic localization of kynurenine aminotransferase II in the rat brain visualized by immunocytochemistry. Glia. 2007;55(1):78-92.
91. Han Q, Robinson H, Cai T, Tagle DA, Li J. Biochemical and structural properties of mouse kynurenine aminotransferase III. Molecular and cellular biology. 2009;29(3):784-93.
92. Yu P, Li Z, Zhang L, Tagle DA, Cai T. Characterization of kynurenine aminotransferase III, a novel member of a phylogenetically conserved KAT family. Gene. 2006;365:111-8.
93. Moran J, Alavez S, Rivera-Gaxiola M, Valencia A, Hurtado S. Effect of NMDA antagonists on the activity of glutaminase and aspartate aminotransferase in the developing rat cerebellum. International journal of developmental neuroscience : the official journal of the International Society for Developmental Neuroscience. 1999;17(1):57-65.
94. Waagepetersen HS, Sonnewald U, Schousboe A. Compartmentation of glutamine, glutamate, and GABA metabolism in neurons and astrocytes: functional implications. The Neuroscientist : a review journal bringing neurobiology, neurology and psychiatry. 2003;9(5):398-403.
95. Han Q, Robinson H, Cai T, Tagle DA, Li J. Biochemical and structural characterization of mouse mitochondrial aspartate aminotransferase, a newly identified kynurenine aminotransferase-IV. Bioscience reports. 2011;31(5):323-32.
96. Ulvik A, Theofylaktopoulou D, Midttun O, Nygard O, Eussen SJ, Ueland PM. Substrate product ratios of enzymes in the kynurenine pathway measured in plasma as indicators of functional vitamin B-6 status. The American journal of clinical nutrition. 2013;98(4):934-40.
97. Luchowski P, Luchowska E, Turski WA, Urbanska EM. 1-Methyl-4-phenylpyridinium and 3-nitropropionic acid diminish cortical synthesis of kynurenic acid via interference with kynurenine aminotransferases in rats. Neurosci Lett. 2002;330(1):49-52.
98. Csillik A, Knyihar E, Okuno E, Krisztin-Peva B, Csillik B, Vecsei L. Effect of 3-nitropropionic acid on kynurenine aminotransferase in the rat brain. Exp Neurol. 2002;177(1):233-41.
99. Gramsbergen JB, Hodgkins PS, Rassoulpour A, Turski WA, Guidetti P, Schwarcz R. Brain-specific modulation of kynurenic acid synthesis in the rat. J Neurochem. 1997;69(1):290-8.
100. Hodgkins PS, Schwarcz R. Metabolic control of kynurenic acid formation in the rat brain. Developmental Neuroscience. 1998;20(4-5):408-16.
101. Phillips RS. Structure and mechanism of kynureninase. Arch Biochem Biophys. 2014;544:69-74.
102. Lima S, Kumar S, Gawandi V, Momany C, Phillips RS. Crystal structure of the Homo sapiens kynureninase-3-hydroxyhippuric acid inhibitor complex: insights into the molecular basis of kynureninase substrate specificity. J Med Chem. 2009;52(2):389-96.
103. Guillemin GJ, Kerr SJ, Smythe GA, Armati PJ, Brew BJ. Kynurenine pathway metabolism in human astrocytes. 2000. p. 125-31.
104. Fukui S, Schwarcz R, Rapoport SI, Takada Y, Smith QR. Blood-brain barrier transport of kynurenines: implications for brain synthesis and metabolism. J Neurochem. 1991;56(6):2007-17.
105. Gal EM, Sherman AD. Synthesis and metabolism of L-kynurenine in rat brain. J Neurochem. 1978;30(3):607-13.
106. Mellor AL, Munn DH. Ido expression by dendritic cells: tolerance and tryptophan catabolism. Nat Rev Immunol. 2004;4(10):762-74.
107. Fallarino F, Grohmann U, You S, McGrath BC, Cavener DR, Vacca C, et al. The Combined Effects of Tryptophan Starvation and Tryptophan Catabolites Down-Regulate T Cell Receptor Œð-Chain and Induce a Regulatory Phenotype in Naive T Cells. The Journal of Immunology. 2006;176(11):6752-61.

108. Terness P, Bauer TM, Rose L, Dufter C, Watzlik A, Simon H, et al. Inhibition of allogeneic T cell proliferation by indoleamine 2,3-dioxygenase-expressing dendritic cells: mediation of suppression by tryptophan metabolites. The Journal of experimental medicine. 2002;196(4):447-57.
109. Frumento G, Rotondo R, Tonetti M, Damonte G, Benatti U, Ferrara GB. Tryptophan-derived catabolites are responsible for inhibition of T and natural killer cell proliferation induced by indoleamine 2,3-dioxygenase. The Journal of experimental medicine. 2002;196(4):459-68.
110. Munn DH, Shafizadeh E, Attwood JT, Bondarev I, Pashine A, Mellor AL. Inhibition of T cell proliferation by macrophage tryptophan catabolism. The Journal of experimental medicine. 1999;189(9):1363-72.
111. Quintana FJ, Murugaiyan G, Farez MF, Mitsdoerffer M, Tukpah AM, Burns EJ, et al. An endogenous aryl hydrocarbon receptor ligand acts on dendritic cells and T cells to suppress experimental autoimmune encephalomyelitis. Proc Natl Acad Sci U S A. 2010;107(48):20768-73.
112. Vogel CF, Goth SR, Dong B, Pessah IN, Matsumura F. Aryl hydrocarbon receptor signaling mediates expression of indoleamine 2,3-dioxygenase. Biochem Biophys Res Commun. 2008;375(3):331-5.
113. Reyes Ocampo J, Lugo Huitron R, Gonzalez-Esquivel D, Ugalde-Muniz P, Jimenez-Anguiano A, Pineda B, et al. Kynurenines with neuroactive and redox properties: relevance to aging and brain diseases. Oxidative medicine and cellular longevity. 2014;2014:646909.
114. Perkins MN, Stone TW. An iontophoretic investigation of the actions of convulsant kynurenines and their interaction with the endogenous excitant quinolinic acid. Brain Res. 1982;247(1):184-7.
115. Brady RJ, Swann JW. Suppression of ictal-like activity by kynurenic acid does not correlate with its efficacy as an NMDA receptor antagonist. Epilepsy research. 1988;2(4):232-8.
116. Parsons CG, Danysz W, Quack G, Hartmann S, Lorenz B, Wollenburg C, et al. Novel systemically active antagonists of the glycine site of the N-methyl-D-aspartate receptor: electrophysiological, biochemical and behavioral characterization. The Journal of pharmacology and experimental therapeutics. 1997;283(3):1264-75.
117. Hilmas C, Pereira EF, Alkondon M, Rassoulpour A, Schwarcz R, Albuquerque EX. The brain metabolite kynurenic acid inhibits alpha7 nicotinic receptor activity and increases non-alpha7 nicotinic receptor expression: physiopathological implications. J Neurosci. 2001;21(19):7463-73.
118. Marchi M, Risso F, Viola C, Cavazzani P, Raiteri M. Direct evidence that release-stimulating α7* nicotinic cholinergic receptors are localized on human and rat brain glutamatergic axon terminals. Journal of Neurochemistry. 2002;80(6):1071-8.
119. Kozak R, Campbell BM, Strick CA, Horner W, Hoffmann WE, Kiss T, et al. Reduction of brain kynurenic Acid improves cognitive function. J Neurosci. 2014;34(32):10592-602.
120. Fallarino F, Volpi C, Fazio F, Notartomaso S, Vacca C, Busceti C, et al. Metabotropic glutamate receptor-4 modulates adaptive immunity and restrains neuroinflammation. Nature Medicine. 2010;16(8):897-902.
121. Berlinguer-Palmini R, Masi A, Narducci R, Cavone L, Maratea D, Cozzi A, et al. GPR35 activation reduces Ca2+ transients and contributes to the kynurenic acid-dependent reduction of synaptic activity at CA3-CA1 synapses. PLoS One. 2013;8(11):e82180.
122. Wang J, Simonavicius N, Wu X, Swaminath G, Reagan J, Tian H, et al. Kynurenic acid as a ligand for orphan G protein-coupled receptor GPR35. The Journal of biological chemistry. 2006;281(31):22021-8.
123. DiNatale BC, Murray IA, Schroeder JC, Flaveny CA, Lahoti TS, Laurenzana EM, et al. Kynurenic acid is a potent endogenous aryl hydrocarbon receptor ligand that synergistically induces interleukin-6 in the presence of inflammatory signaling. Toxicological sciences : an official journal of the Society of Toxicology. 2010;115(1):89-97.
124. Lugo-Huitron R, Blanco-Ayala T, Ugalde-Muniz P, Carrillo-Mora P, Pedraza-Chaverri J, Silva-Adaya D, et al. On the antioxidant properties of kynurenic acid: free radical scavenging activity and inhibition of oxidative stress. Neurotoxicology and teratology. 2011;33(5):538-47.

125. Stone TW, Behan WMH, Jones PA, Darlington LG, Smith RA. The role of kynurenines in the production of neuronal death, and the neuroprotective effect of purines. Journal of Alzheimer's Disease. 2001;3(4):355-66.
126. de Carvalho LP, Bochet P, Rossier J. The endogenous agonist quinolinic acid and the non endogenous homoquinolinic acid discriminate between NMDAR2 receptor subunits. Neurochemistry international. 1996;28(4):445-52.
127. Schurr A, Rigor BM. Kainate toxicity in energy-compromised rat hippocampal slices: differences between oxygen and glucose deprivation. Brain Res. 1993;614(1-2):10-4.
128. Tavares RG, Tasca CI, Santos CE, Wajner M, Souza DO, Dutra-Filho CS. Quinolinic acid inhibits glutamate uptake into synaptic vesicles from rat brain. Neuroreport. 2000;11(2):249-53.
129. Baverel G, Martin G, Michoudet C. Glutamine synthesis from aspartate in guinea-pig renal cortex. The Biochemical journal. 1990;268(2):437-42.
130. Ganzella M, Jardim FM, Boeck CR, Vendite D. Time course of oxidative events in the hippocampus following intracerebroventricular infusion of quinolinic acid in mice. Neuroscience research. 2006;55(4):397-402.
131. Aguilera P, Chanez-Cardenas ME, Floriano-Sanchez E, Barrera D, Santamaria A, Sanchez-Gonzalez DJ, et al. Time-related changes in constitutive and inducible nitric oxide synthases in the rat striatum in a model of Huntington's disease. Neurotoxicology. 2007;28(6):1200-7.
132. Platenik J, Stopka P, Vejrazka M, Stipek S. Quinolinic acid-iron(ii) complexes: slow autoxidation, but enhanced hydroxyl radical production in the Fenton reaction. Free radical research. 2001;34(5):445-59.
133. Yan E, Castillo-Melendez M, Smythe G, Walker D. Quinolinic acid promotes albumin deposition in Purkinje cell, astrocytic activation and lipid peroxidation in fetal brain. Neuroscience. 2005;134(3):867-75.
134. Braidy N, Grant R, Adams S, Brew B, Guillemin G. Mechanism for Quinolinic Acid Cytotoxicity in Human Astrocytes and Neurons. Neurotoxicity Research. 2009;16(1):77-86.
135. Ting KK, Brew BJ, Guillemin GJ. Effect of quinolinic acid on gene expression in human astrocytes: Implications for Alzheimer's disease. In: Takai K, editor. 2007. p. 384-8.
136. Guillemin GJ, Croitoru-Lamoury J, Dormont D, Armati PJ, Brew BJ. Quinolinic acid upregulates chemokine production and chemokine receptor expression in astrocytes. GLIA. 2003;41(4):371-81.
137. Croitoru-Lamoury J, Guillemin GJ, Dormont D, Brew BJ. Quinolinic acid up-regulates chemokine production and chemokine receptor expression in astrocytes. 2003. p. 37-45.
138. Guillemin GJ, Brew BJ. Implications of the kynurenine pathway and quinolinic acid in Alzheimer's disease. Redox Report. 2002;7(4):199-206.
139. Guillemin GJ. Quinolinic acid, the inescapable neurotoxin. The FEBS journal. 2012;279(8):1356-65.
140. Fallarino F, Grohmann U, Vacca C, Bianchi R, Orabona C, Spreca A, et al. T cell apoptosis by tryptophan catabolism. Cell Death and Differentiation. 2002;9(10):1069-77.
141. Belladonna ML, Grohmann U, Guidetti P, Volpi C, Bianchi R, Fioretti MC, et al. Kynurenine pathway enzymes in dendritic cells initiate tolerogenesis in the absence of functional IDO. J Immunol. 2006;177(1):130-7.
142. Stone TW. Neuropharmacology of quinolinic and kynurenic acids. Pharmacol Rev. 1993;45(3):309-79.
143. Smith AJ, Smith RA, Stone TW. 5-Hydroxyanthranilic acid, a tryptophan metabolite, generates oxidative stress and neuronal death via p38 activation in cultured cerebellar granule neurones. Neurotox Res. 2009;15(4):303-10.
144. Wei H, Leeds P, Chen RW, Wei W, Leng Y, Bredesen DE, et al. Neuronal apoptosis induced by pharmacological concentrations of 3-hydroxykynurenine: characterization and protection by dantrolene and Bcl-2 overexpression. J Neurochem. 2000;75(1):81-90.
145. Okuda S, Nishiyama N, Saito H, Katsuki H. Hydrogen peroxide-mediated neuronal cell death induced by an endogenous neurotoxin, 3-hydroxykynurenine. Proceedings of the National Academy of Sciences. 1996;93(22):12553-8.

146. Wang Q, Zhang M, Ding Y, Wang Q, Zhang W, Song P, et al. Activation of NAD(P)H oxidase by tryptophan-derived 3-hydroxykynurenine accelerates endothelial apoptosis and dysfunction in vivo. Circulation research. 2014;114(3):480-92.
147. Okuda S, Nishiyama N, Saito H, Katsuki H. 3-Hydroxykynurenine, an endogenous oxidative stress generator, causes neuronal cell death with apoptotic features and region selectivity. J Neurochem. 1998;70(1):299-307.
148. Leipnitz G, Schumacher C, Dalcin KB, Scussiato K, Solano A, Funchal C, et al. In vitro evidence for an antioxidant role of 3-hydroxykynurenine and 3-hydroxyanthranilic acid in the brain. Neurochemistry international. 2007;50(1):83-94.
149. Braidy N, Grant R, Brew BJ, Adams S, Jayasena T, Guillemin GJ. Effects of Kynurenine Pathway Metabolites on Intracellular NAD Synthesis and Cell Death in Human Primary Astrocytes and Neurons. International journal of tryptophan research : IJTR. 2009;2:61-9.
150. Guidetti P, Schwarcz R. 3-Hydroxykynurenine potentiates quinolinate but not NMDA toxicity in the rat striatum. The European journal of neuroscience. 1999;11(11):3857-63.
151. Taher YA, Piavaux BJA, Gras R, van Esch BCAM, Hofman GA, Bloksma N, et al. Indoleamine 2,3-dioxygenase,Äìdependent tryptophan metabolites contribute to tolerance induction during allergen immunotherapy in a mouse model. Journal of Allergy and Clinical Immunology. 2008;121(4):983-91.e2.
152. Knubel CP, Martinez FF, Acosta Rodriguez EV, Altamirano A, Rivarola HW, Diaz Lujan C, et al. 3-Hydroxy kynurenine treatment controls T. cruzi replication and the inflammatory pathology preventing the clinical symptoms of chronic Chagas disease. PLoS One. 2011;6(10):e26550.
153. Notarangelo FM, Wu HQ, Macherone A, Graham DR, Schwarcz R. Gas chromatography/tandem mass spectrometry detection of extracellular kynurenine and related metabolites in normal and lesioned rat brain. Anal Biochem. 2012;421(2):573-81.
154. Colin-Gonzalez AL, Maldonado PD, Santamaria A. 3-Hydroxykynurenine: an intriguing molecule exerting dual actions in the central nervous system. Neurotoxicology. 2013;34:189-204.
155. Goldstein LE, Leopold MC, Huang X, Atwood CS, Saunders AJ, Hartshorn M, et al. 3-Hydroxykynurenine and 3-Hydroxyanthranilic Acid Generate Hydrogen Peroxide and Promote Œ±-Crystallin Cross-Linking by Metal Ion Reduction,Ä†. Biochemistry. 2000;39(24):7266-75.
156. Thomas SR, Stocker R. Antioxidant activities and redox regulation of interferon-gamma-induced tryptophan metabolism in human monocytes and macrophages. 2000. p. 541-52.
157. Piscianz E, Cuzzoni E, De Iudicibus S, Valencic E, Decorti G, Tommasini A. Differential action of 3-hydroxyanthranilic acid on viability and activation of stimulated lymphocytes. International Immunopharmacology. 2011;11(12):2242-5.
158. Zaher SS, Germain C, Fu H, Larkin DF, George AJ. 3-hydroxykynurenine suppresses CD4+ T-cell proliferation, induces T-regulatory-cell development, and prolongs corneal allograft survival. Investigative ophthalmology & visual science. 2011;52(5):2640-8.
159. Krause D, Suh HS, Tarassishin L, Cui QL, Durafourt BA, Choi N, et al. The tryptophan metabolite 3-hydroxyanthranilic acid plays anti-inflammatory and neuroprotective roles during inflammation: role of hemeoxygenase-1. The American journal of pathology. 2011;179(3):1360-72.
160. Gaubert S, Bouchaut M, Brumas V, Berthon G. Copper--ligand interactions and the physiological free radical processes. Part 3. Influence of histidine, salicylic acid and anthranilic acid on copper-driven Fenton chemistry in vitro. Free radical research. 2000;32(5):451-61.
161. Platten M, Ho PP, Youssef S, Fontoura P, Garren H, Hur EM, et al. Treatment of autoimmune neuroinflammation with a synthetic tryptophan metabolite. Science. 2005;310(5749):850-5.
162. Shiota N, Kovanen PT, Eklund KK, Shibata N, Shimoura K, Niibayashi T, et al. The anti-allergic compound tranilast attenuates inflammation and inhibits bone destruction in collagen-induced arthritis in mice. Br J Pharmacol. 2010;159(3):626-35.
163. Darakhshan S, Pour AB. Tranilast: A review of its therapeutic applications. Pharmacological research : the official journal of the Italian Pharmacological Society. 2014;91C:15-28.

164. Fernandez-Pol JA, Klos DJ, Hamilton PD. Antiviral, cytotoxic and apoptotic activities of picolinic acid on human immunodeficiency virus-1 and human herpes simplex virus-2 infected cells. Anticancer research. 2001;21(6A):3773-6.
165. Cai S, Sato K, Shimizu T, Yamabe S, Hiraki M, Sano C, et al. Antimicrobial activity of picolinic acid against extracellular and intracellular Mycobacterium avium complex and its combined activity with clarithromycin, rifampicin and fluoroquinolones. The Journal of antimicrobial chemotherapy. 2006;57(1):85-93.
166. Grant RS, Coggan SE, Smythe GA. The Physiological Action of Picolinic Acid in the Human Brain. International Journal of Tryptophan Research. 2009;2009(IJTR-2-Grant-et-al):71.
167. Bosco MC, Rapisarda A, Massazza S, Melillo G, Young H, Varesio L. The tryptophan catabolite picolinic acid selectively induces the chemokines macrophage inflammatory protein-1Œ± and -1Œ≤ in macrophages. Journal of Immunology. 2000;164(6):3283-91.
168. Braidy N, Guillemin G, Grant R. Promotion of cellular NAD+ anabolism: Therapeutic potential for oxidative stress in ageing and alzheimer's disease. Neurotoxicity Research. 2008;13(3-4):173-84.
169. Copeland CS, Neale SA, Salt TE. Actions of Xanthurenic Acid, a putative endogenous Group II metabotropic glutamate receptor agonist, on sensory transmission in the thalamus. Neuropharmacology. 2013;66(0):133-42.
170. Nikiforuk A, Popik P, Drescher KU, van Gaalen M, Relo AL, Mezler M, et al. Effects of a positive allosteric modulator of group II metabotropic glutamate receptors, LY487379, on cognitive flexibility and impulsive-like responding in rats. The Journal of pharmacology and experimental therapeutics. 2010;335(3):665-73.
171. Neale SA, Copeland CS, Salt TE. Effect of VGLUT inhibitors on glutamatergic synaptic transmission in the rodent hippocampus and prefrontal cortex. Neurochemistry international. 2014;73:159-65.
172. Neale SA, Copeland CS, Uebele VN, Thomson FJ, Salt TE. Modulation of hippocampal synaptic transmission by the kynurenine pathway member xanthurenic acid and other VGLUT inhibitors. Neuropsychopharmacology. 2013;38(6):1060-7.
173. Fazio F, Lionetto L, Molinaro G, Bertrand HO, Acher F, Ngomba RT, et al. Cinnabarinic Acid, an Endogenous Metabolite of the Kynurenine Pathway, Activates Type 4 Metabotropic Glutamate Receptors. Molecular Pharmacology. 2012;81(5):643-56.
174. Fazio F, Zappulla C, Notartomaso S, Busceti C, Bessede A, Scarselli P, et al. Cinnabarinic acid, an endogenous agonist of type-4 metabotropic glutamate receptor, suppresses experimental autoimmune encephalomyelitis in mice. Neuropharmacology. 2014;81(0):237-43.
175. Schmidt JV, Su GH, Reddy JK, Simon MC, Bradfield CA. Characterization of a murine Ahr null allele: involvement of the Ah receptor in hepatic growth and development. Proc Natl Acad Sci U S A. 1996;93(13):6731-6.
176. Fernandez-Salguero P, Pineau T, Hilbert DM, McPhail T, Lee SS, Kimura S, et al. Immune system impairment and hepatic fibrosis in mice lacking the dioxin-binding Ah receptor. Science. 1995;268(5211):722-6.
177. Nguyen LP, Bradfield CA. The search for endogenous activators of the aryl hydrocarbon receptor. Chemical research in toxicology. 2008;21(1):102-16.
178. Murray IA, Morales JL, Flaveny CA, Dinatale BC, Chiaro C, Gowdahalli K, et al. Evidence for ligand-mediated selective modulation of aryl hydrocarbon receptor activity. Mol Pharmacol. 2010;77(2):247-54.
179. Heath-Pagliuso S, Rogers WJ, Tullis K, Seidel SD, Cenijn PH, Brouwer A, et al. Activation of the Ah receptor by tryptophan and tryptophan metabolites. Biochemistry. 1998;37(33):11508-15.
180. Wincent E, Amini N, Luecke S, Glatt H, Bergman J, Crescenzi C, et al. The suggested physiologic aryl hydrocarbon receptor activator and cytochrome P4501 substrate 6-formylindolo[3,2-b]carbazole is present in humans. The Journal of biological chemistry. 2009;284(5):2690-6.
181. Zelante T, Iannitti RG, Cunha C, De Luca A, Giovannini G, Pieraccini G, et al. Tryptophan catabolites from microbiota engage aryl hydrocarbon receptor and balance mucosal reactivity via interleukin-22. Immunity. 2013;39(2):372-85.

182. Seidel SD, Winters GM, Rogers WJ, Ziccardi MH, Li V, Keser B, et al. Activation of the Ah receptor signaling pathway by prostaglandins. Journal of biochemical and molecular toxicology. 2001;15(4):187-96.
183. McIntosh BE, Hogenesch JB, Bradfield CA. Mammalian Per-Arnt-Sim proteins in environmental adaptation. Annual review of physiology. 2010;72:625-45.
184. Quintana FJ, Sherr DH. Aryl hydrocarbon receptor control of adaptive immunity. Pharmacol Rev. 2013;65(4):1148-61.
185. Dere E, Lo R, Celius T, Matthews J, Zacharewski TR. Integration of genome-wide computation DRE search, AhR ChIP-chip and gene expression analyses of TCDD-elicited responses in the mouse liver. BMC genomics. 2011;12:365.
186. Lo R, Matthews J. High-resolution genome-wide mapping of AHR and ARNT binding sites by ChIP-Seq. Toxicological sciences : an official journal of the Society of Toxicology. 2012;130(2):349-61.
187. Schodel J, Oikonomopoulos S, Ragoussis J, Pugh CW, Ratcliffe PJ, Mole DR. High-resolution genome-wide mapping of HIF-binding sites by ChIP-seq. Blood. 2011;117(23):e207-17.
188. Vogel CF, Matsumura F. A new cross-talk between the aryl hydrocarbon receptor and RelB, a member of the NF-kappaB family. Biochem Pharmacol. 2009;77(4):734-45.
189. Denison MS, Soshilov AA, He G, DeGroot DE, Zhao B. Exactly the same but different: promiscuity and diversity in the molecular mechanisms of action of the aryl hydrocarbon (dioxin) receptor. Toxicological sciences : an official journal of the Society of Toxicology. 2011;124(1):1-22.
190. Oeckinghaus A, Hayden MS, Ghosh S. Crosstalk in NF-kappaB signaling pathways. Nat Immunol. 2011;12(8):695-708.
191. Vogel CF, Khan EM, Leung PS, Gershwin ME, Chang WL, Wu D, et al. Cross-talk between aryl hydrocarbon receptor and the inflammatory response: a role for nuclear factor-kappaB. The Journal of biological chemistry. 2014;289(3):1866-75.
192. Allan LL, Sherr DH. Constitutive activation and environmental chemical induction of the aryl hydrocarbon receptor/transcription factor in activated human B lymphocytes. Mol Pharmacol. 2005;67(5):1740-50.
193. Tian Y. Ah receptor and NF-kappaB interplay on the stage of epigenome. Biochem Pharmacol. 2009;77(4):670-80.
194. Vogel CF, Wu D, Goth SR, Baek J, Lollies A, Domhardt R, et al. Aryl hydrocarbon receptor signaling regulates NF-kappaB RelB activation during dendritic-cell differentiation. Immunol Cell Biol. 2013;91(9):568-75.
195. Hershko A, Ciechanover A. The ubiquitin system. Annual review of biochemistry. 1998;67:425-79.
196. Ohtake F, Baba A, Takada I, Okada M, Iwasaki K, Miki H, et al. Dioxin receptor is a ligand-dependent E3 ubiquitin ligase. Nature. 2007;446(7135):562-6.
197. Baglole CJ, Maggirwar SB, Gasiewicz TA, Thatcher TH, Phipps RP, Sime PJ. The aryl hydrocarbon receptor attenuates tobacco smoke-induced cyclooxygenase-2 and prostaglandin production in lung fibroblasts through regulation of the NF-kappaB family member RelB. The Journal of biological chemistry. 2008;283(43):28944-57.
198. Thatcher TH, Maggirwar SB, Baglole CJ, Lakatos HF, Gasiewicz TA, Phipps RP, et al. Aryl hydrocarbon receptor-deficient mice develop heightened inflammatory responses to cigarette smoke and endotoxin associated with rapid loss of the nuclear factor-kappaB component RelB. The American journal of pathology. 2007;170(3):855-64.
199. Leidner J, Palkowitsch L, Marienfeld U, Fischer D, Marienfeld R. Identification of lysine residues critical for the transcriptional activity and polyubiquitination of the NF-kappaB family member RelB. The Biochemical journal. 2008;416(1):117-27.
200. Matsumura F. The significance of the nongenomic pathway in mediating inflammatory signaling of the dioxin-activated Ah receptor to cause toxic effects. Biochem Pharmacol. 2009;77(4):608-26.
201. Frame MC. Src in cancer: deregulation and consequences for cell behaviour. Biochimica et biophysica acta. 2002;1602(2):114-30.

202. Dong B, Cheng W, Li W, Zheng J, Wu D, Matsumura F, et al. FRET analysis of protein tyrosine kinase c-Src activation mediated via aryl hydrocarbon receptor. Biochimica et biophysica acta. 2011;1810(4):427-31.
203. Shi C, Ma Y, Liu H, Zhang Y, Wang Z, Jia H. The non-receptor tyrosine kinase c-Src mediates the PDGF-induced association between Furin and pro-MT1-MMP in HPAC pancreatic cells. Mol Cell Biochem. 2012;362(1-2):65-70.
204. Yang Y, Bai ZG, Yin J, Wu GC, Zhang ZT. Role of c-Src activity in the regulation of gastric cancer cell migration. Oncology reports. 2014;32(1):45-9.
205. Khalil N. TGF-beta: from latent to active. Microbes and infection / Institut Pasteur. 1999;1(15):1255-63.
206. Kamato D, Burch ML, Piva TJ, Rezaei HB, Rostam MA, Xu S, et al. Transforming growth factor-beta signalling: role and consequences of Smad linker region phosphorylation. Cellular signalling. 2013;25(10):2017-24.
207. Quintana FJ, Iglesias AH, Farez MF, Caccamo M, Burns EJ, Kassam N, et al. Adaptive autoimmunity and Foxp3-based immunoregulation in zebrafish. PLoS One. 2010;5(3):e9478.
208. Quintana FJ, Jin H, Burns EJ, Nadeau M, Yeste A, Kumar D, et al. Aiolos promotes TH17 differentiation by directly silencing Il2 expression. Nat Immunol. 2012;13(8):770-7.
209. Apetoh L, Quintana FJ, Pot C, Joller N, Xiao S, Kumar D, et al. The aryl hydrocarbon receptor interacts with c-Maf to promote the differentiation of type 1 regulatory T cells induced by IL-27. Nat Immunol. 2010;11(9):854-61.
210. Veldhoen M, Hirota K, Westendorf AM, Buer J, Dumoutier L, Renauld JC, et al. The aryl hydrocarbon receptor links TH17-cell-mediated autoimmunity to environmental toxins. Nature. 2008;453(7191):106-9.
211. Ciofani M, Madar A, Galan C, Sellars M, Mace K, Pauli F, et al. A validated regulatory network for Th17 cell specification. Cell. 2012;151(2):289-303.
212. Kimura A, Naka T, Nohara K, Fujii-Kuriyama Y, Kishimoto T. Aryl hydrocarbon receptor regulates Stat1 activation and participates in the development of Th17 cells. Proc Natl Acad Sci U S A. 2008;105(28):9721-6.
213. Puccetti P, Fallarino F. Generation of T cell regulatory activity by plasmacytoid dendritic cells and tryptophan catabolism. Blood Cells, Molecules, and Diseases. 2008;40(1):101-5.
214. Quintana FJ. The aryl hydrocarbon receptor: a molecular pathway for the environmental control of the immune response. Immunology. 2013;138(3):183-9.
215. Lin CH, Chen CC, Chou CM, Wang CY, Hung CC, Chen JY, et al. Knockdown of the aryl hydrocarbon receptor attenuates excitotoxicity and enhances NMDA-induced BDNF expression in cortical neurons. J Neurochem. 2009;111(3):777-89.
216. Latchney SE, Hein AM, O'Banion MK, DiCicco-Bloom E, Opanashuk LA. Deletion or activation of the aryl hydrocarbon receptor alters adult hippocampal neurogenesis and contextual fear memory. J Neurochem. 2013;125(3):430-45.
217. Mukai M, Lin TM, Peterson RE, Cooke PS, Tischkau SA. Behavioral rhythmicity of mice lacking AhR and attenuation of light-induced phase shift by 2,3,7,8-tetrachlorodibenzo-p-dioxin. Journal of biological rhythms. 2008;23(3):200-10.
218. Huang X, Powell-Coffman JA, Jin Y. The AHR-1 aryl hydrocarbon receptor and its co-factor the AHA-1 aryl hydrocarbon receptor nuclear translocator specify GABAergic neuron cell fate in C. elegans. Development. 2004;131(4):819-28.
219. Filbrandt CR, Wu Z, Zlokovic B, Opanashuk L, Gasiewicz TA. Presence and functional activity of the aryl hydrocarbon receptor in isolated murine cerebral vascular endothelial cells and astrocytes. Neurotoxicology. 2004;25(4):605-16.
220. Takanaga H, Kunimoto M, Adachi T, Tohyama C, Aoki Y. Inhibitory effect of 2,3,7,8-tetrachlorodibenzo-p-dioxin on cAMP-induced differentiation of rat C6 glial cell line. J Neurosci Res. 2001;64(4):402-9.
221. Takanaga H, Yoshitake T, Yatabe E, Hara S, Kunimoto M. Beta-naphthoflavone disturbs astrocytic differentiation of C6 glioma cells by inhibiting autocrine interleukin-6. J Neurochem. 2004;90(3):750-7.

222. Gramatzki D, Pantazis G, Schittenhelm J, Tabatabai G, Kohle C, Wick W, et al. Aryl hydrocarbon receptor inhibition downregulates the TGF-beta/Smad pathway in human glioblastoma cells. Oncogene. 2009;28(28):2593-605.
223. Kohta M, Kohmura E, Yamashita T. Inhibition of TGF-beta1 promotes functional recovery after spinal cord injury. Neuroscience research. 2009;65(4):393-401.
224. Kimura A, Naka T, Nakahama T, Chinen I, Masuda K, Nohara K, et al. Aryl hydrocarbon receptor in combination with Stat1 regulates LPS-induced inflammatory responses. The Journal of experimental medicine. 2009;206(9):2027-35.
225. Masuda K, Kimura A, Hanieh H, Nguyen NT, Nakahama T, Chinen I, et al. Aryl hydrocarbon receptor negatively regulates LPS-induced IL-6 production through suppression of histamine production in macrophages. Int Immunol. 2011;23(10):637-45.
226. Huai W, Zhao R, Song H, Zhao J, Zhang L, Zhang L, et al. Aryl hydrocarbon receptor negatively regulates NLRP3 inflammasome activity by inhibiting NLRP3 transcription. Nat Commun. 2014;5:4738.
227. Ho LW, Carmichael J, Swartz J, Wyttenbach A, Rankin J, Rubinsztein DC. The molecular biology of Huntington's disease. Psychological medicine. 2001;31(1):3-14.
228. Beal MF, Kowall NW, Ellison DW, Mazurek MF, Swartz KJ, Martin JB. Replication of the neurochemical characteristics of Huntington's disease by quinolinic acid. Nature. 1986;321(6066):168-71.
229. Guidetti P, Luthi-Carter RE, Augood SJ, Schwarcz R. Neostriatal and cortical quinolinate levels are increased in early grade Huntington's disease. Neurobiol Dis. 2004;17(3):455-61.
230. Sathyasaikumar KV, Stachowski EK, Amori L, Guidetti P, Muchowski PJ, Schwarcz R. Dysfunctional kynurenine pathway metabolism in the R6/2 mouse model of Huntington's disease. J Neurochem. 2010;113(6):1416-25.
231. Jauch D, Urbanska EM, Guidetti P, Bird ED, Vonsattel JP, Whetsell WO, Jr., et al. Dysfunction of brain kynurenic acid metabolism in Huntington's disease: focus on kynurenine aminotransferases. J Neurol Sci. 1995;130(1):39-47.
232. Giorgini F, Guidetti P, Nguyen Q, Bennett SC, Muchowski PJ. A genomic screen in yeast implicates kynurenine 3-monooxygenase as a therapeutic target for Huntington disease. Nat Genet. 2005;37(5):526-31.
233. Citron M. Alzheimer's disease: strategies for disease modification. Nature reviews Drug discovery. 2010;9(5):387-98.
234. Guillemin GJ, Brew BJ, Noonan CE, Takikawa O, Cullen KM. Indoleamine 2,3 dioxygenase and quinolinic acid Immunoreactivity in Alzheimer's disease hippocampus. Neuropathology and Applied Neurobiology. 2005;31(4):395-404.
235. Unger JW. Glial reaction in aging and Alzheimer's disease. Microscopy Research and Technique. 1998;43(1):24-8.
236. Rahman A, Ting K, Cullen KM, Braidy N, Brew BJ, Guillemin GJ. The excitotoxin quinolinic acid induces tau phosphorylation in human neurons. PLoS ONE. 2009;4(7).
237. Ting KK, Brew B, Guillemin G. The involvement of astrocytes and kynurenine pathway in Alzheimer's disease. Neurotoxicity Research. 2007;12(4):247-62.
238. Cooper NR, Bradt BM, O'Barr S, Yu JX. Focal inflammation in the brain: Role in Alzheimer's disease. Immunologic Research. 2000;21(2-3):159-65.
239. Baran H, Jellinger K, Deecke L. Kynurenine metabolism in Alzheimer's disease. Journal of Neural Transmission. 1999;106(2):165-81.
240. Hernandez CM, Kayed R, Zheng H, Sweatt JD, Dineley KT. Loss of alpha7 nicotinic receptors enhances beta-amyloid oligomer accumulation, exacerbating early-stage cognitive decline and septohippocampal pathology in a mouse model of Alzheimer's disease. J Neurosci. 2010;30(7):2442-53.
241. Lee DR, Semba R, Kondo H, Goto S, Nakano K. Decrease in the levels of NGF and BDNF in brains of mice fed a tryptophan-deficient diet. Bioscience, Biotechnology and Biochemistry. 1999;63(2):337-40.
242. Widner B, Ledochowski M, Fuchs D. Sleep disturbances and tryptophan in patients with Alzheimer's disease. The Lancet. 2000;355(9205):755-6.

243. Hartai Z, Klivenyi P, Janaky T, Penke B, Dux L, Vecsei L. Kynurenine metabolism in plasma and in red blood cells in Parkinson's disease. J Neurol Sci. 2005;239(1):31-5.
244. Ogawa T, Matson WR, Beal MF, Myers RH, Bird ED, Milbury P, et al. Kynurenine pathway abnormalities in Parkinson's disease. Neurology. 1992;42(9):1702-6.
245. Knyihar-Csillik E, Csillik B, Pakaski M, Krisztin-Peva B, Dobo E, Okuno E, et al. Decreased expression of kynurenine aminotransferase-I (KAT-I) in the substantia nigra of mice after 1-methyl-4-phenyl-1,2,3,6-tetrahydropyridine (MPTP) treatment. Neuroscience. 2004;126(4):899-914.
246. Stone R. Parkinson's disease. Coincidence or connection? Science. 2002;296(5567):451-2.
247. Merino M, Vizuete ML, Cano J, Machado A. The non-NMDA glutamate receptor antagonists 6-cyano-7-nitroquinoxaline-2,3-dione and 2,3-dihydroxy-6-nitro-7-sulfamoylbenzo(f)quinoxaline, but not NMDA antagonists, block the intrastriatal neurotoxic effect of MPP+. J Neurochem. 1999;73(2):750-7.
248. Zhang H, Andrekopoulos C, Joseph J, Chandran K, Karoui H, Crow JP, et al. Bicarbonate-dependent peroxidase activity of human Cu,Zn-superoxide dismutase induces covalent aggregation of protein: intermediacy of tryptophan-derived oxidation products. The Journal of biological chemistry. 2003;278(26):24078-89.
249. Noack H, Lindenau J, Rothe F, Asayama K, Wolf G. Differential expression of superoxide dismutase isoforms in neuronal and glial compartments in the course of excitotoxically mediated neurodegeneration: relation to oxidative and nitrergic stress. Glia. 1998;23(4):285-97.
250. Ilzecka J, Kocki T, Stelmasiak Z, Turski WA. Endogenous protectant kynurenic acid in amyotrophic lateral sclerosis. Acta neurologica Scandinavica. 2003;107(6):412-8.
251. Carson MJ. Microglia as liaisons between the immune and central nervous systems: functional implications for multiple sclerosis. Glia. 2002;40(2):218-31.
252. Monaco F, Fumero S, Mondino A, Mutani R. Plasma and cerebrospinal fluid tryptophan in multiple sclerosis and degenerative diseases. Journal of neurology, neurosurgery, and psychiatry. 1979;42(7):640-1.
253. Hartai Z, Klivenyi P, Janaky T, Penke B, Dux L, Vecsei L. Kynurenine metabolism in multiple sclerosis. Acta neurologica Scandinavica. 2005;112(2):93-6.
254. Rejdak K, Bartosik-Psujek H, Dobosz B, Kocki T, Grieb P, Giovannoni G, et al. Decreased level of kynurenic acid in cerebrospinal fluid of relapsing-onset multiple sclerosis patients. Neurosci Lett. 2002;331(1):63-5.
255. Chiarugi A, Cozzi A, Ballerini C, Massacesi L, Moroni F. Kynurenine 3-mono-oxygenase activity and neurotoxic kynurenine metabolites increase in the spinal cord of rats with experimental allergic encephalomyelitis. Neuroscience. 2001;102(3):687-95.
256. O'Connor JC, Andre C, Wang Y, Lawson MA, Szegedi SS, Lestage J, et al. Interferon-gamma and tumor necrosis factor-alpha mediate the upregulation of indoleamine 2,3-dioxygenase and the induction of depressive-like behavior in mice in response to bacillus Calmette-Guerin. J Neurosci. 2009;29(13):4200-9.
257. Smith AK, Simon JS, Gustafson EL, Noviello S, Cubells JF, Epstein MP, et al. Association of a polymorphism in the indoleamine- 2,3-dioxygenase gene and interferon-alpha-induced depression in patients with chronic hepatitis C. Molecular psychiatry. 2012;17(8):781-9.
258. Steiner J, Walter M, Gos T, Guillemin GJ, Bernstein HG, Sarnyai Z, et al. Severe depression is associated with increased microglial quinolinic acid in subregions of the anterior cingulate gyrus: evidence for an immune-modulated glutamatergic neurotransmission? J Neuroinflammation. 2011;8:94.
259. Laugeray A, Launay JM, Callebert J, Surget A, Belzung C, Barone PR. Peripheral and cerebral metabolic abnormalities of the tryptophan-kynurenine pathway in a murine model of major depression. Behavioural brain research. 2010;210(1):84-91.
260. Biskup CS, Sanchez CL, Arrant A, Van Swearingen AE, Kuhn C, Zepf FD. Effects of acute tryptophan depletion on brain serotonin function and concentrations of dopamine and norepinephrine in C57BL/6J and BALB/cJ mice. PLoS One. 2012;7(5):e35916.
261. Lewis DA, Hashimoto T, Volk DW. Cortical inhibitory neurons and schizophrenia. Nat Rev Neurosci. 2005;6(4):312-24.

262. Coyle JT. NMDA receptor and schizophrenia: a brief history. Schizophr Bull. 2012;38(5):920-6.
263. Schwarcz R, Rassoulpour A, Wu HQ, Medoff D, Tamminga CA, Roberts RC. Increased cortical kynurenate content in schizophrenia. Biological psychiatry. 2001;50(7):521-30.
264. Alexander KS, Wu HQ, Schwarcz R, Bruno JP. Acute elevations of brain kynurenic acid impair cognitive flexibility: normalization by the alpha7 positive modulator galantamine. Psychopharmacology (Berl). 2012;220(3):627-37.
265. Wonodi I, Stine OC, Sathyasaikumar KV, Roberts RC, Mitchell BD, Hong LE, et al. Downregulated kynurenine 3-monooxygenase gene expression and enzyme activity in schizophrenia and genetic association with schizophrenia endophenotypes. Arch Gen Psychiatry. 2011;68(7):665-74.
266. Miller CL, Llenos IC, Dulay JR, Weis S. Upregulation of the initiating step of the kynurenine pathway in postmortem anterior cingulate cortex from individuals with schizophrenia and bipolar disorder. Brain Res. 2006;1073-1074:25-37.
267. Turski WA, Schwarcz R. On the disposition of intrahippocampally injected kynurenic acid in the rat. Experimental brain research. 1988;71(3):563-7.
268. Heyes MP, Brew BJ, Martin A, Price RW, Salazar AM, Sidtis JJ, et al. Quinolinic acid in cerebrospinal fluid and serum in HIV-1 infection: relationship to clinical and neurological status. Annals of neurology. 1991;29(2):202-9.
269. Rodgers J, Stone TW, Barrett MP, Bradley B, Kennedy PG. Kynurenine pathway inhibition reduces central nervous system inflammation in a model of human African trypanosomiasis. Brain. 2009;132(Pt 5):1259-67.
270. Miu J, Ball HJ, Mellor AL, Hunt NH. Effect of indoleamine dioxygenase-1 deficiency and kynurenine pathway inhibition on murine cerebral malaria. International journal for parasitology. 2009;39(3):363-70.
271. Speciale C, Schwarcz R. On the production and disposition of quinolinic acid in rat brain and liver slices. J Neurochem. 1993;60(1):212-8.
272. Dinuzzo M, Mangia S, Maraviglia B, Giove F. The role of astrocytic glycogen in supporting the energetics of neuronal activity. Neurochem Res. 2012;37(11):2432-8.
273. Fernandez-Fernandez S, Almeida A, Bolaños JP. Antioxidant and bioenergetic coupling between neurons and astrocytes. Biochemical Journal. 2012;443(1):3-11.
274. van der Windt Gerritje JW, Everts B, Chang C-H, Curtis Jonathan D, Freitas Tori C, Amiel E, et al. Mitochondrial Respiratory Capacity Is a Critical Regulator of CD8+ T Cell Memory Development. Immunity.36(1):68-78.
275. Guillemin GJ, Cullen KM, Lim CK, Smythe GA, Garner B, Kapoor V, et al. Characterization of the Kynurenine Pathway in Human Neurons. The Journal of Neuroscience. 2007;27(47):12884-92.
276. Vandesompele J, De Preter K, Pattyn F, Poppe B, Van Roy N, De Paepe A, et al. Accurate normalization of real-time quantitative RT-PCR data by geometric averaging of multiple internal control genes. Genome biology. 2002;3(7):RESEARCH0034.
277. Sofroniew MV, Vinters HV. Astrocytes: biology and pathology. Acta Neuropathol. 2010;119(1):7-35.
278. Sofroniew MV. Molecular dissection of reactive astrogliosis and glial scar formation. Trends in neurosciences. 2009;32(12):638-47.
279. Mayo L, Trauger SA, Blain M, Nadeau M, Patel B, Alvarez JI, et al. Regulation of astrocyte activation by glycolipids drives chronic CNS inflammation. Nat Med. 2014;20(10):1147-56.
280. LaFrance-Corey RG, Howe CL. Isolation of brain-infiltrating leukocytes. Journal of visualized experiments : JoVE. 2011(52).
281. Martinez Gomez JM, Croxford JL, Yeo KP, Angeli V, Schwarz H, Gasser S. Development of experimental autoimmune encephalomyelitis critically depends on CD137 ligand signaling. J Neurosci. 2012;32(50):18246-52.
282. Sobczak M, Dargatz J, Chrzanowska-Wodnicka M. Isolation and culture of pulmonary endothelial cells from neonatal mice. Journal of visualized experiments : JoVE. 2010(46).
283. Seluanov A, Vaidya A, Gorbunova V. Establishing primary adult fibroblast cultures from rodents. Journal of visualized experiments : JoVE. 2010(44).

284. Guillemin GJ, Smythe G, Takikawa O, Brew BJ. Expression of indoleamine 2,3-dioxygenase and production of quinolinic acid by human microglia, astrocytes, and neurons. GLIA. 2005;49(1):15-23.
285. Derecki NC, Katzmarski N, Kipnis J, Meyer-Luehmann M. Microglia as a critical player in both developmental and late-life CNS pathologies. Acta Neuropathol. 2014;128(3):333-45.
286. Starossom SC, Mascanfroni ID, Imitola J, Cao L, Raddassi K, Hernandez SF, et al. Galectin-1 Deactivates Classically Activated Microglia and Protects from Inflammation-Induced Neurodegeneration. Immunity. 2012;37(2):249-63.
287. Martinez FO, Sica A, Mantovani A, Locati M. Macrophage activation and polarization. Frontiers in bioscience : a journal and virtual library. 2008;13:453-61.
288. Mantovani A, Sica A, Sozzani S, Allavena P, Vecchi A, Locati M. The chemokine system in diverse forms of macrophage activation and polarization. Trends Immunol. 2004;25(12):677-86.
289. Miyamoto A, Wake H, Moorhouse AJ, Nabekura J. Microglia and synapse interactions: fine tuning neural circuits and candidate molecules. Frontiers in cellular neuroscience. 2013;7:70.
290. Chhor V, Le Charpentier T, Lebon S, Ore MV, Celador IL, Josserand J, et al. Characterization of phenotype markers and neuronotoxic potential of polarised primary microglia in vitro. Brain Behav Immun. 2013;32:70-85.
291. Rivest S. Regulation of innate immune responses in the brain. Nat Rev Immunol. 2009;9(6):429-39.
292. Butovsky O, Jedrychowski MP, Cialic R, Krasemann S, Murugaiyan G, Fanek Z, et al. Targeting miR-155 restores abnormal microglia and attenuates disease in SOD1 mice. Annals of neurology. 2014.
293. Miron VE, Boyd A, Zhao JW, Yuen TJ, Ruckh JM, Shadrach JL, et al. M2 microglia and macrophages drive oligodendrocyte differentiation during CNS remyelination. Nat Neurosci. 2013;16(9):1211-8.
294. Butovsky O, Jedrychowski MP, Moore CS, Cialic R, Lanser AJ, Gabriely G, et al. Identification of a unique TGF-beta-dependent molecular and functional signature in microglia. Nat Neurosci. 2014;17(1):131-43.
295. Abbas AK, Lichtman AH. Basic Immunology: Functions and Disorders of the Immune System: Saunders/Elsevier; 2010.
296. Szabo SJ, Kim ST, Costa GL, Zhang X, Fathman CG, Glimcher LH. A novel transcription factor, T-bet, directs Th1 lineage commitment. Cell. 2000;100(6):655-69.
297. Zheng W, Flavell RA. The transcription factor GATA-3 is necessary and sufficient for Th2 cytokine gene expression in CD4 T cells. Cell. 1997;89(4):587-96.
298. Acosta-Rodriguez EV, Rivino L, Geginat J, Jarrossay D, Gattorno M, Lanzavecchia A, et al. Surface phenotype and antigenic specificity of human interleukin 17-producing T helper memory cells. Nat Immunol. 2007;8(6):639-46.
299. Hori S, Nomura T, Sakaguchi S. Control of regulatory T cell development by the transcription factor Foxp3. Science. 2003;299(5609):1057-61.
300. Fu S, Zhang N, Yopp AC, Chen D, Mao M, Chen D, et al. TGF-beta induces Foxp3 + T-regulatory cells from CD4 + CD25 - precursors. American journal of transplantation : official journal of the American Society of Transplantation and the American Society of Transplant Surgeons. 2004;4(10):1614-27.
301. Gorina R, Font-Nieves M, Márquez-Kisinousky L, Santalucia T, Planas AM. Astrocyte TLR4 activation induces a proinflammatory environment through the interplay between MyD88-dependent NFκB signaling, MAPK, and Jak1/Stat1 pathways. GLIA. 2011;59(2):242-55.
302. Dejardin E. The alternative NF-kappaB pathway from biochemistry to biology: pitfalls and promises for future drug development. Biochem Pharmacol. 2006;72(9):1161-79.
303. Farina C, Aloisi F, Meinl E. Astrocytes are active players in cerebral innate immunity. Trends Immunol. 2007;28(3):138-45.
304. Grassl C, Luckow B, Schlondorff D, Dendorfer U. Transcriptional regulation of the interleukin-6 gene in mesangial cells. Journal of the American Society of Nephrology : JASN. 1999;10(7):1466-77.

305. Chan C, Li L, McCall CE, Yoza BK. Endotoxin tolerance disrupts chromatin remodeling and NF-kappaB transactivation at the IL-1beta promoter. J Immunol. 2005;175(1):461-8.
306. Dounay AB, Anderson M, Bechle BM, Evrard E, Gan X, Kim JY, et al. PF-04859989 as a template for structure-based drug design: identification of new pyrazole series of irreversible KAT II inhibitors with improved lipophilic efficiency. Bioorganic & medicinal chemistry letters. 2013;23(7):1961-6.
307. Neumann M, Naumann M. Beyond IkappaBs: alternative regulation of NF-kappaB activity. FASEB journal : official publication of the Federation of American Societies for Experimental Biology. 2007;21(11):2642-54.
308. Weih F, Warr G, Yang H, Bravo R. Multifocal defects in immune responses in RelB-deficient mice. J Immunol. 1997;158(11):5211-8.
309. Shih VF, Davis-Turak J, Macal M, Huang JQ, Ponomarenko J, Kearns JD, et al. Control of RelB during dendritic cell activation integrates canonical and noncanonical NF-kappaB pathways. Nat Immunol. 2012;13(12):1162-70.
310. Kerkvliet NI. AHR-mediated immunomodulation: the role of altered gene transcription. Biochem Pharmacol. 2009;77(4):746-60.
311. Soshilov AA, Denison MS. Ligand promiscuity of aryl hydrocarbon receptor agonists and antagonists revealed by site-directed mutagenesis. Molecular and cellular biology. 2014;34(9):1707-19.
312. Petkov PI, Rowlands JC, Budinsky R, Zhao B, Denison MS, Mekenyan O. Mechanism-based common reactivity pattern (COREPA) modelling of aryl hydrocarbon receptor binding affinity. SAR and QSAR in environmental research. 2010;21(1):187-214.
313. Zhao B, Degroot DE, Hayashi A, He G, Denison MS. CH223191 is a ligand-selective antagonist of the Ah (Dioxin) receptor. Toxicological sciences : an official journal of the Society of Toxicology. 2010;117(2):393-403.
314. Bastien D, Lacroix S. Cytokine pathways regulating glial and leukocyte function after spinal cord and peripheral nerve injury. Exp Neurol. 2014;258:62-77.
315. Guerrero AR, Uchida K, Nakajima H, Watanabe S, Nakamura M, Johnson WE, et al. Blockade of interleukin-6 signaling inhibits the classic pathway and promotes an alternative pathway of macrophage activation after spinal cord injury in mice. J Neuroinflammation. 2012;9:40.
316. Zhou Z, Peng X, Insolera R, Fink DJ, Mata M. IL-10 promotes neuronal survival following spinal cord injury. Exp Neurol. 2009;220(1):183-90.
317. Vezzani A, Viviani B. Neuromodulatory properties of inflammatory cytokines and their impact on neuronal excitability. Neuropharmacology. 2014.
318. Okada S, Nakamura M, Mikami Y, Shimazaki T, Mihara M, Ohsugi Y, et al. Blockade of interleukin-6 receptor suppresses reactive astrogliosis and ameliorates functional recovery in experimental spinal cord injury. J Neurosci Res. 2004;76(2):265-76.
319. Boulland ML, Marquet J, Molinier-Frenkel V, Moller P, Guiter C, Lasoudris F, et al. Human IL4I1 is a secreted L-phenylalanine oxidase expressed by mature dendritic cells that inhibits T-lymphocyte proliferation. Blood. 2007;110(1):220-7.
320. Thackray SJ, Mowat CG, Chapman SK. Exploring the mechanism of tryptophan 2,3-dioxygenase. Biochemical Society Transactions. 2008;36(6):1120-3.
321. Bender DA, McCreanor GM. The preferred route of kynurenine metabolism in the rat. Biochimica et biophysica acta. 1982;717(1):56-60.
322. Goldstein LE, Leopold MC, Huang X, Atwood CS, Saunders AJ, Hartshorn M, et al. 3-Hydroxykynurenine and 3-hydroxyanthranilic acid generate hydrogen peroxide and promote alpha-crystallin cross-linking by metal ion reduction. Biochemistry. 2000;39(24):7266-75.
323. Srinivasan S, Avadhani NG. Cytochrome c oxidase dysfunction in oxidative stress. Free Radical Biology and Medicine. 2012;53(6):1252-63.
324. Murphy MP, Holmgren A, Larsson NG, Halliwell B, Chang CJ, Kalyanaraman B, et al. Unraveling the biological roles of reactive oxygen species. Cell metabolism. 2011;13(4):361-6.
325. Murphy MP. How mitochondria produce reactive oxygen species. The Biochemical journal. 2009;417(1):1-13.

326. Celsi F, Pizzo P, Brini M, Leo S, Fotino C, Pinton P, et al. Mitochondria, calcium and cell death: a deadly triad in neurodegeneration. Biochimica et biophysica acta. 2009;1787(5):335-44.
327. Gutteridge JM, Halliwell B. Antioxidants: Molecules, medicines, and myths. Biochem Biophys Res Commun. 2010;393(4):561-4.
328. Cozzi A, Carpenedo R, Moroni F. Kynurenine Hydroxylase Inhibitors Reduce Ischemic Brain Damage[colon] Studies With (m-Nitrobenzoyl)-Alanine (mNBA) and 3,4-Dimethoxy-[lsqb]-N-4-(Nitrophenyl)Thiazol-2YL[rsqb]-Benzenesulfonamide (Ro 61-8048) in Models of Focal or Global Brain Ischemia. J Cereb Blood Flow Metab. 1999;19(7):771-7.
329. Clark CJ, Mackay GM, Smythe GA, Bustamante S, Stone TW, Phillips RS. Prolonged survival of a murine model of cerebral malaria by kynurenine pathway inhibition. Infection and immunity. 2005;73(8):5249-51.
330. Zwilling D, Huang S-Y, Sathyasaikumar KV, Notarangelo FM, Guidetti P, Wu H-Q, et al. Kynurenine 3-Monooxygenase Inhibition in Blood Ameliorates Neurodegeneration. Cell. 2011;145(6):863-74.
331. Kim SM, Chung MJ, Ha TJ, Choi HN, Jang SJ, Kim SO, et al. Neuroprotective effects of black soybean anthocyanins via inactivation of ASK1–JNK/p38 pathways and mobilization of cellular sialic acids. Life Sciences. 2012;90(21–22):874-82.
332. Perry SW, Norman JP, Barbieri J, Brown EB, Gelbard HA. Mitochondrial membrane potential probes and the proton gradient: a practical usage guide. BioTechniques. 2011;50(2):98-115.
333. Norman JP, Perry SW, Kasischke KA, Volsky DJ, Gelbard HA. HIV-1 trans activator of transcription protein elicits mitochondrial hyperpolarization and respiratory deficit, with dysregulation of complex IV and nicotinamide adenine dinucleotide homeostasis in cortical neurons. J Immunol. 2007;178(2):869-76.
334. Aguirre E, Rodriguez-Juarez F, Bellelli A, Gnaiger E, Cadenas S. Kinetic model of the inhibition of respiration by endogenous nitric oxide in intact cells. Biochimica et biophysica acta. 2010;1797(5):557-65.
335. Campesan S, Green EW, Breda C, Sathyasaikumar KV, Muchowski PJ, Schwarcz R, et al. The Kynurenine Pathway Modulates Neurodegeneration in a Drosophila Model of Huntington's Disease. Current Biology. 2011;21(11):961-6.
336. Okuda S, Nishiyama N, Saito H, Katsuki H. 3-Hydroxykynurenine, an Endogenous Oxidative Stress Generator, Causes Neuronal Cell Death with Apoptotic Features and Region Selectivity. Journal of Neurochemistry. 1998;70(1):299-307.
337. Pesta D, Gnaiger E. High-resolution respirometry: OXPHOS protocols for human cells and permeabilized fibers from small biopsies of human muscle. Methods in molecular biology. 2012;810:25-58.
338. Riobo NA, Melani M, Sanjuan N, Fiszman ML, Gravielle MC, Carreras MC, et al. The modulation of mitochondrial nitric-oxide synthase activity in rat brain development. The Journal of biological chemistry. 2002;277(45):42447-55.
339. Greaves LC, Nooteboom M, Elson JL, Tuppen HA, Taylor GA, Commane DM, et al. Clonal Expansion of Early to Mid-Life Mitochondrial DNA Point Mutations Drives Mitochondrial Dysfunction during Human Ageing. PLoS genetics. 2014;10(9):e1004620.
340. Navarro A, Boveris A. The mitochondrial energy transduction system and the aging process. American journal of physiology Cell physiology. 2007;292(2):C670-86.
341. Wu G, Fang YZ, Yang S, Lupton JR, Turner ND. Glutathione metabolism and its implications for health. The Journal of nutrition. 2004;134(3):489-92.
342. Kirkman HN, Gaetani GF. Catalase: a tetrameric enzyme with four tightly bound molecules of NADPH. Proc Natl Acad Sci U S A. 1984;81(14):4343-7.
343. Rover S, Cesura AM, Huguenin P, Kettler R, Szente A. Synthesis and biochemical evaluation of N-(4-phenylthiazol-2-yl)benzenesulfonamides as high-affinity inhibitors of kynurenine 3-hydroxylase. J Med Chem. 1997;40(26):4378-85.
344. Braidy N, Guillemin GJ, Grant R. Effects of Kynurenine Pathway Inhibition on NAD Metabolism and Cell Viability in Human Primary Astrocytes and Neurons. International journal of tryptophan research : IJTR. 2011;4:29-37.

345. Carpenedo R, Meli E, Peruginelli F, Pellegrini-Giampietro DE, Moroni F. Kynurenine 3-mono-oxygenase inhibitors attenuate post-ischemic neuronal death in organotypic hippocampal slice cultures. Journal of Neurochemistry. 2002;82(6):1465-71.
346. Prochazkova D, Bousova I, Wilhelmova N. Antioxidant and prooxidant properties of flavonoids. Fitoterapia. 2011;82(4):513-23.
347. Murakami A, Ohnishi K. Target molecules of food phytochemicals: food science bound for the next dimension. Food & function. 2012;3(5):462-76.
348. Cusi MG, Del Vecchio MT, Terrosi C, Savellini GG, Di Genova G, La Placa M, et al. Immune-reconstituted influenza virosome containing CD40L gene enhances the immunological and protective activity of a carcinoembryonic antigen anticancer vaccine. Journal of Immunology. 2005;174(11):7210-6.
349. Takahashi A, Watanabe T, Mondal A, Suzuki K, Kurusu-Kanno M, Li Z, et al. Mechanism-based inhibition of cancer metastasis with (-)-epigallocatechin gallate. Biochem Biophys Res Commun. 2014;443(1):1-6.
350. Katiyar S, Elmets CA, Katiyar SK. Green tea and skin cancer: photoimmunology, angiogenesis and DNA repair. The Journal of nutritional biochemistry. 2007;18(5):287-96.
351. Singh T, Katiyar SK. Green tea catechins reduce invasive potential of human melanoma cells by targeting COX-2, PGE2 receptors and epithelial-to-mesenchymal transition. PLoS One. 2011;6(10):e25224.
352. Singh BN, Shankar S, Srivastava RK. Green tea catechin, epigallocatechin-3-gallate (EGCG): mechanisms, perspectives and clinical applications. Biochem Pharmacol. 2011;82(12):1807-21.
353. Fu Z, Zhen W, Yuskavage J, Liu D. Epigallocatechin gallate delays the onset of type 1 diabetes in spontaneous non-obese diabetic mice. The British journal of nutrition. 2011;105(8):1218-25.
354. Mandel SA, Avramovich-Tirosh Y, Reznichenko L, Zheng H, Weinreb O, Amit T, et al. Multifunctional activities of green tea catechins in neuroprotection. Modulation of cell survival genes, iron-dependent oxidative stress and PKC signaling pathway. Neurosignals. 2005;14(1-2):46-60.
355. Zhang HS, Wu TC, Sang WW, Ruan Z. EGCG inhibits Tat-induced LTR transactivation: role of Nrf2, AKT, AMPK signaling pathway. Life Sci. 2012;90(19-20):747-54.
356. Narkar VA, Downes M, Yu RT, Embler E, Wang YX, Banayo E, et al. AMPK and PPARdelta agonists are exercise mimetics. Cell. 2008;134(3):405-15.
357. Rietveld A, Wiseman S. Antioxidant effects of tea: evidence from human clinical trials. The Journal of nutrition. 2003;133(10):3285S-92S.
358. Schroeder EK, Kelsey NA, Doyle J, Breed E, Bouchard RJ, Loucks FA, et al. Green tea epigallocatechin 3-gallate accumulates in mitochondria and displays a selective antiapoptotic effect against inducers of mitochondrial oxidative stress in neurons. Antioxidants & redox signaling. 2009;11(3):469-80.
359. Dragicevic N, Smith A, Lin X, Yuan F, Copes N, Delic V, et al. Green tea epigallocatechin-3-gallate (EGCG) and other flavonoids reduce Alzheimer's amyloid-induced mitochondrial dysfunction. Journal of Alzheimer's disease : JAD. 2011;26(3):507-21.
360. Arnold S. The power of life. Cytochrome c oxidase takes center stage in metabolic control, cell signalling and survival. Mitochondrion. 2012;12(1):46-56.
361. Haslam G, Wyatt D, Kitos PA. Estimating the number of viable animal cells in multi-well cultures based on their lactate dehydrogenase activities. Cytotechnology. 2000;32(1):63-75.
362. Norman JP, Perry SW, Kasischke KA, Volsky DJ, Gelbard HA. HIV-1 Trans Activator of Transcription Protein Elicits Mitochondrial Hyperpolarization and Respiratory Deficit, with Dysregulation of Complex IV and Nicotinamide Adenine Dinucleotide Homeostasis in Cortical Neurons. The Journal of Immunology. 2007;178(2):869-76.
363. Pendergrass W, Wolf N, Poot M. Efficacy of MitoTracker Green™ and CMXrosamine to measure changes in mitochondrial membrane potentials in living cells and tissues. Cytometry Part A. 2004;61A(2):162-9.
364. Schneider CA, Rasband WS, Eliceiri KW. NIH Image to ImageJ: 25 years of image analysis. Nature methods. 2012;9(7):671-5.

365. Duchen MR. Mitochondria in health and disease: perspectives on a new mitochondrial biology. Molecular Aspects of Medicine. 2004;25(4):365-451.
366. Nicholls DG, Budd SL. Mitochondria and Neuronal Survival2000 2000-01-01 00:00:00. 315-60 p.
367. Hutter E, Unterluggauer H, Garedew A, Jansen-Durr P, Gnaiger E. High-resolution respirometry--a modern tool in aging research. Experimental gerontology. 2006;41(1):103-9.
368. Kelly DP, Scarpulla RC. Transcriptional regulatory circuits controlling mitochondrial biogenesis and function. Genes & development. 2004;18(4):357-68.
369. Wick AN, Drury DR, Nakada HI, Wolfe JB. Localization of the primary metabolic block produced by 2-deoxyglucose. The Journal of biological chemistry. 1957;224(2):963-9.
370. Sugioka K, Nakano M, Totsune-Nakano H, Minakami H, Tero-Kubota S, Ikegami Y. Mechanism of O2- generation in reduction and oxidation cycle of ubiquinones in a model of mitochondrial electron transport systems. Biochimica et biophysica acta. 1988;936(3):377-85.
371. Jellinger KA. Basic mechanisms of neurodegeneration: a critical update. Journal of cellular and molecular medicine. 2010;14(3):457-87.
372. Valenti D, De Rasmo D, Signorile A, Rossi L, de Bari L, Scala I, et al. Epigallocatechin-3-gallate prevents oxidative phosphorylation deficit and promotes mitochondrial biogenesis in human cells from subjects with Down's syndrome. Biochimica et biophysica acta. 2013;1832(4):542-52.
373. Zhang Z, Ding Y, Dai X, Wang J, Li Y. Epigallocatechin-3-gallate protects pro-inflammatory cytokine induced injuries in insulin-producing cells through the mitochondrial pathway. Eur J Pharmacol. 2011;670(1):311-6.
374. Hardie DG, Ross FA, Hawley SA. AMPK: a nutrient and energy sensor that maintains energy homeostasis. Nat Rev Mol Cell Biol. 2012;13(4):251-62.
375. Mihaylova MM, Shaw RJ. The AMPK signalling pathway coordinates cell growth, autophagy and metabolism. Nature cell biology. 2011;13(9):1016-23.
376. Collins QF, Liu HY, Pi J, Liu Z, Quon MJ, Cao W. Epigallocatechin-3-gallate (EGCG), a green tea polyphenol, suppresses hepatic gluconeogenesis through 5'-AMP-activated protein kinase. The Journal of biological chemistry. 2007;282(41):30143-9.
377. Li Y, Zhao S, Zhang W, Zhao P, He B, Wu N, et al. Epigallocatechin-3-O-gallate (EGCG) attenuates FFAs-induced peripheral insulin resistance through AMPK pathway and insulin signaling pathway in vivo. Diabetes research and clinical practice. 2011;93(2):205-14.
378. Cai EP, Lin JK. Epigallocatechin gallate (EGCG) and rutin suppress the glucotoxicity through activating IRS2 and AMPK signaling in rat pancreatic beta cells. J Agric Food Chem. 2009;57(20):9817-27.
379. Hwang JT, Ha J, Park IJ, Lee SK, Baik HW, Kim YM, et al. Apoptotic effect of EGCG in HT-29 colon cancer cells via AMPK signal pathway. Cancer letters. 2007;247(1):115-21.
380. Huang CH, Tsai SJ, Wang YJ, Pan MH, Kao JY, Way TD. EGCG inhibits protein synthesis, lipogenesis, and cell cycle progression through activation of AMPK in p53 positive and negative human hepatoma cells. Molecular nutrition & food research. 2009;53(9):1156-65.
381. Park SY, Jung CH, Song B, Park OJ, Kim YM. Pro-apoptotic and migration-suppressing potential of EGCG, and the involvement of AMPK in the p53-mediated modulation of VEGF and MMP-9 expression. Oncology letters. 2013;6(5):1346-50.
382. Chen C, Shen G, Hebbar V, Hu R, Owuor ED, Kong AN. Epigallocatechin-3-gallate-induced stress signals in HT-29 human colon adenocarcinoma cells. Carcinogenesis. 2003;24(8):1369-78.
383. Spasic MR, Callaerts P, Norga KK. AMP-activated protein kinase (AMPK) molecular crossroad for metabolic control and survival of neurons. The Neuroscientist : a review journal bringing neurobiology, neurology and psychiatry. 2009;15(4):309-16.
384. Dasgupta B, Milbrandt J. Resveratrol stimulates AMP kinase activity in neurons. Proc Natl Acad Sci U S A. 2007;104(17):7217-22.
385. Ludwig B, Bender E, Arnold S, Huttemann M, Lee I, Kadenbach B. Cytochrome C oxidase and the regulation of oxidative phosphorylation. Chembiochem : a European journal of chemical biology. 2001;2(6):392-403.

386. Arnold S, Kadenbach B. The intramitochondrial ATP/ADP-ratio controls cytochrome c oxidase activity allosterically. FEBS Lett. 1999;443(2):105-8.
387. Huttemann M, Kadenbach B, Grossman LI. Mammalian subunit IV isoforms of cytochrome c oxidase. Gene. 2001;267(1):111-23.
388. Misiak M, Singh S, Drewlo S, Beyer C, Arnold S. Brain region-specific vulnerability of astrocytes in response to 3-nitropropionic acid is mediated by cytochrome c oxidase isoform expression. Cell and tissue research. 2010;341(1):83-93.
389. Horvat S, Beyer C, Arnold S. Effect of hypoxia on the transcription pattern of subunit isoforms and the kinetics of cytochrome c oxidase in cortical astrocytes and cerebellar neurons. J Neurochem. 2006;99(3):937-51.
390. Collman JP, Dey A, Barile CJ, Ghosh S, Decreau RA. Inhibition of electrocatalytic O(2) reduction of functional CcO models by competitive, non-competitive, and mixed inhibitors. Inorganic chemistry. 2009;48(22):10528-34.
391. Arnold S, Goglia F, Kadenbach B. 3,5-Diiodothyronine binds to subunit Va of cytochrome-c oxidase and abolishes the allosteric inhibition of respiration by ATP. European journal of biochemistry / FEBS. 1998;252(2):325-30.
392. Fukuda R, Zhang H, Kim JW, Shimoda L, Dang CV, Semenza GL. HIF-1 regulates cytochrome oxidase subunits to optimize efficiency of respiration in hypoxic cells. Cell. 2007;129(1):111-22.
393. Pope S, Land JM, Heales SJ. Oxidative stress and mitochondrial dysfunction in neurodegeneration; cardiolipin a critical target? Biochimica et biophysica acta. 2008;1777(7-8):794-9.
394. Helling S, Huttemann M, Ramzan R, Kim SH, Lee I, Muller T, et al. Multiple phosphorylations of cytochrome c oxidase and their functions. Proteomics. 2012;12(7):950-9.
395. Piccoli C, Scrima R, Boffoli D, Capitanio N. Control by cytochrome c oxidase of the cellular oxidative phosphorylation system depends on the mitochondrial energy state. The Biochemical journal. 2006;396(3):573-83.
396. Lu LY, Ou N, Lu QB. Antioxidant induces DNA damage, cell death and mutagenicity in human lung and skin normal cells. Scientific reports. 2013;3:3169.
397. Lee YJ, Choi DY, Yun YP, Han SB, Oh KW, Hong JT. Epigallocatechin-3-gallate prevents systemic inflammation-induced memory deficiency and amyloidogenesis via its anti-neuroinflammatory properties. The Journal of nutritional biochemistry. 2013;24(1):298-310.
398. Dauer W, Przedborski S. Parkinson's disease: mechanisms and models. Neuron. 2003;39(6):889-909.
399. Banchereau J, Pascual V, O'Garra A. From IL-2 to IL-37: the expanding spectrum of anti-inflammatory cytokines. Nat Immunol. 2012;13(10):925-31.
400. Yang Z, Mu Z, Dabovic B, Jurukovski V, Yu D, Sung J, et al. Absence of integrin-mediated TGFbeta1 activation in vivo recapitulates the phenotype of TGFbeta1-null mice. The Journal of cell biology. 2007;176(6):787-93.
401. Li MO, Flavell RA. TGF-beta: a master of all T cell trades. Cell. 2008;134(3):392-404.
402. Shi M, Zhu J, Wang R, Chen X, Mi L, Walz T, et al. Latent TGF-beta structure and activation. Nature. 2011;474(7351):343-9.
403. Wang R, Zhu J, Dong X, Shi M, Lu C, Springer TA. GARP regulates the bioavailability and activation of TGFbeta. Molecular biology of the cell. 2012;23(6):1129-39.
404. Miyazono K, Olofsson A, Colosetti P, Heldin CH. A role of the latent TGF-beta 1-binding protein in the assembly and secretion of TGF-beta 1. The EMBO journal. 1991;10(5):1091-101.
405. Tran DQ, Andersson J, Wang R, Ramsey H, Unutmaz D, Shevach EM. GARP (LRRC32) is essential for the surface expression of latent TGF-beta on platelets and activated FOXP3+ regulatory T cells. Proc Natl Acad Sci U S A. 2009;106(32):13445-50.
406. Rifkin DB. Latent transforming growth factor-beta (TGF-beta) binding proteins: orchestrators of TGF-beta availability. The Journal of biological chemistry. 2005;280(9):7409-12.
407. Buscemi L, Ramonet D, Klingberg F, Formey A, Smith-Clerc J, Meister JJ, et al. The single-molecule mechanics of the latent TGF-beta1 complex. Current biology : CB. 2011;21(24):2046-54.

408. Schultz-Cherry S, Chen H, Mosher DF, Misenheimer TM, Krutzsch HC, Roberts DD, et al. Regulation of transforming growth factor-beta activation by discrete sequences of thrombospondin 1. The Journal of biological chemistry. 1995;270(13):7304-10.
409. Barcellos-Hoff MH, Dix TA. Redox-mediated activation of latent transforming growth factor-beta 1. Molecular endocrinology. 1996;10(9):1077-83.
410. Yee JA, Yan L, Dominguez JC, Allan EH, Martin TJ. Plasminogen-dependent activation of latent transforming growth factor beta (TGF beta) by growing cultures of osteoblast-like cells. J Cell Physiol. 1993;157(3):528-34.
411. Dewerchin M, Nuffelen AV, Wallays G, Bouche A, Moons L, Carmeliet P, et al. Generation and characterization of urokinase receptor-deficient mice. The Journal of clinical investigation. 1996;97(3):870-8.
412. Carmeliet P, Schoonjans L, Kieckens L, Ream B, Degen J, Bronson R, et al. Physiological consequences of loss of plasminogen activator gene function in mice. Nature. 1994;368(6470):419-24.
413. Worthington JJ, Klementowicz JE, Travis MA. TGFbeta: a sleeping giant awoken by integrins. Trends in biochemical sciences. 2011;36(1):47-54.
414. Hirota S, Liu Q, Lee HS, Hossain MG, Lacy-Hulbert A, McCarty JH. The astrocyte-expressed integrin alphavbeta8 governs blood vessel sprouting in the developing retina. Development. 2011;138(23):5157-66.
415. Cambier S, Gline S, Mu D, Collins R, Araya J, Dolganov G, et al. Integrin alpha(v)beta8-mediated activation of transforming growth factor-beta by perivascular astrocytes: an angiogenic control switch. The American journal of pathology. 2005;166(6):1883-94.
416. Mobley AK, Tchaicha JH, Shin J, Hossain MG, McCarty JH. Beta8 integrin regulates neurogenesis and neurovascular homeostasis in the adult brain. Journal of cell science. 2009;122(Pt 11):1842-51.
417. Annes JP, Chen Y, Munger JS, Rifkin DB. Integrin alphaVbeta6-mediated activation of latent TGF-beta requires the latent TGF-beta binding protein-1. The Journal of cell biology. 2004;165(5):723-34.
418. Mu D, Cambier S, Fjellbirkeland L, Baron JL, Munger JS, Kawakatsu H, et al. The integrin alpha(v)beta8 mediates epithelial homeostasis through MT1-MMP-dependent activation of TGF-beta1. The Journal of cell biology. 2002;157(3):493-507.
419. Edwards JP, Thornton AM, Shevach EM. Release of active TGF-beta1 from the latent TGF-beta1/GARP complex on T regulatory cells is mediated by integrin beta8. J Immunol. 2014;193(6):2843-9.
420. Gauthy E, Cuende J, Stockis J, Huygens C, Lethe B, Collet JF, et al. GARP is regulated by miRNAs and controls latent TGF-beta1 production by human regulatory T cells. PLoS One. 2013;8(9):e76186.
421. Massague J. How cells read TGF-beta signals. Nat Rev Mol Cell Biol. 2000;1(3):169-78.
422. Schachtrup C, Ryu JK, Helmrick MJ, Vagena E, Galanakis DK, Degen JL, et al. Fibrinogen triggers astrocyte scar formation by promoting the availability of active TGF-beta after vascular damage. J Neurosci. 2010;30(17):5843-54.
423. Klingberg F, Hinz B, White ES. The myofibroblast matrix: implications for tissue repair and fibrosis. The Journal of pathology. 2013;229(2):298-309.
424. Klingberg F, Chow ML, Koehler A, Boo S, Buscemi L, Quinn TM, et al. Prestress in the extracellular matrix sensitizes latent TGF-beta1 for activation. The Journal of cell biology. 2014.
425. Engelhardt B, Coisne C. Fluids and barriers of the CNS establish immune privilege by confining immune surveillance to a two-walled castle moat surrounding the CNS castle. Fluids and barriers of the CNS. 2011;8(1):4.
426. Gomez-Duran A, Carvajal-Gonzalez JM, Mulero-Navarro S, Santiago-Josefat B, Puga A, Fernandez-Salguero PM. Fitting a xenobiotic receptor into cell homeostasis: how the dioxin receptor interacts with TGFbeta signaling. Biochem Pharmacol. 2009;77(4):700-12.
427. Saxena V, Lienesch DW, Zhou M, Bommireddy R, Azhar M, Doetschman T, et al. Dual roles of immunoregulatory cytokine TGF-beta in the pathogenesis of autoimmunity-mediated organ damage. J Immunol. 2008;180(3):1903-12.

428. Santiago-Josefat B, Mulero-Navarro S, Dallas SL, Fernandez-Salguero PM. Overexpression of latent transforming growth factor-beta binding protein 1 (LTBP-1) in dioxin receptor-null mouse embryo fibroblasts. Journal of cell science. 2004;117(Pt 6):849-59.
429. Raposo C, Graubardt N, Cohen M, Eitan C, London A, Berkutzki T, et al. CNS repair requires both effector and regulatory T cells with distinct temporal and spatial profiles. J Neurosci. 2014;34(31):10141-55.
430. Schwartz M, Baruch K. Breaking peripheral immune tolerance to CNS antigens in neurodegenerative diseases: Boosting autoimmunity to fight-off chronic neuroinflammation. Journal of autoimmunity. 2014;54C:8-14.